Prognostic and predictive testing of molecular markers in breast cancer by real-time quantitative PCR

Anieta M. Sieuwerts

Prognostic and predictive testing of molecular markers in breast cancer by real-time quantitative PCR

Prognostisch en predicatief testen van moleculaire markers in borstkanker met behulp van real-time kwantitative PCR

Proefschrift

ter verkrijging van de graad van doctor aan de
Erasmus Universiteit Rotterdam
op gezag van de
rector magnificus

Prof.dr. S.W.J. Lamberts
en volgens besluit van het College voor Promoties.

De openbare verdediging zal plaatsvinden op
woensdag 5 december 2007 om 09.45 uur

door

Anita Maria Sieuwerts
geboren te 's Hertogenbosch

ERASMUS UNIVERSITEIT ROTTERDAM

Promotiecommissie

Promotor:
Prof.dr. J.G.M. Klijn

Overige leden:
Prof.dr. C.G.J. Sweep
Prof.dr. A.M.M. Eggermont
Dr. P.M.J.J. Berns

Copromotor:
Dr. J.A. Foekens

CONTENTS

CONTENTS

LIST OF ABBREVIATIONS

ACT	actinomycin D
ADAM	a disintegrin and metalloproteinase
ANOVA	analysis of variance
APPBP2	amyloid beta precursor protein (cytoplasmic tail) binding protein 2
AR	androgen receptor
AUC	area under the curve
B2M	β-2-microglobulin
BCIP	5-bromo-4-chloro-3-indolyl phosphate
BLAST	basic local alignment search tool
BRCA1	breast cancer 1
BRCA2	breast cancer 2
CA	cancer antigen
CCNE1	cyclin E1
CCNE2	cyclin E2
CDC42EP4	cell-division cycle 42 effector protein 4
CDK2	cyclin-dependent kinase-2
cDNA	copy DNA
CEA	carcinoembryonic antigen
CGH	comparative genomic hybridization
CHX	cycloheximide
CI	confidence interval
CIT	colloidal intraductal tumors
CMF	cyclophosphamide, methotrexate, 5-fluorouracil
COL1A1	collagen type I alpha 1
CR	complete remission
CRC	colorectal cancer
Ct	cycle threshold
c.v.	coefficient of variation
DCIS	ductal carcinoma *in situ*
DFS	disease-free survival
DM	distant metastasis
DMFS	distant metastasis-free survival
DNA	deoxyribonucleic acid
dsDNA	double-stranded DNA
DTF	desmoid-type fibromatosis
E2	estradiol
E2IG5	E2 induced gene 5
ECM	extracellular matrix
EDTA	ethylenediaminetetraacetic acid
EGF	epidermal growth factor
EIF1	eukaryotic translation initiation factor 1
ELISA,	enzyme-linked immunosorbent assay
EMMPRIN	extracellular MMP-inducer
ER	estrogen receptor
ERBB2	Her-2/neu; erythroblastic leukemia viral oncogene homolog 2, neuro/glioblastoma derived oncogene homolog (avian)
ER-α	estrogen receptor alpha
ESR1	estrogen receptor 1 (formerly *ER-α*) gene
ETS	c-ets proto-oncogene transcription factor
EZH1	enhancer of zeste (Drosophila) homolog 1
FDA	federal drug administration
FDR	false discovery rate
FFPE	formalin-fixed paraffin-embedded
FGF	fibroblast growth factor
FISH	fluorescence *in situ* hybridisation
FMNL	formin-like
GAPDH	glyceraldehyde-3-phosphate dehydrogenase
GGI	genomic grade index
GOBP	gene ontology biological process
GRB7	growth factor receptor-bound protein 7
HE	hematoxylin and eosin
HGF	hepatocyte growth factor
HK	housekeeper
HMBS	hydroxymethylbilane synthase (formerly porphobilinogen deaminase, PBGD)
HOXB13	homeobox B13
HPRT	hypoxanthine-guanine phospho-ribosyltransferase
HR	hazard ratio
HRP	horseradish peroxidase
HSPG	heparan sulphate proteoglycans
IBC	inflammatory breast cancer
IDC	invasive/infiltrating ductal carcinoma
IGF	insulin-like growth factor
IGFBP	insulin-like growth factor binding protein
IL17RB	interleukin 17 receptor B
ILC	infiltrating/invasive lobular cancer
LCIS	lobular carcinoma *in situ*
LMW	low molecular weight
LNN	lymph node-negative
LNP	lymph node-positive
LOE	level of evidence
LRR	local-regional relapse
MC	medullary carcinomas
MEC	medical ethics committee
MFS	metastasis-free survival
MMP	matrix metalloproteinase
mRNA	messenger RNA
N	normal-tissue-derived
NAT9	N-acetyltransferase 9
NBT	nitrotetrazolium blue
NC	no change
NCBI	national center for biotechnology information
NIH	national institute of health
NPI	Nottingham prognostic index
NR1D1	nuclear receptor subfamily 1, group D, member 1
OR	odds ratio
OS	overall survival
p53	tumor suppressor oncoprotein 53
PA	plasminogen activator
PAI	plasminogen activator inhibitor
PAI-1	plasminogen activator inhibitor 1
PBGD	porphobilinogen deaminase
PBS	phosphate buffered saline
PCR	polymerase chain reaction
PD	progressive disease
PFM	protein- and serum-free medium
PFS	progression free survival
PGR	progesterone receptor (formerly PgR) gene
PgR	progesterone receptor
PR	partial remission
PRS	post-relapse survival
ps	primer set
qPCR	quantitative polymerase chain reaction
qRT-PCR	quantitative reverse transcriptase polymerase chain reaction
RBC	recurrent breast cancer
RNA	ribonucleic acid
ROC	receiver operating characteristic
r_s	Spearman rank correlation
RT	reverse transcriptase
RT-PCR	reverse transcriptase polymerase chain reaction
SAM	significance analysis of microarrays
SA-β-gal	senescence associated β-galactosidase
SD	stable disease
SDS	sodium dodecyl sulfate
SEER	surveillance, epidemiology, and end results
SFT	solitary fibrous tumors
SMA	smooth muscle actin

SSC	sodium chloride / sodium citrate
Strept ABC	streptavidin-biotin-peroxidase complex
s-uPAR	soluble urokinase plasminogen activator receptor
T	tumor-tissue-derived
TBP	tributyl phosphine
TC	epithelial tumor cell nuclei
TERC	telomerase RNA component
TERT	reverse transcriptase enzyme telomerase
TGF-β	transforming growth factor β
TIMP	tissue inhibitor of metalloproteinases
TIMP-1	tissue inhibitor of metalloproteinases-1
TIMP1	TIMP metallopeptidase inhibitor 1 gene
TIMP1-v1	TIMP1 full-length variant gene
TIMP1-v2	TIMP1 variant lacking exon 2 gene
TMUGS	tumor marker utility grading system
TNM	tumor node metastases
TNP	trinitrophenyl hapten
tPA	tissue-type plasminogen activator
TRAP	telomerase repeat amplification
TRF2	telomere repeat binding factor 2
TSP-1	thrombospondin 1
UICC	union internationale contre le cancer
uPA	urokinase plasminogen activator
uPAR	urokinase plasminogen activator receptor
VEGF	vascular endothelial growth factor
VIM	vimentin
VTN	vitronectin
XGAL	5-bromo-4-chloro-3-indolyl-β-D-galactopyranoside
α-SMA	α-smooth muscle actin

CHAPTER ONE

General introduction

1. GENERAL INTRODUCTION

This chapter provides a general overview of breast cancer, including the relevance of measuring gene expression in the primary breast tumor in relation to the progression of the disease and the tumor response to treatment. To better understand the concept of breast cancer, extra emphasis will be put on breast cancer subtypes, staging and grading, and the tumor micro-environment that harbors the epithelial cancer cells. Currently available biomarkers to assess outcome of breast cancer patients in general (*i.e.* prognosis) as well as biomarkers currently available to assess patient outcome in response to therapy (*i.e.* prediction) will be discussed. After this it should become clear that there is still an urgent need for new biomarkers. How this search for additional biomarkers can be achieved by measuring mRNA gene expression in the primary tumor of patients diagnosed with breast cancer, will be explained in more detail.

1.1 Breast cancer

Epidemiology

In women breast cancer is, after skin cancer, the most common type of cancer and accounts for about 30% of all cancers in women. For women between 35-55 years of age in the well developed countries it is overall the main cause of death. In the Netherlands the incidence of breast cancer has been rising from 100 cases per 100,000 women in 1989 to 124 cases per 100,000 women in 2003 (www.vikc.nl). The age-adjusted approximate lifetime risk to be diagnosed with breast cancer is currently about 11% (www.kankerregistratie.nl). In the U.S. the probability of developing breast cancer is already as high as 12% (www.seer.cancer.gov).

The good news is that early detection, new treatment modalities and new insights have improved survival rates. An initial analysis of data from the National Cancer Institute's Surveillance, Epidemiology, and End Results (SEER) registries for example, showed that the age-adjusted incidence rate of breast cancer in women in the United States fell sharply (by 6.7%) in 2003, as compared with the rate in 2002. This decrease in breast cancer incidence seems to be temporally related to the first report of the Women's Health Initiative and the ensuing drop in the use of hormone-replacement therapy among postmenopausal women in the United States [1]. Nowadays, about 88% of the women diagnosed with breast cancer in the U.S will survive at least 10 years (www.healthcentral.com).
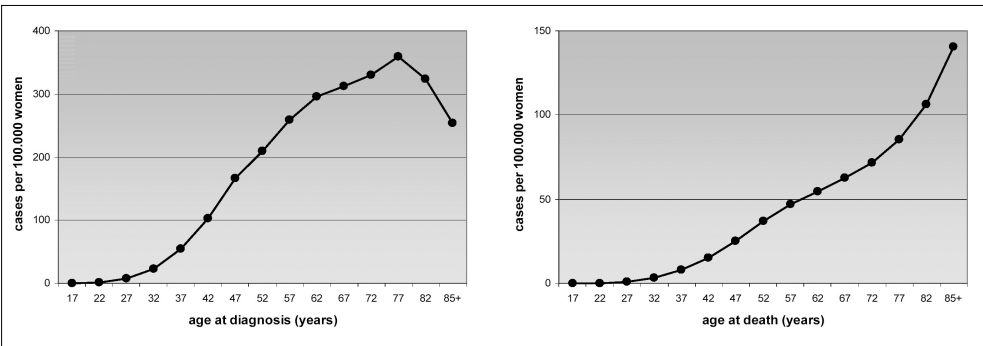

Figure 1.1.1. Malignant breast cancer incidence (left panel) and breast cancer related death (right panel) at various ages.
This graph of breast cancer incidence shows a steeply rising incidence with increasing age. (Complied from Surveillance, Epidemiology, and End Results (SEER) 13 registries for 1995-2004, based on the November 2006 submission; www.seer.cancer.gov).

Risk factors for breast cancer

Risk factors to get diagnosed with breast cancer can be divided in those that you cannot change (inborn) and those related to lifestyle [2]. Well acknowledged inborn risk factors are gender, aging (see also figure 1.1.1), genetic risk factors, family and personal history of breast cancer, race, abnormal breast biopsy, previous chest radiation and time of menstrual periods. Lifestyle related factors involve not having children or delayed childbirth, oral contraceptive use, hormone replacement therapy, breast-feeding and pregnancy, obesity and dietary aspects, especially use of alcohol (www.cancer.org). Note however that most women who have one or more breast cancer risk factors may never develop the disease, while many women who do have breast cancer have no apparent risk factors (other than being a woman and growing older, figure 1.1.1). With our aging population, especially the age-related increase in breast cancer incidence needs our attention. One of the reasons for this age-associated increased risk to get diagnosed with breast cancer (consequences of telomere attrition in stromal cells) will be discussed in chapter 3 of this thesis.

Once the cancer has developed, evaluation of additional risk factors such as the type of the breast cancer, the stage and grade at time of diagnosis, and other intrinsic tumor characteristics such as chromosomal abnormalities, immunological phenotype, cell proliferation index, and levels of proteins/enzymes and receptors for hormones and growth factors become important [3].

Types of breast cancer

In general, cancers can be classified according to their site of tissue origin, with the majority of human tumors arising from epithelial cells, *i.e.*, cells that line the walls of cavities and ducts, or in case of skin, serve as the outside covering of the body. For example carcinomas arise from epithelial cells, adenocarcinomas from secretory epithelial cells, squamous cell carcinomas from epithelial cells that line a duct or the skin and that lack secretory function. These epithelial tumors are responsible for more than 80% of the cancer-related deaths in the Western world. A second class of malignant tumors arises from non-epithelial tissues throughout the body. This class of non-epithelial tumors comprises the sarcomas derived from a variety of mesenchymal cell types such as fibroblasts, adipocytes, osteoblasts and myocytes, the leukemias and lymphomas derived from the blood-forming tissues, and the neuroectodermal tumors derived from components of the nervous system [4]. In addition to this, breast cancers are classified according a more defined site of origin and cell type (see also figure 1.1.2 and table 1.1.1).

Carcinoma sites in Breast

Lymph Nodes

Lobule
Duct
Lobe

Alveoli in Lobule
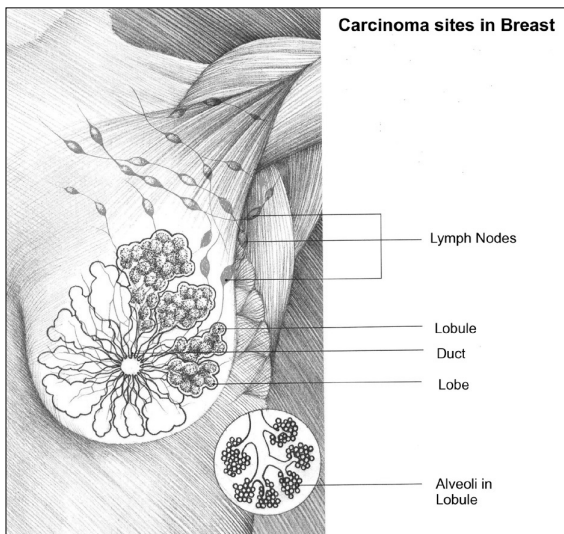
Figure 1.1.2. Carcinoma sites in breast.
Most often breast cancer has only one location in a single breast, almost half of which originate in the upper and outer quadrant of the breast. Though breast cancer has the potential to spread to other regions of the body first, it most commonly spreads first to the axillary (underarm) lymph nodes. This is known as regional spread. From there, the breast cancer can metastasize (spread) systematically to other areas of the body (such as the bone, liver, lung, or brain). Ductal carcinomas comprise about 85% of breast tumors and originate from the epithelium of the mammary ducts. The remaining are mainly lobular carcinomas, which arise from the mammary lobules. (www.MyBreastCancerNetwork.com).

Table 1.1.1. Breast cancer morphological taxonomy.
Freely adapted from www.immunerecovery.net, www.healthcentral.com, and [5].

Subtypes		Brief description
LCIS	Lobular Carcinoma *in Situ*	These are abnormal cells that pose a long-term risk for invasive cancer. LCIS is NOT cancer. But it is a sign that the woman is 6 to 7 times more likely to develop cancer during the course of her lifetime than a woman who does not have LCIS: the same risk one would be at if the mother and a sister both had cancer. Though these lesions are low grade, there is a 30% risk for development of invasive carcinoma in the same or the opposite breast.
DCIS	Ductal Carcinoma *in Situ*	These are cancer cells in the lining of a duct that have not invaded the surrounding breast tissue. DCIS is in 98 to 99 percent curable. It refers to breast cancer that is located in the breast's milk ducts, the tiny tubes that bring milk from where it is manufactured (in the lobules) to the nipple.
ILC	Infiltrating/ Invasive Lobular Cancer	ILC occurs in the milk-producing lobules. While most breast cancers occur in the ducts, just 12% occur in the lobules. Lack of a palpable lump is one aspect of lobular cancer distinguishing it from ductal. The invasive form is frequently diffuse and usually shows multiple sites in the breast. In most cases where both breasts are involved, a phenomena that often occurs in hereditary breast cancer, it is lobular carcinoma.
IDC	Invasive/ Infiltrating Ductal Carcinoma	IDC is the most common type of breast cancer; 70% of women with breast cancer have this diagnosis. Moreover, 80% of the women with invasive breast cancer have IDC.
RBC	Recurrent Breast Cancer	RBC is a cancer that progresses during treatment or recurs after a remission. RBC is generally more serious than a new breast cancer, as it indicates the cancer was not eradicated by the initial treatment, and thus is inherently a "tougher" cancer.
IBC	Inflammatory Breast Cancer	IBC accounts for fewer than 5% of new breast cancers. Unlike most breast cancer, it does not start with a lump, but with a diffuse infiltration.
MC	Medullary Carcinomas	Medullary carcinomas are a special class of ductal carcinoma found more frequently in young patients and likely associated with a family history. The cells are better differentiated and the tumor is often large and soft to palpation. Ironically, with this larger tumor, the prognosis is better than with invasive ductal carcinoma. Medullary carcinoma is less invasive [6].
CIT	Colloidal Intraductal Tumors	Colloidal intraductal tumors (mucinous tumors) are large, gelatin like masses and usually develop in older women; they are slow growing and have a more favorable prognosis.
Others	Papillary, comedo, tubular carcinomas and phyllodes tumors	Papillary and comedo carcinomas are other types of intraductal carcinomas. In tubular carcinoma the neoplastic cells form a single cuboidal layer in small round to teardrop shaped ductules widely spaced in a fibrous stroma. Phyllodes tumors are rare fibroepithelial tumors of the breast.

1.2 Breast cancer staging and grading

Breast cancer is a heterogeneous disease which encompasses several entities with distinct prognosis. Although a comprehensive breast cancer morphological taxonomy has been developed and usefully applied to patient management (see also table 1.1.1), it has become clear that tumors classified under the same descriptive term may have distinct underlying biological features and clinical behavior [7]. Therefore, in addition to histological typing, breast cancer is characterized by stage, grade and molecular markers.

Breast cancer staging

Staging of breast cancer refers to determination of size and location of the disease. There are currently two staging classifications in use: a breast cancer staging system that divides breast cancers in 5 stages for most sites, including a stage 0 for non invasive carcinoma *in situ*, and the more elaborate tumor node metastases (TNM) system. In the latter system, T describes the size of the tumor, N describes whether the cancer has spread to the lymph nodes, and M describes whether the cancer has spread to another part of the body, such as the bone, liver or the lung. In table 1.2.1 the most common breast cancer stages are described. As depicted in figure 1.2.1, especially metastatic disease is associated with a very poor overall survival, thus showing the importance of being able to stage breast cancers and stressing the urgent need for early detection and tumor-specific treatment modalities.

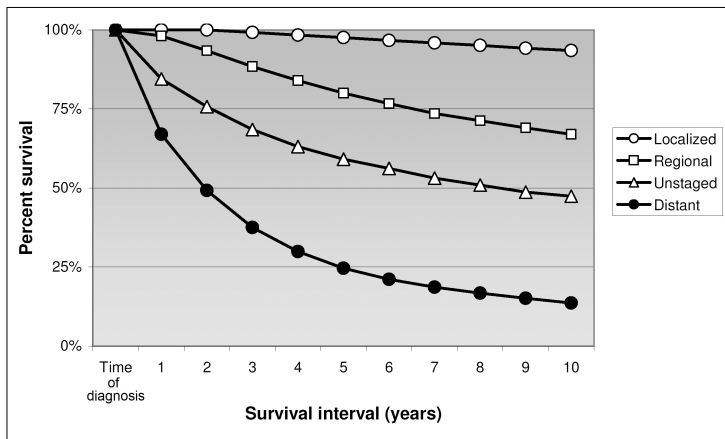*Figure 1.2.1. Relative survival rates for breast cancer in females by stage at diagnosis.*
This graph of breast cancer survival after diagnosis shows a steeply declining survival rate in time, especially for the patients with a distant metastasis.
(Complied from Surveillance, Epidemiology, and End Results (SEER) 9 registries for 1988-2003, based on the November 2006 submission: www.seer.cancer.gov).

Table 1.2.1. Breast cancer staging taxonomy.
Freely adapted from www.immunerecovery.net and www.healthcentral.com (review date: 03/14/2007. Reviewed by: Editorial Team: Greg Juhn, David R. Eltz, Kelli A. Stacy. Previously reviewed by Harvey Simon, M.D., Associate Professor of Medicine, Harvard Medical School; Physician, Massachusetts General Hospital (10/2/2006).

Stage	Brief description and clinical implications
0	Non invasive carcinoma; carcinoma *in situ*; LCIS and DCIS.
I	Localized. No spreading beyond the breast and the tumor diameter is no more than 2 cm across.
II	Regional. The tumor is less than 2 cm across, and the cancer has spread to the lymph nodes under the arm, or the tumor is between 2 and 5 cm with or without spreading to the lymph nodes under the arm, or the tumor is larger than 5 cm but has not spread to the lymph nodes under the arm.
III	Regional. Locally advanced. In this stage, the tumor in the breast is more than 5 cm across, and: - it has spread to the underarm lymph nodes. - it has spread to other lymph nodes or tissues near the breast. Inflammatory breast cancer is also treated as a Stage III cancer. Recurrent breast cancer is considered to be an advanced cancer.
IV	Metastasized cancer; advanced cancer. The cancer has spread from the breast to other parts of the body. In about 75% of cases with metastasis, the cancer has spread to the bone. The cancer at this stage is considered to be chronic and incurable, and the usefulness of treatments is, although improving, still limited. The goals of treatment for Stage IV are a complete or partial response, stabilization of the disease, or slowing disease progression resulting in prolonged survival.

TNM Stage	Brief description
T0	When there is no evidence of a primary tumor.
Tis	Non invasive carcinoma; carcinoma *in situ*; LCIS and DCIS.
T1 to T3	In case of carcinoma of the breast, the designations T1 through T3 are used to describe tumors of increasing size ($\leq$ 2 cm, 2- $\leq$5 cm, and > 5 cm).
T4	Advanced lesions of any size, including those with direct extension to the chest wall or skin.
TX	Whenever the primary tumor cannot be assessed.
N0	No nodal involvement.
N1	Axillary nodal involvement.
N2	Axillary nodal involvement with nodes extended to one another or nearby structures.
N3	Subclavicular nodal involvement or edema of arm caused by lymphatic obstruction.
M0	No metastasis present.
M1	Metastasis present.
MX	Presence of distant metastases cannot be assessed.

Breast cancer grading

While staging of breast cancer refers to determining the size and location of the disease, grading of breast cancer is a term used to describe how closely a tumor resembles normal tissue and gives an idea of how quickly the cancer may develop. Based on the histological appearance as assigned by the pathologist, there are three grades: grade 1 (low-grade), grade 2 (moderate or intermediate grade) and grade 3 (high-grade). Low-grade means that the cancer cells look very like the normal, well-differentiated, cells of the breast. They are usually slow growing and are less likely to spread. In high-grade tumors the cells are poorly differentiated and look very abnormal. They will probably grow more quickly and are more likely to spread.

Other more advanced methods to characterize tumors according established clinical and pathological criteria are based on guidelines such as the St Gallen [8, 9] and the National Institute of Health consensus [10], or by making use of specific prognostic tools such as the Nottingham Prognostic Index (NPI) [11] or Adjuvant-Online algorithm (www.adjuvant-online. com).

Molecular breast cancer markers

Another way of grading primary breast tumors to estimate the risk of cancer progression in aiding the clinician to construct a patient tailored therapy is to make use of molecular profiling and genomic grading indices. Microarray based molecular classification of breast tumors or selection of gene expression panels to improve prediction of risks or treatment outcomes are thought to be theoretically superior to established clinical and pathological criteria, based on guidelines such as the St Gallen and National Institute of Health consensus, or guidelines which use specific prognostic tools, such as the Nottingham Prognostic Index or Adjuvant-Online algorithm [12]. The first well known studies in this field, aimed at classifying breast carcinomas based on gene expression patterns, are those of Perou and Sorlie [13-16]. According these studies, breast carcinomas can now, based on patterns of expression of 496 "intrinsic" genes, be distinguished in tumor subclasses with distinct clinical implications:

1.   Luminal-epithelial group (with sub-classification into types A, B and C), characterized by expression of the estrogen receptor and genes associated with the estrogenic function, *i.e.*, genes that are typically expressed in the luminal epithelium that lines the ducts.
2.   Basal-epithelial group, typically negative for the estrogen and progesterone receptors as well as the ERBB2 (Her2/neu) oncogene ("triple negative").
3.   ERBB2+ group associated with overexpression of the ERBB2 amplicon.
4.   Normal breast-like group.

At the same time, the Genomic Grade Index (GGI), capturing 97 differentially expressed genes, can be used to reclassify patients with histologic grade 2 tumors into two groups with high versus low risks of recurrence [17, 18].

But with respect to implementing microarray data much debate is going on in the field with most clinicians still being more comfortable with the classical ways of grading tumors [12, 18-28].

1.3 The tumor micro-environment

Human breast carcinomas arise via intermediate steps known as precursor or premalignant lesions (see figure 1.3.1). Because the most malignant aspect of abnormal proliferation (*i.e.* neoplasia) is metastasis, recognition of metastatic phenotypes is particularly important [29].

As proposed by Hanahan and Weinberg in 2000 [30], the vast catalogue of cancer cell types can be seen as a manifestation of six essential alterations in cell physiology that dictate malignant growth, collectively called the 'Hallmarks of cancer':

-           self-sufficiency in growth signals;
-           insensitivity to growth-inhibitory signals;
-           evasion of programmed cell death (apoptosis);
-           limitless replicative potential;
-           sustained growth of new blood vessels (angiogenesis);
-           tissue invasion and metastasis.
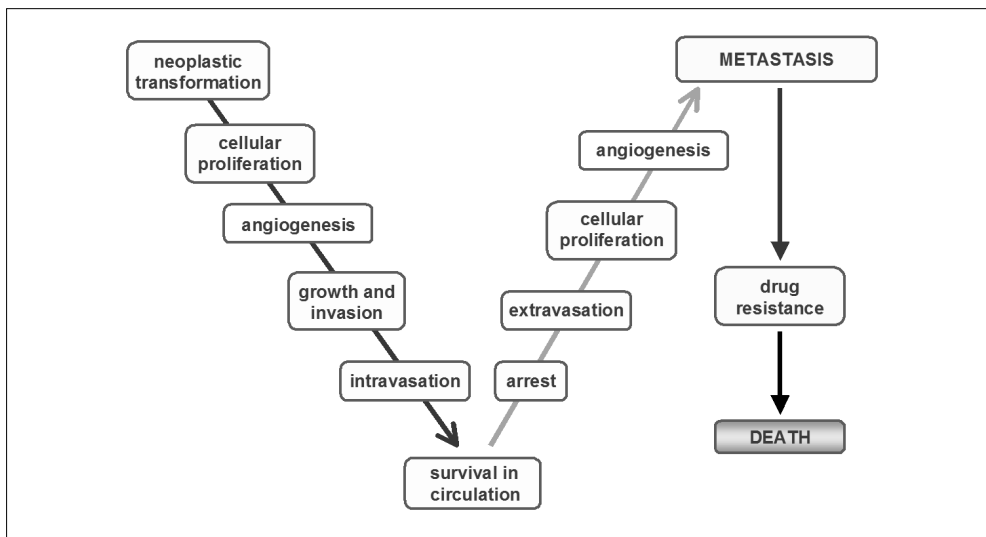
Figure 1.3.1. Steps in tumor progression.
After neoplastic transformation, cells start proliferating abnormally. Formation of new blood vessels supports the growth and invasion of the tumor cells in the extracellular matrix. Cells able to enter and survive in the vasculature may extravasate and form a metastatic lesion. The purpose of molecular breast cancer markers is to recognize and characterize the steps involved in tumor progression.

The players in the tumor micro-environment, *i.e.* the area in which the tumor cells are nested, are multiple, and each of them may contribute to these hallmarks of cancer. For example the stroma or the supportive platform for the epithelial layer, which accounts for more than 80% of the normal breast volume [31], is composed of fibroblasts, endothelial cells, smooth muscle cells, adipocytes, inflammatory cells, nerve cells and a macromolecular network of proteoglycans and glycoproteins collectively termed the extracellular matrix (ECM). Figure 1.3.2 gives two typical examples of hematoxylin-eosin (HE) stained breast tumor sections; one section with predominantly epithelial cancer cells and one section where the epithelial cancer cells are nested in a network of stromal cells.

Figure 1.3.2. Examples of hematoxylin-eosin (HE) stained breast tumor sections.
In the left panel a breast cancer that predominantly consists of epithelial cancer cells (visualized by the darker stained nuclei). In the right panel an example of a breast cancer where the epithelial cancer cells are nested in a network of stromal cells.

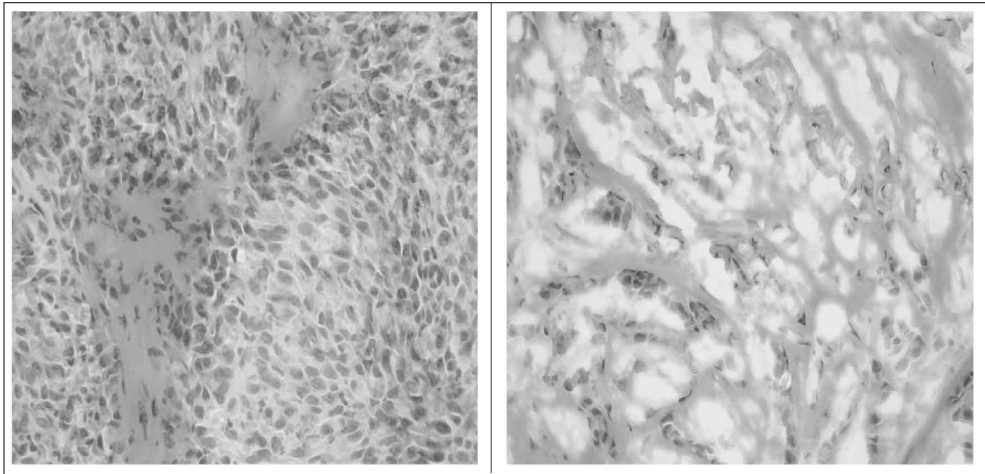There is now an increasing insight that signals provided by the stroma can induce the genetic alterations that underlie tumor formation, can stimulate tumor growth and progression, and can dictate both therapeutic response and ultimate clinical outcome [32-40]. *In vitro* research results, including those of our own group [41-51], and *in vivo* results [52-54] make it clear that non-neoplastic stromal cells, notably the stromal (myo)fibroblast cells of carcinomas, are indeed active participants in promoting growth, invasion and metastasis of tumors. Observations of specific genetic alterations in exclusively the stromal cells present in the tumor environment [55, 56] even extend this heterotypic interplay concept to the stroma being responsible for tumor formation and maintenance.

In addition to the microarray grading signatures mentioned previously, three grading signatures that focus on the stromal micro-environment of the epithelial tumor cells have been described. Firstly, a grading based on characteristic genes found in five cancer tissue categories (epithelial cells, leucocytes, myoepithelium/myofibroblasts, endothelium and stroma) [52]. Secondly, a signature based on differences between 2 types of fibroblastic tumors: desmoid-type fibromatosis (DTF) and solitary fibrous tumors (SFT) [53]. Thirdly, a signature based on gene expression profiles of fibroblasts from ten anatomic sites [57]. In the latter, a stereotyped gene expression program was identified in response to serum exposure that appeared to reflect the multifaceted role of fibroblasts in wound healing. Genes induced in the fibroblast serum-response program are expressed in tumors by the tumor cells themselves, by tumor-associated fibroblasts, or both. These stromal signatures capturing the reciprocal interactions between mesenchymal and epithelial cells might also be considered a way of grading tumors with distinct clinical features [54, 57].

Therefore cancer should be seen as a multicellular program in which the tumor cells themselves, the tumor-associated fibroblasts, and diverse other cells in the tumor micro-environment are active participants [57-60].

1.4 Prognostic and predictive markers

It is important for this thesis to understand the difference between a prognostic and a predictive marker. A prognostic marker predicts disease recurrence or tumor progression, independently of future treatment effects. A predictive biomarker predicts response or resistance to a specific cancer therapy. Any change in disease status during treatment should be reflected by a change in the marker status [61]. Prognostic factors, *e.g.*, metastatic disease, lymph node status, tumor size, histologic grade, proliferation rate, ERBB2, hormone receptors and other biological markers are used to predict the clinical course of breast cancer at the time of primary treatment. Patients with a poor prognosis are offered radiotherapy and systemic adjuvant therapy *i.e.*, endocrine, cytotoxic or biological anticancer therapy following primary surgery for early stage cancer that affects the entire body. Prediction refers to the likelihood of outcome in response to a specific therapy. For the choice of (systemic) adjuvant therapy information about prognostic and predictive factors such as size and shape of the tumor, location of the tumor, proliferation rate and biological markers are useful.

Biomarkers in breast cancer for diagnostics, prognosis and targeted therapies

A biological marker is an indicator or characteristic trait of a disease that facilitates differential diagnosis (the process of distinguishing one disorder from other, similar disorders). Biomarkers are biological substances normally present in small amounts in tumor tissues or body fluids and encompass a wide variety of molecules, including transcription factors, cell surface receptors, and secreted proteins. These are measured in the management of breast cancer patients for the following purposes: (1) early detection, (2) monitoring of advanced breast cancer patients, (3) prediction of disease recurrence or tumor progression, and (4) prediction of therapeutic response. In general, biomarkers can be divided in circulating biomarkers that are detected in body fluids and markers detected in tumor tissue, with one new class of biomarkers, the circulating tumor cells, bridging the two. Examples of established breast biomarkers are the serum-based cancer antigens CA 15-3, CA 125, CA 27-29 and carcinoembryonic antigen (CEA), and the tissue-based estrogen and progesterone hormone receptors, markers measuring DNA-ploidy/ content and/or proliferation, the oncogene ERBB2, the tumor suppressor gene p53, and the protease urokinase plasminogen activator (uPA) and its inhibitor plasminogen activator inhibitor 1 (PAI-1) [3, 9, 62, 63].

An example of a new (class of) biomarker(s) that require further prospective validation is represented by the gene expression profiles [9] that classify breast tumors into histological subtypes [18, 23, 26, 28, 52, 53, 64-67], subgroups with different prognosis [26, 54, 57, 68-78], different sites of relapse [79-81], and different types of response to treatment [82-101]. To evaluate the usefulness of a new biomarker to monitor disease progression, correlation of levels of the marker with tumor size, disease-free, metastasis-free, progression-free, and (post-relapse) overall survival are taken into consideration. Thus a biological prognostic marker refers to a marker that correlates with disease-free, metastasis-free and overall survival; the term predictive marker indicates a marker that is capable of predicting tumor sensitivity or resistance to various therapies. But markers may be applicable to both scenarios. Estrogen receptors for example are weak prognostic indicators and good predictors of response to endocrine therapy. On the other hand, markers measuring proliferation indices are good indicators of prognosis, and, in addition, may directly be related to response to chemotherapy and are closely related to response to endocrine therapy [102]. Ultimately, a useful clinical marker is one that meets two criteria: it can be measured reproducibly by means of a reliable and widely available assay and it conveys information about the disease that is meaningful to the physician and patient.

The tumor marker utility grading system (TMUGS)

As the field of tumor associated biomarkers has rapidly expanded over the last two decades with a concomitant increase in published reports, it has become increasingly apparent that a strong need exists to establish consensus guidelines for the development and use of established as well as novel tumor associated markers [61]. For this purpose, the TMUGS has been introduced as a framework tool consisting of two parts: one part to classify the tumor markers and another part to evaluate the clinical utility of the tumor markers [103].

In the first part the precise characteristics of the marker is clarified. These characteristics include the marker designation, the molecule and/or substance and the relevant alteration from normalcy, the assay format and reagents, the specimen type, and the neoplastic disease for which the marker is being evaluated. In the second part the clinical utility of the marker is evaluated and scaled with respect to risk assessment, screening, differential diagnosis, prognosis with respect to prediction of relapse/ progression, prognosis with respect to response to therapy, and monitoring clinical course. Finally, to define the quality of data that exist, the marker is scaled by placing the available data into one or several levels of evidence (LOE-5 to LOE-1) (table 1.4.1).

Although it seems cumbersome at first, application of this system by expert reviewers should help to separate those markers for which clinical utility clearly exists from those markers for which either more data are necessary or for which further consideration can be discarded [104].

Table 1.4.1. Tumor marker utility grading system to classify the level of evidence of tumor associated biomarker studies.*

Level of evidence (LOE)	Type of evidence
1	Evidence derived from a prospective high-powered clinical trial specifically addressing tumor marker utility or overview or meta (pooled) analysis of lower LOE studies.
2	Evidence from tumor specimens which were collected prospectively and tumor marker utility determined as secondary aim of study in order to get ready for a large clinical trial.
3	Evidence from larger retrospective trials.
4	Evidence from small retrospective studies.
5	Evidence from small pilot studies designed to determine or estimate distribution of tumor biomarker levels in a sample population.

*Schmitt *et al* [61], modified from Hayes *et al* [103].

1.5 Available techniques to study biomarkers in the genomics era

The techniques to search for new biomarkers, to validate their usefulness, and assign biological functions has made great progress in this computerized era of proteomics to study proteins and genomics to study genes. In the last three decades, techniques for the evaluation of gene expression have progressed from methods developed for the analysis of single, specific genes (*e.g.*, Northern, slot, and dot blotting; semi-quantitative and quantitative reverse transcription and PCR; and nuclease protection assays) to gene expression profiling techniques focused on identifying all genes that differ in expression or sequence between or among experimental samples (*e.g.*, subtractive hybridization, differential display, sequencing of expressed sequence tags, serial analysis of gene expression, and hybridization to microarrays). With the vast amount of data generated in these experiments, specialized programs are required to interpret the statistical significance and biological meaning from these data. Pathway analysis is one hot-topic method to find relationships among genes, cell processes and diseases.

The following summary merely serves to give a brief overview of the currently widely used methods. Because this thesis is mainly focused on quantifying gene expression by real-time reverse transcriptase polymerase chain reaction (real-time RT-PCR or qRT-PCR), special emphasis will be put on this technique, its basic principle, the potentials and the limitations.

Gene expression profiling

There are two main applications of gene expression profiling; studies unravelling novel breast cancer classifications and those that aim to identify novel markers for prediction of clinical outcome [20]. Gene expression profiling has for example been applied to classify breast tumors into histological subtypes [18, 23, 26, 52, 53, 64-67], into subgroups with different prognosis [57, 68-78], different sites of relapse [79-81, 105], and different types of response to treatment [54, 82-101]. Note however that gene expression levels cannot always be compared with protein levels. Regulatory mechanisms affecting protein concentrations, activity, and stability can act at the level of DNA and mRNA translation, protein folding, glycosylation, phosphorylation, and (proteosomal) protein degradation. Since it is only the actual protein that is biologically active, a sensitive, protein-based, method is important to determine the actual biological activity of a marker that has been discovered by gene analysis. While the great advantage of identifying a large set of differentially expressed genes between or among experimental samples simultaneously (gene expression profiling) is simply the large number of genes that are analyzed simultaneously, especially low expressed tags might be adversely biased and validation at the single gene level by real-time RT-PCR remains essential.

Real-time PCR method

Real-time PCR is a method that enables detection of sequence-specific PCR gene products as they accumulate in "real-time" during the PCR amplification process. For an example see figure 1.5.1. When the PCR product of interest is produced during cycling (x-axis), real-time PCR can detect their accumulation (y-axis) and quantify the number of gene copies present in the initial PCR mixture before amplification began. With special algorithms the number of copies can be calculated. Real-time PCR can be applied on genomic DNA sequences or on copy DNA (cDNA) generated from mRNA after a reverse transcriptase (RT) reaction.The main differences between the variations in the procedure are found in the fluorophores or dyes to detect the levels. The most sensitive, least expensive, but also least specific method makes use of double-stranded (ds) DNA dyes such as SYBR Green. The lack of specificity is due to the fact that dsDNA dyes will bind all dsDNA PCR products, including nonspecific products such as primer dimers (when two primers used to set up the PCR reaction hybridize). Using fluorescent reporter probes is the most accurate and most reliable method, but also the most expensive
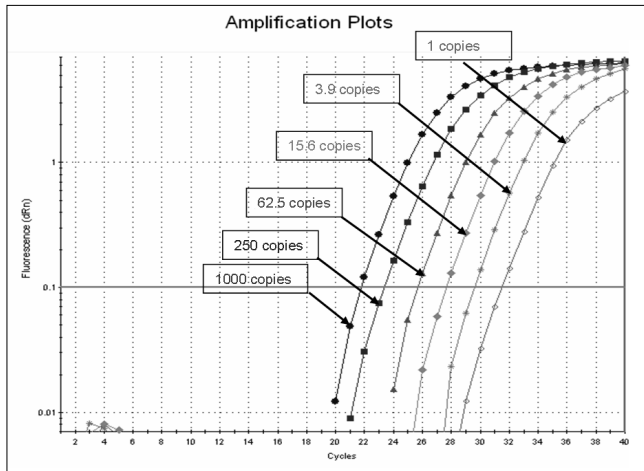
Figure 1.5.1.
Real-time PCR amplification plot.

one. It uses a sequence-specific RNA or DNA-based probe to quantify only the sequence in the gene of interest matching the probe sequence; thus, use of this probe-based method significantly increases specificity, and allows quantification even in the presence of some non-specific DNA amplification. If the necessary precautions are taken, this method potentially allows for multiplexing (assaying for several genes in the same reaction) by using specific probes with different-colored labels.

Quantitation of PCR products

Relative concentrations of PCR products present during the exponential phase of the reaction are determined by plotting fluorescence against cycle number on a logarithmic scale (see figure 1.5.1). A threshold for detection of fluorescence above background is determined. The cycle at which the fluorescence from a sample crosses the threshold (solid horizontal line in figure 1.5.1) is called the cycle threshold, Ct. Since the quantity of PCR product doubles every cycle during the exponential phase, relative amounts of PCR products can be calculated, *e.g.*, a sample whose Ct is 3 cycles earlier than another sample had $2^3 = 8$ times more initial gene copies. The number of (m)RNA or DNA copies are then determined by comparing the results to a standard curve produced by RT-PCR of serial dilutions of a known amount of (m)RNA or DNA copies.

To accurately quantify gene expression, the measured amount of RNA from the gene of interest is divided by the amount of RNA from a reference (housekeeping) gene measured in the same sample to normalize for possible variation in the amount and quality of RNA between different samples. This normalization permits accurate comparison of expression of the gene of interest between different samples, provided that the expression of the reference gene used in the normalization is very similar across all the samples. Choosing a reference gene or set of genes fulfilling this criterion is therefore of high importance, and often challenging, because only very few genes show equal levels of expression across a range of different conditions or tissues [106-110].

Pathway analysis

As described above, microarray technology has successfully classified breast tumors into histological subtypes [18, 23, 26, 52, 53, 64-67], subgroups with different prognosis [57, 68-78], different sites of relapse [79-81, 105], and different types of response to treatment [54, 82-101]. However, it soon became clear that various gene signatures identified for classifying patients with different subtypes of breast cancer or with different prognosis had few genes overlapping [75, 111, 112]. This could be due

to the fact that many genes function in the same biological pathway. Therefore, to place potential suitable biomarkers in a biological context, the biological pathways rather than individual genes related to patient outcomes should be investigated [112-116].

1.6 Tumor tissue, DNA, RNA, and protein bank

A shortage of high-quality human tumor samples might very well be the top barrier to progress in cancer research. With scientists pinning their hopes for new diagnostics and cures on molecular biomarkers, they need access to human tissue samples from large numbers of people. For this, biobanks with stored tissues, body fluids and related products such as DNA, RNA and protein lysates are essential. A biobank allows formal accreditation of ethics and security procedures, and through a dedicated management, processing, storage, retrieval, and release structure, can provide selected and preassembled material and data for research and discovery [117, 118]. Clinical pathology archives are usually extensive but comprise mostly formalin-fixed paraffin-embedded (FFPE) tissue blocks. Although recent progress has been made with tumor RNA and DNA analysis in FFPE tissue, the RNA and DNA fragmentation and chemical modifications that occur with formalin fixation remain significant barriers to biomarker research. In addition, although FFPE tissue microarrays can be very suitable for immunological staining, various specific approaches such as those aimed at protein modifications and mass spectrometry are difficult to apply to formalin-fixed tissue [119]. Therefore the main request for clinical specimens for biomarker research involves fresh frozen tissue.

Power of the Rotterdam fresh frozen breast tissue bank for 'omics' research

The opportunity to collect fresh frozen tumor tissue that is suitable for studies on extracted DNA, RNA and protein has been further reduced by early diagnosis, reduction in surgical extent, and trends towards preoperative therapies. For ethical reasons, trials of therapy in patients with breast cancer no longer include an untreated control group. Therefore, retrospective studies involving well-characterized tumor banks with tumors from untreated patients are necessary to determine whether putative biomarkers are pure prognostic markers in stead of a predictor for the benefits of systemic therapy. One such well characterized fresh frozen tissue bank has been established by the department of Medical Oncology, Erasmus Medical Center, Rotterdam, The Netherlands.

This fresh frozen breast tumor tissue bank currently contains over 14,000 samples stored in liquid nitrogen since 1978. Of 5,500 patients a computerized database with updated clinical follow-up is available. In addition, information on high quality extracts of DNA from 3,000 tissues, RNA from 2,000 tissues, and protein from over 10,000 tissues are stored in accompanying computerized databases. Because of the uniqueness of this bank, these resources are also extensively used in collaborative studies with other European and American research groups [18, 75, 80, 81, 94, 120-124], to name only the 2005-2007 publications that resulted from such collaborative studies. Figure 1 in chapter 6 of this thesis gives a detailed overview of the RNA collection stored in this bank with sufficient clinical follow-up for reliable statistical analyses [125]. These RNA samples were the very important source of clinical samples for the studies included in this thesis [50, 51, 112, 123, 125].

1.7 Aims and outline of this thesis

The aims of this thesis are firstly to gain insight into the interaction between breast tumor cells and the surrounding stromal fibroblasts. Secondly, this concept of a multi-cellular program in which the tumor cells, the tumor-associated fibroblasts, and diverse other cells in the tumor micro-environment are active participants, is integrated in our search for novel prognostic and predictive biomarkers. Finally, the concept of biomarkers is placed in a larger context by looking at pathways rather then individual biomarkers. In summary, the more specific subjects discussed in this thesis are: 1) studies on the

interaction between different biological systems, 2) studies on prognosis, and 3) studies on prediction to tamoxifen therapy response.

In **chapter 2** the role of peri-tumoral fibroblasts in relation to the expression of components of the plasminogen activator (PA) system and the insulin-like growth factor (IGF) system in normal and tumor-tissue-derived human breast fibroblasts exposed to various fibroblast growth factors (FGFs) is discussed [48]. The *in vitro* data presented propose that of the FGFs studied (FGF-1, -2, -4, -5, and -7), FGF-2 is the most attractive target for therapeutical strategies aimed at diminishing the contribution of stromal fibroblasts in the PA-directed breast tumor proteolysis.

With our aging population, especially the age-related increase in breast cancer incidence should worry us. In **chapter 3** the role of peri-tumoral fibroblasts is investigated in relation to this important aspect [49]. For this, we investigated whether breast fibroblasts aged *in vitro* through passage in culture display altered levels of the PA system and growth factors that are known to modulate that system. Our results show that aging accompanied by telomere loss induces *PAI-1* and *FGF-1* mRNA expression in all breast fibroblast strains, increases *uPA* and decreases *IGF-1* mRNA expression in a subset, and increases MMP-2 protein expression only in tumor-derived breast fibroblasts. Thus, the age-induced levels of these biomarkers in stromal breast fibroblasts could contribute to breast cancer progression.

In **chapter 4** the multi-cellular notion is experienced in the clinical setting. In this chapter we evaluated the predictive value of the disintegrin and metalloproteinases, ADAM-9, ADAM-10, ADAM-11, and ADAM-12, and of the matrix metalloproteinases, MMP-2 and MMP-9, in patients with recurrent breast cancer treated with tamoxifen [50]. The data will show that especially for primary tumors containing a high proportion of stromal elements, the assessment of mRNA expression levels of *ADAM-9* and *ADAM-11* could be useful to identify patients with recurrent breast cancer who are likely to benefit or fail from tamoxifen therapy.

One of the applications of real-time RT-PCR is validation of putative biomarkers that emerge from microarray experiments in a larger patient cohort. One such biomarker is cyclin E2 (*CCNE2*), a gene that overlaps between our 76-gene prognostic signature [75] and the 70-gene prognostic signature [70]. In **chapter 5** we describe the prognostic evaluation of cyclin E with this quantitative method in a large cohort of 635 lymph node-negative (LNN) breast cancer patients that did not receive systemic adjuvant therapy [51]. The study shows that both *CCNE1* and *CCNE2* qualify as independent prognostic markers for LNN breast cancer patients, and that *CCNE1* may provide additional information for specific subgroups of patients with stroma-enriched primary tumors.

Another validation study, discussed in **chapter 6**, concerns the *HOXB13*-to-*IL17BR* expression ratio that was previously identified to predict clinical outcome of breast cancer patients treated with adjuvant tamoxifen [125]. In this study we demonstrate that, in addition to tamoxifen therapy failure (prediction), high *HOXB13*-to-*IL17BR* ratio expression levels also associate with tumor aggressiveness (prognosis).

Having discovered and identified two alternatively spliced variants of *TIMP1* mRNA in cancer cell lines and colon cancer tissue [126] (**chapter 7**), the prognostic value of these variants were tested in 1301 primary breast specimens [123] (**chapter 8**). Comparing *TIMP1* mRNA and protein levels revealed that concentrations of *TIMP1* mRNA and one of its splice variants and TIMP-1 protein were differentially associated with prognosis in primary breast cancer. It is discussed how such a differential association might help our understanding of the role of TIMP-1 with respect to breast cancer progression.

As shown in chapter 5, published prognostic gene signatures in breast cancer have few genes in common. In **chapter 9** a rationale for this observation is provided by studying the prognostic power and the underlying biological pathways of different gene signatures [112].

REFERENCES

1. Ravdin PM, Cronin KA, Howlader N, Berg CD, Chlebowski RT, Feuer EJ, Edwards BK, Berry DA. The decrease in breast-cancer incidence in 2003 in the United States. N Engl J Med 2007;356:1670-4.

2. McPherson K, Steel CM, Dixon JM. ABC of breast diseases. Breast cancer-epidemiology, risk factors, and genetics. BMJ 2000;321:624-8.

3. Klijn JGM, Berns EMJJ, Foekens JA. Prognostic and predictive factors and targets for therapy in breast cancer. In: Breast cancer: prognosis, treatment and prevention. (J.R. Pasqualini, ed), Marcel Dekker Inc., New York 2002:79-90.

4. Weinberg RA. The biology of cancer. Garland Science Publishing, London, UK:2007.

5. van de Vijver MJ. The pathology of familial breast cancer: The pre-BRCA1/BRCA2 era: historical perspectives. Breast Cancer Res 1999;1:27-30.

6. Eichhorn JH. Medullary carcinoma, provocative now as then. Semin Diagn Pathol 2004;21:65-73.

7. Reis-Filho JS, Westbury C, Pierga JY. The impact of expression profiling on prognostic and predictive testing in breast cancer. J Clin Pathol 2006;59:225-231.

8. Goldhirsch A, Wood WC, Gelber RD, Coates AS, Thurlimann B, Senn HJ. Meeting highlights: updated international expert consensus on the primary therapy of early breast cancer. J Clin Oncol 2003;21:3357-65.

9. Goldhirsch A, Glick JH, Gelber RD, Coates AS, Thurlimann B, Senn HJ. Meeting highlights: international expert consensus on the primary therapy of early breast cancer 2005. Ann Oncol 2005;16:1569-83.

10. Eifel P, Axelson JA, Costa J, Crowley J, Curran WJ, Jr., Deshler A, Fulton S, Hendricks CB, Kemeny M, Kornblith AB, Louis TA, Markman M, Mayer R, Roter D. National Institutes of Health Consensus Development Conference Statement: adjuvant therapy for breast cancer, November 1-3, 2000. J Natl Cancer Inst 2001; 93:979-89.

11. Blamey RW, Ellis IO, Pinder SE, Lee AH, Macmillan RD, Morgan DA, Robertson JF, Mitchell MJ, Ball GR, Haybittle JL, Elston CW. Survival of invasive breast cancer according to the Nottingham Prognostic Index in cases diagnosed in 1990-1999. Eur J Cancer 2007;43:1548-55.

12. Modlich O, Prisack HB, Bojar H. Breast cancer expression profiling: the impact of microarray testing on clinical decision making. Expert Opin Pharmacother 2006;7:2069-78.

13. Perou CM, Sorlie T, Eisen MB, van de Rijn M, Jeffrey SS, Rees CA, Pollack JR, Ross DT, Johnsen H, Akslen LA, Fluge O, Pergamenschikov A, Williams C, Zhu SX, Lonning PE, Borresen-Dale AL, Brown PO, Botstein D. Molecular portraits of human breast tumours. Nature 2000;406:747-52.

14. Sorlie T, Perou CM, Tibshirani R, Aas T, Geisler S, Johnsen H, Hastie T, Eisen MB, van de Rijn M, Jeffrey SS, Thorsen T, Quist H, Matese JC, Brown PO, Botstein D, Eystein Lonning P, Borresen-Dale AL. Gene expression patterns of breast carcinomas distinguish tumor subclasses with clinical implications. Proc Natl Acad Sci U S A 2001;98:10869-74.

15. Sorlie T, Tibshirani R, Parker J, Hastie T, Marron JS, Nobel A, Deng S, Johnsen H, Pesich R, Geisler S, Demeter J, Perou CM, Lonning PE, Brown PO, Borresen-Dale AL, Botstein D. Repeated observation of breast tumor subtypes in independent gene expression data sets. Proc Natl Acad Sci U S A 2003;100:8418-23.

16. Sorlie T, Perou CM, Fan C, Geisler S, Aas T, Nobel A, Anker G, Akslen LA, Botstein D, Borresen-Dale AL, Lonning PE. Gene expression profiles do not consistently predict the clinical treatment response in locally advanced breast cancer. Mol Cancer Ther 2006; 5:2914-8.

17. Sotiriou C, Wirapati P, Loi S, Harris A, Fox S, Smeds J, Nordgren H, Farmer P, Praz V, Haibe-Kains B, Desmedt C, Larsimont D, Cardoso F, Peterse H, Nuyten D, Buyse M, Van de Vijver MJ, Bergh J, Piccart M, Delorenzi M. Gene expression profiling in breast cancer: understanding the molecular basis of histologic grade to improve prognosis. J Natl Cancer Inst 2006;98:262-72.

18. Loi S, Haibe-Kains B, Desmedt C, Lallemand F, Tutt AM, Gillet C, Ellis P, Harris A, Bergh J, Foekens JA, Klijn JG, Larsimont D, Buyse M, Bontempi G, Delorenzi M, Piccart MJ, Sotiriou C. Definition of clinically distinct molecular subtypes in estrogen receptor-positive breast carcinomas through genomic grade. J Clin Oncol 2007;25:1239-46.

19. Carr KM, Rosenblatt K, Petricoin EF, Liotta LA. Genomic and proteomic approaches for studying human cancer: prospects for true patient-tailored therapy. Hum Genomics 2004;1:134-40.

20. Brenton JD, Carey LA, Ahmed AA, Caldas C. Molecular classification and molecular forecasting of breast cancer: ready for clinical application? J Clin Oncol 2005;23:7350-60.

21. Paik S. Molecular profiling of breast cancer. Curr Opin Obstet Gynecol 2006;18:59-63.

22. Ioannidis JP. Is molecular profiling ready for use in clinical decision making? Oncologist 2007;12:301-11.

23. Loi S, Piccart M, Sotiriou C. The use of gene-expression profiling to better understand the clinical heterogeneity of estrogen receptor positive breast cancers and tamoxifen response. Crit Rev Oncol Hematol 2007;61: 187-94.

24. Pusztai L, Cristofanilli M, Paik S. New generation of molecular prognostic and predictive tests for breast cancer. Semin Oncol 2007;34:S10-6.

25. Symmans WF. A pathologist's perspective on emerging genomic tests for breast cancer. Semin Oncol 2007;34: S4-9.

26. Yoder BJ, Wilkinson EJ, Massoll NA. Molecular and morphologic distinctions between infiltrating ductal and lobular carcinoma of the breast. Breast J 2007;13:172-9.

27. Sorlie T. Molecular classification of breast tumors: toward improved diagnostics and treatments. Methods Mol Biol 2007;360:91-114.

28. Sotiriou C, Piccart MJ. Taking gene-expression profiling to the clinic: when will molecular signatures become relevant to patient care? Nat Rev Cancer 2007;7:545-53.

29. Tsubura A, Yoshizawa K, Uehara N, Yuri T, Matsuoka Y. Multistep mouse mammary tumorigenesis through pre-neoplasia to neoplasia and acquisition of metastatic potential. Med Mol Morphol 2007;40:9-17.

30. Hanahan D, Weinberg RA. The hallmarks of cancer. Cell 2000;100:57-70.

31. Drife JO. Breast development in puberty. Ann N Y Acad Sci 1986;464:58-65.

32. Bissell MJ, Radisky D. Putting tumours in context. Nat Rev Cancer 2001;1:46-54.

33. Liotta LA, Kohn EC. The microenvironment of the tumour-host interface. Nature 2001;411:375-9.

34. De Wever O, Mareel M. Role of tissue stroma in cancer cell invasion. J Pathol 2003;200:429-47.

35. Schmeichel KL, Bissell MJ. Modeling tissue-specific signaling and organ function in three dimensions. J Cell Sci 2003;116:2377-88.

36. Schedin P, Elias A. Multistep tumorigenesis and the microenvironment. Breast Cancer Res 2004;6:93-101.

37. Orimo A, Gupta PB, Sgroi DC, Arenzana-Seisdedos F, Delaunay T, Naeem R, Carey VJ, Richardson AL, Weinberg RA. Stromal fibroblasts present in invasive human breast carcinomas promote tumor growth and angiogenesis through elevated SDF-1/CXCL12 secretion. Cell 2005;121:335-48.

38. Radisky DC, Levy DD, Littlepage LE, Liu H, Nelson CM, Fata JE, Leake D, Godden EL, Albertson DG, Nieto MA, Werb Z, Bissell MJ. Rac1b and reactive oxygen species mediate MMP-3-induced EMT and genomic instability. Nature 2005;436:123-7.

39. Tan PH, Jayabaskar T, Yip G, Tan Y, Hilmy M, Selvarajan S, Bay BH. p53 and c-kit (CD117) protein expression as prognostic indicators in breast phyllodes tumors: a tissue microarray study. Mod Pathol 2005;18: 1527-34.

40. Radisky ES, Radisky DC. Stromal induction of breast cancer: Inflammation and invasion. Rev Endocr Metab Disord 2007;In press.

41. van Roozendaal CE, van Ooijen B, Klijn JG, Claassen C, Eggermont AM, Henzen-Logmans SC, Foekens JA. Stromal influences on breast cancer cell growth. Br J Cancer 1992;65:77-81.

42. van Roozendaal CE, Klijn JG, van Ooijen B, Claassen C, Eggermont AM, Henzen-Logmans SC, Foekens JA. Transforming growth factor beta secretion from primary breast cancer fibroblasts. Mol Cell Endocrinol 1995; 111:1-6.

43. van Roozendaal KE, Klijn JG, van Ooijen B, Claassen C, Eggermont AM, Henzen-Logmans SC, Foekens JA. Differential regulation of breast tumor cell proliferation by stromal fibroblasts of various breast tissue sources. Int J Cancer 1996;65:120-5.

44. van Roozendaal CE, Gillis AJ, Klijn JG, van Ooijen B, Claassen CJ, Eggermont AM, Henzen-Logmans SC, Oosterhuis JW, Foekens JA, Looijenga LH. Loss of imprinting of IGF2 and not H19 in breast cancer, adjacent normal tissue and derived fibroblast cultures. FEBS Lett 1998;437:107-11.

45. Sieuwerts AM, Klijn JG, Henzen-Logmand SC, Bouwman I, Van Roozendaal KE, Peters HA, Setyono-Han B, Foekens JA. Urokinase-type-plasminogen-activator (uPA) production by human breast (myo) fibroblasts in vitro: influence of transforming growth factor-beta(1) (TGF beta(1)) compared with factor(s) released by human epithelial-carcinoma cells. Int J Cancer 1998;76:829-35.

46. Sieuwerts AM, Klijn JG, Foekens JA. Insulin-like growth factor 1 (IGF-1) and urokinase-type plasminogen activator (uPA) are inversely related in human breast fibroblasts. Mol Cell Endocrinol 1999;154:179-85.

47. Sieuwerts AM, Klijn JG, Henzen-Logmans SC, Foekens JA. Cytokine-regulated urokinase-type-plasminogen-activator (uPA) production by human breast fibroblasts in vitro. Breast Cancer Res Treat 1999;55:9-20.

48. Sieuwerts AM, Martens JW, Dorssers LC, Klijn JG, Foekens JA. Differential effects of fibroblast growth factors on expression of genes of the plasminogen activator and insulin-like growth factor systems by human breast fibroblasts. Thromb Haemost 2002;87: 674-83.

49. Martens JW, Sieuwerts AM, Bolt-deVries J, Bosma PT, Swiggers SJ, Klijn JG, Foekens JA. Aging of stromal-derived human breast fibroblasts might contribute to breast cancer progression. Thromb Haemost 2003;89:393-404.

50. Sieuwerts AM, Meijer-van Gelder ME, Timmermans M, Trapman AM, Rodriguez Garcia R, Arnold M, Goedheer AJ, Portengen H, Klijn JG, Foekens JA. How ADAM-9 and ADAM-11 differentially from estrogen receptor predict response to tamoxifen treatment in patients with recurrent breast cancer: a retrospective study. Clin Cancer Res 2005;11:7311-21.

51. Sieuwerts AM, Look MP, Meijer-van Gelder ME, Timmermans M, Trapman AM, Rodriguez Garcia R, Arnold M, Goedheer AJ, de Weerd V, Portengen H, Klijn JG, Foekens JA. Which cyclin E prevails as prognostic marker for breast cancer? Results from a retrospective study involving 635 lymph node-negative breast cancer patients. Clin Cancer Res 2006;12:3319-28.

52. Allinen M, Beroukhim R, Cai L, Brennan C, Lahti-Domenici J, Huang H, Porter D, Hu M, Chin L, Richardson A, Schnitt S, Sellers WR, Polyak K. Molecular characterization of the tumor microenvironment in breast cancer. Cancer Cell 2004;6:17-32.

53. West RB, Nuyten DS, Subramanian S, Nielsen TO, Corless CL, Rubin BP, Montgomery K, Zhu S, Patel R, Hernandez-Boussard T, Goldblum JR, Brown PO, van de Vijver M, van de Rijn M. Determination of stromal signatures in breast carcinoma. PLoS Biol 2005;3:1101-1110.

54. Chang HY, Nuyten DS, Sneddon JB, Hastie T, Tibshirani R, Sorlie T, Dai H, He YD, van't Veer LJ, Bartelink H, van de Rijn M, Brown PO, van de Vijver MJ. Robustness, scalability, and integration of a wound-response gene expression signature in predicting breast cancer survival. Proc Natl Acad Sci U S A 2005; 102:3738-43.

55. Moinfar F, Man YG, Arnould L, Bratthauer GL, Ratschek M, Tavassoli FA. Concurrent and independent genetic alterations in the stromal and epithelial cells of mammary carcinoma: implications for tumorigenesis. Cancer Res 2000;60:2562-6.

56. Pelham RJ, Rodgers L, Hall I, Lucito R, Nguyen KC, Navin N, Hicks J, Mu D, Powers S, Wigler M, Botstein D. Identification of alterations in DNA copy number in host stromal cells during tumor progression. Proc Natl Acad Sci U S A 2006;103:19848-53.

57. Chang HY, Sneddon JB, Alizadeh AA, Sood R, West RB, Montgomery K, Chi JT, van de Rijn M, Botstein D, Brown PO. Gene expression signature of fibroblast serum response predicts human cancer progression: similarities between tumors and wounds. PLoS Biol 2004;2:206-214.

58. Shekhar MP, Pauley R, Heppner G. Host microenvironment in breast cancer development: extracellular matrix-stromal cell contribution to neoplastic phenotype of epithelial cells in the breast. Breast Cancer Res 2003;5:130-5.

59. Radisky DC, Bissell MJ. Cancer. Respect thy neighbor! Science 2004;303:775-7.

60. Orimo A, Weinberg RA. Stromal fibroblasts in cancer: a novel tumor-promoting cell type. Cell Cycle 2006;5: 1597-601.

61. Schmitt M, Harbeck N, Daidone MG, Brynner N, Duffy MJ, Foekens JA, Sweep FC. Identification, validation, and clinical implementation of tumor-associated biomarkers to improve therapy concepts, survival, and quality of life of cancer patients: tasks of the Receptor and Biomarker Group of the European Organization for Research and Treatment of Cancer. Int J Oncol 2004;25: 1397-406.

62. Bast RC, Jr., Ravdin P, Hayes DF, Bates S, Fritsche H, Jr., Jessup JM, Kemeny N, Locker GY, Mennel RG, Somerfield MR. 2000 update of recommendations for the use of tumor markers in breast and colorectal cancer: clinical practice guidelines of the American Society of Clinical Oncology. J Clin Oncol 2001;19:1865-78.

63. Molina R, Barak V, van Dalen A, Duffy MJ, Einarsson R, Gion M, Goike H, Lamerz R, Nap M, Soletormos G, Stieber P. Tumor markers in breast cancer- European Group on Tumor Markers recommendations. Tumour Biol 2005;26:281-93.

64. Huang E, West M, Nevins JR. Gene expression profiling for prediction of clinical characteristics of breast cancer. Recent Prog Horm Res 2003;58:55-73.

65. Calza S, Hall P, Auer G, Bjohle J, Klaar S, Kronenwett U, Liu ET, Miller L, Ploner A, Smeds J, Bergh J, Pawitan Y. Intrinsic molecular signature of breast cancer in a population-based cohort of 412 patients. Breast Cancer Res 2006;8:R34.

66. Ignatiadis M, Desmedt C. Predicting risk of breast cancer recurrence using gene-expression profiling. Pharmacogenomics 2007;8:101-11.

67. Dupont VN, Gentien D, Oberkampf M, De Rycke Y, Blin N. A gene expression signature associated with metastatic cells in effusions of breast carcinoma patients. Int J Cancer 2007;121:1036-46.

68. Hedenfalk I, Duggan D, Chen Y, Radmacher M, Bittner M, Simon R, Meltzer P, Gusterson B, Esteller M, Kallioniemi OP, Wilfond B, Borg A, Trent J, Raffeld M, Yakhini Z, Ben-Dor A, Dougherty E, Kononen J, Bubendorf L, Fehrle W, Pittaluga S, Gruvberger S, Loman N, Johannsson O, Olsson H, Sauter G. Gene-expression profiles in hereditary breast cancer. N Engl J Med 2001;344:539-48.

69. Ahr A, Karn T, Solbach C, Seiter T, Strebhardt K, Holtrich U, Kaufmann M. Identification of high risk breast-cancer patients by gene expression profiling. Lancet 2002;359:131-2.

70. van de Vijver MJ, He YD, van't Veer LJ, Dai H, Hart AA, Voskuil DW, Schreiber GJ, Peterse JL, Roberts C, Marton MJ, Parrish M, Atsma D, Witteveen A, Glas A, Delahaye L, van der Velde T, Bartelink H, Rodenhuis S, Rutgers ET, Friend SH, Bernards R. A gene-expression signature as a predictor of survival in breast cancer. N Engl J Med 2002;347:1999-2009.

71. Huang E, Cheng SH, Dressman H, Pittman J, Tsou MH, Horng CF, Bild A, Iversen ES, Liao M, Chen CM, West M, Nevins JR, Huang AT. Gene expression predictors of breast cancer outcomes. Lancet 2003;361:1590-6.

72. Ramaswamy S, Ross KN, Lander ES, Golub TR. A molecular signature of metastasis in primary solid tumors. Nat Genet 2003;33:49-54.

73. Bertucci F, Borie N, Ginestier C, Groulet A, Charafe-Jauffret E, Adelaide J, Geneix J, Bachelart L, Finetti P, Koki A, Hermitte F, Hassoun J, Debono S, Viens P, Fert V, Jacquemier J, Birnbaum D. Identification and validation of an ERBB2 gene expression signature in breast cancers. Oncogene 2004; 23:2564-75.

74. Miller LD, Smeds J, George J, Vega VB, Vergara L, Ploner A, Pawitan Y, Hall P, Klaar S, Liu ET, Bergh J. An expression signature for p53 status in human breast cancer predicts mutation status, transcriptional effects, and patient survival. Proc Natl Acad Sci U S A 2005; 102:13550-5.

75. Wang Y, Klijn JG, Zhang Y, Sieuwerts AM, Look MP, Yang F, Talantov D, Timmermans M, Meijer-van Gelder ME, Yu J, Jatkoe T, Berns EM, Atkins D, Foekens JA. Gene-expression profiles to predict distant metastasis of lymph-node-negative primary breast cancer. Lancet 2005;365:671-9.

76. Foekens JA, Atkins D, Zhang Y, Sweep FC, Harbeck N, Paradiso A, Cufer T, Sieuwerts AM, Talantov D, Span PN, Tjan-Heijnen VC, Zito AF, Specht K, Hoefler H, Golouh R, Schittulli F, Schmitt M, Beex LV, Klijn JG, Wang Y. Multicenter validation of a gene expression-based prognostic signature in lymph node-negative primary breast cancer. J Clin Oncol 2006; 24:1665-71.

77. Liu R, Wang X, Chen GY, Dalerba P, Gurney A, Hoey T, Sherlock G, Lewicki J, Shedden K, Clarke MF. The prognostic role of a gene signature from tumorigenic breast-cancer cells. N Engl J Med 2007;356:217-26.

78. Ma Y, Qian Y, Wei L, Abraham J, Shi X, Castranova V, Harner EJ, Flynn DC, Guo L. Population-based molecular prognosis of breast cancer by transcriptional profiling. Clin Cancer Res 2007;13:2014-22.

79. Woelfle U, Cloos J, Sauter G, Riethdorf L, Jänicke F, van Diest P, Brakenhoff R, Pantel K. Molecular signature associated with bone marrow micrometastasis in human breast cancer. Cancer Res 2003;63:5679-84.

80. Smid M, Wang Y, Klijn JG, Sieuwerts AM, Zhang Y, Atkins D, Martens JW, Foekens JA. Genes associated with breast cancer metastatic to bone. J Clin Oncol 2006; 24:2261-7.

81. Minn AJ, Gupta GP, Padua D, Bos P, Nguyen DX, Nuyten D, Kreike B, Zhang Y, Wang Y, Ishwaran H, Foekens JA, van de Vijver M, Massague J. Lung metastasis genes couple breast tumor size and metastatic spread. Proc Natl Acad Sci U S A 2007;104:6740-5.

82. Sotiriou C, Powles TJ, Dowsett M, Jazaeri AA, Feldman AL, Assersohn L, Gadisetti C, Libutti SK, Liu ET. Gene expression profiles derived from fine needle aspiration correlate with response to systemic chemotherapy in breast cancer. Breast Cancer Res 2002;4:R3.

83. Chang JC, Wooten EC, Tsimelzon A, Hilsenbeck SG, Gutierrez MC, Elledge R, Mohsin S, Osborne CK, Chamness GC, Allred DC, O'Connell P. Gene expression profiling for the prediction of therapeutic response to docetaxel in patients with breast cancer. Lancet 2003; 362:362-9.

84. Ayers M, Symmans WF, Stec J, Damokosh AI, Clark E, Hess K, Lecocke M, Metivier J, Booser D, Ibrahim N, Valero V, Royce M, Arun B, Whitman G, Ross J, Sneige N, Hortobagyi GN, Pusztai L. Gene expression profiles predict complete pathologic response to neoadjuvant paclitaxel and fluorouracil, doxorubicin, and cyclophosphamide chemotherapy in breast cancer. J Clin Oncol 2004;22:2284-93.

85. Bertucci F, Finetti P, Rougemont J, Charafe-Jauffret E, Nasser V, Loriod B, Camerlo J, Tagett R, Tarpin C, Houvenaeghel G, Nguyen C, Maraninchi D, Jacquemier J, Houlgatte R, Birnbaum D, Viens P. Gene expression profiling for molecular characterization of inflammatory breast cancer and prediction of response to chemotherapy. Cancer Res 2004;64:8558-65.

86. Paik S, Shak S, Tang G, Kim C, Baker J, Cronin M, Baehner FL, Walker MG, Watson D, Park T, Hiller W, Fisher ER, Wickerham DL, Bryant J, Wolmark N. A multigene assay to predict recurrence of tamoxifen-treated, node-negative breast cancer. N Engl J Med 2004;351:2817-26.

87. Troester MA, Hoadley KA, Sorlie T, Herbert BS, Borresen-Dale AL, Lonning PE, Shay JW, Kaufmann WK, Perou CM. Cell-type-specific responses to chemotherapeutics in breast cancer. Cancer Res 2004; 64:4218-26.

88. Chang JC, Wooten EC, Tsimelzon A, Hilsenbeck SG, Gutierrez MC, Tham YL, Kalidas M, Elledge R, Mohsin S, Osborne CK, Chamness GC, Allred DC, Lewis MT, Wong H, O'Connell P. Patterns of resistance and incomplete response to docetaxel by gene expression profiling in breast cancer patients. J Clin Oncol 2005; 23:1169-77.

89. Folgueira MA, Carraro DM, Brentani H, Patrao DF, Barbosa EM, Netto MM, Caldeira JR, Katayama ML, Soares FA, Oliveira CT, Reis LF, Kaiano JH, Camargo LP, Vencio RZ, Snitcovsky IM, Makdissi FB, e Silva PJ, Goes JC, Brentani MM. Gene expression profile associated with response to doxorubicin-based therapy in breast cancer. Clin Cancer Res 2005;11:7434-43.

90. Glinsky GV, Berezovska O, Glinskii AB. Microarray analysis identifies a death-from-cancer signature predicting therapy failure in patients with multiple types of cancer. J Clin Invest 2005;115:1503-21.

91. Hannemann J, Oosterkamp HM, Bosch CA, Velds A, Wessels LF, Loo C, Rutgers EJ, Rodenhuis S, van de Vijver MJ. Changes in gene expression associated with response to neoadjuvant chemotherapy in breast cancer. J Clin Oncol 2005;23:3331-42.

92. Iwao-Koizumi K, Matoba R, Ueno N, Kim SJ, Ando A, Miyoshi Y, Maeda E, Noguchi S, Kato K. Prediction of docetaxel response in human breast cancer by gene expression profiling. J Clin Oncol 2005;23:422-31.

93. Jansen MP, Foekens JA, van Staveren IL, Dirkzwager-Kiel MM, Ritstier K, Look MP, Meijer-van Gelder ME, Sieuwerts AM, Portengen H, Dorssers LC, Klijn JG, Berns EM. Molecular classification of tamoxifen-resistant breast carcinomas by gene expression profiling. J Clin Oncol 2005;23:732-40.

94. Martens JW, Nimmrich I, Koenig T, Look MP, Harbeck N, Model F, Kluth A, Bolt-de Vries J, Sieuwerts AM, Portengen H, Meijer-Van Gelder ME, Piepenbrock C, Olek A, Hofler H, Kiechle M, Klijn JG, Schmitt M, Maier S, Foekens JA. Association of DNA methylation of phosphoserine aminotransferase with response to endocrine therapy in patients with recurrent breast cancer. Cancer Res 2005;65:4101-17.

95. Andre F, Mazouni C, Hortobagyi GN, Pusztai L. DNA arrays as predictors of efficacy of adjuvant/neoadjuvant chemotherapy in breast cancer patients: current data and issues on study design. Biochim Biophys Acta 2006; 1766:197-204.

96. Andre F, Pusztai L. Molecular classification of breast cancer: implications for selection of adjuvant chemotherapy. Nat Clin Pract Oncol 2006;3:621-32.

97. Buyse M, Loi S, van't Veer L, Viale G, Delorenzi M, Glas AM, d'Assignies MS, Bergh J, Lidereau R, Ellis P, Harris A, Bogaerts J, Therasse P, Floore A, Amakrane M, Piette F, Rutgers E, Sotiriou C, Cardoso F, Piccart MJ. Validation and clinical utility of a 70-gene prognostic signature for women with node-negative breast cancer. J Natl Cancer Inst 2006;98:1183-92.

98. Paik S. Methods for gene expression profiling in clinical trials of adjuvant breast cancer therapy. Clin Cancer Res 2006;12:1019-1023.

99. Paik S, Tang G, Shak S, Kim C, Baker J, Kim W, Cronin M, Baehner FL, Watson D, Bryant J, Costantino JP, Geyer CE, Jr., Wickerham DL, Wolmark N. Gene expression and benefit of chemotherapy in women with node-negative, estrogen receptor-positive breast cancer. J Clin Oncol 2006;24: 3726-34.

100. Potti A, Dressman HK, Bild A, Riedel RF, Chan G, Sayer R, Cragun J, Cottrill H, Kelley MJ, Petersen R, Harpole D, Marks J, Berchuck A, Ginsburg GS, Febbo P, Lancaster J, Nevins JR. Genomic signatures to guide the use of chemotherapeutics. Nat Med 2006;12:1294-300.

101. Paik S. Development and clinical utility of a 21-gene recurrence score prognostic assay in patients with early breast cancer treated with tamoxifen. Oncologist 2007; 12:631-5.

102. Ravaioli A, Bagli L, Zucchini A, Monti F. Prognosis and prediction of response in breast cancer: the current role of the main biological markers. Cell Prolif 1998;31:113-26.

103. Hayes DF, Bast RC, Desch CE, Fritsche H, Jr., Kemeny NE, Jessup JM, Locker GY, Macdonald JS, Mennel RG, Norton L, Ravdin P, Taube S, Winn RJ. Tumor marker utility grading system: a framework to evaluate clinical utility of tumor markers. J Natl Cancer Inst 1996;88: 1456-66.

104. Hayes DF. Determination of clinical utility of tumor markers: a tumor marker utility grading system. Recent Results Cancer Res 1998;152:71-85.

105. Smid M, Wang Y, Zhang Y, Sieuwerts A, Yu J, Klijn J, Foekens J, Martens J. Subtypes of breast cancer show preferential site of relapse. (submitted) 2007.

106. Janssens N, Janicot M, Perera T, Bakker A. Housekeeping genes as internal standards in cancer research. Mol Diagn 2004;8:107-13.

107. Szabo A, Perou CM, Karaca M, Perreard L, Quackenbush JF, Bernard PS. Statistical modeling for selecting housekeeper genes. Genome Biol 2004;5:R59.

108. de Kok JB, Roelofs RW, Giesendorf BA, Pennings JL, Waas ET, Feuth T, Swinkels DW, Span PN. Normalization of gene expression measurements in tumor tissues: comparison of 13 endogenous control genes. Lab Invest 2005;85:154-9.

109. Nailis H, Coenye T, Van Nieuwerburgh F, Deforce D, Nelis HJ. Development and evaluation of different normalization strategies for gene expression studies in Candida albicans biofilms by real-time PCR. BMC Mol Biol 2006;7:25.

110. Nolan T, Hands RE, Bustin SA. Quantification of mRNA using real-time RT-PCR. Nat Protoc 2006;1:1559-82.

111. Fan C, Oh DS, Wessels L, Weigelt B, Nuyten DS, Nobel AB, van't Veer LJ, Perou CM. Concordance among gene-expression-based predictors for breast cancer. N Engl J Med 2006;355:560-9.

112. Yu J, Sieuwerts AM, Zhang Y, Martens JW, Smid M, Klijn JG, Wang Y, Foekens JA. Pathway analysis of gene signatures predicting metastasis of node-negative primary breast cancer. BMC Cancer 2007;7:182.

113. Hu Z, Fan C, Oh DS, Marron JS, He X, Qaqish BF, Livasy C, Carey LA, Reynolds E, Dressler L, Nobel A, Parker J, Ewend MG, Sawyer LR, Wu J, Liu Y, Nanda R, Tretiakova M, Ruiz Orrico A, Dreher D, Palazzo JP, Perreard L, Nelson E, Mone M, Hansen H, Mullins M, Quackenbush JF, Ellis MJ, Olopade OI, Bernard PS, Perou CM. The molecular portraits of breast tumors are conserved across microarray platforms. BMC Genomics 2006;7:96.

114. Bild AH, Yao G, Chang JT, Wang Q, Potti A, Chasse D, Joshi MB, Harpole D, Lancaster JM, Berchuck A, Olson JA, Jr., Marks JR, Dressman HK, West M, Nevins JR. Oncogenic pathway signatures in human cancers as a guide to targeted therapies. Nature 2006;439:353-7.

115. Rhodes DR, Kalyana-Sundaram S, Tomlins SA, Mahavisno V, Kasper N, Varambally R, Barrette TR, Ghosh D, Varambally S, Chinnaiyan AM. Molecular concepts analysis links tumors, pathways, mechanisms, and drugs. Neoplasia 2007;9:443-54.

116. Saal LH, Johansson P, Holm K, Gruvberger-Saal SK, She QB, Maurer M, Koujak S, Ferrando AA, Malmstrom P, Memeo L, Isola J, Bendahl PO, Rosen N, Hibshoosh H, Ringner M, Borg A, Parsons R. Poor prognosis in carcinoma is associated with a gene expression signature of aberrant PTEN tumor suppressor pathway activity. Proc Natl Acad Sci U S A 2007;104:7564-9.

117. Coebergh JW, van Veen EB, Vandenbroucke JP, van Diest P, Oosterhuis W. One-time general consent for research on biological samples: opt out system for patients is optimal and endorsed in many countries. BMJ 2006;332:665.

118. Snell L, Watson PH. Breast tissue banking: collection, handling, storage, and release of tissue for breast cancer research. Methods Mol Med 2006;120:3-24.

119. Abramovitz M, Braga S, Ellis M, Forbes J, Harbeck N, Hewitt S, Leyland-Jones B, Mook S, Olson J, Rojo F, Seth A, Singh B, van 't Veer L, Watson M, Zujewski J, Enos R. Guideline for collection, handling, and storage of Specimens from Breast International Group (BIG) and National Cancer Institute (NCI) Cooperative Group breast cancer clinical trials. Ctep.cancer.gov/forms/guidelines_fresh_tissue 2006:1-27.

120. Schrohl AS, Meijer-van Gelder ME, Holten-Andersen MN, Christensen IJ, Look MP, Mouridsen HT, Brunner N, Foekens JA. Primary tumor levels of tissue inhibitor of metalloproteinases-1 are predictive of resistance to chemotherapy in patients with metastatic breast cancer. Clin Cancer Res 2006;12:7054-8.

121. Yang F, Foekens JA, Yu J, Sieuwerts AM, Timmermans M, Klijn JG, Atkins D, Wang Y, Jiang Y. Laser microdissection and microarray analysis of breast tumors reveal ER-alpha related genes and pathways. Oncogene 2006;25:1413-9.

122. Umar A, Dalebout JC, Timmermans AM, Foekens JA, Luider TM. Method optimisation for peptide profiling of microdissected breast carcinoma tissue by matrix-assisted laser desorption/ionisation-time of flight and matrix-assisted laser desorption/ionisation-time of flight/time of flight-mass spectrometry. Proteomics 2005;5:2680-8.

123. Sieuwerts AM, Usher PA, Meijer-van Gelder ME, Timmermans M, Martens JW, Brunner N, Klijn JG, Offenberg H, Foekens JA. Concentrations of TIMP1 mRNA splice variants and TIMP-1 protein are differentially associated with prognosis in primary breast cancer. Clin Chem 2007;53:1280-8.

124. Umar A, Luider TM, Foekens JA, Pasa-Tolic L. NanoLC-FT-ICR MS improves proteome coverage attainable for approximately 3000 laser-microdissected breast carcinoma cells. Proteomics 2007;7:323-9.

125. Jansen MP, Sieuwerts AM, Look MP, Ritstier K, Meijer-van Gelder ME, van Staveren IL, Klijn JG, Foekens JA, Berns EM. HOXB13-to-IL17BR expression ratio is related with tumor aggressiveness and response to tamoxifen of recurrent breast cancer: a retrospective study. J Clin Oncol 2007;25:662-8.

126. Usher PA, Sieuwerts AM, Bartels A, Lademann U, Nielsen HJ, Holten-Andersen L, Foekens JA, Brunner N, Offenberg H. Identification of alternatively spliced TIMP-1 mRNA in cancer cell lines and colon cancer tissue. Mol Oncol 2007;1:205-215.

CHAPTER TWO

Differential effects of fibroblast growth factors on expression of genes of the plasminogen activator and insulin-like growth factor systems by human breast fibroblasts

Anieta M. Sieuwerts[1], John W. M. Martens[1], Lambert C. J. Dorssers[2], Jan G. M. Klijn[1] and John A. Foekens[1]

[1]Department of Medical Oncology, Erasmus MC, Rotterdam, The Netherlands
[2]Department of Pathology, Erasmus MC, Rotterdam, The Netherlands

ABSTRACT

In breast stroma urokinase plasminogen activator (uPA) is predominantly expressed by fibroblasts located in the near vicinity of tumor cells, and fibroblast-derived insulin-like growth factor-1 (IGF-1) may be involved in inhibiting the expression of uPA in these fibroblasts. To investigate a possible role for fibroblast growth factors (FGFs), we evaluated the expression of components of the PA system and the IGF system in normal and tumor-tissue-derived human breast fibroblasts exposed to various FGFs *in vitro*. mRNA analysis revealed that FGF-1, FGF-2 and FGF-4 induced the mRNA expression levels of *uPA*, *tPA*, *uPAR*, *PAI-1* and *PAI-2*, and reduced those of *IGF-1*, *IGF-1R*, *IGF-2R* and *IGFBP-4*, without significantly affecting the levels of *IGFBP-3*, *IGFBP-5* and *IGFBP-6* mRNA. Concerning the expression of *IGF-2* mRNA, the effects mediated by FGF-1, FGF-2 and FGF-4 were divergent. In general, the effects elicited by FGF-1 on the various mRNA levels studied were rapid and short-term. Those mediated by FGF-2 overall lagged behind but were longer-lasting. For FGF-4 an in between pattern was observed. Blocking transcription and translation demonstrated that a) both the FGF-1 and FGF-2 induced effects were the result of altered gene transcription or mRNA stability, b) the short-term effects mediated by FGF-1 and FGF-2 required *de novo* protein synthesis, and c) the long-term effects elicited by FGF-2 did not depend on *de novo* protein synthesis during the first 24 h, but were triggered by proteins produced or made available thereafter. The data presented propose that of the FGFs studied (FGF-1, -2, -4, -5, and -7), FGF-2 is the most attractive target for therapeutical strategies aimed at diminishing the contribution of stromal fibroblasts in the PA-directed breast tumor proteolysis.

INTRODUCTION

In breast cancer, peritumoral stromal fibroblast-like cells have been shown to express proteolytic enzymes such as the metalloproteinases MMP-2 [1], MMP-11 [1, 2], MMP-13 [3] and MMP-14 [4] and the urokinase-type plasminogen activator uPA [1, 5, 6]. In particular the uPA system, constituting uPA, its cell-bound receptor (uPAR), and its main inhibitors plasminogen activator inhibitors type 1 and 2 (PAI-1 and PAI-2) have been shown to be involved in the process of matrix degradation, tumor cell migration and invasion, and angiogenesis. Upon binding to its receptor, uPA converts plasminogen into plasmin. Plasmin is able to directly degrade a variety of extracellular matrix (ECM) proteins, and can activate several MMPs, which in turn are also able to dissolve ECM components. Tissue-type plasminogen activator (tPA) on the other hand has been shown to play a major role in plasmin-directed lysis of fibrin clots (reviewed in [7]). Many research groups have reported high breast tumor levels of uPA, uPAR and PAI-1 to be associated with poor prognosis (reviewed in [8-10]). Ergo, an understanding of the behavior of potential inducers and modifiers of components of the PA system may be helpful in designing future therapeutic strategies.

We have shown previously that out of a panel of various cytokines and growth factors, the fibroblast growth factors FGF-1 and FGF-2 were amongst the most potent inducers, and the insulin-like growth factors IGF-1 and IGF-2 amongst the most potent inhibitors of uPA protein production by human breast fibroblasts [11]. Noteworthy in view of the present study is the detection of FGF-1 protein in peritumoral stromal cells of breast tumor tissue treated with protease inhibitors [12], and the significant association observed between FGF-2 and uPA staining of peritumoral stromal cells [13]. The FGF family of soluble growth factors is

composed of a large number of structurally related proteins. Extracellular FGF binds with low affinity to heparan sulphate proteoglycans (HSPGs), which protect FGF from degradation and serve as FGF-reservoirs to promote longterm availability [14-16], and with high affinity to one or more of the 4 identified FGF tyrosine kinase receptors (FGF-Rs) [17]. For uPA induction by FGF-2, the involvement of ETS transcription factors has been described [18-20]. Although FGFs have been shown to induce expression of components of the PA system in a direct manner [21, 22], also indirect pathways have been described. For example, induction of the PA system by VEGF, another angiogenic factor capable of inducing the transcription factor ETS, is dependent on the presence of FGF-2 [23]. There are no published data available on a possible role for the IGF system in relation to the FGF-induced up-regulation of the PA system. This would be of interest to know, since we have demonstrated that IGF-1 and uPA are inversely related in human breast fibroblasts, and showed data suggesting that IGF-1 controls the expression of uPA [24]. Like FGFs, IGFs interact with their own tyrosine kinase receptor, the IGF-1R. Although IGF-2 compared with IGF-1 binds with a 2 to 50-fold lower affinity to the IGF-1R, both ligands can mediate the same functions via this receptor [reviewed in [25]]. The mannose-6-phosphate receptor/IGF-2R, however, binds IGF-2 and not IGF-1. Furthermore, the activities of both IGF-1 and IGF-2 are modulated by their association with six different high affinity IGF binding proteins (IGFBPs) [25-28].

To examine a possible regulation of the PA and IGF systems by FGFs in human breast fibroblasts, and to shed in this respect some light on the tumor biology of normal versus tumor-tissue-derived fibroblasts, we analysed in this study the FGF-induced mRNA expression of components of the PA system and of the IGF system in a set of paired cultured normal and tumor-tissue-derived human breast fibroblasts. To examine a possible differential regulation of components of the PA and IGF system by various known FGFs, we selected the following FGF panel for our study: FGF-1 and FGF-2,

being the FGFs present in almost all breast cancer cases studied, FGF-5 and FGF-7, representing the group of FGFs with a more restricted level of expression in breast cancer, and FGF-4, representing the group of FGFs not known to play a role in breast cancer [29-31].

MATERIALS AND METHODS

Culture of fibroblast strains

The human fibroblast strains T and N were established from an invasive ductal breast adenocarcinoma tumor-tissue-derived (T) fragment and from adjacent normal breast tissue (N) of the same patient, as described in detail before [32]. The original tumor tissue and adjacent normal breast tissue, as well as the resulting T and N fibroblast populatons isolated from these two tissues, were characterised using standard immunocytochemical procedures, as described [33]. Fibroblasts were propagated in medium containing 10% foetal calf serum and for experimentation transferred to protein-free medium in 6-well tissue culture plates, coated with the recombinant cell-attachment factor Pronectin®F (ICN Biomedicals, Cleveland, OH, USA), as described [11].

Experimental culture conditions

To obtain quiescent fibroblasts, they were cultured for 4 days in protein-free medium. Then the protein-free medium was replaced by 2 ml experimental medium, that is, protein-free medium containing either the relevant vehicle or one of the human recombinant FGFs (all obtained from R&D systems, Minneapolis, MN) at the concentrations indicated in the text. For neutralisation purposes, the FGF-specific neutralising antibodies (R&D systems) were used against their proper isotype-matched control antibodies (R&D systems) in the absence and presence of the relevant FGFs according to the manufacturer's advise. For studying the effects of the mRNA synthesis inhibitor actinomycin D (ACT), quiescent fibroblasts were pre-incubated for 15 min in protein-free medium supplemented with 5 µg/ml ACT (Sigma, St.

Louis, MO) or with the vehicle only (final concentration of 0.05% ethanol). After a double wash with PBS, they were cultured for an additional 24 h in fresh protein-free medium in the absence or presence of FGFs. For studying the effects of the protein synthesis inhibitor cycloheximide (CHX), quiescent fibroblasts were cultured for up to 48 h in protein-free medium supplemented with 50 µg/ml cycloheximide (Sigma) or with the vehicle only (protein-free medium) in the absence or presence of FGFs. At the indicated time-points, the amount of uPA protein released into the culture medium and the expression levels of the various mRNA transcripts were evaluated (see below for followed procedures).

Measurement of the amount of uPA by immunoassay

Fifty µl of the 2 ml experimental medium was used to measure uPA antigen by an enzyme-linked immunosorbent assay (ELISA) involving 4 different polyclonal antibodies, which has been characterised in detail [34], as described [11]. We established previously that the levels of uPA protein released by these quiescent and growth factor activated fibroblasts into the culture medium correlate significantly (Spearman rank correlation r_s=+0.96, P<0.001; n=24] with the functional ability of uPA to convert plasminogen into plasmin [11].

RNA isolation and first strand cDNA synthesis

To enable measurement of specific mRNA species from a relatively small number of fibroblasts, we quantitated mRNA transcripts by reverse transcriptase polymerase chain reaction (RT-PCR). Cellular RNA from fibroblasts, cultured in duplicate for up to 4 days in experimental protein-free medium, was isolated using the guanidium salt extraction with RNAzol B (Campro, Veenendaal, The Netherlands) according to the manufacturer's instruction. 1.0 µg RNA samples were reverse-transcribed at 37° C for 60 min in a total volume of 80 µl containing Superscript II RNase H-RT, DTT, first-strand buffer, RNasin, dNTP, oligo(dT) 12-18, random hexamer primers, and first-strand buffer

(GibcoBRL, Grand Island, NY, USA) according to the manufacturer's instruction. The resulting cDNA samples were aliquoted, and stored at −80° C before PCR amplification.

PCR-amplification of specific mRNA sequences

To enable comparison of the levels of specific mRNAs in different samples, they were evaluated as a ratio of the medium abundance housekeeping gene hypoxanthine-guanine phosphoribosyltransferase (HPRT). Utilising the primer sets depicted in Table 1, the specific sequences in each cDNA sample were amplified by PCR. The specificities of these intron-spanning primer sets were verified by sequencing the PCR products. Because some of the primer sets interfered with the other primer sets, and to enable divergence in the number of PCR cycles between gene-sequences (see Table 1), we chose to amplify each sequence separately. To maximise uniformity in this setting, complete 110 µl cDNA PCR mixtures [containing 5% (v/v) cDNA in a final concentration of 1.5 x Taq DNA polymerase buffer with 1.5 mM MgCl$_2$ (Promega, Leiden, The Netherlands), 1.5 mM each dNTP (Amersham Pharmacia Biotech, Roosendaal, The Netherlands), supplemented with 2.5 U of Taq DNA polymerase (Promega)] were equally divided at 20 µl over 5 tubes containing the respective primer sets in 10 µl at a final concentration of 0.5 µM of each primer. In each PCR experiment one of the tubes always contained the HPRT primer set to allow normalisation of the other mRNA expression levels. After an initial denaturation of 4 min at 94° C, cDNA was amplified in 23-31 PCR cycles, with denaturation for 45 s at 94° C, annealing for 45 s at 57° C and extension for 45 s at 72° C per cycle, with an additional extension for 6 min at 72° C after the last cycle. Initial experiments were performed to establish conditions to ensure that all genes were amplified linearly in this experimental setting. Negative controls included samples without reverse transcriptase (RNA control), and samples where cDNA was omitted (water control). Equal volumes of PCR products were visualised in duplicate against HPRT on 2% MetaPhor agarose gels (FMC

Table 1. Primer sets used for amplification of mRNA by RT-PCR.

mRNA	primer sequence[a] (5' → 3')	cycli no[b]	size bp[c]	mRNA	primer sequence[a] (5' → 3')	cycli no[b]	size bp[c]
uPA	AGAATTCACCACCATCGAG GCAGGAATCTGTTTTCCAC	28	571	**IGF-1[5]**	GACAGGGGCTTTTATTTCAAC GACAGAGCGAGCTGACTTG	31	159
tPA	GTACAGCCAGCCTCAGTTTC GTCGCATGTTGTCACGAATC	27	776	**IGF-2**	GCGGCTTCTACTTCAGCAG CAGGTGTCATATTGGAAGAAC	31	214
uPAR	AATGGCCGCCAGTGTTACAG CAGGAGACATCAATGTGGTTC	26	227	**IGF-1R**	TCAGTTAATCGTGAAGTGGAAC GTCCTTGCAAAGACGAAGTTG	27	600
s-uPAR[1]	AATGGCCGCCAGTGTTACAG CCAGCTTCCCCAGAGTGAG	28	144	**IGF-2R**	GTGTCTTCCCCTTCATATTC CAGGTAGTTGTCCCCATTG	27	809
PAI-1	CATCAATGACTGGGTGAAGAC CATAAGGGGCAGCAATGAAC	23	320	**IGFBP-1**	TCGTAGAGAGTTTAGCCAAG GCTGTGATAAAATCCATTCTTG	28	165
PAI-2	AACCCCAGGCAGTAGACTTC GTGCCCTCCTCATTCACATC	31	648	**IGFBP-2[6]**	CTGGAGGAGCCCAAGAAG GCCATGCTTGTCACAGTTG	28	162
FGF-2[2]	GAGCGACCCTCACATCAAG TTTCAGTGCCACATACCAAC	25	220	**IGFBP-3[7]**	CCCTCCATTCAAAGATAATC TCCACACACCAGCAGAAG	23	298
VEGF[3]	CCTTGCCTTGCTGCTCTAC GGTACTCCTGGAAGATGTC	26	165	**IGFBP-4**	CTGGGCGACGAAGCCATC GGGGTGGAAGTTGCCGTTG	23	579
ETS-1[4]	GTTAATGGAGTCAACCCAGC GGGTGACGACTTCTTGTTTG	25	274	**IGFBP-5**	GGGTTTGCCTCAACGAAAAG TTTCTGCGGTCCTTCTTCAC	23	181
HPRT	ATGGACAGGACTGAACGTC GGTCCTTTTCACCAGCAAG	27	378	**IGFBP-6**	GCGACTGCTCTGGAAGGAG TGGTAGAGGTGCCTGGATTC	23	478

a   All primer sets (top=sense, bottom=anti-sense) were constructed and optimised for a 57°C annealing-temperature, are intron-spanning, amplify a region within the coding region of the mature peptide, and showed product formation in at least one fibroblast strain or cell line.

b   Initial experiments were performed to establish the optimal number of cycles required in our experimental set-up to certify that the analysis of the PCR products would occur during the amplification phase, prior to reaching the plateau phase.

c   All PCR products were verified by sequence analysis and tested to agree with the expected size.

1   Reverse primer constructed in the reported alternative exon 7 of the uPAR gene to detect the soluble uPA binding protein (s-uPAR), which arises from an alternative splicing in the middle of the third domain of uPAR, resulting in an alternative exon 7 lacking the carboxy-terminal membrane attachment [50].

2   Primers constructed in the sequence of the mature peptide of the 18 kDa FGF-2 downstream the initiation sites of the reported 22.5 kDa and 21 kDa high molecular mass forms of FGF-2, and therefore applicable to detect all different FGF-2 mass forms [51].

3   Primers constructed to detect both the reported 121 kDa and 165 kDa secreted VEGF forms and the 189 kDa and 206 kDa VEGF forms that remain cell associated (reviewed in [52]). With isoform specific primers we found that in our fibroblasts the 121 and 165 kDa splice variants were the isoforms most prominently present (data not shown).

4   Primers constructed within the exon 5 to exon 6 region, upstream the reported alternative splicing variant, ETS-1b, lacking exon 7, therefore constructed to detect both the ETS-1a and ETS-1b variant, and downstream the reported splice variant lacking exon 4 [53].

5   To detect both the alternatively spliced IGF-1A and IGF-1B precursors, primers were constructed to span intron 2 and 3 [54].

6   Used in the presence of 1 M betaine for optimal PCR amplification.

7   Used in the presence of 2.5 mM MgCl2 for optimal PCR amplification.

Bioproducts, Rockland, ME) stained with ethidium-bromide, and band intensities were measured by UV scanning using the Scanalytics ONE-Dscan 1.0 software (Alpha Innotech Corporation, Biozym). Figure 1 shows a representative example of a gel electrophoresis analysis of uPA, uPAR, VEGF and HPRT mRNA expression levels after RT-PCR amplification. For all individual cDNAs, amplification of each specific mRNA sequence was performed in at least 3 independently performed PCR experiments.

The inter-assay coefficient of variation (c.v.) for control samples (cDNA of tumor-derived fibroblasts pre-cultured to near confluence in growth medium, and analysed for specific uPA and IGF-1 sequences against HPRT), for 12 independently performed PCRs over a period of 6 months was 25%. This inter-assay c.v. includes all prior handling involved in obtaining the PCR products as well as the variation introduced by gel electrophoresis.

Statistical analysis

In all individual cell culture experiments, factors were tested in duplicate. Results of one representative experiment are expressed as means ± SD. Results of more than one independently performed experiment are expressed as means ± SEM. To test for differences between 2 groups, the 2-sided Student's t-test was used, with $P<0.05$ considered as statistically significant.

RESULTS

Basal mRNA levels

To investigate the basal and FGF-induced capacity of human breast fibroblasts to express components of the PA and IGF systems *in vitro*, we used a protein-free culture system. All mRNA expression data were obtained from RT-PCR experiments and normalised against the housekeeping gene *HPRT* as shown in Figure 1. Comparison of various basal steady-state mRNA levels after normalisation against *HPRT* in quiescent normal (N) and tumor-derived (T) fibroblasts from the same patient are presented in Figure 2. Although we were able to detect *IGFBP-1* mRNA transcripts in human MDA-MB-231 breast cancer cells, and *IGFBP-2* mRNA transcripts in human MCF7, T47-D, ZR75.1 and SKBR-3 breast cancer cells (data

not shown), we were unable to detect *IGFBP-1* and *IGFBP-2* mRNA transcripts in quiescent and FGF-activated N and T fibroblasts. As shown in Figure 2 for the other mRNAs studied, quiescent N and T fibroblasts expressed similar amounts of *tPA*, *PAI-2*, *IGF-2R*, *IGFBP-4*, *IGFBP-6*, and *FGF-2* mRNA transcripts. *uPAR*, its soluble form *s-uPAR*, *IGF-2*, and *ETS-1* mRNA levels were only slightly (less than 1.5-fold) elevated ($P<0.05$) and *IGF-1R* only slightly decreased ($P<0.01$) in T fibroblasts when compared with N fibroblasts. However, the T fibroblasts expressed over 1.5-fold more ($P<0.01$) *PAI-1*, *uPA*, *IGFBP-3* and *VEGF* mRNA transcripts and over 1.5-fold less ($P<0.01$) *IGF-1* and *IGFBP-5* mRNA transcripts when compared with N fibroblasts.

FGF-mediated alterations in mRNA expression and uPA protein production

Previously we showed that FGF-1 and FGF-2 are able to induce *uPA* expression by fibroblasts [11]. In addition, we have shown that *IGF-1* and *uPA* are inversely related, and that IGF-1, either directly or indirectly, down-regulates uPA [24]. To further explore these latter findings, we investigated a possible role for the FGFs in these processes. To optimise and confirm the specificity of our experimental approach, we exposed both N and T fibroblasts for up to 4
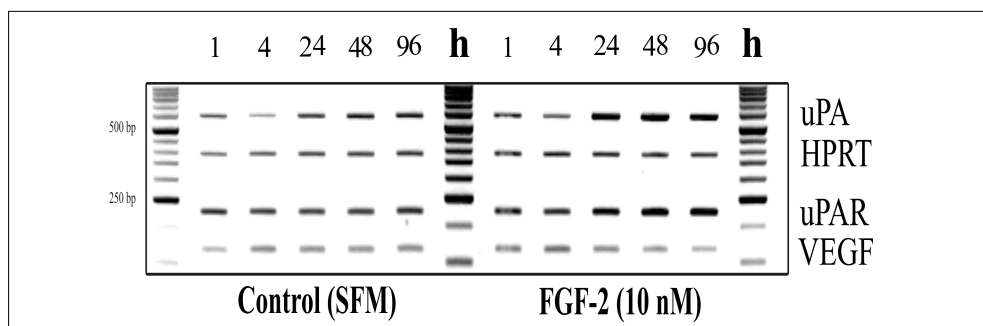
Figure 1. An example of a gel electrophoresis of RT-PCR amplified uPA, uPAR and VEGF mRNA normalised against HPRT mRNA.

Quiescent fibroblasts were cultured for up to 4 days in experimental protein-free medium in the absence (control) or presence of 10 nM FGF-2. Total RNA was isolated 1, 4, 24, 48, and 96 h after the addition of experimental medium and analysed by RT-PCR to obtain uPA, uPAR, VEGF, and HPRT mRNA. For each time-point separately, equal volumes of the different products were loaded together in one gel slot with the corresponding HPRT mRNA product to allow subsequent normalisation of the uPA, uPAR, and VEGF mRNA expression levels.
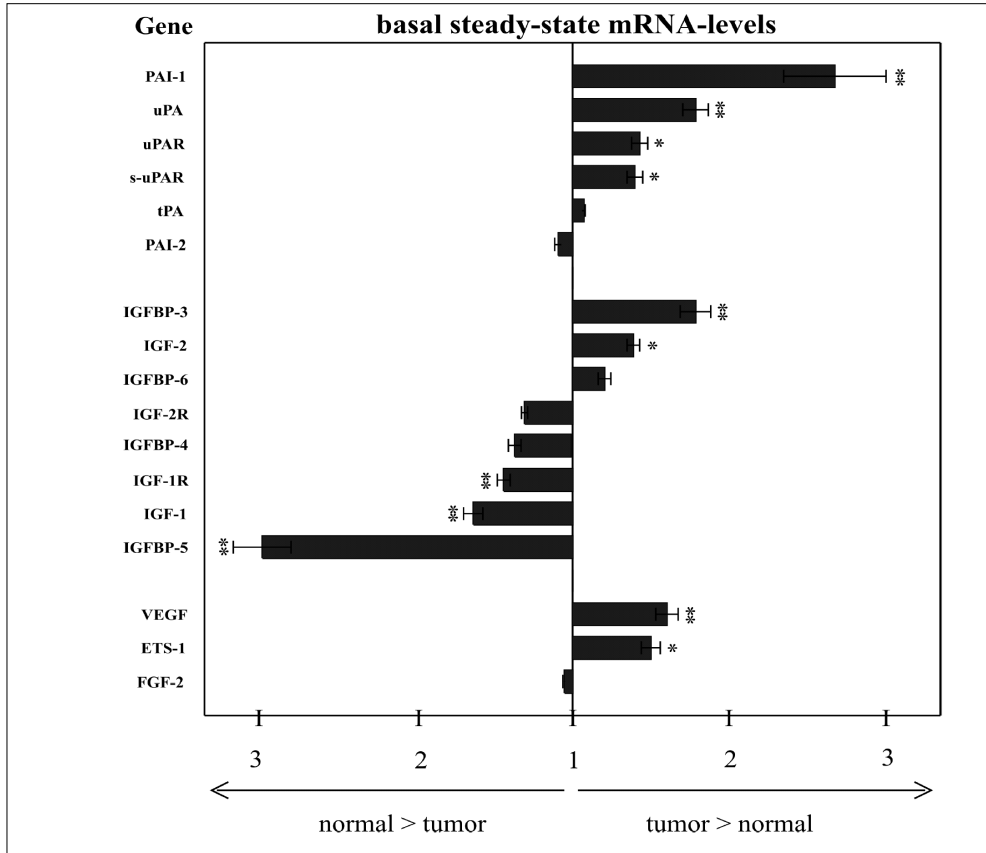
Figure 2. Comparison of basal steady-state mRNA expression levels in quiescent N and T human breast fibroblasts.
Quiescent N and T fibroblasts were cultured for up to 4 days in protein-free medium as described in the materials and methods section. Total RNA was isolated 1, 2, and 4 days after the addition of protein-free medium and analysed by RT-PCR to quantify the basal mRNA expression levels of the PA-, IGF-, and FGF-related genes as described in the materials and methods section. Bars represent the means ± SEM of the 3 time-points (days 1, 2 and 4), as obtained from 3 independent cell culture experiments, each performed in duplicate, and are expressed as fold-difference compared with the counter-part fibroblast strain. */** = significantly different from the counter-part fibroblast strain (P<0.05/P<0.01).

days to various concentrations of FGF-1 (0, 1, 2, 3.3, 10, 33 nM), FGF-2 (0, 1, 3.3, 10, 33 nM), FGF-4 (0, 1, 2, 10 nM), FGF-5 (0, 5, 10, 50 nM), and FGF-7 (0, 1, 10 nM) before measuring the amount of uPA protein released into the medium during this time. These experiments showed that neither FGF-5 nor FGF-7 were able to significantly affect the amount of uPA protein produced by these fibroblasts. In addition, as analysed by RT-PCR 1, 4, 24, 48, and 96 h after the addition of 10 nM, neither FGF-5 nor FGF-7 were able to significantly affect any of the studied mRNA levels (*uPA*, *tPA*, *uPAR*, *PAI-1*, *PAI-2*, *IGF-1*, *IGF-2*, *IGF-1R*, *IGF-2R* and *FGF-2*). Therefore we decided to further focus our experiments on FGF-1, FGF-2, and FGF-4. For all three, a time- and dose-dependent induction of uPA protein and *uPA* mRNA was observed, peaking between 24 and 48 h and reaching a plateau at the 10 nM concentration (data not shown). The data presented in Figure 3 show that with 10 nM FGF-1, FGF-2, or FGF-4, the levels of uPA protein released into the culture medium during 4 days peaked between 24

Figure 3. FGF-1, FGF-2, and FGF-4 induced effects on uPA mRNA and uPA protein..
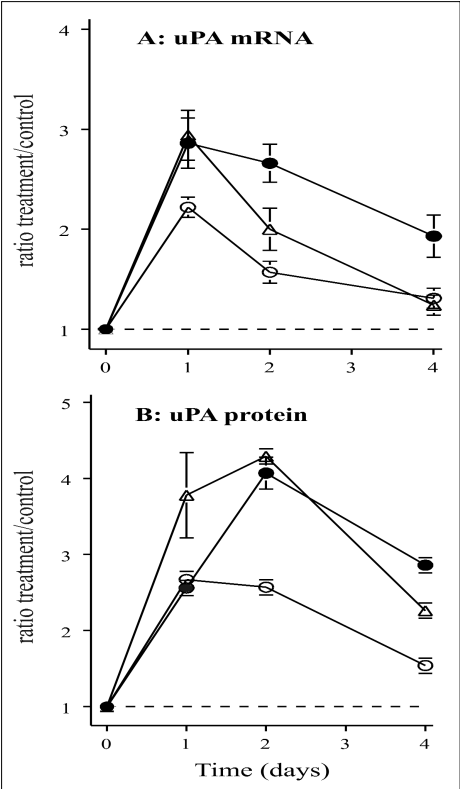*Quiescent N fibroblasts were cultured for up to 4 days in experimental protein-free medium in the absence (control: - - -) or presence of 10 nM FGF-1 (-○-), 10 nM FGF-2 (-●-), or 10 nM FGF-4 (-Δ-). Total RNA and conditioned medium were isolated 1, 2, and 4 days after the addition of experimental medium and analysed by RT-PCR and ELISA to quantify uPA mRNA expression levels (panel A) and accumulated uPA protein release into the culture medium (panel B). Data are expressed as ratio treatment/control ± SD of one cell culture experiment performed in duplicate. Similar results were obtained in other experiments with T fibroblasts.*

Table 2. Neutralisation of FGF-induced effects on uPA and uPAR mRNA.

	uPA mRNA (treatment/control)			uPAR mRNA (treatment/control)		
Addition	+ anti-FGF	+ FGF	+ FGF + anti-FGF	+ anti-FGF	+ FGF	+ FGF + anti-FGF
(anti-) FGF-1	0.8 ± 0.1	1.7 ± 0.2*	0.8 ± 0.0▪	0.8 ± 0.1	2.8 ± 0.3*	1.1 ± 0.1▪
(anti-) FGF-2	0.6 ± 0.0*	2.3 ± 0.1*	1.1 ± 0.4▪	0.8 ± 0.2	2.6 ± 0.6*	1.2 ± 0.4▪
(anti-) FGF-4	1.1 ± 0.2	3.0 ± 0.5*	2.2 ± 0.4▪	0.9 ± 0.2	3.7 ± 0.4*	1.8 ± 0.2▪
(anti-) FGF-7	0.9 ± 0.1	1.0 ± 0.0	1.0 ± 0.1	0.8 ± 0.2	1.0 ± 0.2	0.8 ± 0.2

Culture conditions of T fibroblasts exposed for 48 h to FGFs at the minimal dose required to elicit an uPA-inducing effect (2 nM FGF-1, 1 nM FGF-2, 1 nM FGF-4, and a high dose of 10 nM FGF-7) in the absence or presence of specific neutralising antibodies to block these FGF-induced effects, were as described in the materials and methods section. For controls, FGFs and anti-FGFs were replaced for the proper vehicles (rabbit and goat IgG at the same concentrations used for the neutralising antibodies). RT-PCR analysis of uPA and uPAR mRNA expression was performed as described in the materials and methods section. Data shown are those of one experiment performed in duplicate, expressed as mean ratio treatment/control ± SD.
* = significantly different from controls cultured in the absence of (anti-)FGF;
▪ = significantly different from controls cultured in the presence of FGF ($P<0.05$).

and 48 h (Figure 3B), and mimicked the levels of *uPA* mRNA measured in these cultures, that reached an optimum at 24 h (Figure 3A).

To verify the specificity of the FGF-induced effects, we cultured the human breast T fibroblasts for 48 h in the absence and presence of FGFs at the minimal dose required to elicit a uPA-inducing effect (2 nM FGF-1, 1 nM FGF-2, 1 nM FGF-4, and as a control a high dose of 10 nM FGF-7), and studied the ability of specific neutralising antibodies to block these FGF-induced effects. While neither FGF-7 nor anti-FGF-7 affected *uPA* and *uPAR* mRNA levels, all other antibodies were able to significantly inhibit the 1.7 to 3.7-fold FGF-mediated increases in *uPA* and *uPAR* mRNA levels by 25-100% (Table 2). Judged by the effects of the antibodies on the basal *uPA* mRNA expression levels in the control cultures (40% inhibition in *uPA* mRNA), these fibroblasts expressed basal *uPA*-inducing FGF-2 activity.

Differential effects of FGF-1, FGF-2, and FGF-4

Having established the optimal dose of 10 nM and the specificity of the FGF-1, FGF-2, and FGF-4 induced effects, we next investigated the effects of these FGFs on the expression of PA- and IGF-related mRNA transcripts. Despite the differences in the basal steady-state mRNA levels between N and T human breast fibroblasts (Figure 2), no differences were observed between the responses of N fibroblasts to FGFs compared with those exhibited by the T fibroblasts. Therefore, the results of the experiments with N and T fibroblasts were combined. Figure 4 shows the kinetics of the mRNA expression levels as a result of incubation with FGF-1 and FGF-2. These graphs clearly show an inverse relation between the mRNA expression levels of the components of the PA system (Figure 4A) and several of those of the IGF system (Figure 4B) following stimulation with FGF-1 and FGF-2. A FGF-1- and FGF-2-induced up to 3-fold up-regulation of mRNA levels of components of the PA system was accompanied by an up to 8-fold down-regulation of IGF-1 and an up to 2-fold down-regulation of *IGF-1R*, *IGF-2R*, and *IGFBP-4* mRNA levels. Interestingly,
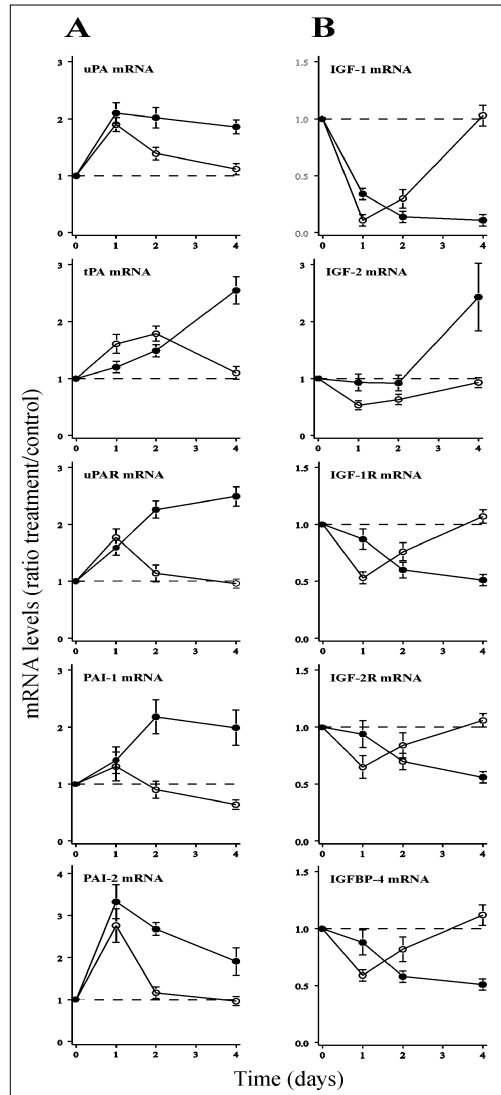
Figure 4. Differential effects of FGF-1 and FGF-2 on PA- and IGF-related mRNA levels.

Quiescent N and T fibroblasts were cultured for up to 4 days in experimental protein-free medium in the absence (control: - - -) or presence of 10 nM FGF-1 (-○-) or 10 nM FGF-2 (-●-). Total RNA was isolated 1, 2, and 4 days after the addition of experimental medium and analysed by RT-PCR to quantify the PA-related (panel A) and IGF-related (panel B) mRNA expression levels. No differences were observed between the responses of N fibroblasts to FGFs compared with those exhibited by the T fibroblasts. Therefore, the results of the experiments with N and T fibroblasts are combined in these figures. Data are expressed as ratio treatment/control ± SEM of 6 independent cell culture experiments (n=3 for both N and T fibroblasts), each performed in duplicate.

the effects elicited on *IGF-2* mRNA levels diverged distinctly between FGF-1 and FGF-2 (Figure 4B). Both FGF-1 and FGF-2 were unable at any of the time-points to elicit a more then 1.5-fold difference in the mRNA levels of *IGFBP-3*, *IGFBP-5* and *IGFBP-6* compared with controls (data not shown).

Despite the comparable up- and down-regulations mediated by both FGF-1 and FGF-2, the curves do show a time-dependent divergence in the effects elicited by FGF-1 when compared with those elicited by FGF-2. FGF-1 is able to induce PA-related mRNA levels within 1 day, followed by a rapid decrease back to base-line levels. The FGF-2-induced effects tend to increase further after the first day where after they remain relatively stably increased for up to 4 days. Similarly, although both FGF-1 and FGF-2 reduce *IGF-1*, *IGF-1R*, *IGF-2R* and *IGFBP-4* mRNA levels, these effects are rapid and short-term when elicited by FGF-1. The FGF-2-mediated inhibitions on these mRNAs on the other hand, overall lag behind for one day before they remain stably reduced for up to 4 days. For FGF-4 an in-between pattern of time-dependent inductions and reductions emerged for these mRNAs when compared with those elicited by FGF-1 and FGF-2 (data not shown).

Effect of blocking RNA synthesis on FGF-1- and FGF-2-induced uPA expression

Our results thus far indicate a time-dependent difference in the effects elicited by FGF-1 compared with those elicited by FGF-2, with the effects of FGF-1 being rapid and short-term and those of FGF-2 overall lagging behind but longer-lasting. This raised the question whether FGF-1 and FGF-2 utilise different pathways and/or whether an additional signal-transduction pathway might be involved. To address this question at the transcriptional level, we pre-incubated fibroblasts for 15 min with the transcription inhibitor actinomycin D (ACT) or vehicle control, followed by an additional 24 h culturing in the absence or presence of FGF-1 or FGF-2. While ACT did not change the *uPA* mRNA stability in unstimulated control cultures

(data not shown), both FGF-1 and FGF-2 completely lost their ability to stimulate *uPA* mRNA synthesis after pre-incubation with ACT (Figure 5A) as well as their full ability to stimulate the amount of uPA protein released into the culture medium (Figure 5B). Similarly, all the other inductions and reductions elicited by FGF-1 and FGF-2 on the mRNA levels shown in Figure 4 were completely nullified after pre-incubation with ACT (data not shown). This indicated that the FGF-1- and FGF-2-mediated short-term effects investigated in this study were the result of altered gene transcription or altered mRNA stability. In our culturing system the fibroblasts were extremely sensitive to ACT. Once exposed to ACT, even for only 15 min, we were unable to culture these fibroblasts for longer than 24 h without affecting their ability to stay adherent to the culture surface. Therefore, the prolonged effects elicited by FGF-2 on the various mRNA levels compared with the effects elicited by FGF-1 could as such not be addressed by these experiments.

Effect of blocking protein synthesis on FGF-1- and FGF-2-induced uPA expression

To address the existence of possible different pathways at the translational level, we cultured quiescent and FGF-activated fibroblasts for up to 48 h in the absence and presence of the translation inhibitor cycloheximide (CHX). Adherence to the culture surface only became a problem for fibroblasts cultured for over 48 h in the continuous presence of CHX. All FGF-1- and FGF-2-mediated alterations on the PA- and IGF-related mRNAs were annulled in cultures treated for 24 and 48 h with CHX compared with control cultures. Therefore, all the observed short-term (24 h) and longer-term (48 h) effects mediated by both FGF-1 and FGF-2 had to be triggered by proteins that required *de novo* synthesis. As an example, the results of the 24 h incubation in the presence of CHX on the expression levels of *uPA* mRNA are presented in Figure 6A, and on the amount of uPA protein released into the culture medium during this 24 h in Figure 6B. However, a difference between FGF-1- and FGF-2-induced effects emerged for
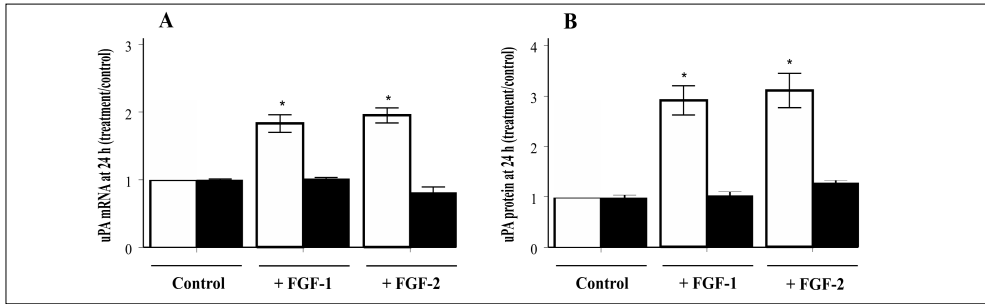
Figure 5. FGF-1 and FGF-2 mediated changes in uPA mRNA and protein levels after blocking gene transcription.
Quiescent N and T fibroblasts, pre-incubated for 15 min with 5 µg/ml ACT (black bars) or with the vehicle only (open bars), were cultured for an additional 24 h in fresh protein-free and ACT-free medium in the absence (control) or presence of 10 nM FGF-1 or 10 nM FGF-2. Total RNA and conditioned medium were isolated 24 h after the addition of experimental medium and analysed by RT-PCR and ELISA to quantify uPA mRNA expression levels (panel A) and uPA protein release into the culture medium (panel B). No differences were observed between the responses of N fibroblasts to FGFs compared with those exhibited by the T fibroblasts. Therefore, the results of the experiments with N and T fibroblasts are combined in these figures. Data are expressed as ratio treatment/control ± SEM of 5 independent cell culture experiments (n=2 for N and n=3 for T fibroblasts), each performed in duplicate. * = significantly different from controls cultured in the absence or presence of ACT (P<0.05).
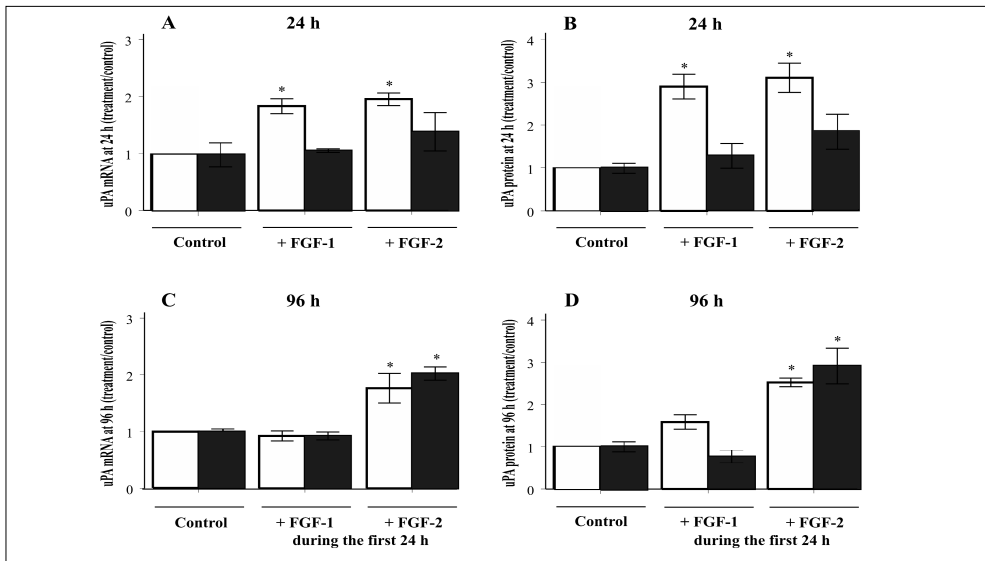
Figure 6. FGF-1 and FGF-2 mediated changes in uPA mRNA and protein levels after blocking mRNA translation.
Quiescent N and T fibroblasts were cultured for 24 h, either in the presence of 50 µg/ml CHX (black bars) or in the presence of the vehicle only (open bars), in experimental medium in the absence (control) or presence of 10 nM FGF-1 or 10 nM FGF-2. Total RNA and conditioned medium were isolated 24 h (panels A and B), and 96 h (panels C and D) after the addition of experimental medium. For the latter, cultures were thoroughly washed with PBS after the 24 h incubation period and subcultured for an additional 72 h in fresh protein-free medium lacking CHX and FGFs. uPA mRNA levels and uPA protein release into the culture medium were analysed with RT-PCR and ELISA. No differences were observed between the responses of N fibroblasts to FGFs compared with those exhibited by the T fibroblasts. Therefore, the results of the experiments with N and T fibroblasts are combined in these figures. Data are expressed as ratio treatment/control ± SEM of 4 independent cell culture experiments (n=2 for N and n=2 for T fibroblasts), each performed in duplicate. * = significantly different from controls cultured in the absence or presence of CHX (P<0.05).

fibroblasts cultured for 24 h in the presence of CHX and allowed to recover for an additional 3 days in protein-free medium lacking FGF-1, FGF-2 and CHX (Figure 6C and 6D). In this case, despite the inhibition of translation during the first 24 h, FGF-2 pre-treatment was still able to induce *uPA* mRNA and protein expression as measured 3 days later. Thus, the observed long-term effects elicited by FGF-2 resulted from proteins produced or made available during the 72 h recovery period, following the 24 h incubation in the presence of CHX. Similarly, the long-term effects elicited by FGF-2 on the mRNA levels of *tPA*, *uPAR*, *PAI-1*, *PAI-2*, *IGF-1*, *IGF-2*, *IGF-1R*, *IGF-2R*, and *IGFBP-4* (see Figure 4) were not significantly affected by the presence of CHX during the first 24 h.

DISCUSSION

Results only recently published on a randomised prospective study of 556 patients with lymph node-negative breast cancer [35], confirm that uPA and PAI-1 are strong and independent prognostic factors for patients with primary breast cancer and that uPA and PAI-1 measurements are especially useful for risk-adapted individualized treatment strategies for patients with node-negative disease. These new clinically important level of evidence 1 type studies [36], clearly indicate that a better understanding of the regulation of the PA system is needed to explore these factors as targets for tumor biology-oriented therapies. Stromal involvement in tumor progression in general, and in ECM degradation in particular, is a topic of increasing interest. An understanding of the behavior of stromal fibroblasts in the process of plasminogen activator directed tumor invasion and angiogenesis might be helpful in designing future therapeutic strategies. For that purpose we investigated the FGF-mediated alterations in the mRNA levels of components related to the PA- and IGF-systems in human breast fibroblasts *in vitro*.

In the absence of exogenously added FGFs we noticed distinct mRNA expression profiles in quiescent N fibroblasts compared with T fibroblasts. While N fibroblasts expressed higher levels of mRNAs related to the IGF-1 system, T fibroblasts expressed higher levels of mRNAs related to the PA system, as well as *IGFBP-3* and *IGF-2*. Although *FGF-2* mRNA levels did not differ between N and T fibroblasts, quiescent T fibroblasts expressed higher levels of *VEGF* and *ETS-1* mRNA. These data indicate a difference between this set of human fibroblasts established from malignant breast-tumor tissue (T) and from adjacent normal breast tissue (N) of the same patient. *In vivo*, similar differences in PA-related [1, 5, 6], *IGF-1* and *IGF-2* [37], *VEGF* [38] and *ETS-1* [18] mRNA expression profiles have been observed in fibroblasts in the near vicinity of the tumor cells compared with fibroblasts located in histologically normal breast tissue. This indicates that the cultured N and T fibroblasts used in this study still displayed at large their original and distinct phenotypes. Notwithstanding, we can not exclude that other distinct phenotypical differences were not as well preserved in these cultured fibroblasts removed from their *in vivo* environment.

Despite the differences in the basal steady-state mRNA levels of N and T human breast fibroblasts, no differences were observed between the responses of the N fibroblasts to FGFs compared with those displayed by the T fibroblasts. Thus, FGFs are able to induce the various responses described in this study irrespective of the distinct phenotypes of N and T fibroblasts, suggesting that also N fibroblasts, once present in a FGF-rich environment, are at risk of becoming potent PA-producing cells. Both N and T fibroblasts exhibited a time-dependent difference in gene expression alterations elicited by FGF-1 compared with those induced by FGF-2, with the effects of FGF-1 being rapid and short-term and those of FGF-2 overall lagging behind but longerlasting. This raised the question whether FGF-1 and FGF-2 might use distinct signaling pathways. To answer this question, we performed experiments aimed at blocking transcription and translation. Blocking transcription and translation demonstrated that a) both the FGF-1- and FGF-2-induced effects were the result of altered gene transcription or mRNA stability, b) the short-term effects mediated by FGF-1 and FGF-2 required *de novo* pro-

tein synthesis, and c) even if the stimulus was removed after a 24 h incubation, the long-term effects elicited by FGF-2 remained. These data suggest that accumulated mRNAs (with long stability), which attribute to the FGF-2 signaling, can induce the prolonged effect after removal of the protein synthesis blockade. Alternatively, the long-term effects did not require the sustained presence of FGF-2 because FGF-2 was stored and released after the 24 h pre-incubation with CHX.

This latter mechanism is likely connected to the binding-kinetics of FGFs to heparan proteoglycans (HSPGs). In 3T3 mouse fibroblasts for example, active HSPGs have been shown to contribute to the increased sensitivity of these cells to FGF-2 compared to FGF-1 [39]. In MDA-MB-231 human breast cancer cells, a differential sensitivity to FGF-1 and FGF-2 has been shown to be related to their binding-kinetics to HSPG. While for FGF-1 there was only one high affinity binding site with a fast association rate (fast/high HSPG-R), for FGF-2 there was, in addition to this fast/high HSPG-R, also a lower affinity binding site with a slow association rate [15]. FGF bound to HSPG can be released by plasmin, which will increase the availability of biologically active FGF [40, 41]. Since uPA is able to convert inactive plasminogen into active plasmin [7], FGFs are able to control their own bioavailability through their action on the PA system. From the literature we deduce that the binding-kinetics of FGF-4 to HSPG are in between those of FGF-1 and FGF-2 [42]. Therefore, the differential binding of FGFs to fibroblast-associated HSPGs may very well explain the rapid but transient response to FGF-1 (one binding site for HSPG), the biphasic sustained response to FGF-2 (two binding sites for HSPG), and the intermediate response to FGF-4.

Like we showed previously for human breast fibroblasts at the level of *uPA* mRNA, uPA and PAI-1 protein, and their ability to generate plasmin [11, 24], uPA activity in the conditioned medium of osteosarcoma cells decreased significantly when they were cultured in the presence of exogenously added IGF-1 [43]. These studies are in contrast to the study of Dunn *et al.*, which

reported an up-regulation of uPA in the human breast cancer cell line MDA-MB-231 by IGF-1 [44]. The present study however confirms the negative correlation between IGF-1 and uPA in human breast fibroblasts and extends this to all components of the PA system (uPA, tPA, uPAR, PAI-1 and PAI-2) being inversely related to IGF-1, IGF-1R, IGF-2R, and IGFBP-4. The action of IGF-1 on the PA system may, like discussed by Lalou and co-workers for osteosarcoma cells [43], involve a regulatory loop whereby IGF-1 controls its own bioavailability through its action on the PA system, which regulates dissociation of IGF-1 from IGFBPs. At the cellular level IGFBPs are thought to inhibit the actions of the IGFs, but under specific circumstances they may potentiate their metabolic and mitogenic effects (reviewed in [25-28]). In this study, of the six IGFBPs examined, only *IGFBP-4* mRNA expression was notably affected by the presence of FGF-1, FGF-2, and FGF-4. Therefore, our results do not indicate that *IGFBP* mRNA expression levels in general are greatly affected by FGFs. This does however not exclude FGF-induced differences in the regulation at protein level or changes in the extracellular activities of IGFBPs. Similarly like described above for FGF-HSPG complexes, plasmin (generated through PA catalysed activation of plasminogen) is able to increase the availability of biologically active IGF in the pericellular environment by dissociation of IGF-IGFBP complexes [43, 45].

Only in case of *IGF-2* mRNA expression the effects mediated by FGF-1 (a short-term 2-fold down-regulation) and FGF-2 (a 2.5-fold up-regulation after 3 days) diverged distinctly. In various studies, high stromal-derived IGF-2 levels have been correlated with increased tumorigenicity (reviewed in [37, 46]). Our results implicate FGF-2 as a potential factor responsible for these high stromal-derived IGF-2 levels.

Several research groups have examined a possible correlation between expression levels and localisation of FGF and prognosis in patients with breast cancer [13, 29, 30, 47, 48]. Although these reports show discrepancies, possibly due to the different techniques used to assess the

expression levels and localisation of the FGFs, the overall consensus appears to be that high levels of FGF-1 and FGF-2 in human breast carcinoma are associated with good prognostic features such as low stage and small tumor size. In the micro-environment, in contrast to IGF-2, which is also produced by the epithelial tumor cells, fibroblasts are the main suppliers of IGF-1, a potent mitogen for epithelial cells [49]. From our mRNA expression data it can be deduced that FGFs are able to decrease the levels of mitogenic IGF-1 which otherwise would have been available for the breast epithelial (tumor) cells. This may be an explanation for the overall consensus that high levels of FGF are associated with favorable prognosis in patients with breast cancer. On the other hand, we have shown that FGF-2 and, although to a lesser extent, FGF-1 and FGF-4 are powerful inducers of the PA system in these fibroblasts, which would indicate a poor prognosis (reviewed in [8-10]). This might suggest that the balance of the FGF-induced effects on the IGF-system (decrease in production of mitogens for tumor cells = good prognosis) and PA-system (increase in production of factors associated with migration, invasion, and angiogenesis = poor prognosis) is of influence on the overall prognosis.

In conclusion, our data show that FGFs differentially affect the mRNA expression of components related to the PA and IGF systems in human breast fibroblasts. Furthermore, the data imply that of the FGFs studied, especially FGF-2 may be an effective target for therapeutical strategies aimed at diminishing the contribution of stromal fibroblasts in the PA-directed breast tumor proteolysis.

ACKNOWLEDGEMENT

REFERENCES

1. Wolf C, Rouyer N, Lutz Y, Adida C, Loriot M, Bellocq JP, Chambon P, Basset P. Stromelysin 3 belongs to a subgroup of proteinases expressed in breast carcinoma fibroblasts cells and possibly implicated in tumor progression. Proc Natl Acad Sci USA 1993;90: 1843-7.

2. Basset P, Bellocq JP, Wolf C, Stoll I, Hutin P, Limacher JM, Podhajcer OL, Chenard MP, Rio MC, Chambon P. A novel metalloproteinase gene specifically expressed in stromal cells of breast carcinomas. Nature 1990;348:699-704.

3. Uría JA, Stahle-Bäckdahl M, Seiki M, Fueyo A, López-Otin C. Regulation of collagenase-3 expression in human breast carcinomas is mediated by stromal-epithelial cell interactions. Cancer Res 1997;57: 4882-8.

4. Okada A, Bellocq JP, Rouyer N, Chenard MP, Rio MC, Chambon P, Basset P. Membrane-type matrix metalloproteinase (MT-MMP) gene is expressed in stromal cells of human colon, breast, and head and neck carcinomas. Proc Natl Acad Sci USA 1995;92:2730-4.

5. Rømer J, Pyke C, Lund LR, Eriksen J, Kristensen P, Rønne E, Høyer- Hansen G, Danø K, Brünner N. Expression of uPA and its receptor by both neoplastic and stromal cells during xenograft invasion. Int J Cancer 1994;57:553-60.

6. Nielsen BS, Sehested M, Tiomshel S, Pyke C, Danø K. Messenger RNA for urokinase plasminogen activator is expressed in myofibroblasts adjacent to cancer cells in human breast cancer. Lab Invest 1996;74:168-77.

7. Andreasen PA, Egelund R, Petersen HH. The plasminogen activation system in tumor growth, invasion, and metastasis. Cell Mol Life Sci 2000;57:25-40.

8. Duffy MJ, Duggan C, Maguire T, Mulcahy K, Elvin P, McDermott E, Fennelly JJ, O'Higgins N. Urokinase plasminogen activator as a predictor of aggressive disease in breast cancer. Enzyme Protein 1996;49:85-93.

9. Schmitt M, Harbeck N, Thomssen C, Wilhelm O, Magdolen V, Reuning U, Ulm K, Höfler H, Jänicke F, Graeff H. Clinical impact of the plasminogen activation system in tumor invasion and metastasis: prognostic relevance and target for therapy. Thromb Haemost 1997; 78:285-96.

10. Look MP, Foekens JA. Clinical relevance of the urokinase plasminogen activator system in breast cancer. Apmis 1999;107:150-9.

11. Sieuwerts AM, Klijn JG, Henzen-Logmans SC, Foekens JA. Cytokine-regulated urokinase-type-plasminogen-activator (uPA) production by human breast fibroblasts *in vitro*. Breast Cancer Res Treat 1999; 55:9-20.

12. Coope RC, Browne PJ, Yiangou C, Bansal GS, Walters J, Groome N, Shousha S, Johnston CL, Coombes RC, Gomm JJ. The location of acidic fibroblast growth factor in the breast is dependent on the activity of proteases present in breast cancer tissue. Br J Cancer 1997;75: 621-30.

13. Visscher DW, DeMattia F, Ottosen S, Sarkar FH, Crissman JD. Biologic and clinical significance of basic fibroblast growth factor immunostaining in breast carcinoma. Mod Pathol 1995;8:665-70.

14. Quarto N, Amalric F. Heparan sulfate proteoglycans as transducers of FGF- 2 signalling. J Cell Sci 1994; 107: 3201-12.

15. Fernig DG, Chen HL, Rahmoune H, Descamps S, Boilly B, Hondermarck H. Differential regulation of FGF-1 and -2 mitogenic activity is related to their kinetics of binding to heparan sulfate in MDA-MB-231 human breast cancer cells. Biochem Biophys Res Commun 2000;267:70-6.

16. Sperinde GV, Nugent MA. Mechanisms of fibroblast growth factor 2 intracellular processing: a kinetic analysis of the role of heparan sulfate proteoglycans. Biochemistry 2000;39:3788-96.

17. Johnson DE, Williams LT. Structural and functional diversity in the FGF receptor multigene family. Adv Cancer Res 1993;60:1-41.

18. Wernert N, Gilles F, Fafeur V, Bouali F, Raes MB, Pyke C, Dupressoir T, Seitz G, Vandenbunder B, Stehelin D. Stromal expression of c-Etsl transcription factor correlates with tumor invasion. Cancer Res 29994;54:5683-8.

19. D'Orazio D, Besser D, Marksitzer R, Kunz C, Hume DA, Kiefer B, Nagamine Y. Cooperation of two PEA3/AP1 sites in uPA gene induction by TPA and FGF-2. Gene 1997;201:179-87.

20. Kitange G, Shibata S, Tokunaga Y, Yagi N, Yasunaga A, Kishikawa M, Naito S. Ets-1 transcription factor-mediated urokinase-type plasminogen activator expression and invasion in glioma cells stimulated by serum and basic fibroblast growth factors. Lab Invest 1999;79:407-16.

21. Pepper MS, Sappino AP, Stocklin R, Montesano R, Orci L, Vassalli JD. Upregulation of urokinase receptor expression on migrating endothelial cells. J Cell Biol 1993;122:673-84.

22. Sandberg T, Eriksson P, Gustavsson B, Casslen B. Differential regulation of the plasminogen activator inhibitor-1 (PAI-1) gene expression by growth factors and progesterone in human endometrial stromal cells. Mol Hum Reprod 1997;3:781-7.

23. Mandriota SJ, Pepper MS. Vascular endothelial growth factor-induced *in vitro* angiogenesis and plasminogen activator expression are dependent on endogenous basic fibroblast growth factor. J Cell Sci 1997;110:2293-302.

24. Sieuwerts AM, Klijn JG, Foekens JA. Insulin-like growth factor 1 (IGF-1) and urokinase-type plasminogen activator (uPA) are inversely related in human breast fibroblasts. Mol Cell Endocrinol 1999;154:179-85.

25. O'Connor R. Survival factors and apoptosis. Adv Biochem Eng Biotechnol 1998;62:137-66.

26. Baxter RC. Insulin-like growth factor (IGF)-binding proteins: interactions with IGFs and intrinsic bioactivities. Am J Physiol Endocrinol Metab 2000;278: E967-76.

27. Butt AJ, Firth SM, Baxter RC. The IGF axis and programmed cell death. Immunol Cell Biol 1999;77: 256-62.

28. Lee AV, Hilsenbeck SG, Yee D. IGF system components as prognostic markers in breast cancer. Breast Cancer Res Treat 1998;47:295-302.

29. Smith J, Yelland A, Baillie R, Coombes RC. Acidic and basic fibroblast growth factors in human breat tissue. Eur J Cancer 1994;4:496-503.

30. Anandappa SY, Winstanley JH, Leinster S, Green B, Rudland PS, Barraclough R. Comparative expression of fibroblast growth factor mRNAs in benign and malignant breast disease. Br J Cancer 1994;69:772-6.

31. Penault-Llorca F, Bertucci F, Adelaide J, Parc P, Coulier F, Jacquemier J, Birnbaum D, de Lapeyriere O. Expression of FGF and FGF receptor genes in human breast cancer. Int J Cancer 1995;61:170-6.

32. van Roozendaal CEP, van Ooijen B, Klijn JGM, Claassen C, Eggermont AMM, Henzen-Logmans SC, Foekens JA. Stromal influences on breast cancer cell growth. Br J Cancer 1992;65:77-81.

33. van Roozendaal CEP, Klijn JGM, van Ooijen B, Claassen C, Eggermont AMM, Henzen-Logmans SC, Foekens JA. Transforming growth factor beta secretion from primary breast cancer fibroblasts. Mol Cell Endocrinol 1995;111:1-6.

34. Grebenschikov N, Geurts-Moespot A, De Witte H, Heuvel J, Leake R, Sweep F, Benraad T. A sensitive and robust assay for urokinase and tissue-type plasminogen activators (uPA and tPA) and their inhibitor type I (PAI-1) in breast tumor cytosols. Int J Biol Markers 1997;12:6-14.

35. Jänicke F, Prechtl A, Thomssen C, Harbeck N, Meisner C, Untch M, Sweep CG, Selbmann HK, Graeff H, Schmitt M. Randomized adjuvant chemotherapy trial in high-risk, lymph node-negative breast cancer patients identified by urokinase-type plasminogen activator and plasminogen activator inhibitor type 1. J Natl Cancer Inst 2001;93:913-20.

36. Hayes DF, Bast RC, Desch CE, Fritsche H, Jr., Kemeny NE, Jessup JM, Locker GY, Macdonald JS, Mennel RG, Norton L, Ravdin P, Taube S, Winn RJ. Tumor marker utility grading system: a framework to evaluate clinical utility of tumor markers. J Natl Cancer Inst 1996;88: 456-66.

37. Rasmussen AA, Cullen KJ. Paracrine/autocrine regulation of breast cancer by the insulin-like growth factors. Breast Cancer Res Treat 1998;47:219-33.

38. Speirs V, Atkin SL. Production of VEGF and expression of the VEGF receptors Flt-1 and KDR in primary cultures of epithelial and stromal cells derived from breast tumours. Br J Cancer 1999;80:898-903.

39. Zhou FY, Owens RT, Hermonen J, Jalkanen M, Hook M. Is the sensitivity of cells for FGF-1 and FGF-2 regulated by cell surface heparan sulfate proteoglycans? Eur J Cell Biol 1997;73:166-74.

40. Saksela O, Rifkin DB. Release of basic fibroblast growth factor-heparan sulfate complexes from endothelial cells by plasminogen activator-mediated proteolytic activity. J Cell Biol 1990;110:767-75.

41. Ribatti D, Leali D, Vacca A, Giuliani R, Gualandris A, Roncali L, Nolli ML, Presta M. In vivo angiogenic activity of urokinase: role of endogenous fibroblast growth factor-2. J Cell Sci 1999;112:4213-21.

42. Guimond S, Maccarana M, Olwin BB, Lindahl U, Rapraeger AC. Activating and inhibitory heparin sequences for FGF-2 (basic FGF). Distinct requirements for FGF-1, FGF-2, and FGF-4. J Biol Chem 1993;268: 23906-14.

43. Lalou C, Silve C, Rosato R, Segovia B, Binoux M. Interactions between insulin-like growth factor-I (IGF-I) and the system of plasminogen activators and their inhibitors in the control of IGF-binding protein-3 production and proteolysis in human osteosarcoma cells. Endocrinology 1994;135:2318-26.

44. Dunn SE, Torres JV, Oh JS, Cykert DM, Barrett JC. Up-regulation of urokinase-type plasminogen activator by insulin-growth factor-I depends upon phosphatidyl-inositol-3 kinase and mitogen-activated protein kinase kinase. Cancer Res 2001;61:1367-74.

45. Campbell PG, Novak JF, Yanosick TB, McMaster JH. Involvement of the plasmin system in dissociation of the insulin-like growth factor-binding protein complex. Endocrinology 1992;130:1401-12.

46. Hasnain M, Khndwala HM, McCutcheon IE, Flyvbjerg A, Friendl KE. The effects of insulin-like growth factors on tumorigenesis and neoplastic growth. Endocr Rev 2000;21:215-44.

47. Colomer R, Aparicio J, Montero S, Guzman C, Larrodera L, Cortes-Funes H. Low levels of basic fibroblast growth factor (bFGF) are associated with a poor prognosis in human breast carcinoma. Br J Cancer 1997;76:1215-20.

48. Yiangou C, Gomm JJ, Coope RC, Law M, Luqmani YA, Shousha S, Coombes RC, Johnston CL. Fibroblast growth factor 2 in breast cancer: occurrence and prognostic significance. Br J Cancer 1997;75:28-33.

49. Rosen N, Yee D, Lippman ME, Paik S, Cullen KJ. Insulin-like growth factors in human breast cancer. Breast Cancer Res Treat 1991;18 Suppl 1:S55-62.

50. Pyke C, Eriksen J, Solberg H, Nielsen BS, Kristensen P, Lund LR, Danø K. An alternatively spliced variant of mRNA for the human receptor for urokinase plasminogen activator. FEBS Lett 1993;326:69-74.

51. Prats H, Kaghad M, Prats AC, Klagsbrun M, Lelias JM, Liauzun P, Chalon P, Tauber JP, Amalric F, Smith JA, *et al*. High molecular mass forms of basic fibroblast growth factor are initiated by alternative CUG codons. Proc Natl Acad Sci USA 1989;86:1836-40.

52. Neufeld G, Cohen T, Gitay-Goren H, Poltorak Z, Tessler S, Sharon R, Gengrinovitch S, Levi BZ. Similarities and differences between the vascular endothelial growth factor (VEGF) splice variants. Cancer Metastasis Rev 1996;15:153-8.

53. Jorcyk CL, Watson DK, Mavrothalassitis GJ, Papas TS. The human ETS1 gene: genomic structure, promoter characterization and alternative splicing. Oncogene 1991;6:523-32.

54. Jansen M, van Schaik FM, Ricker AT, Bullock B, Woods DE, Gabbay KH, Nussbaum AL, Sussenbach JS, Van den Brande JL. Sequence of cDNA encoding human insulin-like growth factor I precursor. Nature 1983;306:609-11.

CHAPTER THREE

Aging of stromal-derived human breast fibroblasts might contribute to breast cancer progression

John W. M. Martens[1], Anieta M. Sieuwerts[1], Joan Bolt-de Vries[1], Peter T. Bosma[1], Susan J. J. Swiggers[2], Jan G. M. Klijn[1] and John A. Foekens[1]

[1]Department of Medical Oncology, Erasmus MC, Rotterdam, The Netherlands
[2]Department of Haemotology, Erasmus MC, Rotterdam, The Netherlands

ABSTRACT

Age is an important factor in the development and spread of breast cancer. Stromal cells also contribute to breast cancer growth and metastasis through the production of extracellular matrix (ECM) modifiers such as urokinase type plasminogen activator (uPA), its receptor (uPAR), its inhibitors (PAI-1 and PAI-2), matrix metalloproteinases (MMPs), and growth factors, including the fibroblast and insulin-like growth factors (FGFs and IGFs). In the present study we have investigated whether breast fibroblasts aged *in vitro* through passage in culture display altered levels of the plasminogen activator system and growth factors that are known to modulate that system.

With real-time RT-PCR we found that during passage human breast fibroblasts, whether derived from the tumor burden or from matched adjacent normal breast tissue, exhibited a consistent increase in *PAI-1* and *FGF-1* and a decrease in *MMP-2* mRNA expression. In addition, in 5 out of 7 fibroblast strains we observed an induction of *uPA* expression in combination with a reduced *IGF-1* expression. Interestingly, while during aging MMP-2 protein increased in all tumor-derived fibroblast strains, these protein levels were reduced in all normal-tissue-derived fibroblasts. No other clear-cut age-dependent alterations were found in the all-together 26 factors investigated. We furthermore demonstrate in one tumor-derived fibroblast strain that the increases in *uPA* and *PAI-1* mRNA and MMP-2 protein production are inversely related to the telomere length. Artificially increasing telomere length in this fibroblast strain by expressing human telomerase reverse transcriptase (*hTERT*) prevented senescence and resulted in late passage cultures with early passage *uPA*, *PAI-1* and MMP-2 levels.

Our results show that aging accompanied by telomere loss induces *PAI-1* and *FGF-1* and reduces *MMP-2* mRNA expression in all breast fibroblast strains, increases *uPA* and decreases *IGF-1* mRNA expression in a subset, and increases MMP-2 protein expression only in tumor-derived breast fibroblasts. These age-induced levels of *PAI-1*, *FGF-1*, *uPA* and MMP-2 in stromal breast fibroblast could contribute to breast cancer progression.

INTRODUCTION

ECM modifiers such as uPA, its receptor uPAR and its inhibitor PAI-1, MMPs, and cathepsins, are linked to poor prognosis in breast cancer [1-8]. Interestingly, the expression of these remodelling proteins is not always increased in the tumor cells but quite often in the adjacent stromal tissue [9-14]. Some of those (PAI-1, uPA, MMP-2, MMP-9, MMP-11 and MMP-13) are particularly increased in stromal cells that border the expanding tumor [11-16]. The pivotal role of these stromal derived matrix remodelling proteins in cancer biology is underscored in knock out mice models where in the absence of stromal uPA, PAI-1, MMP-2 or MMP-9, tumor growth and/or spread to distant locations is clearly impaired [17-20]. Thus, the local microenvironment is an important driving force stimulating the invasive and malignant behavior of primary tumor cells [21-26].

Age is an important risk factor in many cancers, including breast cancer, but its role in cancer has predominantly been linked to the accumulation of DNA damage in the primary tumor [27]. Much less attention has been paid to the role of stromal cells in this process. In contrast, delayed wound healing and impaired migration in the skin as a result of aging has been ascribed to altered levels of stromal ECM modulators [28]. Furthermore, skin fibroblasts aged *in vitro* to senescence secrete increasing amounts of uPA, PAI-1, MMPs and tissue inhibitors of MMPs (TIMP) [29-34]. Similar to wound healing and migration, breast cancer growth and metastasis require ECM remodelling processes. Thus, age related changes in the urokinase system might contribute to metastasis in the breast. The contribution of aging to breast cancer growth and

Table 1. Intron-spanning primers used for quantitative real-time RT-PCR.

Gene	Forward primer	Reverse primer	Product size
uPA	AGAATTCACCACCATCGAG	ATCAGCTTCACAACAGTCAT	474
uPAR	AATGGCCGCCAGTGTTACAG	CAGGAGACATCAATGTGGTTC	227
s-uPAR	AATGGCCGCCAGTGTTACAG	CCAGCTTCCCCAGAGTGAG	144
PAI-1	GCTGGTGAATGCCCTCTAC	GGCAGCCTGGTCATGTTG	318
PAI-2	GGGTCAAGACTCAAACCAAAG	CCTTTGAAGTAGACAGCATTC	103
IGF-1	TGGTGGATGCTCTTCAGTTC	GACAGAGCGAGCTGACTTG	191
IGF-2	GCGGCTTCTACTTCAGCAG	CAGGTGTCATATTGGAAGAAC	214
IGF1-R	AATCCCCATCAGGAAGTATG	TATCCACTCTGCTCTCAAAG	350
IGFBP-2	CTGGAGGAGCCCAAGAAG	GCCATGCTTGTCACAGTTG	162
IGFBP-3	CCCTCCATTCAAAGATAATC	TCCACACACCAGCAGAAG	298*
IGFBP-5	GGGTTTGCCTCAACGAAAAG	TTTCTGCGGTCCTTCTTCAC	180
IGFBP-6	GCGTGGAGGAGGAGGATG	TGGTAGAGGTGCCTGGATTC	306
TGF-β1	GCCCTGGACACCAACTATTG	CGTGTCCAGGCTCCAAATG	168
FGF-1	ACAAGGGACAGGAGCGAC	TCCAGCCTTTCCAGGAACA	171
FGF-2	GAGCGACCCTCACATCAAG	TTTCAGTGCCACATACCAAC	220
FGF-7	CATGGAAGGAGGGGATATAAG	CCTTTTGATTTAAGGCAACAAAC	338
TSP-1	CTGCTCCAATGCCACAGTTC	GGAGCCCTCACATCGGTTG	178
ETS-1	GTTAATGGAGTCAACCCAGC	GGGTGACGACTTCTTGTTTG	274
HGF	ATTACTGCCGAAATCCAGATG	CACTGTCGTGCAGTAAGAAC	292
EMMPRIN	TCACTACCGTAGAAGACCTTG	TCCCCCTCGTTGATGTGTTC	280
VEGF	TACCTCCACCATGCCAAG	GGTACTCCTGGAAGATGTC	148
MMP-2	CGCAGTGACGGAAAGATGTG	TGGGACAGACGGAAGTTCTTG	203
MMP-9	TGCCCGGACCAAGGATACAG	GGCACTGAGGAATGATCTAAG	83
HPRT	TATTGTAATGACCAGTCAACAG	GGTCCTTTTCACCAGCAAG	192

1 mM MgCl$_2$ added to the final 25 µl PCR mixture.

metastasis was recently underlined by demonstrating that senescent fibroblasts stimulated *in vitro* growth of mouse and human mammary epithelial cells more efficiently when compared to younger fibroblasts [35]. Similarly, in mice senescent human fibroblasts stimulated epithelial mammary tumor cell growth more effectively than young fibroblasts [35]. To follow-up on this work, we studied changes in factors related to the plasminogen activator system in aging human breast fibroblasts.

In the past we have isolated different sets of breast fibroblast strains derived from the primary tumor and from normal breast tissue adjacent to the tumor of the same patient. In these strains, we determined expression of components of the IGF and urokinase system and showed that the levels of these components can be modulated by several known growth factors including FGF-1, -2 and -4, TGF-ß$_1$ and IGF-1 [36-38].

In the present study we have used *in vitro* passaging of these normal- and tumor-tissue-derived breast fibroblast strains as a model system for aging *in vivo*. For this, early and late passage cultures were compared. We initially focussed on uPA but later we extended our study to other components of the urokinase system as well as modulatory factors. Since aging and subsequent senescence *in vitro* has been ascribed to telomere attrition in many different stromal cells [39], we determined telomere length decline after passaging in these strains. In order to revert the aging process, we extended telomere length in one of the fibroblast strains through the introduction of human telomerase reverse transcriptase.

The results show that upon aging all fibroblast strains induce *PAI-1* and *FGF-1* mRNA and only a subset of the strains *uPA* mRNA. Furthermore, while in tumor-derived fibroblasts the levels of MMP-2 protein increase, those meas-

ured in normal-tissue-derived fibroblasts decrease with age. In one of the strains we show that introduction of human telomerase reverse transcriptase reverts the changes in *PAI-1*, *uPA* and MMP-2, suggesting that telomere attrition with increasing passages is responsible for these inductions in this aging tumor-derived human breast fibroblast strain.

MATERIALS AND METHODS

Tissue culture

Eight different human fibroblast strains described in detail before [40] were used. The strains were established from invasive ductal breast adenocarcinoma tumor-tissue fragments (T) and from adjacent normal breast tissue (N) of the same patients. Due to the large size of the primary tumor, one patient (n° 26) received chemotherapy (FEC) before the tumor was removed. The human MDA-MB-231-BAG and MCF7-BAG breast cancer cell lines (which contain the *LacZ* gene, encoding β-galactosidase) were kindly provided by Dr. N. Brünner (Finsen Laboratory, Copenhagen, Denmark). Fibroblast strains and epithelial cell lines were maintained as described [37].

Culture of fibroblast strains in protein-free medium

Different passages and strains of normal and tumor-derived breast fibroblasts were split one to three into 162 cm² culture flasks. To deplete the cells of exogenous serum-related factors, the cells were at 90% confluence washed twice with PBS and placed overnight on serum- and protein-free medium (PFM) [37]. The next day the cells were washed again with PBS and placed on fresh PFM. After 4 days the cells were harvested for RNA and protein isolation (see below).

uPA ELISA

For uPA protein production, fibroblasts were plated in PFM in 6-well Pronectin F coated tissue culture plates (ICN Biomedicals, Cleveland, OH) as described [37]. After 4 days, PFM was replaced and cells were allowed to accumulate uPA protein for four days. After 4 days medium and cells were harvested and prepared for measurement of released and cell-bound uPA by ELISA [37, 41].

RNA isolation, cDNA synthesis and quantification of specific mRNA species

Total RNA was extracted with RNAzol B (Campro, Veenendaal, The Netherlands) according to the manufacturer from fibroblasts cultured as described above. Total RNA (6 μg) was reverse-transcribed using oligo(dT)12-18 and random hexamer primers (Superscript RNAse H- kit, Invitrogen, Breda, The Netherlands) according to the manufacturer's instruction. Copy DNA samples were treated with RNase H- (Promega, Leiden, The Netherlands). Real-time quantitative PCR was performed in an ABI Prism 7700 apparatus (Applied Biosystems, Foster City, USA) using for each cDNA quantified the intron-spanning forward and reverse primer combination (Table 1). The PCR products were generated in 35-40 cycles of 15 s denaturing at 95° C, 30 s annealing at 62° C, 20 s extension at 72° C and an additional 20 s extension at 79° C in a volume of 25 μl containing 30 ng cDNA, 330 nM forward and reverse primer and 12.5 μl SYBR-green PCR-master-mixture (Applied Biosystems). Depending on the melting temperature of the products, SYBR-green fluorescent signals were acquired after each cycle at 72° C or at 79° C. The size of each PCR product was initially verified as well as the efficiency of amplification. Each run included a calibration curve of a serial diluted cDNA pool of human breast fibroblasts and cell lines. Cycle threshold (Ct) values were obtained at a fixed threshold value of 0.02. For all individual cDNAs, amplification of each specific mRNA sequence was performed in at least 2 independently performed PCR experiments. The errors in duplicates were always less than 25%, else the PCR was repeated. Target gene levels were calculated as the mean mRNA-level relative to the housekeeping gene hypoxanthine-guanine phosphoribosyltransferase (*HPRT*) using Ct values

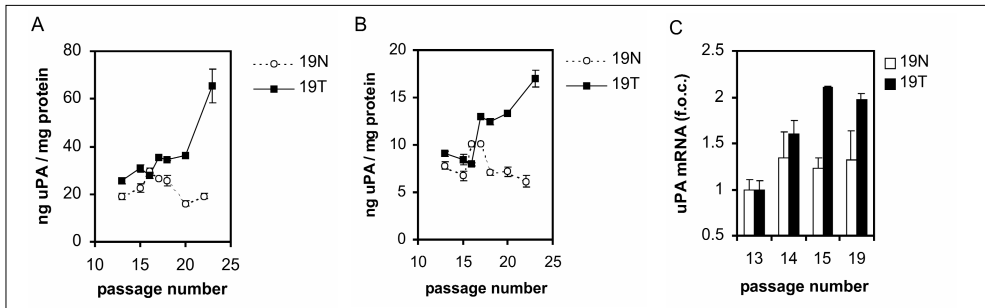(mRNA target = $2^{(\text{mean Ct HPRT - mean Ct target})}$).

Figure 1. uPA protein production and mRNA expression in aging 19N and 19T breast fibroblasts.
Indicated passages of subconfluent (90%) 19T and 19N breast fibroblast were plated, cultured in duplicate and serum-starved for 4 days in PFM in Pronectin F coated plates. After that, uPA accumulation was allowed to proceed for 4 days and the amount of released (A) and cell-bound (B) uPA was measured by ELISA. Data shown are the means ± SD of duplicate cell cultures. Basal uPA mRNA levels (C) were determined by quantitative real-time RT-PCR as described in the material and methods. Data shown are expressed as fold of the levels measured in passage number 13 (expression set at 1.0) and are the means ± SD of two independently performed PCR reactions.

Methylation status of CpG island in the uPA promoter

Genomic DNA from different fibroblast strains, MDA-MB-231-BAG and MCF7-BAG was isolated as described [42]. Genomic DNA (4 µg) was digested with *Pst I*, *Pst I*/*Hpa II*, *Pst I*/*Hha I* or *Pst I*/*Msp I*, phenol/chloroform extracted and precipitated. To determine if the CpG island of the *uPA* promoter was methylated, a PCR (30 cycles and an annealing temperature of 58° C) was performed on digested genomic DNA with primers that flank the CpG island (TGGGC-GAGGTAGAGAGTCTCCTGTGC and CTG-CGGTCTCCGACTGTGCTGCG). PCR products were analysed on 2.0% metaphore agarose gels.

Western blotting and immunostaining

Sub-confluent fibroblasts serum-starved as described above were washed twice with 10 mM Tris-HCl (pH=7.4), scraped, pelleted and stored at −80° C until further use. Proteins were extracted from the cell pellets using the 3-step extraction protocol (ReadyPrep™ Sequential extraction kit; Biorad, Veenendaal, The Netherlands). Briefly, cells were resuspended in 40 mM ice-cold Tris base supplemented with 10% (v/v) of a protease inhibitor cocktail (#P-9599, Sigma, Zwijndrecht, The Netherlands), 1 mM PMFS (#P-7626, Sigma), DNAse I (#DNEP,

Sigma), and RNAse A (#R4642, Sigma). Cells were disrupted by 3 repetitive freeze/thaw cycles followed by a 10 min ultrasound sonication. Soluble proteins were separated from the intermediate soluble and insoluble proteins by centrifugation. The remaining pellet used in our analysis was dissolved in 40 mM Tris base containing 8 M urea, 4% (w/v) CHAPS, 0.2% (w/v) BioLyte 3/10 ampholyte and 20 mM TBP. Samples (3-5 µg) were separated in denaturing MOPS/SDS buffer on a 4 to 12 % gradient NuPAGE Bis-Tris gel (Invitrogen) according to the manufacturer. Subsequently, proteins were electroblotted to HyBond-P PVDF membranes. Membranes blocked overnight in blocking buffer [3% BSA in 20 mM Tris-HCl (pH=7.4), 150 mM NaCl (TBS) and 0.05% Tween] were incubated for 1 h at room temperature in blocking buffer with primary antibody (anti-hα-SMA clone 1A4 (Dako, Glostrup, Denmark); anti-hMMP-2 clone Ab-3 (Oncogene Research products, Boston, USA); anti-hp53 clone DO-1 or clone Pab-240 (sc-126 and sc-99, respectively, Santa Cruz Biotechnology, CA, USA), antipropyl 4-hydroxylase clone 5B5 (M0877, Dako), anti-vimentin clone V9 (M0725, Dako), anti-hGAPDH (Chemicon International, Temecula, USA), or mouse IgG1k (X0931, DAKO)). Blots were developed with peroxidase labelled rabbit anti-mouse IgG (P0161, Dako; 1:5000 in blocking buffer) followed by

ECL chemiluminescence (Amersham, Eindhoven, The Netherlands). Expected product sizes were verified with reference proteins (#161-0318, Biorad). Quantification of the intensity of the protein bands relative to band of the housekeeper GAPDH was determined using Scanalytics ONE-D scan software (Alpha Innotech Ltd., Cannock, United Kingdom).

Retroviral gene transfer

The retroviral expression construct containing *hTERT*, *pBabe-hTERT*, and the empty retroviral expression vector *pBabe-puro* used have been described [43, 44]. The retroviral packaging cell line Phoenix-AMPHO was a gift from Dr. Gary Nolan (Stanford University, Stanford, CA) and was maintained as described previously (http://www.stanford.edu/group/nolan/). Retroviral gene transfer was performed essentially as described previously [45]. Briefly, Phoenix-AMPHO cells were transfected with retroviral transfer plasmid (4 µg per well) using Fugene-6 reagent (Roche Diagnostics, Indianapolis, IN, USA). Two days after transfection, the medium containing the retroviruses was applied to a fibroblast culture at 40% confluence and infection was allowed to proceed for 24 h. Then a second batch of medium containing retroviruses made as described above was added and infection was proceeded for another 24 h. Fibroblasts that had successfully incorporated a retroviral copy were selected with puromycin (2 µg/ml; Sigma).

Telomere length measurements, TRAP assay and senescence associated β-galactosidase staining

For telomere length measurements genomic DNA was isolated as described above. DNA (3 µg) was digested with *Hinf I* and *Rsa I*, separated on 0.7% agarose, blotted to Hybond N$^+$ nylon membrane (Amersham) and hybridised with a ^{32}P-labelled telomeric (CCCTAA)^4 probe as described [46]. The blot was exposed to a PhosphorImager screen to visualise bound telomeric probe. To determine telomerase activity, cell pellets were solubilised and assayed for telomerase activity by using a PCR-based telomere repeat amplification protocol assay

[47] according to the manufacturer (TRAPeze Telomerase detection kit, Intergen, Purchase, NY, USA). For senescence associated β-galactosidase staining, fibroblasts (50% confluent) were fixed in 3.7% formadehyde in PBS for 10 min and stained for 3 to 4 days at 37° C with 5-bromo-4-chloro-3-indolyl-β-D-galactopyranoside (XGAL) at pH=6 as described [48].

RESULTS

Cell-bound and secreted uPA accumulation in aging breast fibroblasts

The significance of uPA protein production in breast fibroblasts during passage *in vitro* as a model for aging was studied first in one normal (19N) and one tumor-derived breast fibroblast strain (19T) that were both obtained from one patient. Comparison of basal uPA protein production in aging fibroblasts is best studied in serum-starved sub-confluent cultures in culture plates coated with Pronectin F [29, 30, 38]. In the tumor-tissue-derived fibroblast strain the levels of released (Figure 1A) and cell-associated uPA (Figure 1B) increased with increasing passage number. The difference was most striking in the cultures of fibroblasts reaching senescence, which produced 2- to 3-fold more uPA protein when compared to the earliest passage studied. In contrast, no such increase in released (Figure 1A) or cell-bound uPA (Figure 1B) was seen in the normal fibroblast strain 19N cultured under similar conditions. To determine whether the upregulation of uPA protein during passage *in vitro* was at the protein or at the mRNA level, we compared *uPA* mRNA levels between different passages of serum-starved 19N and 19T fibroblasts that were cultured in Pronectin F coated plates. Upon passage, the basal *uPA* mRNA levels of 19T fibroblast increased 1.8-fold while those of 19N fibroblast did not clearly change (Figure 1C). Thus, uPA protein levels reflect mRNA levels indicating that the upregulation of uPA protein in 19T fibroblasts during passage *in vitro* is at the mRNA level.
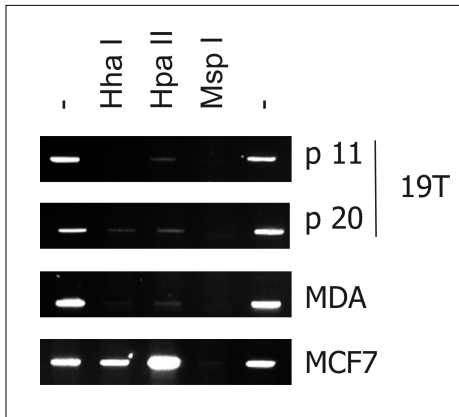
Figure 2. Methylation status of the CpG island in the uPA promoter does not change between young and aged 19T fibroblasts.
Genomic DNA was isolated from young (passage number 11) and aged (passage number 20) 19T fibroblasts, from MCF7-BAG and from MDA-MB-231-BAG cells.The genomic DNA was digested with Pst I to allow efficient amplification.The methylation status was determined by digestion with either a methylation sensitive (Hha I or Hpa II) or a methylation insensitive enzyme (Msp I), that all recognise the targeted CpG island, followed by subsequent amplification of the CpG island with primers flanking the island as described in the material and methods.To control for amplification, DNA digested with Pst I alone was included. PCR fragments (330 bp) generated are shown for each different cell line studied.

Methylation of the uPA promoter

Increased expression of the *uPA* gene in the 19T breast fibroblast strain during passage *in vitro* could be responsible for the increased mRNA levels. Recently, in the breast cancer cell line MCF7 the *uPA* promoter was shown to be silenced through methylation at the CpG island present in its promoter [49]. Thus, a relieve of repression through the loss of methylation of the CpG island in the *uPA* promoter might explain the increase in mRNA levels during passage. Therefore, the methylation status of the CpG island in the human *uPA* promoter was determined in early and late passage 19T fibroblasts. To determine the methylation status of the CpG island in the *uPA* promoter we used methylation sensitive (*Hha I* and *Hpa II*) and insensitive (*Msp I*) restriction enzymes followed by PCR amplification with primers flanking the CpG island (Figure 2). As controls

we included MCF7 and MDA-MB-231 cells from which the methylation status has been studied before [49]. The results show that, similar to MDA-MB-231 cells, the promoter of *uPA* is hardly methylated in early as well as in late passage 19T fibroblasts because after digestion of genomic DNA with both methylation sensitive and insensitive enzymes little PCR product was generated from the CpG island studied (Figure 2). Also in other young fibroblast strains tested (19N, 26T and 26N) the CpG island in the *uPA* promoter was not methylated (not shown). On the other hand, and in line with previous work [49], the CpG island in MCF7 cells was methylated. Hence, unlike the breast cancer cell line MCF7, the transcription of *uPA* in 19T fibroblasts is not negatively regulated through methylation of the CpG island in its promoter. Therefore, loss of methylation of the CpG island in the *uPA* promoter does not explain increased *uPA* mRNA levels observed in late passage 19T fibroblasts.

Quantification of components in aging fibroblasts that are relevant to breast cancer metastasis

Next, we examined whether the difference in *uPA* levels between normal (19N) and tumor-derived (19T) breast fibroblast strains was observed in other sets of aging fibroblast strains. In addition, to get a broader understanding of age related changes in breast fibroblasts we broadened our analysis and included 26 markers relevant to the role of stromal fibroblasts in breast cancer growth and metastasis [11-16, 36-38, 50]. The study included ECM proteases and inhibitors (uPA, uPAR and soluble uPAR, PAI-1 and PAI-2, MMP-2 and MMP-9), growth factors known to modulate ECM proteases and their inhibitors (TGF-β1, FGFs, IGFs and IGFBPs, HGF, EMMPRIN, TSP-1 and VEGF), the myofibroblast differentiation marker α-SMA [51], and the fibroblast markers 5B5 and VIM [52, 53]. In addition, we measured wild type p53 levels, a marker for senescence [54]. Early and late passages of 4 sets of matched human breast fibroblasts strains were compared. Unfortunately, one strain of normal

Table 2. Relative basal mRNA and protein expression of 26 markers in aging fibroblasts.[1]

mRNA level[1]	Median	(range)	P-value[3]
uPA	1.21	(0.59-3.05)	0.18
uPAR	1.05	(0.8-1.27)	0.95
s-uPAR	0.92	(0.33-1.41)	0.51
ETS	1.11	(0.40-1.40)	0.59
PAI-1	1.85	(1.20-2.25)	**0.01**
PAI-2	1.29	(0.29-4.10)	0.29
IGF-1	0.69	(0.14-2.52)	0.67
IGF-2	1.28	(0.09-5.07)	0.25
IGF1-R	0.95	(0.47-1.49)	0.74
IGFBP-2	0.49	(0.23-6.41)	0.71
IGFBP-3	2.62	(1.31-11.6)	0.07
IGFBP-5	0.79	(0.38-2.97)	0.59
IGFBP-6	1.22	(0.48-2.05)	0.16
FGF-1	1.32	(0.92-1.63)	**0.01**
FGF-2	1.02	(0.84-1.38)	0.23
FGF-7	0.93	(0.68-1.19)	0.38
VEGF	1.17	(0.8-1.67)	0.10
TSP-1	1.79	(0.42-2.54)	0.07
TGF-β1	0.91	(0.69-1.18)	0.60
EMMPRIN	0.80	(0.62-1.55)	0.57
HGF	1.53	(0.34-2.32)	0.26
MMP-2	0.74	(0.72-1.05)	**0.02**
Protein level[2]			
5B5	1.06	(0.28-3.52)	0.58
SMA	2.77	(0.09-8.25)	0.08
VIM	1.24	(0.15-2.44)	0.56
MMP-2	1.35	(0.43-3.30)	0.20
p53	0.65	(0.35-3.41)	0.72

1   mRNA values (median and range) of 7 late passage breast fibroblasts are expressed relative to the levels measured in early passage (set at 1.0). All mRNA levels were measured in duplicate by quantative real-time RT-PCR as described in materials and methods using the housekeeping gene HPRT as standard.

2   Protein levels (median and range) of late passage breast fibroblasts are expressed relative to the levels measured in early passage. All protein levels were measured in duplicate on Western blots using chemiluminescence as described in materials and methods. The signals were normalised against the signal obtained from the GAPDH protein.

3   A two-sided paired t-test was used to compare normalised levels of early passage versus late passage fibroblasts.

fibroblasts from one patient could not be analysed due to lack of late-passage material (poor growth). Before analysis, the different passages of the different strains were made quiescent by serum-starvation in PFM. The majority of the markers were analysed at the mRNA level and basal mRNA levels were measured by quantitative real-time PCR using the housekeeping gene *HPRT* as a reference (Table 2). In some cases basal protein levels were determined. These were the (myo)fibroblast markers (SMA, 5B5 and VIM), and MMP-2 and p53 that are well-known to be regulated at the protein level [55]. Protein levels were measured on western blots relative to GAPDH protein levels (Table 2).

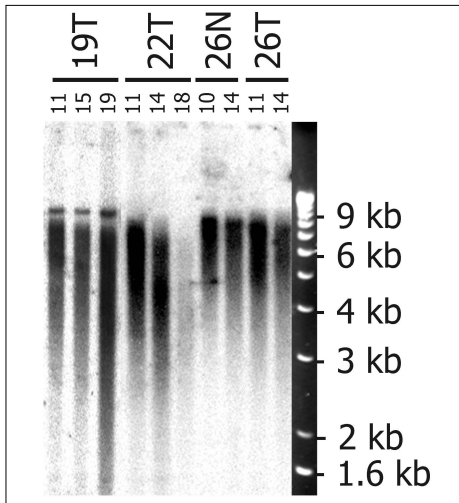From the mRNA's quantified of the uPA system, the basal mRNA expression levels of only

Figure 3. Telomere length declines during passage of breast fibroblasts.
Hinf1 and RsaI digested genomic DNA isolated from indicated passages of indicated fibroblast strains (19T, 22T, 26N and 26T) were separated on 0.7% agarose gels before hybridization with a telomeric probe to detect telomere repeat as described in the materials and methods section.

PAI-1 (*P*=0.01) correlated positively with increasing passage number (Table 2). *uPA* mRNA showed only a very weak trend (*P*=0.18) towards increased expression but a subset of the strains (19T, 22T, 25N, 25T and 26N) showed a consistent increase (1.2- to 3-fold). Of the other factors, *FGF-1* mRNA correlated positively (*P*=0.01) and *MMP-2* mRNA negatively (*P*=0.02) with increasing passage number. The other mRNA levels did not change significantly with increasing age of the culture (Table 2). *MMP-9* mRNA levels were too low to be accurately analysed with SYBR-green (Ct-values higher than 33). This low expression of *MMP-9* mRNA is in line with previous work on breast fibroblasts [56].
Interestingly, MMP-2 protein levels in all normal fibroblast strains tended towards a decrease (0.62 ± 0.17; *P*=0.06, n=3, two-sided paired t-test) and followed the mRNA levels. In contrast, MMP-2 protein levels in tumor-associated fibroblast showed a tendency to an increase (2.43 ± 1.00; *P*=0.06, n=4, two-sided paired t-test). The response of tumor-derived fibroblasts

was significantly different from that of normal fibroblasts (*P*=0.03, two-sided standard t-test), suggesting that MMP-2 protein production downstream of the messenger during aging is changed in tumor-derived fibroblasts. p53 levels did not change nor did the fibroblast markers 5B5 and VIM. The levels of α-SMA showed a wide variation but tended towards an increase with increasing passage number (*P*=0.08).

All fibroblast strains loose telomere length upon passage in vitro

Many human fibroblast strains become senescent upon extensive passage due to telomere attrition [57]. We determined telomere length with increasing passage number in our fibroblast strains (Figure 3 and results not shown). Since telomere length is hard to measure accurately due to large intercellular variation, we
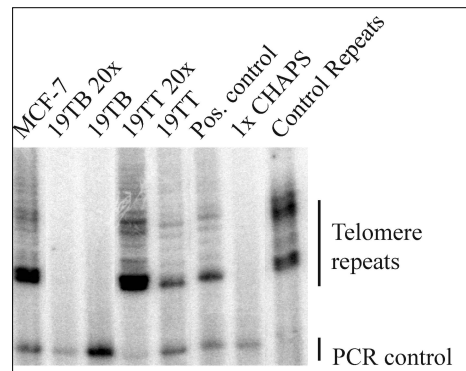
Figure 4. Telomerase activity is successfully introduced in 19T fibroblasts.
Lysates from 19T fibroblasts (500 cells) infected with empty vector (19TB) or with a retroviral vector containing hTERT (19TT) were analysed for telomerase activity using a standard TRAP assay as described in the materials and methods. Lysates (500 cells) from MCF7-BAG cells that contain telomerase activity [59] as well as a buffer control (1xCHAPS) were included. Lysates of 19TB and 19TT containing 10,000 cells were also analysed (19TB 20x and 19TT 20x). Heat-inactivated samples did not show any specific amplification products.
Telomerase repeats, indicative of telomerase activity, are visible as a ladder. Note that, due to the increased amplification efficiency, the smallest repeat is usually most abundant. When no repeats were observed, as is the case in lysates from empty vector infected fibroblasts, a short synthetic 36 bp telomere repeat present in the PCR serves to confirm a successful amplification procedure.
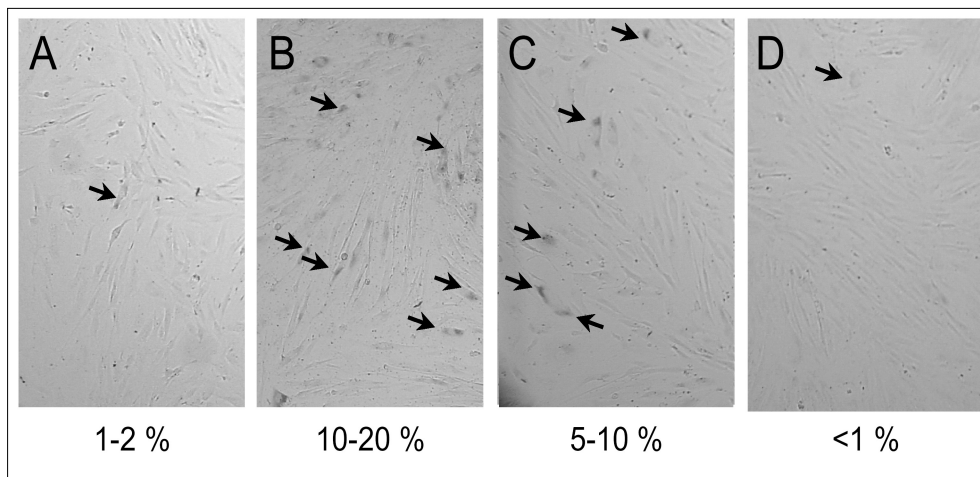
Figure 5. Senescence associated β-galactosidase staining in young and old fibroblasts with or without telomerase.
Subconfluent young (passage number 13; A) and old (passage number 27; B) 19T fibroblast and old 19T fibroblasts (passage number 27) infected with empty vector (C) or hTERT (D) were stained for senescence associated β-galactosidase activity as descibed in material and methods. Positive stained cells are indicated with an arrow.
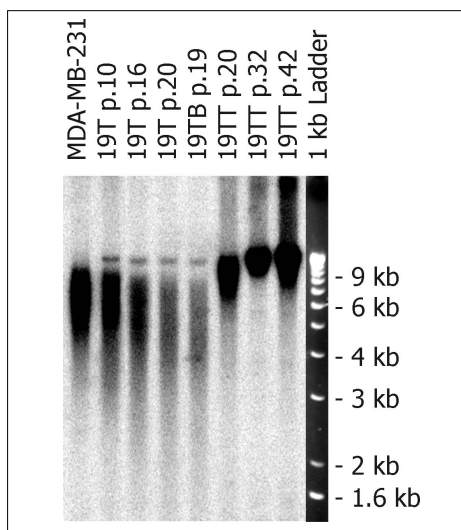
Figure 6. Telomere length is extended after the introduction of telomerase in 19T fibroblasts.
Hinfl and RsaI digested genomic DNA isolated from a control breast carcinoma line MDA-MB-231, from 19T fibroblasts (passage number 10, 16 and 20) and from empty vector infected 19TB fibroblasts (passage number 19) and from hTERT-infected 19TT fibroblasts (passage number 20, 32 and 42), was separated on 0.7% agarose gel and blotted to a nylon membrane.The blot was hybridised with a telomeric probe to detect telomere repeats as described in Figure 3.

have included additional passages (*i.e.* 19T and 22T). All strains showed a decrease in telomere length with increasing passage number (Figure 3, only 19T, 22T, 26N, and 26T are shown). Concluding, in all breast fibroblast strains telomere length declined with increasing passage number but in some less dramatically than others. Thus, the strains are ageing due to the end replication problem resulting in replicative senescence [58].

Human telomerase reverse transcriptase restores telomere length loss as well as uPA and PAI-1 mRNA levels and MMP-2 protein levels in 19T fibroblasts

To study the direct role of telomere loss on the induction of *uPA* and *PAI-1* mRNA and MMP-2 protein during passage *in vitro*, we introduced human telomerase reverse transcriptase (*hTERT*) into the tumor-derived fibroblast strain 19T. This strain showed an increase in *PAI-1* and *uPA* mRNA and MMP-2 protein during passage. Since fibroblasts are hard to transfect we introduced *hTERT* into this fibroblast strain using a retroviral delivery system [45]. Retroviruses were introduced in pre-senescent fibroblasts at passage number 16. We generated one
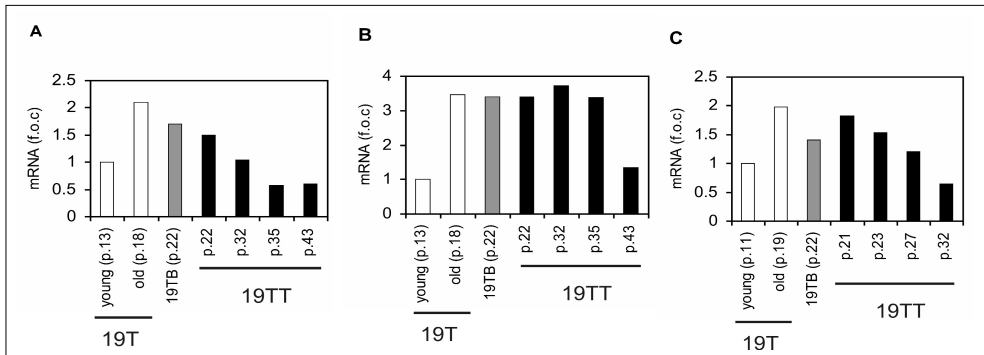
Figure 7. uPA and PAI-1 mRNA and MPP2 protein levels return to the levels seen in young fibroblasts.
Young and aged 19T breast fibroblast of indicated passage number (open bars), late passage empty vector infected 19TB (passage number 22) (shaded bars) and different passages of hTERT-infected 19TT fibroblasts (black bars) were all at 90% confluence serum-starved for 4 days prior to RNA isolation. Basal uPA (A) and PAI-1 (B) mRNA levels were determined by quantitative real-time RT-PCR as described in the material and methods. Basal MMP-2 protein levels (C) were determined by Western blot as described in the material and methods. The levels shown in the graph are all relative to levels in early passage 19T fibroblasts (expression set at 1.0).

fibroblast subculture, 19TB, infected with the empty retroviral vector *pBabe-puro* [44] and another, 19TT, with the retroviral vector containing human telomerase reverse transcriptase (*phTERT*) [43]. To test successful delivery we measured telomerase activity in both subcultures (Figure 4). While in the 19TB subculture no telomerase activity could be measured using a standard TRAP assay [47], telomerase activity was readily detectable in 19TT fibroblasts, indicating that the transduction was successful. The activity was approximately 5% of that present in MCF7 cells, a cell line known to have considerable telomerase activity [59]. To further verify the significance of this amount of telomerase, we performed senescence-associated β-galactosidase staining (SA-β-gal staining) on 19TB and 19TT fibroblasts and in early and late passage 19T fibroblasts (Figure 5). SA-β-gal staining is a marker for senescence indicative of aging fibroblasts [48]. The 19TB fibroblast cells infected with the empty vector showed SA-β-gal staining (5-10%; Figure 5C) which was comparable to the levels observed in the parental 19T fibroblast strain of similar passage (Figure 5B). In contrast, less than 1% staining was seen in the 19TT line that contains *hTERT* (Figure 5D). Similar levels were seen in early passage 19T fibroblasts (Figure 5A). Concluding, senescence was not observed in the late

passage 19TT fibroblast line. Absence of senescence was further substantiated by successful passaging of the 19TT line currently beyond passage number 55. This passage number was never reached by 19TB fibroblasts nor by the parental 19T fibroblasts.

Next, we determined telomere length in 19TB and 19TT fibroblasts (Figure 6). While telomere length (approx. 6 kb) in 19TB fibroblasts (passage number 19) was comparable to the parental fibroblasts of the similar passage, telomeres of 19TT fibroblast were clearly elongated (approximately 10 kb). Telomeres of 19TT fibroblasts at this passage were even longer than the telomere length of early passage 19T fibroblasts. Interestingly, upon continued culturing *in vitro* of the 19TT strain, telomere length further increased and reached a length of approximately 12 kb in passage number 32 and 42 (Figure 6). In humans, telomeres of this length are only seen in germ cells that do contain telomerase activity [39]. Concluding, loss of telomeres and occurrence of senescence can be overcome by the introduction of human telomerase reverse transcriptase in this tumor-derived breast fibroblast strain.

Finally, we determined the levels of *uPA* and *PAI-1* mRNA and MMP-2 protein in different passages of *hTERT*-infected fibroblasts (Figure 7A, 7B and 7C). To study the effect of *hTERT*

expression on *uPA* and *PAI-1* mRNA expression we measured their levels in senescent 19TB fibroblasts (passage number 22) and in 19TT fibroblasts from passage number 22 onwards (Figure 7A and 7B). Similar to a late passage parental strain (passage number 18), line 19TT (passage number 22) and near-senescent 19TB (passage number 22) fibroblasts had approximately 1.8-fold more *uPA* mRNA and 2.6-fold more *PAI-1* mRNA levels compared with the early passage parental 19T fibroblast strain (passage number 13). The levels of *uPA* mRNA declined gradually in the next 10 passages to return to the levels seen in early passage 19T fibroblasts (passage number 13) (Figure 7A). For *PAI-1*, mRNA levels also declined, but this decline took 10 passages more to return to the levels seen in young fibroblasts (Figure 7B). MMP-2 protein levels were 1.5- to 1.8-fold upregulated as well in late passage 19T and 19TB fibroblasts and in 19TT fibroblast of similar passage number (Figure 7C). Those levels also declined gradually with increasing passage to the levels seen in early passage 19T fibroblasts. Thus, in this tumor-derived fibroblast strain telomere reconstitution results in mRNA levels of *uPA* and *PAI-1*, and protein levels of MMP-2 comparable to the levels in early passage 19T fibroblasts.

DISCUSSION

Breast cancer metastasis requires ECM remodelling. Aging of stromal fibroblasts might contribute to this process by increased production of proteins with metastatic potential. Here, we studied during aging in human breast fibroblasts changes in the urokinase system, in MMPs and in relevant modulating factors. The fibroblast strains were isolated either from the tumor burden or from adjacent normal tissue; each set from one and the same patient. Among the ECM remodelling proteins studied, only *PAI-1* mRNA consistently increased during aging in all strains. *uPA* mRNA was increased only in some of the strains. An increase in PAI-1 and uPA protein and mRNA during aging has been observed before in fibroblasts from skin and lung [30, 34]. PAI-1 protein was also elevated in

endothelial cells aged *in vitro* [30], suggesting that age related induction of particularly PAI-1 is a general phenomenon.

Besides changes in the uPA system, we found that MMP-2 protein levels were upregulated in aged tumor-derived fibroblast strains. In normal breast-derived strains, MMP-2 protein levels followed the decrease in expression of the mRNA during passage. Upregulation of MMPs (MMP-1, -2 and -3) as well as of one of their inhibitors (TIMP-2) has also been observed in other fibroblast strains aged *in vitro* [29, 31, 32]. In contrast, MMP-9 expression was undetectable in all strains independent of age. This contrasts the abundant presence of MMP-9 in the fibroblasts bordering the tumor burden [12] suggesting that MMP-9 expression in breast fibroblast is completely dependent on inducing factors from the tumor [56].

What is causing the age related changes in ECM remodelling proteins is poorly understood. It is clear from previous work that short telomeres lead, presumably via the release of telomere binding proteins, to upregulation of proteins involved in cell cycle arrest such as p16 and in certain cases p53 [39, 60-62]. p16 and p53 might subsequently upregulate PAI-1, uPA and MMP-2. p53 has previously been shown to regulate *PAI-1* promoter activity directly through binding to a p53 response element in the promoter [63]. A similar link of p53 to the induction of *uPA* mRNA has not been described. In the current work we did not find a role for p53 since the levels of p53 protein did not consistently change during passage. Thus, the upregulation of *PAI-1* mRNA during passage of breast fibroblast does not appear to result from increased levels of p53 protein.

Among the growth factors analysed we only observed a consistent increase of *FGF-1,* but the relatively slight changes in *FGF-1* during aging can probably not explain the larger changes in *PAI-1* mRNA. We have previously shown that FGF-1 can modestly upregulate *PAI-1* mRNA in 19T and 19N fibroblasts [50]. The response of uPA to FGF-1 was more pronounced which would be inconsistent with the current observation made in all the strains. Besides FGF-1, the modulating factors

IGFBP3, TSP-1 and VEGF tended towards increased expression during aging and, therefore, these may become statistically significant if a larger panel is studied. Altered TGF-β response has been suggested to regulate MMPs in aging skin fibroblasts [64], yet, *TGF-β₁* mRNA levels did not change in our breast fibroblasts during passage *in vitro*. Thus, altered *TGF-β₁* mRNA levels can not explain increased levels of *PAI-1*. Still though, bioavailability might have changed during passage. Even so, changing TGF-β activity alone cannot explain the increase in *PAI-1* and *uPA* levels seen in the majority of the aging breast fibroblast because TGF-β generally stimulates PAI-1 expression [65], while it decreases uPA expression in human fibroblasts [37].

The inverse correlation between *IGF-1* and *uPA* in breast fibroblasts that we observed before [36] is also seen here in all the strains during aging *in vitro*. This confirms that IGF-I and uPA either regulate each other via an autocrine loop [36, 50] or are co-regulated. Interestingly, the moderate to large increases in *IGFBP3* seen in a number of the lines will cooperate with loss of *IGF-1* expression and indicates that most aging breast fibroblasts are devoid of IGF signalling similar to other aging fibroblasts [66].

Besides the consistent increase of some markers, most of them did not change consistent with increased passage number. Even analysis of all changes in expression during passage in all strains did not reveal a clear clustering of fibroblasts according to the patient they were derived from, nor according to whether the fibroblast were derived from normal or tumor tissue (not shown). This suggests a large heterogeneity among the strains. Large heterogeneity is also observed in fibroblasts from different sources (*e.g.* skin versus lung) and from elder donors [67, 68]. Due to this heterogeneity, the contribution of age-induced stromal factors to breast cancer may be very dependent on the individual.

Recently, it was reported that breast fibroblasts derived from normal donors could not be immortalised by expression of *hTERT* alone [69]. Our tumor-derived fibroblast strain 19T was, however, immortalised after the introduc-

tion of *hTERT* and has now been cultured for over 55 passages. Our results are more in line with the view that short telomeres induce senescence in human fibroblasts [39, 57]. However, our immortalised fibroblast strain was derived from tumor tissue and may behave different from fibroblasts derived from normal breast tissue. Indeed, our tumor-derived strain can be passaged several population doublings more than the normal breast-derived fibroblast strain that was derived at the same time from the same patient. Also 19N and 19T fibroblasts produce different amounts of uPA [50]. Furthermore, during aging MMP-2 levels change differently in normal compared with tumor-derived fibroblasts. From this we can conclude that tumor-derived breast fibroblasts even upon extensive passaging *in vitro* behave different from normal breast fibroblasts, confirming that breast fibroblasts are programmed by the primary tumor.

Not all fibroblast strains seem to arrest at the same telomere length (Figure 3). The tumor-derived strain 22T arrests with telomeres of approximately 6 kb while other strains such 26N and 26T arrest already with telomeres of around 8 kb. This is in line with the view that not the average telomere length determines senescence but rather the number of chromosomes that lack telomeres. In addition, telomere length may not be the only factor that controls the onset of senescence [61].

Telomere elongation using *hTERT* in the 19T strain not only overcomes replicative senescence but it also restores *uPA* and *PAI-1* mRNA levels and MMP-2 protein levels to the levels of early passage fibroblasts. This directly implies that telomere reconstitution by telomerase regulates changes in uPA, PAI-1 and MMP-2 in this fibroblast strain. However, since the levels of *uPA*, *PAI-1* and MMP-2 decline only after several passages, while telomere reconstitution is almost instantaneous, the mechanism that is responsible for the induction of *PAI-1*, *uPA* and MMP-2 must be stable for several passages. Methylation of the CpG islands as we have studied for the *uPA* promoter does not seem responsible for such programming because the methylation status of the *uPA* CpG island was not altered in aging 19T fibroblasts. The true

mechanism underlying this response thus remains unknown. However, it may be related to the mechanism that causes replicative senescence itself, a mechanism that is considered poorly reversible.

Finally, Campisi and coworkers [35] have recently shown that senescent fibroblasts are more potent growth promoters of epithelial tumor cells *in vitro* and of tumor growth and metastasis in mice *in vivo*. An effect that might be explained by the increased levels of PAI-1 and FGF-1 and possibly uPA and MMP-2 in senescent breast fibroblasts. Translating these data to humans, this suggests that increased stromal levels of *PAI-1*, *uPA* and *FGF-1* mRNA and MMP-2 protein could contribute to breast cancer progression in older women.

ACKNOWLEDGEMENTS

REFERENCES

1. Jänicke F, Schmitt M, Graeff H. Clinical relevance of the urokinase-type and tissue-type plasminogen activators and of their type 1 inhibitor in breast cancer. Semin Thromb Hemost 1991;17:303-12.

2. Duffy MJ, O'Grady P, Devaney D, O'Siorain L, Fennelly JJ, Lijnen HJ. Urokinase-plasminogen activator, a marker for aggressive breast carcinomas. Preliminary report. Cancer 1988;62:531-3.

3. Look MP, van Putten WLJ, Duffy MJ, Harbeck N, Christensen IJ, Thomssen C, Kates R, Spyratos F, Ferno M, Eppenberger- Castori S, Sweep CG, Ulm K, Peyrat JP, Martin PM, Magdelenat H, Brunner N, Duggan C, Lisboa BW, Bendahl PO, Quillien V, Daver A, Ricolleau G, Meijer-Van Gelder ME, Manders P, Fiets WE, Blankenstein MA, Broet P, Romain S, Daxenbichler G, Windbichler G, Cufer T, Borstnar S, Kueng W, Beex LV, Klijn JGM, O'Higgins N, Eppenberger U, Jänicke F, Schmitt M, Foekens JA. Pooled analysis of prognostic impact of urokinase-type plasminogen activator and its inhibitor PAI-1 in 8377 Breast Cancer Patients. J Natl Cancer Inst 2002;94:116-28.

4. Thorpe SM, Rochefort H, Garcia M, Freiss G, Christensen IJ, Khalaf S, Paolucci F, Pau B, Rasmussen BB, Rose C. Association between high concentrations of Mr 52,000 cathepsin D and poor prognosis in primary human breast cancer. Cancer Res 1989;49:6008-14.

5. Spyratos F, Maudelonde T, Brouillet JP, Brunet M, Defrenne A, Andrieu C, Hacene K, Desplaces A, Rouesse J, Rochefort H. Cathepsin D: an independent prognostic factor for metastasis of breast cancer. Lancet 1989;2:1115-8.

6. Duffy MJ. Proteases as prognostic markers in cancer. Clin Cancer Res 1996;2:613-8.

7. Schmitt M, Harbeck N, Thomssen C, Wilhelm O, Magdolen V, Reuning U, Ulm K, Hofler H, Jänicke F, Graeff H. Clinical impact of the plasminogen activation system in tumor invasion and metastasis: prognostic relevance and target for therapy. Thromb Haemost 1997; 78:285-96.

8. Foekens JA, Kos J, Peters HA, Krasovec M, Look MP, Cimerman N, Meijer-van Gelder ME, Henzen-Logmans SC, van Putten WLJ, Klijn JGM. Prognostic significance of cathepsins B and L in primary human breast cancer. J Clin Oncol 1998;16:1013-21.

9. Castiglioni T, Merino MJ, Elsner B, Lah TT, Sloane BF, Emmert-Buck MR. Immunohistochemical analysis of cathepsins D, B, and L in human breast cancer. Hum Pathol 1994;25:857-62.

10. Unden AB, Sandstedt B, Bruce K, Hedblad M, Stahle-Backdahl M. Stromelysin-3 mRNA associated with myofibroblasts is overexpressed in aggressive basal cell carcinoma and in dermatofibroma but not in dermatofibrosarcoma. J Invest Dermatol 1996;107:147-53.

11. Nielsen BS, Rank F, López JM, Balbin M, Vizoso F, Lund LR, Danø K, Lopez-Otín C. Collagenase-3 expression in breast myofibroblasts as a molecular marker of transition of ductal carcinoma in situ lesions to invasive ductal carcinomas. Cancer Res 2001;61:7091-100.

12. Nielsen BS, Sehested M, Kjeldsen L, Borregaard N, Rygaard J, Danø K. Expression of matrix metalloprotease-9 in vascular pericytes in human breast cancer. Lab Invest 1997;77:345-55.

13. Nielsen BS, Sehested M, Duun S, Rank F, Timshel S, Rygaard J, Johnsen M, Danø K. Urokinase plasminogen activator is localized in stromal cells in ductal breast cancer. Lab Invest 2001;81:1485-501.

14. Basset P, Bellocq JP, Wolf C, Stoll I, Hutin P, Limacher JM, Podhajcer OL, Chenard MP, Rio MC, Chambon P. A novel metalloproteinase gene specifically expressed in stromal cells of breast carcinomas. Nature 1990;348:699-704.

15. Bianchi E, Cohen RL, Dai A, Thor AT, Shuman MA, Smith HS. Immunohistochemical localization of the plasminogen activator inhibitor-1 in breast cancer. Int J Cancer 1995;60:597-603.

16. Pappot H, Gardsvoll H, Romer J, Pedersen AN, Grondahl-Hansen J, Pyke C, Brunner N. Plasminogen activator inhibitor type 1 in cancer: therapeutic and prognostic implications. Biol Chem Hoppe Seyler 1995; 376:259-67.

17. Bajou K, Noël A, Gerard RD, Masson V, Brünner N, Holst-Hansen C, Skobe M, Fusenig NE, Carmeliet P, Collen D, Foidart JM. Absence of host plasminogen activator inhibitor 1 prevents cancer invasion and vascularization. Nat Med 1998;4:923-8.

18. Frandsen TL, Holst-Hansen C, Nielsen BS, Christensen IJ, Nyengaard JR, Carmeliet P, Brünner N. Direct evidence of the importance of stromal urokinase plasminogen activator (uPA) in the growth of an experimental human breast cancer using a combined uPA genedisrupted and immunodeficient xenograft model. Cancer Res 2001;61:532-7.

19. Coussens LM, Tinkle CL, Hanahan D, Werb Z. MMP-9 supplied by bone marrow-derived cells contributes to skin carcinogenesis. Cell 2000;103:481-90.

20. Bergers G, Brekken R, McMahon G, Vu TH, Itoh T, Tamaki K, Tanzawa K, Thorpe P, Itohara S, Werb Z, Hanahan D. Matrix metalloproteinase-9 triggers the angiogenic switch during carcinogenesis. Nat Cell Biol 2000;2:737-44.

21. Liotta LA, Kohn EC. Stromal therapy: the next step in ovarian cancer treatment. J Natl Cancer Inst 2002; 94: 1113-4.

22. Krtolica A, Campisi J. Cancer and aging: a model for the cancer promoting effects of the aging stroma. Int J Biochem Cell Biol 2002;34:1401.

23. Tlsty TD. Stromal cells can contribute oncogenic signals. Semin Cancer Biol 2001;11:97-104.

24. Chang C, Werb Z. The many faces of metalloproteases: cell growth, invasion, angiogenesis and metastasis. Trends Cell Biol 2001;11:S37-43.

25. Bergers G, Coussens LM. Extrinsic regulators of epithelial tumor progression: metalloproteinases. Curr Opin Genet Dev 2000;10:120-7.

26. McCawley LJ, Matrisian LM. Tumor progression: defining the soil round the tumor seed. Curr Biol 2001; 11:R25-7.

27. DePinho RA. The age of cancer. Nature 2000;408:248-54.

28. Ashcroft GS, Horan MA, Ferguson MW. The effects of ageing on cutaneous wound healing in mammals. J Anat 1995;187(Pt 1):1-26.

29. West MD, Pereira-Smith OM, Smith JR. Replicative senescence of human skin fibroblasts correlates with a loss of regulation and overexpression of collagenase activity. Exp Cell Res 1989;184:138-47.

30. West MD, Shay JW, Wright WE, Linskens MHK. Altered expression of plasminogen activator and plasminogen activator inhibitor during cellular senescence. Exp Gerontol 1996;31:175-93.

31. Zeng G, Millis AJT. Differential regulation of collagenase and stromelysin mRNA in late passage cultures of human fibroblasts. Exp Cell Res 1996; 222: 150-6.

32. Zeng G, Millis AJT. Expression of 72-kDa gelatinase and TIMP-2 in early and late passage human fibroblasts. Exp Cell Res 1994;213:148-55.

33. Wick M, Bürger C, Brüsselbach S, Lucibello FC, Müller R. A novel member of human tissue inhibitor of metalloproteinases (TIMP) gene family is regulated during G1 progression, mitogenic stimulation, differentiation, and senescence. J Biol Chem 1994; 269: 18953-60.

34. Linskens MHK, Feng J, Andrews WH, Enlow BE, Saati SM, Tonkin LA, Funk WD, Villeponteau B. Cataloging altered gene expression in young and senescent cells using enhanced differential display. Nucleic Acids Res 1995;23:3244-51.

35. Krtolica A, Parrinello S, Lockett S, Desprez PY, Campisi J. Senescent fibroblasts promote epithelial cell growth and tumorigenesis: a link between cancer and aging. Proc Natl Acad Sci U S A 2001;98:12072-7.

36. Sieuwerts AM, Klijn JGM, Foekens JA. Insulin-like growth factor 1 (IGF-1) and urokinase-type plasminogen activator (uPA) are inversely related in human breast fibroblasts. Mol Cell Endocrinol 1999;154:179-85.

37. Sieuwerts AM, Klijn JGM, Henzen-Logmand SC, Bouwman I, Van Roozendaal CEP, Peters HA, Setyono-Han B, Foekens JA. Urokinasetype-plasminogen-activator (uPA) production by human breast (myo) fibroblasts in vitro: influence of transforming growth factor-β1 (TGFβ1) compared with factor(s) released by human epithelial-carcinoma cells. Int J Cancer 1998;76:829-35.

38. Sieuwerts AM, Klijn JGM, Henzen-Logmans SC, Foekens JA. Cytokine-regulated urokinase-type-plasminogen-activator (uPA) production by human breast fibroblasts in vitro. Breast Cancer Res Treat 1999; 55:9-20.

39. Bodnar AG, Ouellette M, Frolkis M, Holt SE, Chiu CP, Morin GB, Harley CB, Shay JW, Lichtsteiner S, Wright WE. Extension of life-span by introduction of telomerase into normal human cells. Science 1998; 279: 349-52.

40. Van Roozendaal CEP, van Ooijen B, Klijn JGM, Claassen C, Eggermont AMM, Henzen-Logmans SC, Foekens JA. Stromal influences on breast cancer cell growth. Br J Cancer 1992;65:77-81.

41. Grebenschikov N, Geurts-Moespot A, De Witte H, Heuvel J, Leake R, Sweep F, Benraad T. A sensitive and robust assay for urokinase and tissue-type plasminogen activators (uPA and tPA) and their inhibitor type I (PAI-1) in breast tumor cytosols. Int J Biol Markers 1997;12:6-14.

42. Berns EM, Klijn JGM, van Putten WLJ, van Staveren IL, Portengen H, Foekens JA. c-myc amplification is a better prognostic factor than HER2/neu amplification in primary breast cancer. Cancer Res 1992;52:1107-13.

43. Counter CM, Hahn WC, Wei W, Caddle SD, Beijersbergen RL, Lansdorp PM, Sedivy JM, Weinberg RA. Dissociation among in vitro telomerase activity, telomere maintenance, and cellular immortalization. Proc Natl Acad Sci U S A 1998;95: 14723-8.

44. Morgenstern JP, Land H. Advanced mammalian gene transfer: high titre retroviral vectors with multiple drug selection markers and a complementary helper-free packaging cell line. Nucleic Acids Res 1990;18:3587-96.

45. Pear WS, Nolan GP, Scott ML, Baltimore D. Production of high-titer helper-free retroviruses by transient transfection. Proc Natl Acad Sci U S A 1993;90:8392-6.

46. Counter CM, Avilion AA, LeFeuvre CE, Stewart NG, Greider CW, Harley CB, Bacchetti S. Telomere shortening associated with chromosome instability is arrested in immortal cells which express telomerase activity. Embo J 1992;11:1921-9.

47. Kim NW, Wu F. Advances in quantification and characterization of telomerase activity by the telomeric repeat amplification protocol (TRAP). Nucleic Acids Res 1997;25:2595-7.

48. Dimri GP, Lee X, Basile G, Acosta M, Scott G, Roskelley C, Medrano EE, Linskens M, Rubelj I, Pereira-Smith O, Peacocke M, Campisi J. A biomarker that identifies senescent human cells in culture and in aging skin in vivo. Proc Natl Acad Sci U S A 1995;92: 9363-7.

49. Xing RH, Rabbani SA. Transcriptional regulation of urokinase (uPA) gene expression in breast cancer cells: role of DNA methylation. Int J Cancer 1999;81:443-50.

50. Sieuwerts AM, Martens JWM, Dorssers LC, Klijn JGM, Foekens JA. Differential effects of fibroblast growth factors on expression of genes of the plasminogen activator and insulin-like growth factor systems by human breast fibroblasts. Thromb Haemost 2002;87: 674-83.

51. Sappino AP, Skalli O, Jackson B, Schurch W, Gabbiani G. Smooth-muscle differentiation in stromal cells of malignant and non-malignant breast tissues. Int J Cancer 1988;41:707-12.

52. Schwachula A, Riemann D, Kehlen A, Langner J. Characterization of the immunophenotype and functional properties of fibroblast- like synoviocytes in comparison to skin fibroblasts and umbilical vein endothelial cells. Immunobiology 1994;190:67-92.

53. Sommers CL, Heckford SE, Skerker JM, Worland P, Torri JA, Thompson EW, Byers SW, Gelmann EP. Loss of epithelial markers and acquisition of vimentin expression in adriamycin- and vinblastine-resistant human breast cancer cell lines. Cancer Res 1992; 52: 5190-7.

54. Shay JW, Pereira-Smith OM, Wright WE. A role for both RB and p53 in the regulation of human cellular senescence. Exp Cell Res 1991;196:33-9.

55. Alarcon-Vargas D, Ronai Z. p53-Mdm2--the affair that never ends. Carcinogenesis 2002;23:541-7.

56. Singer CF, Kronsteiner N, Marton E, Kubista M, Cullen KJ, Hirtenlehner K, Seifert M, Kubista E. MMP-2 and MMP-9 expression in breast cancer-derived human fibroblasts is differentially regulated by stromal-epithelial interactions. Breast Cancer Res Treat 2002; 72:69-77.

57. Lansdorp PM. Repair of telomeric DNA prior to replicative senescence. Mech Ageing Dev 2000;118:23-34.

58. Harley CB, Goldstein S. Cultured human fibroblasts: distribution of cell generations and a critical limit. J Cell Physiol 1978;97:509-16.

59. Kyo S, Takakura M, Kanaya T, Zhuo W, Fujimoto K, Nishio Y, Orimo A, Inoue M. Estrogen activates telomerase. Cancer Res 1999;59:5917-21.

60. Counter CM, Meyerson M, Eaton EN, Ellisen LW, Caddle SD, Haber DA, Weinberg RA. Telomerase activity is restored in human cells by ectopic expression of hTERT (hEST2), the catalytic subunit of telomerase. Oncogene 1998;16:1217-22.

61. Karlseder J, Smogorzewska A, de Lange T. Senescence induced by altered telomere state, not telomere loss. Science 2002;295:2446-9.

62. Smogorzewska A, de Lange T. Different telomere damage signaling pathways in human and mouse cells. EMBO J 2002;21:4338-48.

63. Kunz C, Pebler S, Otte J, von der Ahe D. Differential regulation of plasminogen activator and inhibitor gene transcription by the tumor suppressor p53. Nucleic Acids Res 1995;23:3710-7.

64. Zeng G, McCue HM, Mastrangelo L, Millis AJT. Endogenous TGF-beta activity is modified during cellular aging: effects on metalloproteinase and TIMP-1 expression. Exp Cell Res 1996;228:271-6.

65. Thalacker FW, Nilsen-Hamilton M. Opposite and independent actions of cyclic AMP and transforming growth factor beta in the regulation of type 1 plasminogen activator inhibitor expression. Biochem J 1992;287(Pt 3):855-62.

66. Grigoriev VG, Moerman EJ, Goldstein S. Overexpression of insulin-like growth factor binding protein-3 by senescent human fibroblasts: attenuation of the mitogenic response to IGF-I. Exp Cell Res 1995; 219:315-21.

67. Reed MJ, Ferara NS, Vernon RB. Impaired migration, integrin function, and actin cytoskeletal organization in dermal fibroblasts from a subset of aged human donors. Mech Ageing Dev 2001;122:1203-20.

68. Campisi J. From cells to organisms: can we learn about aging from cells in culture? Exp Gerontol 2001;36:607-18.

69. O'Hare MJ, Bond J, Clarke C, Takeuchi Y, Atherton AJ, Berry C, Moody J, Silver AR, Davies DC, Alsop AE, Neville AM, Jat PS. Conditional immortalization of freshly isolated human mammary fibroblasts and endothelial cells. Proc Natl Acad Sci USA 2001;98:646-51.

How ADAM-9 and ADAM-11 differentially from estrogen receptor predict response to tamoxifen treatment in patients with recurrent breast cancer: a retrospective study

Anieta M. Sieuwerts, Marion E. Meijer-van Gelder, Mieke Timmermans,
Anita M.A.C.Trapman, Roberto Rodriguez Garcia, Miranda Arnold,
Anneke J.W. Goedheer, Henk Portengen, Jan G.M. Klijn and John A. Foekens

Department of Medical Oncology, Erasmus MC, Rotterdam, The Netherlands

ABSTRACT

Purpose: To evaluate the predictive value of the disintegrin and metalloproteinases, *ADAM-9*, *ADAM-10*, *ADAM-11*, and *ADAM-12*, and of the matrix metalloproteinases, *MMP-2* and *MMP-9*, in patients with recurrent breast cancer treated with tamoxifen.

Experimental Design: A retrospective study was done on 259 frozen specimens of estrogen receptor-positive primary breast carcinomas from patients who developed recurrent disease and were treated with tamoxifen as the first line of therapy. The expression levels of the biological factors were assessed by real-time quantitative reverse transcriptase PCR.

Results: Using log-transformed continuous variables, increasing levels of *ADAM-9* (odds ratio (OR)=1.41; *P*=0.015) and decreasing levels of *MMP-9* (OR, 0.81; *P*=0.035) predicted favorable disease control independent from the traditional predictive factors. Furthermore, when tumors were dichotomized at the median level of 70% epithelial tumor cell nuclei, our univariate analysis showed particularly strong results for the group of 153 patients with primary tumors containing 30% or more stromal cells. Although estrogen receptor levels lost their predictive power for this group of patients, high levels of *ADAM-9* (OR,1.59; *P*=0.007) and *ADAM-11* (OR,1.65; *P*=0.001) were significantly associated with a higher efficacy of tamoxifen therapy.

Conclusions: Our results show that especially for primary tumors containing stromal elements, the assessment of mRNA expression levels of *ADAM-9* and *ADAM-11* could be useful to identify patients with recurrent breast cancer who are likely to benefit or fail from tamoxifen therapy.

INTRODUCTION

The ADAMs, which stands for a disintegrin and metalloproteinase, also known as MDCs, are a newly discovered family of membrane proteins. All ADAMs possess some or all of the following domains: a signal peptide, a propeptide, a metalloprotease, a disintegrin, a cysteine-rich domain, an epidermal growth factor–like domain, a transmembrane sequence, and a cytoplasmic tail. The propeptide might be involved in latency with activation upon loss, the metalloprotease domain in proteolysis, the disintegrin domain in adhesion, the cysteine-rich domain in fusion and adhesion, the epidermal growth factor–like domain in growth factor activity, and the cytoplasmic tail in cell signaling. The possession of these multiple domains with their potential functions makes them likely candidates to play a role in cancer cell invasion and metastasis. Indeed, some of these ADAMs have already been linked to various diseases including cancer [1–5]. Despite the above findings, a definite role for any ADAM in either cancer formation, progression, or response to therapy, remains to be shown.

In recurrent breast cancer, steroid hormone receptor status is one of the variables often used to determine the choice of endocrine therapy. Thus far, tamoxifen is the most extensively used hormonal treatment, although only 50% to 60% of the treated patients will benefit [6–8]. Because proteases such as the urokinase-type plasminogen activator have been shown to be associated with failure of tamoxifen therapy in patients with recurrent breast cancer [9, 10], we hypothesized that specific ADAMs might also be associated with therapeutic failure.

Thus far, over 30 different ADAMs have been described, of which 19 appear in humans. For our study, we selected four ADAMs for which no pseudogenes have been described and which have already been shown to be expressed to some extent in human breast cancer. Of these four, only *ADAM-11*, also named *MDC*, does not possess an active matrix metalloproteinase (MMP)–like domain. However, based on its location within a loss of heterozygosity region of chromosome 17q21 [11, 12], *ADAM-11* has

been proposed to be a candidate tumor suppressor gene for human breast cancer [13, 14] and was therefore included in our study. The other three members included in this study, *ADAM-9* (*MDC9*, *meltrin-γ*), *ADAM-10* (*Kuz*, *SUP-17*, *MADM*), and *ADAM-12* (*meltrin-α*) all possess an active MMP-like domain, and in addition have all been reported to be increased in malignant compared with normal breast tissue [3, 15]. We also included two well-known members of the MMP-family, *MMP-2* and *MMP-9*, which have also been reported to be increased in malignant compared with normal breast tissue [16–20]. Because most MMPs are localized to the tumor stroma [17, 21], we suspected that this might also be the case for the ADAMs. We therefore compared mRNA levels measured from human breast tissue sections containing predominantly (>70%) epithelial tumor cells with those measured in sections containing at least 30% stromal cells.

In this report of our retrospective study which includes 259 patients with estrogen receptor (ER)–positive primary breast tumors treated with tamoxifen for recurrent breast cancer, we show that, especially in stroma-enriched primary tumors, *ADAM-9* and *ADAM-11* are able to predict the efficacy of first-line tamoxifen therapy.

PATIENTS AND METHODS

Patients

The Medical Ethical Committee of the Erasmus Medical Center Rotterdam, the Netherlands, approved our study design (MEC 02.953). This retrospective study included 259 female breast cancer patients for which the following inclusion criteria were used: all patients should have measurable disease that was treated with tamoxifen as first-line treatment for metastatic disease; all patients underwent primary surgery for breast cancer; diagnosis took place between 1979 and 1996; the primary tumor should be ER-positive and >100 mg tissue should be available. Exclusion criteria were: neo-adjuvant therapy or adjuvant hormonal treatment; if the follow-up period during tamoxifen treatment

was only 6 months or less and patient was still alive but showed no response or therapy was stopped for other reasons than progression (*e.g.*, subjective or objective toxicity) during these 6 months; if previous other cancers were experienced (except basal cell skin cancer or early-stage cervical cancer stage Ia/Ib). Following the above criteria, 340 tumors were available for analysis. Of the tissues, 15% were excluded from this study because the sections contained <30% tumor cell nuclei (see below). Another 9% were excluded because of poor RNA quality (see below). The remaining 259 eligible patients were treated either with breast-conserving surgery (36%) or with modified mastectomy (64%). An axillary dissection was done in 94% of the patients (n=244). Twenty-five patients received cyclophosphamide, methotrexate, 5-fluorouracil, whereas 17 patients received anthracyclin-containing adjuvant chemotherapy. Relevant clinicopathologic characteristics of the patients and their primary tumor are given in Table 1. Follow-up scheduling of physical and instrumental exams, which, depending on the type of metastasis, included computerized tomography scan, bone scan, magnetic resonance imaging, X-rays as well as plasma tumor marker levels, were done as described recently in detail [22]. The date of diagnosis of metastasis was defined as that at confirmation of metastasis after symptoms reported by the patient, detection of clinical signs, or at regular follow-up. Twenty-four patients presented with distant metastasis at diagnosis or developed distant metastasis (including supraclavicular lymph node metastasis) within 1 month after primary surgery (M1 patients). These 24 patients and the 235 patients who developed a recurrence during follow-up (24 patients with local-regional relapse, 211 patients with distant metastasis) were treated with first-line tamoxifen (40 mg daily). Of the 235 M0 patients, the median time between primary surgery and start of therapy was 27 months (range, 4-164 months). At the time of surgical removal of the primary tumor, the median age of the patients was 58 years (range, 26-89 years), and at the start of tamoxifen therapy for recurrent disease, the median age of the patients was 61 years (range, 29-90

Table 1. Associations of biological factors with clinicopathologic factors.

Clinicopathologic factors	No. of patients[†]	Median (and interquartile range) of biological factors after normalization to the housekeeper set*							
		ER-α ($\times 10^0$)	PgR ($\times 10^0$)	ADAM-9 ($\times 10^0$)	ADAM-10 ($\times 10^{-1}$)	ADAM-11 ($\times 10^{-3}$)	ADAM-12 ($\times 10^{-4}$)	MMP-2 ($\times 10^0$)	MMP-9 ($\times 10^{-1}$)
Menopausal status[‡]									
Premenopausal	68	3.30 (4.83)	1.04 (1.79)	4.32 (7.53)	3.34 (2.38)	3.85 (7.94)	4.76 (7.03)	5.91 (9.53)	4.34 (10.57)
Postmenopausal	191	8.39 (12.56)	0.67 (3.03)	4.17 (7.13)	3.12 (2.09)	3.15 (7.17)	3.99 (6.77)	4.70 (7.25)	3.86 (8.64)
		$P < 0.01^\S$	$P = 0.84^\S$	$P = 0.85^\S$	$P = 0.43^\S$	$P = 0.71^\S$	$P = 0.41^\S$	$P = 0.18^\S$	$P = 0.99^\S$
Tumor size (cm)									
≤ 2	71	8.30 (11.30)	0.53 (2.20)	4.97 (9.33)	3.29 (1.92)	3.41 (9.28)	4.76 (7.37)	5.59 (8.71)	4.79 (10.36)
>2 to ≤ 5	147	6.79 (10.59)	1.06 (3.42)	4.32 (6.41)	3.15 (2.28)	3.17 (6.46)	4.22 (6.47)	4.90 (8.13)	4.19 (9.32)
>5 + pT4	41	4.96 (8.14)	0.67 (2.23)	3.60 (5.34)	2.82 (1.66)	2.48 (4.42)	3.00 (7.17)	3.29 (6.41)	1.88 (3.61)
		$P = 0.16^\|$	$P = 0.19^\|$	$P = 0.57^\|$	$P = 0.11^\|$	$P = 0.20^\|$	$P = 0.06^\|$	$P = 0.04^\|$	$P < 0.01^\|$
Tumor grade									
Good/moderate	32	10.31 (12.90)	0.73 (2.47)	3.22 (8.01)	3.20 (2.16)	4.25 (12.22)	3.99 (7.32)	5.12 (6.64)	3.61 (9.83)
Poor	137	4.93 (8.01)	0.67 (2.55)	4.11 (6.89)	3.12 (2.25)	2.39 (5.50)	4.15 (6.84)	4.63 (7.26)	4.19 (8.02)
		$P < 0.01^\S$	$P = 0.49^\S$	$P = 0.57^\S$	$P = 0.16^\S$	$P = 0.11^\S$	$P = 0.71^\S$	$P = 0.63^\S$	$P = 0.84^\S$
Histologic type									
Infiltrating ductal carcinoma	155	6.47 (10.93)	0.53 (2.24)	3.91 (7.19)	2.93 (1.87)	3.20 (6.98)	4.49 (6.41)	4.97 (6.91)	4.18 (10.03)
Infiltrating lobular carcinoma	31	7.24 (10.66)	1.16 (3.65)	4.01 (9.29)	3.56 (2.51)	4.30 (8.82)	3.40 (4.90)	4.39 (9.66)	2.86 (9.74)
Ductal carcinoma *in situ* + infiltrating ductal carcinoma	17	4.48 (4.85)	1.01 (0.90)	3.55 (12.93)	3.22 (3.04)	2.13 (3.57)	5.61 (10.77)	7.84 (12.27)	4.80 (5.76)
		$P = 0.17^\|$	$P = 0.12^\|$	$P = 0.97^\|$	$P = 0.02^\|$	$P = 0.21^\|$	$P = 0.58^\|$	$P = 0.72^\|$	$P = 0.66^\|$
Nodal status									
N_0	118	7.63 (12.94)	0.40 (1.99)	5.22 (7.74)	3.20 (2.46)	4.32 (7.41)	4.76 (6.82)	4.85 (9.04)	3.84 (8.65)
N_{1-3}	54	6.03 (9.47)	1.12 (3.14)	3.67 (7.82)	3.00 (2.55)	2.81 (7.97)	4.03 (8.66)	5.20 (7.81)	4.35 (7.92)
$N_{>3}$	72	4.78 (8.21)	1.15 (3.14)	2.87 (4.39)	3.07 (1.74)	2.25 (3.94)	3.32 (4.62)	3.62 (6.37)	3.51 (10.66)
		$P = 0.02^\|$	$P < 0.01^\|$	$P = 0.01^\|$	$P = 0.27^\|$	$P = 0.01^\|$	$P = 0.01^\|$	$P = 0.15^\|$	$P = 0.89^\|$
Dominant site of relapse									
Soft	30	5.45 (12.34)	0.72 (2.26)	4.21 (7.26)	3.15 (2.48)	4.59 (9.46)	2.30 (6.09)	4.69 (6.03)	3.75 (11.21)
Bone	133	6.78 (8.39)	0.67 (2.25)	4.38 (7.97)	3.20 (2.25)	3.27 (7.27)	4.13 (7.70)	4.63 (8.92)	3.83 (6.49)
Viscera	96	7.44 (11.81)	0.92 (3.25)	3.98 (5.53)	3.08 (1.88)	3.04 (5.57)	4.53 (6.52)	4.91 (6.80)	4.27 (9.45)
		$P = 0.28^\|$	$P = 0.90^\|$	$P = 0.79^\|$	$P = 0.82^\|$	$P = 0.48^\|$	$P = 0.27^\|$	$P = 0.59^\|$	$P = 0.92^\|$
Disease-free interval (y)									
≤ 1	64	6.68 (8.89)	0.59 (1.70)	4.05 (6.08)	3.01 (2.09)	2.23 (6.03)	4.05 (6.51)	4.65 (6.90)	4.27 (10.01)
1-3	119	7.11 (10.65)	0.85 (2.44)	4.52 (8.15)	3.14 (2.23)	3.55 (5.65)	4.43 (7.71)	4.67 (9.08)	4.13 (8.10)
>3	76	6.07 (14.33)	1.00 (3.34)	4.08 (6.80)	3.30 (2.18)	3.18 (9.42)	3.65 (6.48)	4.90 (6.37)	3.83 (9.18)
		$P = 0.92^\|$	$P = 0.12^\|$	$P = 0.75^\|$	$P = 0.52^\|$	$P = 0.22^\|$	$P = 0.34^\|$	$P = 0.74^\|$	$P = 0.93^\|$

* *Due to different assay conditions and amplicon lengths, absolute values of the biological factors can only be compared within a gene assay.*

† *Because of others and unknowns, numbers do not always add up to 259.*

‡ *At start of first-line therapy for recurrent disease.*

§ *P for Mann-Whitney U test.*

‖ *P for Kruskal-Wallis test, including a Wilcoxon-type test for trend when appropriate.*

years). Response to tamoxifen therapy was defined by standard Unio Internationale Contra Cancrum criteria [23]. Objective response was observed in 53 patients (12 complete remission and 41 partial remission), and 87 patients had an increase in tumor size of 25% or more, or showed new tumor lesions within 3 months (progressive disease). The 119 patients with no evident tumor reduction of 50% or more (complete remission and partial remission) or a tumor-progression (progressive disease), were considered as patients with no change. These patients with no change were divided into 103 patients who had no change at >6 months (defined as stable disease) and 16 patients with no change at ≤6 months. The median progression-free survival ratios were: complete remission, 37 months; partial remission, 16 months; stable disease, 14 months; no change at ≤6 months, 5 months; and for progressive disease, 3 months. Because the patients with stable disease had a progression-free survival similar to patients with partial remission, we classified these patients as responders to tamoxifen as advised by the European Organization for Research and Treatment of Cancer [24]. There-

fore, as has been done before [25–27], disease control was defined in our study as complete remission + partial remission + stable disease. For 156 patients (60%), disease was controlled by tamoxifen therapy. The median follow-up of patients alive after surgery was 90 months (range, 10-190 months) and 37 months (range, 4-131 months) after start of tamoxifen therapy. At the end of the follow-up period, 238 (92%) patients had developed tumor progression and 202 (78%) patients had died.

Tissue processing

After primary surgery, a representative part of the tumor was selected by the pathologist, frozen in liquid nitrogen, and sent to our laboratory for routine determination of ER and progesterone receptor (PgR) by ligand binding assay or enzyme immunoassay [28]. Tumor cytosols were prepared and processed as recommended by the European Organization for Research and Treatment of Cancer [29]. The cut-point used to classify tumors as ER- or PgR-positive was 10 fmol/mg cytosolic protein. The remainder of the tumor tissue was stored in our liquid nitrogen tumor bank at the Erasmus MC. For RNA isolation, 20 to 60 cryostat sections of 30 µm, corresponding to 30 to 100 mg, were cut from these tissues. Before, during, and after cutting the sections for RNA isolation, 5 µm sections were cut for H&E staining to assess the amount of tumor cells relative to the amount of surrounding stromal cells. The amount of nuclei evidently of epithelial tumor cell origin relative to the amount of surrounding stromal cells was estimated with a 100-fold magnification in 10 different areas covering the area of each of the three H&E sections. The fraction of tumor cells over stromal cells throughout the sections did not change greatly between the first and last section (mean coefficient of variation, 6%). Only specimens with at least 30% of the nuclei evidently of epithelial tumor cell origin and distributed uniformly over at least 70% of the section area were included.

RNA isolation and cDNA synthesis

Total RNA was extracted with RNAzol B (Campro, Veenendaal, the Netherlands) according to the manufacturer and stored aliquoted in RNase/DNase-free water at –80° C. Five micrograms of total RNA sample aliquots were reverse-transcribed with oligo(dT)$_{12-18}$ and random hexamer primers in a final volume of 40 µl using the Superscript II RNase H- kit from Invitrogen (Breda, the Netherlands) and used according to the manufacturer's instructions. Prior to PCR, the resulting cDNA samples were treated for 30 min at 37° C with four units of RNase H- (Ambion, Huntington, United Kingdom). The quantity and quality of the isolated RNA was established by UV spectroscopy, by examination of ribosomal RNA bands after agarose gel electrophoresis, and by the ability of the sample to be linearly amplified in a serial dilution with our housekeeping gene set (see next section for further details). Samples of total RNA not showing both the 18S and 28S bands (6%) or at 15 ng reverse-transcribed total RNA not amplifiable within 26 cycles at our fixed threshold value of 0.02 (see below) with our housekeeping set, which was the case for 3% of our samples, were excluded from this study.

Quantification of specific mRNA species

Real-time quantitative PCR was done in an ABI Prism 7700 Sequence Detection System (Applied Biosystems, Nieuwerkerk a/d IJssel, the Netherlands) using both the Assay-on-Demand kits from Applied Biosystems and the intron spanning forward and reverse primer combinations shown in Table 2. PCR reactions were done in a final volume of 25 µl containing cDNA synthesized from 5 to 15 ng of total RNA, 330 nmol/l forward and reverse primer and 12.5 µl SYBR-green PCR master mixture (Applied Biosystems) or Brilliant SYBR Green Master Mix (Stratagene, Amsterdam, the Netherlands). For the Assay-on-Demand kits, the protocol with 40 rounds of amplification recommended by the manufacturer was used. For the SYBR-based assays, the following protocol was used. After 10 min of denaturation and activation of the Taq-DNA polymerase, PCR products were amplified in 35 cycles with 15 s of denaturing at 95° C, 30 s of annealing at

Table 2. Intron-skipping primers used for real-time PCR.

Gene	Assay-on-Demand kit	Exon boundary spanned according to product insert	
ADAM-9*	Hs00177638_m1	15-16	
ADAM-10*	Hs00153853_m1	11-12	
ADAM-11*	Hs00253742_m1	26-27	
ADAM-12*	Hs00222216_m1	18-19	

Gene	Forward primer, sequence 5′→3′	Reverse primer, sequence 5′→3′	Product size (bp)
ADAM-9 †	exon 16, CCAGCTAGGATCAGATGTTC	exon 18, CACTTCCTCCGTATCCTTTAG	230
ADAM-11 †	exon 3, CCAGCCTTCAACTCAAACTTC	exon 5, GAGCTTCCCCTGGTAGTAG	147
MMP-2 ‡	exon 7, CGCAGTGACGGAAAGATGTG	exon 8, TGGGACAGACGGAAGTTCTTG	203
MMP-9 †	exon 7, TGCCCGGACCAAGGATACAG	exon 8, GGCACTGAGGAATGATCTAAG	83
ER-α ‡	exon 4, ATCCTACCAGACCCTTCAGTG	exon 5, GCCAGACGAGACCAATCATC	186
PgR ‡	exon 6, CAAGTTAGCCAAGAAGAGTTC	exon 7, ACTTCGTAGCCCTTCCAAAG	78
HPRT ‡	exon 3 TATTGTAATGACCAGTCAACAG	exon 7 GGTCCTTTTCACCAGCAAG	192
PBGD ‡	exon 1, CATGTCTGGTAACGGCAATG	exon 4, GTACGAGGCTTTCAATGTTG	139
β2M ‡	exon 2, CTTTGTCACAGCCCAAGATAG	exon 4, CAATCCAAATGCGGCATCTTC	83

NOTE: Twenty-seven percent of the samples analyzed for ADAM-11 with the SYBR-based assay and 2% of the samples analyzed for ADAM-12 with the probe-based assay did not show detectable levels after, respectively, 35 and 40 cycles of amplification. To validate our personally designed SYBR-based ADAM-9 and ADAM-11 assays, we also analyzed samples with the commercially available probe-based Assay-on-Demand kits for ADAM-9 and ADAM-11. These assays correlated well with our personally-designed SYBR-based assays (Spearman r_s=0.75; n=245, P<0.001 for ADAM-9 and rs=0.45; n=243, P<0.001 for ADAM-11). We chose to use our personally designed SYBR-based quantitative PCR assays for all factors, except for ADAM-10 and ADAM-12, for which we used the Assay-on-Demand kit.

Abbreviations: HPRT, hypoxanthine-guanine phosphoribosyltransferase; PBGD, porphobilinogen deaminase; β2M, β-2-microglobulin.

* Assay done with TaqMan probes in Universal PCR master mixture (Applied Biosystems).

† Assay done in Brilliant SYBR green PCR master mixture (Stratagene).

‡ Assay done in SYBR green PCR master mixture (Applied Biosystems).

62° C, 10 s of ramping to 72° C, 20 s of extension at 72° C, 10 s of ramping to 79° C, and 20 s at 79° C. To avoid possible detection of primer-dimers, which usually melt at lower temperatures, SYBR green fluorescent signals of the products were acquired after each cycle at 79° C for PCR products with melting temperatures >80° C and only at 72° C for those with melting temperatures <80° C. A reference dye, ROX, was included in all assays to normalize data for non–PCR related signal variation. Initial PCRs followed by product-melting curve analyses and gel electrophoresis experiments were done to ensure that with the PCR conditions and the different primer sets used, only one product of the expected size was amplified, and that for each gene an additional cycle resulted in a doubling of PCR product, *i.e.*, that all genes were amplified with an efficiency of at least 95%. In addition, the PCR efficiency of each gene-specific real-time PCR session was validated with a standard curve constructed from a simultaneously run serially diluted cDNA pool of human breast fibroblasts and cell-lines. Negative controls included samples without reverse transcriptase and samples where total RNA and cDNA was replaced with genomic DNA. Quantitative values were obtained from the threshold cycle (Ct) at which the increase in SYBR green or TaqMan probe fluorescent signal associated with an exponential increase of PCR products reached the fixed threshold value of 0.02, which was in all cases, at least 10-fold the standard deviation of the background signal. To enable comparison of the levels of specific mRNAs in different samples, they were evaluated relative to the average expression levels of three housekeeping genes: the low abundance housekeeping gene porphobilinogen deaminase (*PBGD*), the medium abundance housekeeping gene hypoxanthine-guanine phosphoribosyltransferase (*HPRT*), and the high abundance housekeeping gene β-2-microglobulin (*β2M*). With this set of housekeeping genes, the potential influence of sample-specific fluctuations in one of the housekeeping genes will be minimized. Levels of the target genes expressed relative to this

housekeeping set were quantified as follows:
mRNA target $= 2^{\text{(mean Ct housekeeping genes - mean Ct target)}}$.

Immunohistochemistry

To assess the source of the relevant mRNA species for this study, formalin-fixed, paraffin-embedded breast tumor tissues were analyzed by immunohistochemistry. Formalin-fixed, paraffin-embedded tumors were sectioned at 5 μm, mounted on StarFrost slides, dried, deparaffinized in xylene and rehydrated in graded solutions of ethanol and distilled water. Prior to immunostaining, specimens were pre-treated with 1 mmol/l EDTA (pH 8.0) for 10 min at 121° C in an autoclave, cooled to room temperature, rinsed in PBS followed by a 15 min peroxidase (0.3%) and a 30 min bovine serum albumin (5%) block. The following primary antibodies were used: anti-ADAM-9 goat polyclonal antibody (Santa Cruz Biotechnology, Santa Cruz, CA; clone C-15; dilution 1:200); anti- ADAM-11 goat polyclonal antibody (Santa Cruz Biotechnology, clone H-19; dilution 1:200); anti-PR mouse monoclonal antibody (Dako Diagnostica GmbH, Hamburg, Germany; clone 1A6; dilution 1:320); anti-ER-α mouse monoclonal antibody (Dako Diagnostica; clone 1D5; dilution 1:320). After the primary antibody, ADAM-9 and ADAM-11 immunoreactions were visualized by a standard streptavidin-biotinperoxidase complex (Strept ABC) method (DAKO, Diagnostica GmbH, Hamburg, Germany) followed by 3,3′-diaminobenzidine enzymatic development. ER-α and PgR were visualized using the DAKO EnVision+System-HRP mouse kit (DAKO). Sections were counterstained with hematoxylin. The specificity of immunostaining was con-

Table 3. Cox univariate and multivariate regression analysis for disease control with first-line tamoxifen therapy.

Factor	No of [†] patients	Disease control	Univariate analysis			Multivariate analysis*		
			OR	95% CI	*P*	OR	95% CI	*P*
	259	60%						
Menopausal status[‡]								
premenopausal	68	51%	1			1		
postmenopausal	191	63%	1.63	(0.93-2.85)	0.087	1.36	(0.72-2.59)	0.342
DSR								
LRR	30	63%	1			1		
bone	133	58%	0.80	(0.35-1.80)		0.91	(0.37-2.24)	
viscera	96	63%	0.96	(0.41-2.26)	0.730	0.90	(0.36-2.26)	0.840
DFI								
≤ 1 yr	64	34%	1			1		
1-3 yr	119	66%	3.77	(1.99-7.16)		3.94	(2.03-7.68)	
> 3 yr	76	72%	5.00	(2.43-10.28)	< 0.001	4.95	(2.32-10.56)	< 0.001
*ER-α**	259		1.66	(1.21-2.28)	0.002	1.55	(1.08-2.22)	0.018
*PGR**	259		1.16	(1.02-1.31)	0.024	1.10	(0.96-1.27)	0.172
						Additions to the base model		
*ADAM-9**	259		1.39	(1.07-1.79)	0.012	1.41	(1.06-1.85)	0.015
*ADAM-10**	250		1.61	(0.89-2.91)	0.114	1.35	(0.71-2.58)	0.363
*ADAM-11**	259		1.30	(1.05-1.61)	0.016	1.20	(0.95-1.51)	0.126
*ADAM-12**	250		0.82	(0.61-1.10)	0.189	0.78	(0.56-1.08)	0.137
*MMP-2**	259		0.85	(0.64-1.12)	0.245	0.80	(0.59-1.08)	0.138
*MMP-9**	259		0.82	(0.68-0.98)	0.034	0.81	(0.66-0.98)	0.035

* *Biological factors were separately introduced as log-transformed continuous variable to the base multivariate model that included the factors menopausal status, DSR (dominant site of relapse), DFI (disease-free interval) and ER-α and PGR mRNA levels as log-transformed continuous variables.*

† *Because of missing values, numbers do not always add up to 259.*

‡ *At start of first-line therapy for recurrent disease.*

trolled using normal goat and mouse IgG and by omitting the primary antibodies.

To assess the correlation between *ER-α* and *PGR* mRNA and protein levels, ER-α and PgR immunoreactivity was also assessed in 108 randomly selected frozen sections matching the frozen sections used for RNA isolation. These sections were cut, fixed in 4% paraformaldehyde, and analyzed for ER-α and PgR immunoreactivity as described above for the paraffin-embedded samples, except for the deparaffinization and pretreatment steps and with antibodies diluted 1:320. The percentage of epithelial tumor cells with positive nuclei was estimated with a 100-fold magnification in 10 different areas covering the section and scored in five categories as follows: 0% (1), <10% (2), 10% to 25% (3), 25% to 50% (4), >50% (5).

Statistics

Differences in levels were assessed with the Mann-Whitney *U* test or Kruskal-Wallis test, including a Wilcoxon-type test for trend, when appropriate. In these tests, patient and tumor characteristics were used as grouping variables. The strengths of the associations between continuous variables were tested with the Spearman rank correlation (r_s). For the analysis of treatment benefit, transformations of the variables were explored with fractional polynomials. The gain in χ^2 values was not substantial when using transformations other than log-transformations. Fractional polynomials did not result in statistically significantly better fit. The relation with disease control-to-therapy was examined with logistic regression analysis. Odds ratios (OR) were calculated and are presented with their 95% confidence interval (CI). The likelihood ratio test in logistic regression models was used to test for differences. The Cox proportional hazard model was used to calculate the hazard ratio and 95% CI in the analysis of progression-free survival. Progression-free survival was the time that the patients were treated with tamoxifen as first-line systemic treatment for recurrent disease. The start of tamoxifen therapy was set at zero and the end point at the stop-date of

tamoxifen therapy or last date of follow-up. The proportionality assumption was investigated using a test based on the Schoenfeld residuals [30]. Three equal thirds were used to categorize the variable to low, intermediate, and high. Survival curves were generated using the method of Kaplan and Meier (1958) and the logrank test was used to test for differences. All *P* values are two-sided and *P*<0.05 was considered statistically significant. Computations were done with the use of STATA statistical package, release 8.2 (STATA Corp., College Station, TX).

RESULTS

Correlations between biological factors

To verify that the sections used for RNA isolation were representative of the whole tumor with respect to ER and PgR levels, all samples were analyzed for *ER* and *PGR* mRNA expression. In agreement with the selection of ER protein–positive samples, none of the RNA samples tested negative for *ER* mRNA. In addition, *ER* and *PGR* mRNA levels correlated significantly with the amount of ER or PgR protein as measured in the cytosols (Spearman rank correlation, r_s=0.62; *P*<0.001 for *ER*, *n*=259; and r_s=0.63; *P*<0.001 for *PGR*; *n*=255) and by immunohistochemistry (Kruskal-Wallis test: χ^2=31.09; *df*=4; *P*<0.001 for ER, *n*=108; and χ^2=55.95; *df*=4; *P*<0.001 for PgR, *n*=108). Spearman rank correlation further revealed meaningful (defined as *P*<0.001 for *n*=250 to 259) correlations between *ADAM-9* and *ADAM-10* (r_s=0.28), *ADAM-12* (r_s=0.28), *MMP-2* (r_s=0.36), and *MMP-9* (r_s=0.27). In addition, *ADAM-10* correlated with *ADAM-12* (r_s=0.41), *MMP-2* (r_s=0.34), and *MMP-9* (r_s=0.24), *ADAM-12* with *MMP-2* (r_s=0.69) and *MMP-9* (r_s=0.34), and *MMP-2* with *MMP-9* (r_s=0.34). *ER-α* mRNA only correlated with *PGR* mRNA (r_s=0.25), and *ADAM-11* showed no correlation (*P*<0.001) with any of the biological factors studied.

Associations of the expression levels with clinicopathologic factors

The associations of clinicopathologic factors

Table 4. Cox univariate regression analysis for disease control with first-line tamoxifen.

Factor*	Primary tumors with ›70% tumor cell nuclei			Primary tumors with ≤70% tumor cell nuclei		
	No. of patients [†]	OR (95% CI)	*P*	No. of patients [†]	OR (95% CI)	*P*
ER-α	106	2.10 (1.27-3.49)	0.004	153	1.35 (0.88-2.06)	0.164
PgR	106	1.24 (1.03-1.50)	0.025	153	1.10 (0.92-1.30)	0.291
ADAM-9	106	1.18 (0.77-1.80)	0.442	153	1.59 (1.14-2.22)	0.007
ADAM-10	102	2.31 (0.91-5.89)	0.078	148	1.27 (0.58-2.78)	0.554
ADAM-11	106	0.96 (0.69-1.32)	0.780	153	1.65 (1.22-2.23)	0.001
ADAM-12	102	0.68 (0.40-1.16)	0.157	148	0.97 (0.67-1.42)	0.884
MMP-2	106	0.80 (0.49-1.32)	0.387	153	0.92 (0.64-1.30)	0.622
MMP-9	106	0.90 (0.68-1.19)	0.462	153	0.78 (0.60-0.99)	0.045

NOTE: Biological factors separately evaluated for primary tumors with >70% and ≤70% tumor cell nuclei.

* Log-transformed continuous variable.

† Includes 259 patients separately evaluated, based on the median level of 70% tumor nuclei in the whole population of 259 primary tumors, for106 patients with >70% tumor cell nuclei and 153 patients with ≤70% tumor cell nuclei in their primary tumor. Because of missing values, numbers do not always add up to 259.

with the biological factors at the median mRNA level are depicted in Table 1. None of the mRNA levels correlated with the dominant site of relapse or disease-free interval. *ER-α* mRNA levels were inversely related with grade and were higher in tumors from postmenopausal patients compared with premenopausal patients. *MMP-2* and *MMP-9* mRNA expression levels were inversely related with tumor size, and *ADAM-10* expression levels varied between histologic subtypes. The association with nodal status is less straightforward. Although *PGR* mRNA levels in these ER-positive tumors were significantly lower in node-negative patients, *ER-α*, *ADAM-9*, *ADAM-11*, and *ADAM-12* mRNA levels were negatively related with the number of positive lymph nodes.

Univariate and multivariate analysis for disease control

In our analysis of the predictive value of the ADAMs and the MMPs, the main clinical end point was the measurable effect of tamoxifen therapy on tumor size (disease control) from the start of therapy. In univariate analysis using log-transformed continuous variables, increasing levels of *ER-α*, *PGR*, *ADAM-9*, and *ADAM-11*, and decreasing levels of *MMP-9* predicted a favorable disease control (Table 3). In contrast, no significant associations with treatment benefit were observed for *ADAM-10*, *ADAM-12*, and *MMP-2* (Table 3). The predictive value of the factors for disease control was studied with multivariate logistic regression analysis (Table

3). For this multivariate analysis, we used the same base multivariate model including the traditional predictive factors as described previously for a larger group of 691 patients treated with first-line tamoxifen for recurrent disease [10]. This base multivariate model includes the traditional predictive factors menopausal status, dominant site of relapse, disease-free interval, and ER and PGR tumor levels. The contributions of the biological factors that were shown to be significantly related with benefit of tamoxifen treatment in the univariate analysis were separately included as log-transformed continuous variables (Table 3). The analyses showed that only *ADAM-9* (OR, 1.41; *P*=0.015) and *MMP-9* (OR, 0.81; *P*=0.035) provided additional predictive information over the traditional predictive factors of the base model.

Effect of tumor cell percentage

Because most MMPs are localized to the tumor stroma, we hypothesized that this might be the case for the related ADAMs as well. Therefore, we also checked for possible correlations between the fraction of epithelial tumor cell nuclei (range, 30-90%; median, 70%) and stromal-derived cell nuclei in the primary tumor and the predictive power of the various biological factors with respect to tamoxifen benefit. For this, we split our samples at the median level of 70% tumor cell nuclei. The respective groups consisted of *n*=106 patients with >70% tumor cell nuclei (>70% TC) and a group of *n*=153 patients containing ≤70% tumor cell

nuclei (≤70% TC) in their primary tumor. In the group of patients with >70% TC tumors (Table 4), only mRNA levels of *ER-α* (OR, 2.10; *P*=0.004) and *PGR* (OR, 1.24; *P*=0.025) showed significant correlations with treatment outcome. On the other hand, whereas the traditional predictive factors *ER-α* and *PGR* lost their predictive power in the group of tumors containing at least 30% stromal cells, *ADAM-9*, *ADAM-11*, and *MMP-9* mRNA levels gained predictive power with respect to benefit of tamoxifen treatment (OR, 1.59; *P*=0.007 for *ADAM-9*; OR, 1.65; *P*=0.001 for *ADAM-11*; and OR, 0.78; *P*=0.045, for *MMP-9*, respectively; Table 4).

Having established that the predictive power of some of the biological factors, as log-transformed continuous variables, depended on the

cell type composition of the primary tumor, we extended our analysis for these factors. For this, we explored the significance of these factors with respect to disease control and progression-free survival after categorizing the mRNA levels of the biological variables in the specific tumor cell subpopulations in three equal thirds (low, intermediate, high; Table 5). Figure 1 shows progression-free survival as a function of the categorized *ER-α* tumor levels in all 259 patients (Figure 1A) against the 106 patients with >70% TC tumors (Figure 1B) and likewise for *ADAM-9* in all patients (Figure 1C) against the 153 patients with ≤70% TC tumors (Figure 1D). Because the proportional hazards assumptions for *ER-α*, *ADAM-9*, and *ADAM-11* were violated for the total follow-up time of 130 months (*P*<0.005), we analyzed the relation-

Table 5. Cox univariate regression analysis of biological factors in primary tumors with >70% or ≤70% tumor cell nuclei for disease control with first-line tamoxifen and progression-free survival (restricted to the first 9 months) after start of tamoxifen therapy.

Factor and levels*	Tumor cells (%) [†]	No. of patients [‡]	Disease control (%) [‡]	Disease control		Progression-free survival	
				OR (95% CI)	P	Hazard ratio (95% CI)	P
ER-α							
($\times 10^{-6}$)	>70						
<5.0		36	50	1		1	
5.0-13.6		35	57	1.33 (0.52-3.40)		1.19 (0.66-2.14)	
>13.6		35	86	6.00 (1.90-18.96)	0.003	0.28 (0.12-0.64)	<0.001
PgR							
($\times 10^{-6}$)	>70						
<0.2		36	53	1		1	
0.2-1.8		35	63	1.51 (0.59-3.91)		0.72 (0.38-1.36)	
>1.8		35	77	3.02 (1.08-8.42)	0.094	0.58 (0.30-1.12)	0.253
ADAM-9							
($\times 10^{-6}$)	≤70						
<2.9		51	37	1		1	
2.9-7.6		51	69	3.68 (1.62-8.36)		0.36 (0.21-0.64)	
>7.6		51	67	3.37 (1.49-7.60)	0.002	0.47 (0.28-0.80)	<0.001
ADAM-11							
($\times 10^{-3}$)	≤70						
<1.7		51	45	1		1	
1.7-5.0		51	49	1.17 (0.54-2.55)		0.84 (0.50-1.40)	
>5.0		51	78	4.43 (1.86-10.52)	<0.001	0.48 (0.27-0.85)	0.029
MMP-9							
($\times 10^{-6}$)	≤70						
<0.3		51	67	1		1	
0.3-1.0		51	51	0.52 (0.23-1.16)		1.45 (0.83-2.51)	
>1.0		51	55	0.61 (0.27-1.36)	0.245	1.33 (0.76-2.33)	0.388

NOTE: Due to different assay conditions and amplicon lengths, absolute values can only be compared within a gene assay.

* Three equal thirds were used to categorize the variable in the specific tumor cell subpopulation in low, intermediate, and high.

† Based on the median level of 70% tumor cell nuclei in the whole population of 259 primary tumors, separately evaluated for 106 patients with >70% tumor cell nuclei and 153 patients with ≤70% tumor cell nuclei in their primary tumor.

‡ Number of patients entered into the study and corresponding disease control data are given for the low, intermediate, and high mRNA expression levels in the specific tumor cell subpopulation.

ships of these factors with progression-free survival during the first 9 months of follow-up, the time that half of the patients treated for advanced disease showed disease progression on tamoxifen [10, 31]. In this short-term analysis (Figure 1), with 130 failures in all 259 patients, 53 in the group of 106 patients with >70% TC tumors, and 77 failures in the 153 patients with ≤70% TC tumors, the proportional hazards assumption was no longer violated (P>0.1) for any of the factors further evaluated. We therefore restricted our exploration of the relationship of the factors with progression-free survival to failures during the first 9 months of follow-up (Table 5). The most notable findings in these univariate analyses were: (*a*) that *MMP-9* mRNA levels analyzed as a categorized variable lost its predictive value and (*b*) that *ER-α* mRNA levels when measured in >70% TC tumors and *ADAM-9* and *ADAM-11* mRNA levels when measured in ≤70% TC tumors were strong predictors for disease control by first-line tamoxifen therapy and for the length of progression-free survival after the start of treatment.

Localization of ER-α, ADAM-9, and ADAM-11 protein in human breast tissues

Finally, we employed immunohistochemistry to determine the location of ADAM-9 and ADAM-11 protein in our human breast tumor tissues and compared this with the location of ER-α protein. Representative results are shown in Figure 2 for staining of pre-existent mammary gland tissue (Figure 2A-D), carcinoma *in situ* components (Figure 2E-H), and lobular breast carcinomas (Figure 2I-L). Whereas ER-α staining is mainly localized to the nuclei of tumor cells, ADAM-9 and ADAM-11 are most commonly found in the cytoplasm and less commonly at the cell membrane. Immunohistochemical staining of ADAM-9 and ADAM-11 protein in human breast carcinomas yielded heterogeneous results with both proteins found in tumor cells (Figure 2J and K), adipocytes, smooth muscle cells of vessel walls, and the myoepithelial and luminal layers of nonneoplastic epithelium of the mammary gland (Figure 2B and C).

DISCUSSION

Endocrine therapy is the most common treatment in breast cancer patients with tumors that express ER-α and/or PgR. Even though the ER-α is the prime target for endocrine therapy, the failure or success of this therapy is poorly understood. Systemic endocrine therapy in patients with recurrent disease at distant sites is merely palliative and accomplishes a disease control in about 50% to 60% of the patients. However, progression is inevitable in these patients because of the occurrence of acquired therapy resistance. From a biological point of view, first-line single-agent endocrine therapy in patients with recurrent breast cancer is an excellent setting to study response to therapy because it is less subject to prognostic influences unavoidably present when a similar study would be done in the adjuvant setting. In the present study, the effect of endocrine therapy on size of the metastatic or the occurrence of new lesions were used as the main clinical end point. We defined the type of response strictly beforehand, and when there was any doubt, patients were not included in this study. The size of the metastases or the occurrence of new lesions is an objective measure of treatment effect. However, because of the retrospective nature of our study, the differentiation between partial remission and no change was difficult to assess, especially in patients with bone metastasis (60%). In our study, the progression-free survival of patients with stable disease (no change >6 months) was comparable with the progression-free survival of patients with partial remission and could therefore be considered as responders. This is in agreement with a previously published prospective study which also reported that objective benefit was not always easy to assess and in which prolonged stable disease was categorized as response [6].

In this study, ER and PgR were determined in cytosols by biochemical methods and the cutoff used to classify tumors as ER- or PgR-positive was 10 fmol/mg cytosolic protein. These data correlated significantly with *ER* and *PGR* mRNA expression levels. However, although these quantitative procedures are the most accu-
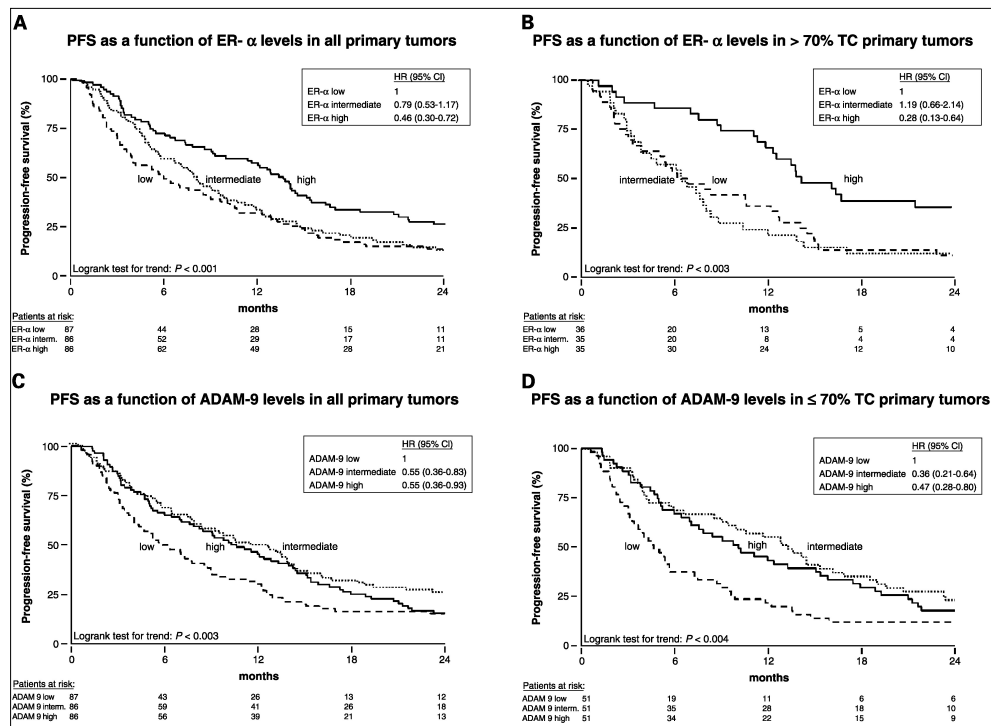
Figure 1. Kaplan-Meier curves of progression-free survival with log-rank testing restricted to the first 9 months of follow-up for patients with advanced disease treated with first-line tamoxifen.
The mRNA levels divided in three equal thirds given in Table 5 for ER-α (A + B) and ADAM-9 (C + D) were assessed in tumors before (A + C) and after (B + D) dichotomization on the basis of the median level of 70% tumor cell nuclei in the total group of 259 patients. Numbers below the x-axis show the patients at risk at the indicated time points.

rate methods, it is not currently the most widely used method to evaluate hormonal receptor status in breast cancer. In fact, immunohistochemistry is nowadays more commonly used for routine ER and PgR measurements. Because this study shows a possible application for current clinical practice, we compared the biochemical and immunohistochemical methods in a randomly selected subgroup of patients. In agreement with a previously published study in which ligand binding assay and immunohistochemistry were compared in predicting response to tamoxifen in 205 patients with ER-positive metastatic breast cancer [32], ER and PgR levels also showed comparable differences in response rates in our study, whether defined by mRNA, by biochemical methods, or by immunohistochemistry.

The main findings of our study are that *ADAM-*

9 and *ADAM-11* differentially from ER predict the type of response to tamoxifen treatment in patients with recurrent breast cancer and that the fraction of tumor cells and stromal elements are important in this respect. The actual ER level in the ER-positive tumors (>10 fmol/mg cytosol protein) containing >30% stromal elements did not further contribute to the rate of response. This finding supports the results of a previous report that showed an association between ER level and the volume fraction of actual cancer cells present in the tumors [33]. Therefore, it was advised that, when quantitative ER levels are used to predict the response of tumors to hormonal therapy, the cellularity of tumors should be taken into consideration. We followed this approach in our study by discriminating between tumors with >70% epithelial tumor cells and tumors with 30% to 70% epithelial

tumor cells. Our results show that for tumors with a relatively low percentage of epithelial tumor cells, a marker set including ADAM-9 and ADAM-11 may have potential to assess the efficacy of tamoxifen therapy.

Of the ADAMs and MMPs studied, all, except *ADAM-11*, were readily detected by real-time RT-PCR in all samples. The absence of detectable *ADAM-11* mRNA levels in 29% of our primary breast tumors is most likely a reflection of the loss of heterozygosity on chromosome 17q21, where *ADAM-11* is located [13], as described to be the case for 30% of the tumors [11]. Patterns of copy number gains and losses define breast tumors with distinct clinicopathologic features and patient prognosis [34]. Several studies have already shown that *ERBB2* amplification is associated with a shorter disease-free and overall survival in the subgroup of patients receiving adjuvant tamoxifen therapy

when compared with the untreated group [35–37]. However, whereas *ERBB2* is located on cytoband 17q12, a region of copy gain, *ADAM-11* is located on cytoband 17q21, a region of copy loss. Our finding that low tumor *ADAM-11* mRNA levels are associated with poor efficacy of tamoxifen treatment supports the hypothesis that *ADAM-11* is a candidate tumor suppressor gene for human breast cancer [13, 14], and extends its role as a candidate tumor suppressor gene to a candidate gene associated with tamoxifen responsiveness.

Our study shows that *ADAM-9* and *ADAM-11* mRNA levels are especially informative with respect to tamoxifen treatment outcome in tumors containing a relatively large proportion of stromal cells. In agreement with a previously published study describing the expression of ADAM-9, ADAM-10, ADAM-12, ADAM-15, and ADAM-17 in breast cancer specimens [38],

Figure 2. Immunohistochemical localization of ER-α, ADAM-9, and ADAM-11 in breast cancer tissue.

A-D, ×20 magnification. Pre-existent mammary gland tissue expressing occasional positive nuclear staining for ER-α (A), abundant staining of the myoepithelial layer and weak staining of the luminal layer for ADAM-9 (B), and weak staining of both layers for ADAM-11 (C). E-H, ×40 magnification. Carcinoma in situ component expressing positive nuclear staining for ER-α (E), intermediate cytoplasmic staining for ADAM-9 (F) and abundant cytoplasmic and membrane staining for ADAM-11 (G). I-L, ×40 magnification. Lobular carcinoma expressing positive nuclear staining for ER-α (I), weak cytoplasmic staining for ADAM-9 (J), and medium cytoplasmic staining for ADAM-11 (K). The specificity of immunostaining was controlled using normal goat and mouse IgG and by omitting the primary antibodies (negative controls, D, H, and L).
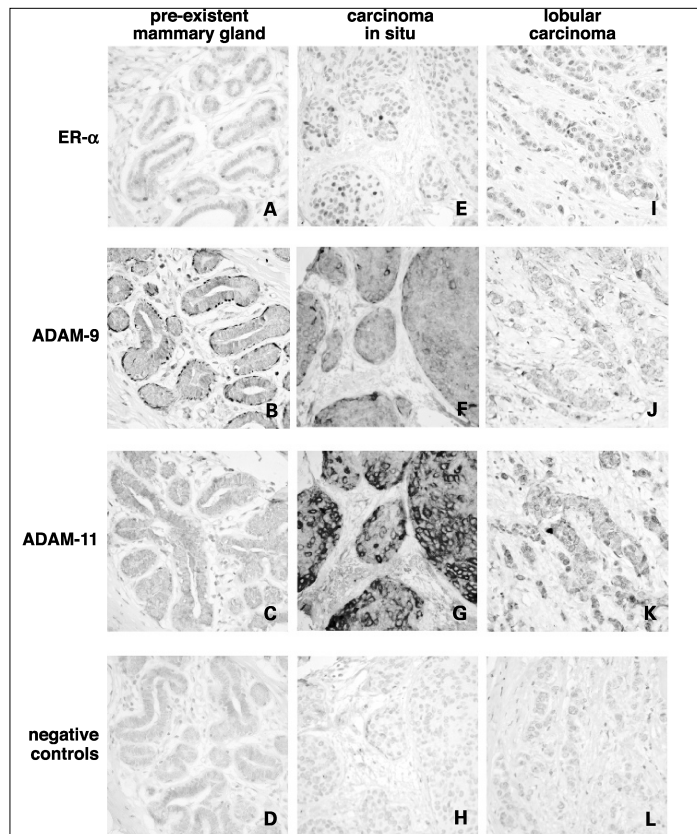
immunohistochemical staining of ADAM-9 and ADAM-11 protein in human breast carcinomas yielded heterogeneous results with both proteins found in tumor cells, adipocytes, nonneoplastic epithelium of the mammary gland, and smooth muscle cells of vessel walls. The question of how ADAM-11 and ADAM-9, either stromal or tumor cell–derived, might prevent the development of tamoxifen resistance remains to be solved. Because proteases such as urokinase-type plasminogen activator [9, 10] and MMP-2 [39] have been shown to be related to tamoxifen resistance, we hypothesized that specific ADAMs might also be related to tamoxifen resistance. We found that high levels of *ADAM-9* and *ADAM-11* mRNA were related to a better response rate. This is in contrast with the findings for urokinase-type plasminogen activator [10], showing high levels to be associated with poor benefit of tamoxifen treatment in recurrent breast cancer, and for MMP-2 [39], showing that high levels predicted failure to adjuvant antiestrogen therapy. This suggests that ADAM-9 and ADAM-11 function differently from urokinase-type plasminogen activator and MMP-2, and that it is therefore perhaps not the protease function of the ADAMs that is important in the prevention or delay of tamoxifen resistance. Increasing evidence indicates that abnormalities occurring in growth factor signaling pathways, as currently well-documented for epidermal growth factor receptor (ERBB1) and ERBB2 (HER2/neu), could dramatically influence steroid hormone action and may be critical for anti–hormonal-resistant breast cancer cell growth [7, 8, 36, 40–43]. From this point of view, one might expect factors that target growth factor signaling pathways are potentially able to prevent the development of tamoxifen resistance. Many intercellular signaling molecules are membrane-anchored proteins, which are proteolytically processed after becoming membrane-bound, to liberate their extracellular domains (ectodomain shedding). Genetic and biochemical studies have shown that some ADAMs participate in these events [3]. Therefore, it is perhaps the ectodomain shedding function of the ADAMs that plays a role in the prevention of tamoxifen resistance.

Furthermore, the disintegrin domain of ADAM-9 can function as an adhesion molecule by interacting with an $\alpha(v)\beta(5)$ integrin [44], thus limiting the metastatic potential of the cell.

In summary, our study shows that patients with primary tumors exhibiting a high percentage of epithelial tumor cell nuclei over stromal cells combined with high levels of ER-α have a good chance to benefit from tamoxifen therapy. For patients with tumors displaying $\geq 30\%$ stromal components intermingled with epithelial tumor cells, the additional assessment of tumor mRNA levels of ADAM-9 and ADAM-11 could be helpful to refine treatment strategies for these patients. However, taking into account that only patients with ER-positive primary tumors entered this study, this may only apply to patients with ER-positive primary tumors. Further studies are required to verify whether the results of our study can be adapted to fit all patients, irrespective of the ER status of the primary tumor. Based on recent advances in breast cancer management, endocrine therapy with aromatase inhibitors may become the treatment of choice for postmenopausal women [45]. Because both aromatase inhibitors and tamoxifen aim to deprive the ER from estrogens, it would be interesting to learn whether ADAM-9 and ADAM-11 could also be linked to disease control of aromatase inhibitors. In addition, as the majority of patients receive adjuvant treatment today, it will be important to learn whether ADAM-9 and ADAM-11 could also be informative for determining the outcome of breast cancer patients treated with adjuvant endocrine therapy.

ACKNOWLEDGEMENTS

REFERENCES

1. Wolfsberg TG, Primakoff P, Myles DG, White JM. ADAM, a novel family of membrane proteins containing A Disintegrin And Metalloprotease domain: multipotential functions in cell-cell and cell-matrix interactions. J Cell Biol 1995;131:275-8.

2. Schlondorff J, Blobel CP. Metalloprotease-disintegrins: modular proteins capable of promoting cell-cell interactions and triggering signals by protein-ectodomain shedding. J Cell Sci 1999;112 (Pt 21):3603-17.

3. Duffy MJ, Lynn DJ, Lloyd AT, O'Shea CM. The ADAMs family of proteins: from basic studies to potential clinical applications. Thromb Haemost 2003; 89:622-31.

4. White JM. ADAMs: modulators of cell-cell and cell-matrix interactions. Curr Opin Cell Biol 2003;15: 598-606.

5. Seals DF, Courtneidge SA. The ADAMs family of metalloproteases: multidomain proteins with multiple functions. Genes Dev 2003;17:7-30.

6. Ravdin PM, Green S, Dorr TM, McGuire WL, Fabian C, Pugh RP, Carter RD, Rivkin SE, Borst JR, Belt RJ. Prognostic significance of progesterone receptor levels in estrogen receptor-positive patients with metastatic breast cancer treated with tamoxifen: results of a prospective Southwest Oncology Group study. J Clin Oncol 1992;10:1284-91.

7. Nicholson RI, Gee JM, Knowlden J, McClelland R, Madden TA, Barrow D, Hutcheson I. The biology of antihormone failure in breast cancer. Breast Cancer Res Treat 2003;80 Suppl 1:S29-34; discussion S35.

8. Hayes DF. Tamoxifen: Dr. Jekyll and Mr. Hyde? J Natl Cancer Inst 2004;96:895-897.

9. Foekens JA, Look MP, Peters HA, van Putten WL, Portengen H, Klijn JG. Urokinase-type plasminogen activator and its inhibitor PAI-1: predictors of poor response to tamoxifen therapy in recurrent breast cancer. J Natl Cancer Inst 1995;87:751-6.

10. Meijer-van Gelder ME, Look MP, Peters HA, Schmitt M, Brunner N, Harbeck N, Klijn JG, Foekens JA. Urokinase-type plasminogen activator system in breast cancer: association with tamoxifen therapy in recurrent disease. Cancer Res 2004;64:4563-8.

11. DeMarchis L, Cropp C, Sheng ZM, Bargo S, Callahan R. Candidate target genes for loss of heterozygosity on human chromosome 17q21. Br J Cancer 2004; 90: 2384-9.

12. Orsetti B, Nugoli M, Cervera N, Lasorsa L, Chuchana P, Ursule L, Nguyen C, Redon R, du Manoir S, Rodriguez C, Theillet C. Genomic and expression profiling of chromosome 17 in breast cancer reveals complex patterns of alterations and novel candidate genes. Cancer Res 2004;64:6453-60.

13. Emi M, Katagiri T, Harada Y, Saito H, Inazawa J, Ito I, Kasumi F, Nakamura Y. A novel metalloprotease/disintegrin-like gene at 17q21.3 is somatically rearranged in two primary breast cancers. Nat Genet 1993;5:151-7.

14. Katagiri T, Harada Y, Emi M, Nakamura Y. Human metalloprotease/disintegrin-like (MDC) gene: exon-intron organization and alternative splicing. Cytogenet Cell Genet 1995;68:39-44.

15. O'Shea C, McKie N, Buggy Y, Duggan C, Hill AD, McDermott E, O'Higgins N, Duffy MJ. Expression of ADAM-9 mRNA and protein in human breast cancer. Int J Cancer 2003;105:754-61.

16. Azzam HS, Arand G, Lippman ME, Thompson EW. Association of MMP-2 activation potential with metastatic progression in human breast cancer cell lines independent of MMP-2 production. J Natl Cancer Inst 1993;85:1758-64.

17. Heppner KJ, Matrisian LM, Jensen RA, Rodgers WH. Expression of most matrix metalloproteinase family members in breast cancer represents a tumor-induced host response. Am J Pathol 1996;149:273-82.

18. Duffy MJ, Maguire TM, Hill A, McDermott E, O'Higgins N. Metalloproteinases: role in breast carcinogenesis, invasion and metastasis. Breast Cancer Res 2000;2:252-7.

19. Ranuncolo SM, Armanasco E, Cresta C, Bal De Kier Joffe E, Puricelli L. Plasma MMP-9 (92 kDa-MMP) activity is useful in the follow-up and in the assessment of prognosis in breast cancer patients. Int J Cancer 2003; 106:745-51.

20. Tester AM, Waltham M, Oh SJ, Bae SN, Bills MM, Walker EC, Kern FG, Stetler-Stevenson WG, Lippman ME, Thompson EW. Pro-matrix metalloproteinase-2 transfection increases orthotopic primary growth and experimental metastasis of MDA-MB-231 human breast cancer cells in nude mice. Cancer Res 2004;64:652-8.

21. Jones JL, Glynn P, Walker RA. Expression of MMP-2 and MMP-9, their inhibitors, and the activator MT1-MMP in primary breast carcinomas. J Pathol 1999; 189:161-8.

22. Martens JW, Nimmrich I, Koenig T, Look MP, Harbeck N, Model F, Kluth A, Bolt-de Vries J, Sieuwerts AM, Portengen H, Meijer-Van Gelder ME, Piepenbrock C, Olek A, Hofler H, Kiechle M, Klijn JG, Schmitt M, Maier S, Foekens JA. Association of DNA methylation of phosphoserine aminotransferase with response to endocrine therapy in patients with recurrent breast cancer. Cancer Res 2005;65:4101-17.

23. Hayward JL, Carbone PP, Heuson JC, Kumaoka S, Segaloff A, Rubens RD. Assessment of response to therapy in advanced breast cancer: a project of the Programme on Clinical Oncology of the International Union Against Cancer, Geneva, Switzerland. Cancer 1977;39:1289-94.

24. European Organization for Research and Treatment of Cancer Breast Cancer Cooperative group. Manual for clinical research and treatment in breast cancer, in Excerpta Medica. 2000: Almere, The Netherlands. p.116-7.

25. Ravdin PM, Burris HA, 3rd, Cook G, Eisenberg P, Kane M, Bierman WA, Mortimer J, Genevois E, Bellet RE. Phase II trial of docetaxel in advanced anthracycline-resistant or anthracenedione-resistant breast cancer. J Clin Oncol 1995;13:2879-85.

26. Foekens JA, Portengen H, Look MP, van Putten WL, Thirion B, Bontenbal M, Klijn JG. Relationship of PS2 with response to tamoxifen therapy in patients with recurrent breast cancer. Br J Cancer 1994;70:1217-23.

27. Robertson JF, Willsher PC, Cheung KL, Blamey RW. The clinical relevance of static disease (no change) category for 6 months on endocrine therapy in patients with breast cancer. Eur J Cancer 1997;33:1774-9.

28. Foekens JA, Portengen H, van Putten WL, Peters HA, Krijnen HL, Alexieva-Figusch J, Klijn JG. Prognostic value of estrogen and progesterone receptors measured by enzyme immunoassays in human breast tumor cytosols. Cancer Res 1989;49:5823-8.

29. European Organization for Research and Treatment of Cancer Breast Cancer Cooperative group. Revision of the standards for the assessment of hormone receptors in human breast cancer; report of the second E.O.R.T.C. Workshop, held on 16-17 March, 1979, in the Netherlands Cancer Institute. Eur J Cancer 1980;16: 1513-5.

30. Grambsch P, Louis TA, Bostick RM, Grandits GA, Fosdick L, Darif M, Potter JD. Statistical analysis of proliferative index data in clinical trials. Stat Med 1994; 13:1619-34.

31. Bonneterre J, Thurlimann B, Robertson JF, Krzakowski M, Mauriac L, Koralewski P, Vergote I, Webster A, Steinberg M, von Euler M. Anastrozole versus tamoxifen as first-line therapy for advanced breast cancer in 668 postmenopausal women: results of the Tamoxifen or Arimidex Randomized Group Efficacy and Tolerability study. J Clin Oncol 2000;18:3748-57.

32. Elledge RM, Green S, Pugh R, Allred DC, Clark GM, Hill J, Ravdin P, Martino S, Osborne CK. Estrogen receptor (ER) and progesterone receptor (PgR), by ligand-binding assay compared with ER, PgR and pS2, by immuno-histochemistry in predicting response to tamoxifen in metastatic breast cancer: a Southwest Oncology Group Study. Int J Cancer 2000;89:111-7.

33. Helle M, Helin H, Isola J, Krohn K. Oestrogen receptor content and cancer cell/stroma ratio in mammary carcinoma. Apmis 1988;96:1140-2.

34. Rennstam K, Ahlstedt-Soini M, Baldetorp B, Bendahl PO, Borg A, Karhu R, Tanner M, Tirkkonen M, Isola J. Patterns of chromosomal imbalances defines subgroups of breast cancer with distinct clinical features and prognosis. A study of 305 tumors by comparative genomic hybridization. Cancer Res 2003;63:8861-8.

35. Borg A, Baldetorp B, Ferno M, Killander D, Olsson H, Ryden S, Sigurdsson H. ERBB2 amplification is associated with tamoxifen resistance in steroid-receptor positive breast cancer. Cancer Lett 1994;81:137-44.

36. De Placido S, Carlomagno C, De Laurentiis M, Bianco AR. c-erbB2 expression predicts tamoxifen efficacy in breast cancer patients. Breast Cancer Res Treat 1998;52: 55-64.

37. Lipton A, Ali SM, Leitzel K, Demers L, Harvey HA, Chaudri-Ross HA, Brady C, Wyld P, Carney W. Serum HER-2/neu and response to the aromatase inhibitor letrozole versus tamoxifen. J Clin Oncol 2003;21:1967-72.

38. Lendeckel U, Kohl J, Arndt M, Carl-McGrath S, Donat H, Rocken C. Increased expression of ADAM family members in human breast cancer and breast cancer cell lines. J Cancer Res Clin Oncol 2005;131:41-8.

39. Talvensaari-Mattila A, Paakko P, Blanco-Sequeiros G, Turpeenniemi-Hujanen T. Matrix metalloproteinase-2 (MMP-2) is associated with the risk for a relapse in postmenopausal patients with node-positive breast carcinoma treated with antiestrogen adjuvant therapy. Breast Cancer Res Treat 2001;65:55-61.

40. Newby JC, Johnston SR, Smith IE, Dowsett M. Expression of epidermal growth factor receptor and c-erbB2 during the development of tamoxifen resistance in human breast cancer. Clin Cancer Res 1997;3:1643-51.

41. Kurokawa H, Arteaga CL. ErbB (HER) receptors can abrogate antiestrogen action in human breast cancer by multiple signaling mechanisms. Clin Cancer Res 2003; 9:511-5.

42. Schiff R, Massarweh SA, Shou J, Bharwani L, Mohsin SK, Osborne CK. Cross-talk between estrogen receptor and growth factor pathways as a molecular target for overcoming endocrine resistance. Clin Cancer Res 2004; 10:331S-6S.

43. Shou J, Massarweh S, Osborne CK, Wakeling AE, Ali S, Weiss H, Schiff R. Mechanisms of tamoxifen resistance: increased estrogen receptor-HER2/neu cross-talk in ER/HER2-positive breast cancer. J Natl Cancer Inst 2004;96:926-35.

44. Zhou M, Graham R, Russell G, Croucher PI. MDC-9 (ADAM-9/Meltrin gamma) functions as an adhesion molecule by binding the alpha(v)beta(5) integrin. Biochem Biophys Res Commun 2001;280:574-80.

45. Winer EP, Hudis C, Burstein HJ, Wolff AC, Pritchard KI, Ingle JN, Chlebowski RT, Gelber R, Edge SB, Gralow J, Cobleigh MA, Mamounas EP, Goldstein LJ, Whelan TJ, Powles TJ, Bryant J, Perkins C, Perotti J, Braun S, Langer AS, Browman GP, Somerfield MR. American Society of Clinical Oncology technology assessment on the use of aromatase inhibitors as adjuvant therapy for postmenopausal women with hormone receptor-positive breast cancer: status report 2004. J Clin Oncol 2005;23:619-29.

CHAPTER FIVE

Which cyclin E prevails as prognostic marker for breast cancer?
Results from a retrospective study involving 635 lymph node-negative breast cancer patients

Anieta M. Sieuwerts, Maxime P. Look, Marion E. Meijer-van Gelder,
Mieke Timmermans, Anita M.A.C. Trapman, Roberto Rodriguez Garcia,
Miranda Arnold, Anneke J.W. Goedheer, Vanja de Weerd, Henk Portengen,
Jan G.M. Klijn and John A. Foekens

Department of Medical Oncology, Erasmus MC, Rotterdam, The Netherlands

ABSTRACT

Purpose: To evaluate the prognostic value of cyclin E with a quantitative method for lymph node-negative primary breast cancer patients.

Patients and methods: mRNA transcripts of full-length and splice variants of cyclin E1 (*CCNE1*) and cyclin E2 (*CCNE2*) were measured by real-time RT-PCR in frozen tumor samples from 635 lymph node-negative breast cancer patients who had not received neoadjuvant or adjuvant systemic therapy.

Results: None of the PCR assays designed for the specific splice variants of the cyclins gave additional prognosis-related information compared with the common assays able to detect all variants. In Cox multivariate analysis, corrected for the traditional prognostic factors, high levels of cyclin E were independently associated with a short distant metastasis-free survival [hazard ratio (HR), 3.40; $P<0.001$ for *CCNE1* and HR, 1.76; $P<0.001$ for *CCNE2*, respectively]. After dichotomizing the tumors at the median level of 70% epithelial tumor cells, the multivariate analysis showed particularly strong results for *CCNE1* in the group of 433 patients with stroma-rich primary tumors (HR, 5.12; $P<0.001$). In these tumors, the worst prognosis was found for patients with estrogen receptor-negative tumors expressing high *CCNE1* (HR, 9.89; $P<0.001$) and for patients with small (T1) tumors expressing high *CCNE1* (HR, 8.47; $P<0.001$).

Conclusion: Our study shows that both *CCNE1* and *CCNE2* qualify as independent prognostic markers for lymph node - negative breast cancer patients, and that *CCNE1* may provide additional information for specific subgroups of patients.

INTRODUCTION

Dysregulation of the cyclin-dependent kinase-2 (CDK2)–bound cyclins plays an important role in the pathogenesis of cancer. High levels of cyclin E expression are found in many types of cancer, and elevated levels of the E1 cell cycle protein have been associated with a poor prognosis in primary breast cancer patients (reviewed by Yasmeen *et al*.; ref. 1). Although studies have mainly focused on cyclin E1, the human genome encodes two E-type cyclins: *CCNE1* (formerly cyclin E) on chromosome 19q [2, 3] and *CCNE2* on chromosome 8q [4–6]. The encoded human cyclin E2 protein shares 47% overall similarity to cyclin E1 and contains a cyclin box motif that is characteristic of all cyclins [5]. However, whereas a significantly increased expression of cyclin E2 is observed in breast cancers [7], its potential association with tumor aggressiveness is still unknown. Notwithstanding, *CCNE2* and not *CCNE1* overlapped between the 76-gene prediction signature from Wang *et al*. [8] and the 70-gene prediction signature from van't Veer *et al*. [9] for metastasis-free survival (MFS) of lymph node–negative patients. This suggested that at least for microarray techniques, and perhaps for all gene expression levels measuring methods, *CCNE2* might be a better prognostic marker when compared with *CCNE1*.

For both *CCNE1* and *CCNE2*, alternatively spliced transcript variants, which encode distinct protein isoforms, have been reported [5, 10–13]. Once translated in tumor cells, the protein products of such variants can give rise to constitutively active forms of the cyclin E containing complexes. To complicate matters, it has been shown that in breast cancer compared with normal cells and tissues, cyclin E1 protein is overexpressed and post-translationally cleaved by a protease into low molecular weight isoforms [14, 15]. These low molecular weight forms of cyclin E1 show higher CDK2 kinase activity, and the low molecular weight cyclin E1/CDK2 complexes are more resistant to inhibitors and antiestrogens [16]. Keyomarsi *et al*. [17] showed that levels of total cyclin E1 and low molecular weight cyclin E1 in tumor

tissue measured by Western blot assay correlated strongly with survival in patients with breast cancer. A complicating factor was that approximately two thirds of the patients included in this study received either adjuvant chemotherapy or hormonal therapy [18]. Trials of adjuvant therapy in patients with breast cancer no longer include an untreated control group. Therefore, retrospective studies involving well-characterized tumor banks with tumors from untreated patients will be necessary to determine whether cyclin E is a pure prognostic factor instead of a predictor for the benefits of adjuvant systemic therapy. Our current study involves such a cohort of 635 tumors from lymph node–negative patients who did not receive any adjuvant systemic therapy.

PATIENTS AND METHODS

Patients

The study was approved by the institutional medical ethics committee (MEC 02.953). Tumor samples were originally submitted to our reference laboratory from 25 regional hospitals for measurements of steroid hormone receptors. Guidelines for primary treatment were similar for all hospitals. To avoid bias, selection of tumors from our tumor bank at the Erasmus Medical Center (Rotterdam, the Netherlands) was done by processing all available frozen tumor samples from female patients with lymph node–negative breast cancer who entered the clinic during 1979 to 1996 and from whom detailed clinical followup was available. Lymph node negativity and tumor size was based on pathologic examination by regional pathologists. Information on grade was extracted from the pathology records and reflects clinical practice during those years. Exclusion criteria were residual disease or distant spread diagnosed at or within 1 month after primary surgery, noninvasive breast cancer, neoadjuvant or adjuvant systemic therapy, a previous other cancer (except basal cell skin cancer or early-stage cervical cancer stage Ia/Ib), <100 mg frozen tissue available, evaluation of tumor content not reliable (2%), <30% epithelial tumor cell nuclei in

the sample (15%), and poor RNA quality (8%). The thus remaining 635 eligible patients were treated either with breast-conserving surgery (54%) or with modified mastectomy (46%). Forty-one percent of the patients had T1 tumors. The median age of the patients at surgery was 56 years (range, 25-88 years). Three hundred eighty-seven patients (61%) received radiotherapy. Routine post-surgical follow-up and defining the date of MFS was as described [8]. Thirty-seven patients presented with a relapse without signs of a distant metastasis. The median follow-up time was 95 months (range, 11-202 months) with 256 failures in the analysis of MFS and 226 failures in the analysis of overall survival. Other relevant clinicopathologic characteristics are listed in Table 1.

Tissue processing

Tissue processing was done as described in detail before [19]. In brief, 20 to 60 cryostat sections of 30 μm, corresponding to 30 to 100 mg, were cut from frozen tissues. Before, in between, and after cutting the sections for RNA isolation, 5 μm sections were cut for H&E staining to assess the amount of tumor cells relative to the amount of surrounding stromal cells. The amount of nuclei evidently of epithelial tumor cell origin relative to the amount of surrounding stromal cells was estimated with a 100-fold magnification in 10 different areas covering the area of each of the three H&E sections. Only specimen with at least 30% of the nuclei of epithelial tumor cell origin and distributed uniformly over at least 70% of the section area were included. Like done before [19], these estimates were used to dichotomize our tumor cohort at the median level of 70% tumor cell nuclei in stroma-rich (primary tumors containing ≥30% stromal components) and stromapoor (primary tumors containing at least 70% epithelial tumor cells).

RNA isolation, cDNA synthesis, and quantification of specific mRNA species

RNA isolation, cDNA synthesis, quantification of specific mRNA species, and quality control checks were done as described in detail before

Table 1. Associations of CCNE1 and CCNE2 mRNA levels with clinicopathologic factors.

Characteristic	No. patients (%)	Median mRNA levels (and interquartile range)*	
		CCNE1 ($\times 10^{-1}$)	CCNE2 ($\times 10^{0}$)
All patients	635 (100)	0.40 (0.67)	0.71 (0.82)
Age (y)			
≤40	86 (14)	0.53 (0.59)	1.03 (1.15)
41-55	224 (35)	0.52 (0.87)	0.75 (0.87)
56-70	200 (31)	0.38 (0.56)	0.70 (0.70)
›70	125 (20)	0.28 (0.36)	0.56 (0.71)
P		‹0.001[†]	‹0.001[†]
Menopausal status			
Premenopausal	265 (42)	0.50 (0.76)	0.81 (1.06)
Postmenopausal	370 (58)	0.34 (0.57)	0.67 (0.71)
P		‹0.001[‡]	0.029[‡]
Type of surgery			
Breast conserving	340 (54)	0.42 (0.70)	0.76 (0.84)
Mastectomy	295 (46)	0.35 (0.62)	0.68 (0.83)
P		0.234[‡]	0.199[‡]
Pathologic tumor size (cm)			
≤2	260 (41)	0.34 (0.64)	0.65 (0.82)
›2	375 (59)	0.43 (0.68)	0.74 (0.82)
P		0.015[‡]	0.204[‡]
Grade			
Poor	331 (52)	0.47 (0.80)	0.80 (0.95)
Unknown	195 (31)	0.35 (0.53)	0.70 (0.78)
Moderate and good	109 (17)	0.25 (0.52)	0.56 (0.66)
P		‹0.001[§]	0.009[§]
ER status			
Negative, ‹10 fmol/mg protein	180 (28)	0.93 (1.28)	0.77 (0.96)
Positive, ≥10 fmol/mg protein	455 (72)	0.29 (0.40)	0.70 (0.82)
P		‹0.001[†]	0.013[†]
PR status[‖]			
Negative, ‹10 fmol/mg protein	223 (35)	0.74 (1.03)	0.81 (1.09)
Positive, ≥10 fmol/mg protein	381 (60)	0.29 (0.41)	0.67 (0.79)
P		‹0.001[†]	‹0.001[†]
Histologic type			
DCIS + IDC	81 (13)	0.40 (0.59)	0.73 (0.66)
IDC	327 (51)	0.41 (0.69)	0.73 (0.91)
ILC	34 (5)	0.25 (0.37)	0.61 (0.80)
Medullary	25 (4)	0.17 (0.20)	0.32 (0.26)
Mucinous	17 (3)	1.08 (2.22)	0.80 (1.22)
Others	18 (3)	0.27 (0.42)	0.51 (0.48)
Unknown	133 (21)	0.44 (0.81)	0.80 (0.80)
P		‹0.001[§]	0.001[§]

Abbreviations: DCIS, ductal carcinoma in situ; ILC, infiltrating lobular carcinoma; IDC, infiltrating ductal carcinoma.
* Due to different assay conditions, absolute values of the CCNEs can only be compared within a gene assay.
† P for Spearman rank correlation test.
‡ P for Mann-Whitney U test.
§ P for Kruskal-Wallis test.
‖ Due to 31 missing values, numbers do not add up to 635.

[19]. Real-time quantitative PCR was done in an ABI Prism 7700 Sequence Detection System (Applied Biosystems, Nieuwerkerk a/d IJssel, the Netherlands) and a Mx3000P Real-time PCR System (Stratagene, Amsterdam, the Netherlands) using both the Assay-on-Demand assays from Applied Biosystems and the intron-spanning forward and reverse primer combinations at the conditions shown in Table 2A. In our initial screening, we compared *CCNE1* and *CCNE2* mRNA transcript levels of the various variants in a set of 185 primary tumors from breast cancer patients and various cultured cell lines (Table 2B). Primer sequences for estrogen receptor-α (*ER-α*), *PGR*, and the housekeepers, as well as how PCR reactions and validations were done to ensure PCR specificity, have all been previously described [19]. Levels of the

Table 2A: Intron-skipping CCNE variant-specific primers used for real-time RT-PCR.

Gene	Specificity	Assay-on-Demand kit (Applied Biosystems)	Exon boundary spanned according product insert
CCNE1 *	All variants	Hs00233356_m1	4-5
CCNE2 *	Variant 2	Hs00180319_m1	7-8

Gene	Specificity	Forward primer sequence 5′→3′	Reverse primer sequence 5′→3′	Product size (bp)
CCNE1 †	All variants except variant $E1_L$	exon 1, variant 2 TGCCACCCGGGTCCACAG	exon 3, variant 2 GCACGTTGAGTTTGGGTAAAC	271
CCNE1 ‡	Wild type and $E1_L$ not $E1_S$ or $E1_T$	exon 7 CTTCACAGGGAGACCTTTTAC	exon 9 CATTCAGCCAGGACACAATAG	274
CCNE1 ‡	Variant $E1_T$ specific	exon 7 CTTCACAGGGAGACCTTTTAC	exon 10 → 8 GAGATCCAACAGCTTCATAATC	237
CCNE1 §	Variant $E1_S$ specific	exon 6 → 8 GGATTGGTTAATGCAGGAAATC	exon 10 GAAATTCAAGGCAGTCAACATC	290
CCNE2 ‡	Variant 1 + 2	exon 8 TACGTCACTGATGGTGCTTG	exon 10 TACGTCACTGATGGTGCTTG	267

Table 2B: PCR traces of wild-type and CCNE variants in primary breast tumors and cell lines.

	CCNE1					CCNE2	
	All variants ($\times 10^{-2}$)	All variants, except $E1_L$ ($\times 10^{-3}$)	Wild type + $E1_L$, no $E1_S$ or $E1_T$ ($\times 10^{-1}$)	Variant $E1_T$ ($\times 10^{-3}$)	Variant $E1_S$ ($\times 10^{-6}$)	Variant 1 + 2 ($\times 10^{-1}$)	Variant 1 + 2 ($\times 10^{-2}$)
LNN primary breast tumors	4.41	1.14	1.31	2.53	2.13	7.94	7.67
Primary fibroblast strain	7.09	0.84	0.77	0.89	17.86	0.11	0.12
EAHY-926 endothelial cells	11.60	2.50	1.28	1.14	11.79	0.41	0.45
MDA-MB-231	4.58	1.04	0.55	0.15	62.21	2.25	1.16
MCF7	9.42	2.29	0.83	4.95	35.24	1.10	0.71
ZR75.1	11.36	4.74	1.39	0.94	19.01	1.46	1.31
T47-D	12.69	1.07	0.61	0.83	0.15	0.56	1.20
EVSA-T	13.41	1.86	1.14	3.20	11.70	1.86	1.96
CAMA-1	25.20	5.52	1.66	5.24	9.91	1.92	1.68
MDA-MB-435	40.10	1.79	0.87	1.81	1.18	0.27	1.26
SKBR-3	41.17	5.76	1.45	1.71	0.02	0.10	0.29

NOTE: In our initial screening, we compared CCNE1 and CCNE2 mRNA transcript levels of the various variants (A) in a set of 185 primary tumors from breast cancer patients and various cultured cell lines (B). Note that due to different assay conditions, absolute values of the CCNE's can only be compared within a gene assay. The assay designed to detect specifically the $CCNE1_S$ variant required >35 rounds of amplification for any product formation in our tumormaterial and was therefore considered too insensitive for reliable SYBR-based real-time PCR measurement. For the CCNE2 assay aimed to specifically detect the variant lacking part of the cyclin box (variant 2), correlation with the CCNE2 assay designed to detect both variants was highly significant ($r_s = 0.92$, P<0.001, n=185), indicating that this splice variant did not play a role of significant importance. We, therefore, continued with the CCNE2 assay able to detect both variants and the CCNE1 assay able to detect (a) all CCNE1 variants and compared results with the CCNE1 assays able to detect; (b) all variants except variant $E1_L$; (c) all variants except variant $E1_S$ and $E1_T$; and (d) the $CCNE1_T$ variant - specific assay.

* Assay done with Taqman probes in Universal PCR-master-mixture (Applied Biosystems).

† Assay done in Brilliant SYBR Green PCR-master-mixture (Stratagene).

‡ Assay done in SYBR-green PCR-master-mixture (Applied Biosystems).

§ Assay done in Platinum SYBR Green qPCR SuperMix-UDG (Invitrogen).

target genes, expressed relative to our housekeeping set, which included the low abundance housekeeping gene *porphobilinogen deaminase*, the medium abundance housekeeping gene *hypoxanthine-guanine phosphoribosyltransferase*, and the high-abundance housekeeping gene *β-2-microglobulin*, were quantified as follows:

mRNA target = $2^{(\text{mean Ct housekeeping} - \text{mean Ct target})}$.

Statistics

Computations were done with the use of the STATA statistical package, release 8.2 (STATA Corp., College Station, TX). Differences in levels were assessed with the Mann-Whitney *U* test or Kruskal-Wallis test. In these tests, patient and tumor characteristics were used as grouping variables. The strengths of the associations

between continuous variables were tested with the Spearman rank correlation (r_s). Variables were either log transformed or Box-Cox transformed to reduce the skewness. The prognostic values of the clinical and biological variables, with MFS and overall survival as the end point in the univariate, multivariate, and interaction analyses, were investigated with the use of the Cox proportional hazards model. The hazard ratio (HR) and its 95% confidence interval were derived from these results. The proportionality assumption was investigated with a test based on the Schoenfeld residuals. Kaplan-Meier survival plots and log-rank tests were used to assess the differences in time to distant metastasis of the predicted high-risk and low-risk groups. All Ps are two sided, and $P<0.05$ was considered statistically significant.

RESULTS

Correlation between real-time PCR and Affymetrix GeneChip array

Comparing our real-time PCR data for all *CCNE1* and *CCNE2* variants with expression data obtained after hybridizing the same total RNA samples on the Affymetrix oligonucleotide Human U133a GeneChips [8] showed significant correlations between our *CCNE1* and *CCNE2* real-time PCR assays and the *CCNE1* 213523_at and *CCNE2* 205034_at probe-based Affymetrix GeneChip array assays, which also recognize all variants of *CCNE1* and *CCNE2* (r_s=0.70 for *CCNE1* and r_s=0.75 for *CCNE2*, respectively; $P<0.001$, n=248). The Spearman rank correlation between *CCNE1* and *CCNE2* was 0.40 ($P<0.001$, n=635) for the real-time PCR assays and 0.36 ($P<0.001$, n=248) for the probe sets. Relating the *CCNE* expression profiles to the subtypes of breast cancer as defined by global profiling [20] showed for both our real-time PCR and Affymetrix GeneChip array data significant ($P<0.05$) differences in median *CCNE* mRNA levels between the subtypes. For both *CCNE1* and *CCNE2*, levels ranked according to the major breast cancer subtype were luminal A (n=94) > basal (n=42) > normal (n=48).

Associations with clinicopathologic factors

The associations of *CCNE1* and *CCNE2* mRNA expression levels with patient and tumor characteristics are shown in Table 1. Although based on a relatively small number of patients, the lowest median levels of the cyclins were found in the histologic subgroup of medullary tumors. *CCNE1* and *CCNE2* levels were both inversely related with age and steroid hormone receptors and higher in premenopausal patients and poor-grade tumors. Furthermore, *CCNE1* and *CCNE2* levels were higher in larger tumors, although for *CCNE2*, this association was not statistically significant. To further explore the associations between the mRNA levels of the cyclins and steroid hormone receptor status, we correlated *ER-α* and *PGR* mRNA levels measured by quantitative real-time PCR with mRNA levels of the cyclins measured in the same preparations. Although at the mRNA level, a strong negative correlation was present between *CCNE1* and *ER-α* and *PGR* (r_s=-0.54 for *ER-α* and -0.54 for *PGR*, respectively; $P<0.001$, n=635), this was less striking for the correlation between the *CCNE2* and *ER-α* and *PGR* mRNA levels (r_s=-0.16 for *ER-α* and -0.23 for *PGR*, respectively).

Univariate and multivariate analysis

We first did Cox univariate analyses for MFS and overall survival as a function of continuous *CCNE1* and *CCNE2* mRNA levels. In these analyses, *CCNE1* and *CCNE2* were associated with a poor MFS (HR, 1.29 for *CCNE1* and HR, 1.59 for *CCNE2*; both $P<0.001$) and overall survival (HR, 1.24 for *CCNE1* and HR, 1.45 for *CCNE2*: both $P<0.001$). These significant relationships justified the search for a cut point to analyze *CCNE1* and *CCNE2* as dichotomized variables and to allow visualization of their prognostic value in Kaplan-Meier analysis. Because the proportional hazards assumption was violated for grade and *PGR* for the total follow-up time of 202 months ($P<0.05$), we restricted our exploration of the relationships of the cyclins with MFS to the first 5 years of follow-up. In this analysis with 209 failures, the

Table 3. Cox univariate and multivariate analysis for 5 years MFS in 635 lymph node-negative patients.

Factor	No. patients (%)	Univariate analysis		Multivariate analysis*	
		HR (95% confidence interval)	P	HR (95% confidence interval)	P
Age (y)					
≤40	86 (14)	1		1	
41-55	224 (35)	0.78 (0.53-1.14)		0.83 (0.56-1.24)	
56-70	200 (31)	0.64 (0.43-0.95)		0.61 (0.32-1.16)	
>70	125 (20)	0.42 (0.25-0.69)	0.003	0.40 (0.19-0.84)	0.089
Menopausal status					
Premenopausal	265 (42)	1		1	
Postmenopausal	370 (58)	0.70 (0.54-0.92)	0.011	0.96 (0.57-1.64)	0.89
Pathologic tumor size (cm)					
≤2	260 (41)	1		1	
>2	375 (59)	1.21 (0.92-1.60)	0.17	1.14 (0.85-1.52)	0.37
Grade					
Poor	331 (52)	1		1	
Unknown	195 (31)	1.02 (0.76-1.37)		1.17 (0.86-1.58)	
Moderate and good	109 (17)	0.44 (0.27-0.70)	<0.001	0.47 (0.29-0.77)	<0.001
ER-α mRNA level					
Continuous	635 (100)	0.89 (0.82-0.98)	0.011	1.10 (0.98-1.25)	0.11
PR mRNA level					
Continuous	635 (100)	0.89 (0.84-0.94)	<0.001	0.87 (0.80-0.94)	<0.001
				Additions to the base model	
CCNE1 mRNA level					
Continuous	635 (100)	1.36 (1.25-1.47)	<0.001	1.39 (1.25-1.55)	<0.001
CCNE1 mRNA level [†]					
≤median	318 (50)	1		1	
>median	317 (50)	2.89 (2.14-3.90)	<0.001	2.65 (1.89-3.71)	<0.001
CCNE1 mRNA level [‡]					
Low (≤0.03)	251 (40)	1		1	
High (>0.03)	384 (60)	3.83 (2.67-5.49)	<0.001	3.40 (2.31-5.03)	<0.001
CCNE1 mRNA level in stroma rich					
Low in stroma rich	156 (36%)	1		1	
High in stroma rich	277 (64%)	5.38 (3.24-8.94)	<0.001	5.12 (3.00-8.75)	<0.001
CCNE2 mRNA level					
Continuous	635 (100)	1.64 (1.39-1.93)	<0.001	1.47 (1.24-1.74)	<0.001
CCNE2 mRNA level [†]					
≤median	318 (50)	1		1	
>median	317 (50)	1.99 (1.49-2.64)	<0.001	1.69 (1.27-2.26)	<0.001
CCNE2 mRNA level [‡]					
Low (≤1.16)	464 (73)	1		1	
High (>1.16)	171 (27)	2.13 (1.62-2.80)	<0.001	1.76 (1.32-2.34)	<0.001
CCNE2 mRNA level in stroma poor					
Low in stroma poor	144 (71)	1		1	
High in stroma poor	58 (29)	2.77 (1.74-4.48)	<0.001	2.06 (1.23-3.45)	0.007
CCNE1 + *CCNE2*					
CCNE1 continuous	635 (100)	1.36 (1.25-1.47)	<0.001	1.34 (1.20-1.51)	<0.001
CCNE2 continuous	635 (100)	1.64 (1.39-1.93)	<0.001	1.30 (1.10-1.56)	0.003

* Cyclins were separately introduced to the base multivariate model that included the factors age, menopausal status, tumor size, grade, and ER-a and PR mRNA levels as log-transformed continuous variables.
† Dichotomized in high and low levels by median level (0.04; range, 0.003-2.12 for CCNE1 0.70; range, 0.07-9.40 for CCNE2).
‡ Dichotomized in high and low levels by cut points (0.03 for CCNE1 and 1.16 for CCNE2).

proportional hazards assumption was no longer violated (*P*>0.1). The data of the Cox univariate and multivariate analyses are summarized in Table 3 for MFS during the first 5 years and in Table 4 for overall survival during the total follow-up period including all deaths. Both cyclins, either when analyzed at their median level (HR, 2.65 for *CCNE1* and HR, 1.69 for *CCNE2*, respectively) or at their optimized cut point (HR, 3.40 for *CCNE1* and HR, 1.76 for *CCNE2*, respectively), contributed significantly to the multivariate model for MFS (all *P*<0.001; Table 3). Similar significant relationships were observed in the analysis for overall survival

Table 4. Cox univariate and multivariate analysis for overall survival in 635 lymph node-negative patients.

Factor	No. patients (%)	Univariate analysis		Multivariate analysis*	
		HR (95% confidence interval)	P	HR (95% confidence interval)	P
Age (y)					
≤40	86 (14)	1		1	
41-55	224 (35)	0.75 (0.51-1.10)		0.77 (0.52-1.14)	
56-70	200 (31)	0.73 (0.49-1.09)		0.64 (0.33-1.22)	
>70	125 (20)	0.88 (0.57-1.35)	0.39	0.80 (0.41-1.59)	0.36
Menopausal status					
Premenopausal	265 (42)	1		1	
Postmenopausal	370 (58)	1.00 (0.76-1.29)	0.97	1.10 (0.65-1.88)	0.71
Pathologic tumor size (cm)					
≤2	260 (41)	1		1	
>2	375 (59)	1.14 (0.88-1.49)	0.32	1.04 (0.79-1.37)	0.78
Grade					
Poor	331 (52)	1		1	
Unknown	195 (31)	0.95 (0.71-1.27)		1.01 (0.75-1.36)	
Moderate and good	109 (17)	0.58 (0.39-0.87)	0.017	0.61 (0.41-0.92)	0.035
ER-α mRNA level					
Continuous	635 (100)	0.94 (0.86-1.02)	0.14	1.06 (0.94-1.20)	0.31
PR mRNA level					
Continuous	635 (100)	0.91 (0.86-0.96)	0.002	0.89 (0.83-0.97)	0.004
				Additions to the base model	
CCNE1 mRNA level					
Continuous	635 (100)	1.24 (1.15-1.35)	<0.001	1.27 (1.15-1.41)	<0.001
CCNE1 mRNA level [†]					
≤median	318 (50)	1		1	
>median	317 (50)	2.03 (1.54-2.66)	<0.001	1.95 (1.43-2.65)	<0.001
CCNE1 mRNA level [‡]					
Low (≤0.03)	251 (40)	1		1	
High (>0.03)	384 (60)	2.55 (1.87-3.49)	<0.001	2.45 (1.74-3.44)	<0.001
CCNE1 mRNA level in stroma rich [‡]					
Low in stroma rich	156 (36)	1		1	
High in stroma rich	277 (64)	3.28 (2.16-4.97)	<0.001	3.33 (2.13-5.21)	<0.001
CCNE2 mRNA level					
Continuous	635 (100)	1.45 (1.24-1.70)	<0.001	1.38 (1.17-1.63)	<0.001
CCNE2 mRNA level [†]					
≤median	318 (50)	1		1	
>median	317 (50)	1.86 (1.42-2.44)	<0.001	1.76 (1.34-2.32)	<0.001
CCNE2 mRNA level [‡]					
Low (≤1.16)	464 (73)	1		1	
High (>1.16)	171 (27)	1.90 (1.45-2.48)	<0.001	1.75 (1.33-2.30)	<0.001
CCNE2 mRNA level in stroma poor [‡]					
Low in stroma poor	144 (71)	1		1	
High in stroma poor	58 (29)	2.62 (1.67-4.12)	<0.001	2.36 (1.45-3.84)	<0.001
CCNE1 + *CCNE2*					
CCNE1 continuous	635 (100)	1.24 (1.15-1.35)	<0.001	1.23 (1.10-1.36)	<0.001
CCNE2 continuous	635 (100)	1.45 (1.24-1.70)	<0.001	1.26 (1.06-1.50)	0.007

* *Cyclins were separately introduced to the base multivariate model that included the factors age, menopausal status, tumor size, grade, and ER-α and PR mRNA levels as log-transformed continuous variables.*

† *Dichotomized in high and low levels by median level (0.04; range, 0.003-2.12 for CCNE1 and 0.70; range, 0.07-9.40 for CCNE2).*

‡ *Dichotomized in high and low levels by cut points (0.03 for CCNE1 and 1.16 for CCNE2).*

(Table 4). No statistically significant interactions were observed between the cyclins and the prognostic factors included in the base multivariate model, between the cyclins and adjuvant radiotherapy, and between the cyclins themselves. When *CCNE1* and *CCNE2* were added simultaneously to the base model, they both independently contributed to the MFS and overall survival models.

ER status and tumor size

To specifically investigate the differences

Table 5. Cox univariate analysis for 5 years MFS in 635 adjuvant untreated lymph node-negative patients.

Factor (high vs low)*	All primary tumors				Stroma-poor primary tumors[†]				Stroma-rich primary tumors[†]			
	No. patients	High CCNE (%)	HR (95% confidence interval)	P	No. patients	High CCNE (%)	HR (95% confidence interval)	P	No. patients	High CCNE (%)	HR (95% confidence interval)	P
All patients												
CCNE1	635	60	3.82 (2.67-5.48)	<0.001	202	53	2.39 (1.40-4.07)	0.001	433	64	5.38 (3.24-8.94)	<0.001
CCNE2	635	27	2.13 (1.62-2.80)	<0.001	202	29	2.77 (1.71-4.48)	<0.001	433	26	1.86 (1.33-2.62)	0.001
ER negative[‡]												
CCNE1	180	88	5.04 (1.23-20.60)	0.003	39	93	0.35 (0.04-2.71)	0.382	141	87	9.89 (1.36-71.66)	0.001
CCNE2	180	31	1.32 (0.80-2.19)	0.285	39	39	1.43 (0.52-3.96)	0.488	141	29	1.27 (0.71-2.29)	0.425
ER positive[‡]												
CCNE1	455	49	4.08 (2.78-6.00)	<0.001	163	43	2.70 (1.53-4.79)	<0.001	292	53	5.58 (3.25-9.57)	<0.001
CCNE2	455	25	2.63 (1.89-3.66)	<0.001	163	26	3.30 (1.92-5.69)	<0.001	292	25	2.29 (1.51-3.48)	<0.001
Tumor size ≤2 cm												
CCNE1	260	54	5.36 (2.96-9.71)	<0.001	87	49	3.47 (1.56-7.73)	0.001	173	57	8.47 (3.36-21.41)	<0.001
CCNE2	260	26	3.75 (2.41-5.82)	<0.001	87	31	4.54 (2.23-9.23)	<0.001	173	24	3.17 (1.79-5.60)	<0.001
Tumor size >2 cm												
CCNE1	375	65	3.00 (1.91-4.74)	<0.001	115	56	1.78 (0.87-3.63)	0.114	260	69	3.99 (2.18-7.32)	<0.001
CCNE2	375	27	1.49 (1.04-2.14)	0.035	115	28	1.81 (0.92-3.57)	0.093	260	27	1.38 (0.90-2.13)	0.137

* Dichotomized in high and low levels by cut points (0.03 for CCNE1 and 1.16 for CCNE2).
† Dichotomized in stroma-rich and stroma-poor at the median level of 70% tumor cells.
‡ Cut point used for ER is10 fmol/mg protein.

between the two cyclins with respect to the strength of their associations with steroid hormone receptor status and tumor size (see Table 1), we did Cox univariate analyses in the subgroups of ER-negative and ER-positive tumors, and in small ($\leq$2 cm) and larger (>2 cm) tumors (Table 5). Although both cyclins were associated with a poor prognosis in the ER-positive subgroup (HR, 4.08 for *CCNE1* and HR, 2.63 for *CCNE2*, respectively), only *CCNE1* was informative for the ER-negative subgroup (HR, 5.04). With respect to tumor size, high levels of both cyclins were significantly associated with a poor MFS, both for patients with small tumors (HR, 5.36 for *CCNE1* and HR, 3.75 for *CCNE2*) and patients with larger tumors (HR, 3.00 for *CCNE1* and HR, 1.49 for *CCNE2*).

Stroma-rich versus stroma-poor tumors

Interaction analysis showed that patients with high levels of *CCNE1* had an increased risk (*P*=0.03) to develop a metastasis within 5 years if their primary tumor was stroma enriched compared with patients with a high level of *CCNE1* combined with a stroma-poor primary tumor. Hence, a high *CCNE1* level was a better predictor of poor prognosis in the group of 433

patients with stroma-rich tumors (HR, 5.38) compared with the group of 202 patients with stroma-poor tumors (HR, 2.39; Table 5). A high level of *CCNE2* on the other hand was a better predictor for the group of 202 patients with stroma-poor tumors (HR, 2.77 compared with HR, 1.86 for stroma-rich tumors). Note that, whereas median *CCNE2* mRNA levels did not differ between stroma-poor tumors (median level, 0.70; interquartile range, 0.89) and stroma-rich tumors (median level, 0.71; interquartile range, 0.80), median levels of *CCNE1* were higher in the group of stroma-rich tumors (median level, 0.043; interquartile range, 0.066 for stroma-rich tumors and median level, 0.034; interquartile range, 0.059 for stroma-poor tumors; *P*=0.01). In contrast to *CCNE2*, for *CCNE1*, the importance of discriminating between stromal content became even more evident in the subgroups of ER-negative tumors and small tumors. Especially for stroma-rich ER-negative tumors (HR, 9.89) and stroma-rich small tumors (HR, 8.47), a high level of *CCNE1* was a strong factor predicting a poor prognosis (Table 5). The prognostic value of the cyclins in all patients and in the subgroups of tumors with a low and high proportion of tumor cells and separately analyzed for
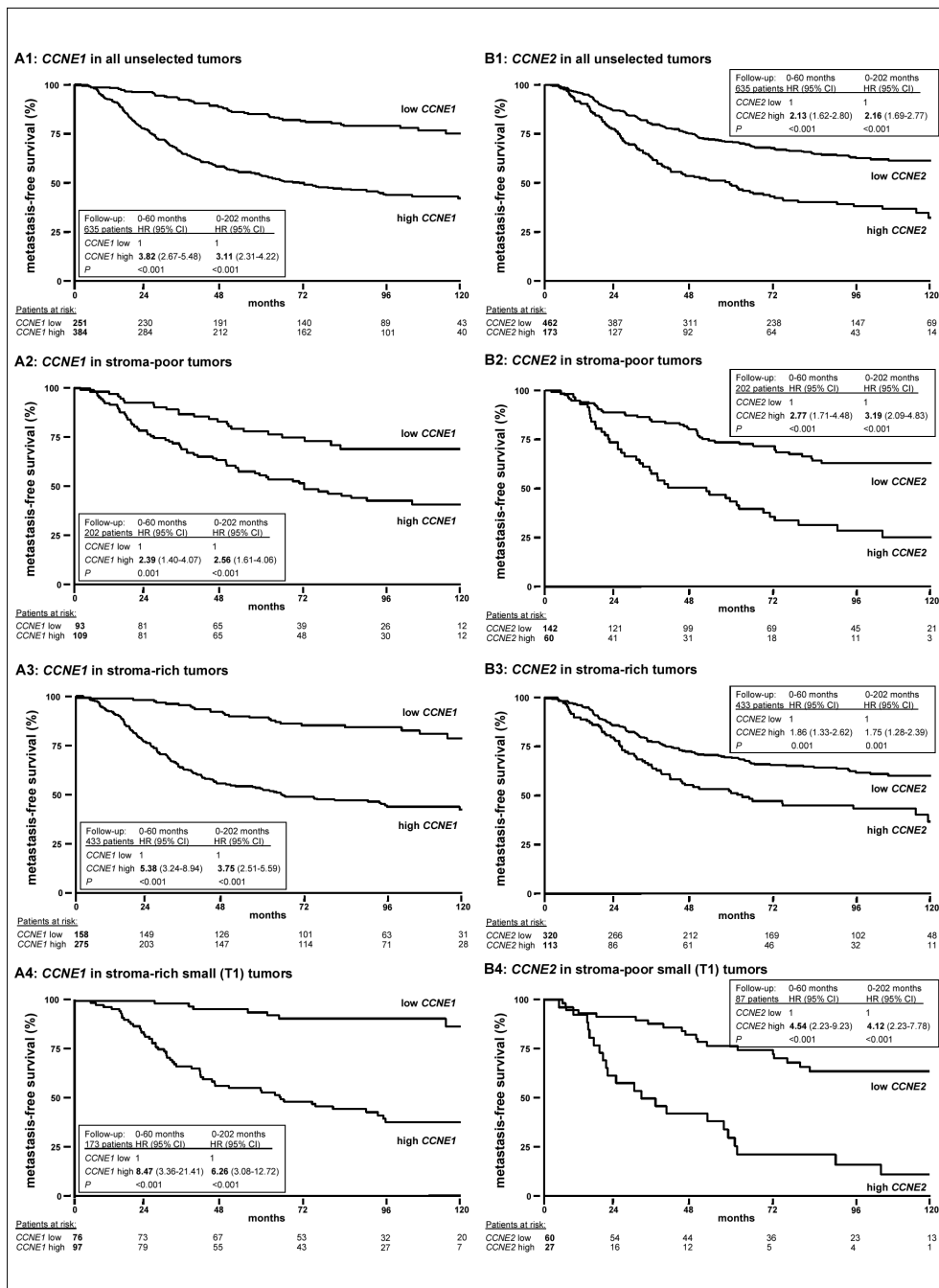
Figure 1. MFS as a function of CCNE1 (A) and CCNE2 (B) in 635 lymph node-negative primary breast cancer patients before (1) and after (2-4) dichotomizing patients according to the percentage of tumor cells present in the primary tumor and tumor size. Patients at risk are indicated. Cut point used for CCNE1 is 0.03 and for CCNE2 is 1.16.

T1 tumors is visualized in Kaplan-Meier curves (Figure 1).

CCNE1 and its mRNA splice variants

The contributions of the various mRNA variants of *CCNE* (see also Table 2A and B) with respect to prognosis was studied in a subgroup of 562 patients. Spearman rank correlation revealed highly significant correlations among all *CCNE1* variants studied (r_s>0.70, *P*<0.001, *n*=562). Irrespective of which splice variant was analyzed, increasing levels of *CCNE1* predicted a poor prognosis. The assay used in this study aimed at detecting all variants of *CCNE1* contributed similarly to MFS and overall survival compared with the various splice variants of *CCNE1* investigated (data not shown).

DISCUSSION

Many research groups have investigated the link between immunohistochemically measured cyclin E1 protein and prognosis in breast cancer, although with conflicting results [1, 17, 21–28]. These heterogeneous results have been attributed to differences in antibodies used to detect cyclin E1 [17] and to differences in the adjuvant treatment of patients [18, 29]. In our present study, we aimed to overcome these pitfalls by using quantitative real-time RT-PCR to evaluate the prognostic value of cyclin E mRNA levels in lymph node–negative breast cancer patients who did not receive adjuvant systemic therapy, which was common practice in the Netherlands in the time period from which we retrieved our primary tumor samples. We evaluated, in addition to various mRNA splice variants of *CCNE1*, the far less extensively studied *CCNE2* member of the cyclin E family, and we are the first to present comprehensive data with respect to the prognostic value of cyclin E2.

The mRNA splice variants of *CCNE1* did not add to the information we obtained from wild-type *CCNE1*. Although our study shows that both *CCNE1* and *CCNE2* are prognosticators for lymph node–negative breast cancer, differences were observed between the two genomic variants of cyclin E. In agreement with previous studies [22], we found that ER-negative tumors expressed significantly higher *CCNE1* mRNA levels. Based on this observation, a potential role for cyclin E1 in mechanisms responsible for estrogen-independent tumor growth has already been suggested [22]. We showed that, in contrast to *CCNE1*, median *CCNE2* levels do not largely differ between ER-negative and ER-positive tumors. Furthermore, only *CCNE1* was a significant prognostic factor in patients with ER-negative tumors.

Other dissimilarities between the two cyclin E members were observed. Only recently, we established that the predictive value of biological factors, among which ER-α, may be further refined by splitting tumor samples at the median level of 70% epithelial tumor cell nuclei in a cohort of stroma-poor tumors and a cohort of stroma-rich tumors [19]. Interaction analyses justified to perform a similar analysis for *CCNE* and showed that high *CCNE1* was a better predictor of poor prognosis in the group of patients with stroma-rich tumors compared with the group of patients with stroma-poor tumors. This strongly suggests a paracrine interaction between tumor cell derived cyclin E1 and a stromal cell–derived factor, resulting in a more aggressive tumor type with a very poor prognosis. High levels of *CCNE2* were similarly associated with poor prognosis in tumors with high and tumors with a relatively low percentage of tumor cell nuclei. For *CCNE2*, such an interaction mechanism between tumor cells and stromal cells does, therefore, not seem to play a role. Profiling studies usually focus on tumors with a relatively high percentage of epithelial tumor cell nuclei. This, together with the already discussed differences associated with ER status, most likely explains why it was the more consistently informative *CCNE2* variant and not the more susceptible to tissue heterogeneity *CCNE1* variant that overlapped between the two gene expression profiles [8, 9]. Success in breast cancer treatment depends greatly upon early detection. More sensitive and specific indicators of prognosis are required to identify those patients at risk for disease progression. Great advantage will be gained with

markers that are able to anticipate disease progress for patients with still small tumors, a group of patients for whom prediction of prognosis is especially difficult to assess. Trials of adjuvant therapy in patients with breast cancer no longer include an untreated control group. Therefore, available tumor banks are very helpful to address specific questions. We did a retrospective study using tumors from patients who had not received systemic adjuvant treatment to determine whether cyclin E is a pure prognostic factor. However, there are obvious limitations to a retrospective study on frozen material that must be acknowledged. The data in Table 1 describe clinicopathologic data that reflect common practice in those days and are not always as comprehensive as the data available nowadays. Due to the frozen nature of our material, (re)examination of histology, grade, proliferation index or, for example, *ERBB2* amplification by fluorescence *in situ* hybridization will not provide the same results as the current standardized methods used for paraffin-embedded material. Furthermore, because our tumor bank consists of frozen tumor material that was left after the biochemical and pathologic examinations, small-sized tumors of ≤1 cm are under represented in this study. Despite this limitation, high levels of *CCNE1* and *CCNE2* as measured by real-time RT-PCR showed to be especially poor predictors of MFS for the 260 of 635 patients with small (T1) tumors.

Although gene expression profiling methods are definitely more comprehensive, and immuno-histochemical methods are more informative with respect to localization of target molecules, real-time PCR is a sensitive, fast, quantitative, and cost-effective method suitable for high-throughput screening. In summary, PCR-based measurement of *CCNE1* and *CCNE2* fulfill the criteria of a clinically attractive biomarker to select early breast cancer patients at high risk for distant metastases.

ACKNOWLEDGEMENTS

REFERENCES

1. Yasmeen A, Berdel WE, Serve H, Muller-Tidow C. E- and A-type cyclins as markers for cancer diagnosis and prognosis. Expert Rev Mol Diagn 2003;3:617-33.

2. Koff A, Cross F, Fisher A, Schumacher J, Leguellec K, Philippe M, Roberts JM. Human cyclin E, a new cyclin that interacts with two members of the CDC2 gene family. Cell 1991;66:1217-28.

3. Lew DJ, Dulic V, Reed SI. Isolation of three novel human cyclins by rescue of G1 cyclin (Cln) function in yeast. Cell 1991;66:1197-206.

4. Zariwala M, Liu J, Xiong Y. Cyclin E2, a novel human G1 cyclin and activating partner of CDK2 and CDK3, is induced by viral oncoproteins. Oncogene 1998;17: 2787-98.

5. Gudas JM, Payton M, Thukral S, Chen E, Bass M, Robinson MO, Coats S. Cyclin E2, a novel G1 cyclin that binds Cdk2 and is aberrantly expressed in human cancers. Mol Cell Biol 1999;19:612-22.

6. Lauper N, Beck AR, Cariou S, Richman L, Hofmann K, Reith W, Slingerland JM, Amati B. Cyclin E2: a novel CDK2 partner in the late G1 and S phases of the mammalian cell cycle. Oncogene 1998;17:2637-43.

7. Payton M, Scully S, Chung G, Coats S. Deregulation of cyclin E2 expression and associated kinase activity in primary breast tumors. Oncogene 2002;21:8529-34.

8. Wang Y, Klijn JG, Zhang Y, Sieuwerts AM, Look MP, Yang F, Talantov D, Timmermans M, Meijer-van Gelder ME, Yu J, Jatkoe T, Berns EM, Atkins D, Foekens JA. Gene-expression profiles to predict distant metastasis of lymph-node-negative primary breast cancer. Lancet 2005;365:671-9.

9. van 't Veer LJ, Dai H, van de Vijver MJ, He YD, Hart AA, Mao M, Peterse HL, van der Kooy K, Marton MJ, Witteveen AT, Schreiber GJ, Kerkhoven RM, Roberts C, Linsley PS, Bernards R, Friend SH. Gene expression profiling predicts clinical outcome of breast cancer. Nature 2002;415:530-6.

10. Ohtsubo M, Theodoras AM, Schumacher J, Roberts JM, Pagano M. Human cyclin E, a nuclear protein essential for the G1-to-S phase transition. Mol Cell Biol 1995;15: 2612-24.

11. Sewing A, Ronicke V, Burger C, Funk M, Muller R. Alternative splicing of human cyclin E. J Cell Sci 1994; 107:581-8.

12. Mumberg D, Wick M, Burger C, Haas K, Funk M, Muller R. Cyclin ET, a new splice variant of human cyclin E with a unique expression pattern during cell cycle progression and differentiation. Nucleic Acids Res 1997;25:2098-105.

13. Keyomarsi K, Conte D, Jr., Toyofuku W, Fox MP. Deregulation of cyclin E in breast cancer. Oncogene 1995;11:941-50.

14. Keyomarsi K, O'Leary N, Molnar G, Lees E, Fingert HJ, Pardee AB. Cyclin E, a potential prognostic marker for breast cancer. Cancer Res 1994;54:380-5.

15. Wang XD, Rosales JL, Magliocco A, Gnanakumar R, Lee KY. Cyclin E in breast tumors is cleaved into its low molecular weight forms by calpain. Oncogene 2003;22: 769-74.

16. Hunt KK, Keyomarsi K. Cyclin E as a prognostic and predictive marker in breast cancer. Semin Cancer Biol 2005;15:319-26.

17. Keyomarsi K, Tucker SL, Buchholz TA, Callister M, Ding Y, Hortobagyi GN, Bedrosian I, Knickerbocker C, Toyofuku W, Lowe M, Herliczek TW, Bacus SS. Cyclin E and survival in patients with breast cancer. N Engl J Med 2002;347:1566-75.

18. Yee D. Cyclin E in breast cancer. N Engl J Med 2003; 348:1063-4; author reply 1063-4.

19. Sieuwerts AM, Meijer-van Gelder ME, Timmermans M, Trapman AM, Rodriguez Garcia R, Arnold M, Goedheer AJ, Portengen H, Klijn JG, Foekens JA. How ADAM-9 and ADAM-11 differentially from estrogen receptor predict response to tamoxifen treatment in patients with recurrent breast cancer: a retrospective study. Clin Cancer Res 2005;11:7311-21.

20. Sorlie T. Molecular portraits of breast cancer: tumour subtypes as distinct disease entities. Eur J Cancer 2004; 40:2667-75.

21. Porter PL, Malone KE, Heagerty PJ, Alexander GM, Gatti LA, Firpo EJ, Daling JR, Roberts JM. Expression of cell-cycle regulators p27[Kip1] and cyclin E, alone and in combination, correlate with survival in young breast cancer patients. Nat Med 1997;3:222-5.

22. Nielsen NH, Arnerlov C, Emdin SO, Landberg G. Cyclin E overexpression, a negative prognostic factor in breast cancer with strong correlation to oestrogen receptor status. Br J Cancer 1996;74:874-80.

23. Kim HK, Park IA, Heo DS, Noh DY, Choe KJ, Bang YJ, Kim NK. Cyclin E overexpression as an independent risk factor of visceral relapse in breast cancer. Eur J Surg Oncol 2001;27:464-71.

24. Loden M, Stighall M, Nielsen NH, Roos G, Emdin SO, Ostlund H, Landberg G. The cyclin D1 high and cyclin E high subgroups of breast cancer: separate pathways in tumorogenesis based on pattern of genetic aberrations and inactivation of the pRb node. Oncogene 2002;21: 4680-90.

25. Kuhling H, Alm P, Olsson H, Ferno M, Baldetorp B, Parwaresch R, Rudolph P. Expression of cyclins E, A, and B, and prognosis in lymph node-negative breast cancer. J Pathol 2003;199:424-31.

26. Rudolph P, Kuhling H, Alm P, Ferno M, Baldetorp B, Olsson H, Parwaresch R. Differential prognostic impact of the cyclins E and B in premenopausal and postmenopausal women with lymph node-negative breast cancer. Int J Cancer 2003;105:674-80.

27. Chappuis PO, Donato E, Goffin JR, Wong N, Begin LR, Kapusta LR, Brunet JS, Porter P, Foulkes WD. Cyclin E expression in breast cancer: predicting germline BRCA1 mutations, prognosis and response to treatment. Ann Oncol 2005;16:735-42.

28. Peters MG, Vidal Mdel C, Gimenez L, Mauro L, Armanasco E, Cresta C, Bal de Kier Joffe E, Puricelli L. Prognostic value of cell cycle regulator molecules in surgically resected stage I and II breast cancer. Oncol Rep 2004;12:1143-50.

29. Span PN, Tjan-Heijnen VC, Manders P, Beex LV, Sweep CG. Cyclin-E is a strong predictor of endocrine therapy failure in human breast cancer. Oncogene 2003; 22:4898-904.

HOXB13-to-IL17BR expression ratio is related with tumor aggressiveness and response to tamoxifen of recurrent breast cancer: a retrospective study

Anieta M. Sieuwerts*, Maurice P.H.M. Jansen*, Maxime P. Look, Kirsten Ritstier,
Marion E. Meijer-van Gelder, Iris L. van Staveren, Jan G.M. Klijn,
John A. Foekens and Els M.J.J. Berns
both authors contributed equally

Department of Medical Oncology, Erasmus MC, Rotterdam, The Netherlands

ABSTRACT

Purpose: A *HOXB13*-to-*IL17BR* expression ratio was previously identified to predict clinical outcome of breast cancer patients treated with adjuvant tamoxifen. However, this ratio may predict a tumor's response to tamoxifen, its intrinsic aggressiveness, or both.

Patients and methods: We have measured the *HOXB13* and *IL17BR* expression levels by real-time polymerase chain reaction in 1,252 primary breast tumor specimens. Expression levels were normalized to housekeeper gene levels and related to clinicopathologic factors for all patients. The primary objective of this study was to determine the relationship of a *HOXB13*-to-*IL17BR* ratio with tumor aggressiveness and/or with response to tamoxifen therapy in estrogen receptor (ER) -positive disease. We selected ER-positive tumors, and clinical end points for the *HOXB13*-to-*IL17BR* ratio were disease-free survival (DFS) in patients with primary breast cancer (n=619) and progression-free survival (PFS) in patients with recurrent breast cancer treated with first-line tamoxifen monotherapy (n=193). The odds ratio (OR) and hazard ratio (HR) and their 95% CI were calculated, and all *P* values were two-sided.

Results: The *HOXB13*-to-*IL17BR* ratio was significantly associated with DFS and PFS. In multivariate analysis, *HOXB13*-to-*IL17BR* ratio expression levels were associated with a shorter DFS for node-negative patients only. Corrected for traditional predictive factors, the dichotomized *HOXB13*-to-*IL17BR* ratio was the strongest predictor in multivariate analysis for a poor response to tamoxifen therapy (OR 0.16; 95% CI, 0.06 to 0.45; *P*<0.001) and a shorter PFS (HR 2.97; 95% CI, 1.82 to 4.86; *P*<0.001).

Conclusion: High *HOXB13*-to-*IL17BR* ratio expression levels associate with both tumor aggressiveness and tamoxifen therapy failure.

INTRODUCTION

Approximately 70% to 75% of invasive breast tumors express the estrogen receptor (ER), the classical prognostic factor, which is an important target for endocrine therapy. In the adjuvant setting, tamoxifen therapy results in a 5.3% to 12.6% improvement in 10-year survival in lymph node-negative (LNN) and lymph node-positive (LNP) patients, respectively [1]. In recurrent disease, approximately half of the patients with ER-positive primary breast tumors will not respond or will rapidly develop resistance to tamoxifen.

Based on genome-wide screening, signatures associated with response to tamoxifen therapy of ER-positive breast cancer have been published by Ma *et al* [2] for adjuvant treatment and published by Jansen *et al* [3] for recurrent disease. Ma *et al* [2] identified a two-gene expression ratio, *HOXB13*-to-*IL17BR*, which predicted clinical outcome in a retrospective study of 60 patients and confirmed this in formalin-fixed paraffin-embedded (FFPE) samples of 20 LNN patients. Reid *et al* [4], however, failed to validate this two-gene ratio on frozen samples from 58 patients, who were mainly node-positive. A drawback in the adjuvant setting is that the tumor's response to tamoxifen and its intrinsic aggressiveness are measured. No accurate determination of response to tamoxifen can be given because these studies lacked randomization and a nontreated control group.

Recent microarray data analyses showed that the *HOXB13*-to-*IL17BR* ratio has no association with relapse-free survival [5] but it does have a weak association with response to first-line tamoxifen therapy [6]. However, data from microarray experiments need to be confirmed with quantitative real-time reverse transcriptase polymerase chain reaction (qRT-PCR), as these data are considered to be more accurate [4]. Therefore, we measured mRNA expression levels of *HOXB13* and *IL17BR* with a qRT-PCR

in RNA isolated from a set of 1,252 frozen breast cancer specimens and related expression levels with clinicopathologic factors. The main clinical end points in ER-positive disease were 1) disease-free survival (DFS) of untreated LNN patients to determine tumor aggressiveness and 2) response to first-line tamoxifen monotherapy for recurrent disease. In addition, we compared for *IL17BR* two primer sets (ps): one at the 3' end region, comparable to the assay of Ma *et al* (*ps3*) [2], and one at the 5' end region, used by Reid *et al* (*ps5*) [4]. Finally, we validated in our cohort predefined cutoff points for untreated patients and tamoxifen-treated patients [7,8].

PATIENTS AND METHODS

Patients

This retrospective study was approved by the

medical ethics committee of the Erasmus MC (Rotterdam, the Netherlands; MEC 02.953), and it included breast tumor tissue specimens of 1,683 female patients with primary operable breast cancer. To avoid bias, frozen tumor samples were processed from patients with breast cancer who entered the clinic between 1979 and 1996 and from whom detailed clinical follow-up was available. Follow-up, tumor staging, and response to therapy was defined by standard International Union Against Cancer (Geneva, Switzerland) classification criteria [9] and applied previously by Foekens *et al* [10]. The cutoff point to classify primary breast tumors as ER and/or progesterone receptor (PgR) -positive was 10 fmol/mg cytosolic protein. The following tumors were excluded from analysis: 1) with distant spread at or within the first month of surgery; 2) with missing values for lymph node status, ER protein status, and *HOXB13*

Table 1. Associations of HOXB13 and IL17BR mRNA levels with clinicopathologic factors.

Factor	No. Patients	%	HOXB13 Median	HOXB13 Δ	HOXB13 P	IL17BRps3 Median	IL17BRps3 Δ	IL17BRps3 P	IL17BRps5 Median	IL17BRps5 Δ	IL17BRps5 P
Total	1,252	100	0.0015	0.050		0.090	0.149		0.015	0.025	
Age in categories, years					.38*			< .001*			< .001*
< 40	166	13	0.0036	0.047		0.084	0.093		0.015	0.020	
40-55	465	37	0.0016	0.045		0.076	0.135		0.012	0.022	
56-70	409	33	0.0019	0.052		0.095	0.161		0.015	0.026	
> 70	212	17	0.0007	0.063		0.116	0.217		0.019	0.032	
Menopausal status					.98†			.005†			.026†
Premenopausal	537	43	0.0016	0.045		0.079	0.123		0.013	0.021	
Postmenopausal	715	57	0.0014	0.056		0.099	0.172		0.016	0.027	
Tumor size					.44‡			.035‡			.098‡
pT1, < 2 cm	392	31	0.0008	0.045		0.095	0.160		0.016	0.025	
pT2, > 2-5 cm	716	57	0.0023	0.050		0.089	0.135		0.014	0.025	
PT3, > 5 cm + pT4	144	12	0.0023	0.077		0.077	0.129		0.013	0.024	
Lymph nodes involved					.37‡			< .001‡			< .001‡
0	653	52	0.0017	0.055		0.104	0.173		0.017	0.028	
1-3	269	21	0.0006	0.045		0.085	0.119		0.014	0.023	
> 3	330	27	0.0023	0.052		0.065	0.095		0.010	0.018	
Grade§					< .001‡			< .001‡			< .001‡
Poor	690	55	0.0051	0.065		0.083	0.121		0.013	0.020	
Good/moderate	184	15	0.0003	0.029		0.109	0.182		0.019	0.033	
ER status‖					< .001*			< .001*			< .001*
Low	335	27	0.0125	0.062		0.053	0.087		0.009	0.015	
High	917	73	0.0005	0.045		0.101	0.173		0.017	0.029	
PgR status‖¶					< .001*			< .001*			< .001*
Low	417	33	0.0106	0.061		0.066	0.113		0.011	0.020	
High	764	61	0.0006	0.044		0.098	0.179		0.016	0.027	

NOTE. All P values are two-sided. The interquartile range is q25-q75.
Abbreviations: ER, estrogen receptor; PgR, progesterone receptor.
* Spearman rank correlation.
† Mann-Whitney U test.
‡ Kruskal-Wallis test, followed by a nonparametric test for trend when appropriate.
§ In 378 samples (30%), grade was unknown. The median expression levels in this subset for HOXB13 was 0.0006 (Δ = 0.045), for IL17BRps3 was 0.091 (Δ =0.172), and for IL17BRps5 was 0.015 (Δ = 0.0027).
‖ Low and high steroid hormone receptor protein status as defined in the Patients and Methods section.
¶ In 71 tumors protein levels of PgR were not determined.

and *IL17BR* expression; 3) with <30% epithelial tumor cells in their tumor specimens; and 4) with specimens of poor RNA quality [11].

After applying the exclusion criteria, tumor specimens of 1,252 patients (74%) were analyzed for *HOXB13* and *IL17BR* expression. From these 1,252 patients (for clinicopathologic details, see Table 1), 543 patients (43%) underwent breast-conserving lumpectomy, and 709 patients (57%) underwent modified mastectomy. The median follow-up time of all 1,252 patients was 72 months (2 to 248 months), of the 692 patients alive was 91 months (3 to 248 months), and of the 560 deaths was 46 months (2 to 205 months). Disease recurrence occurred in 692 (55%) of 1,252 patients.

Four hundred six patients (32%) were treated with adjuvant systemic therapy, of which 177 patients (44%) received hormonal therapy, 214 (53%) received chemotherapy, and 15 (3%) received combination therapy. Of the 846 patients (68%) that had not received (neo)adjuvant systemic therapy, 381 patients (45%) experienced a relapse treated with systemic therapy. Two hundred eighty-five (75%) of these

patients were treated with hormonal therapy, of which 193 patients (68%) received first-line tamoxifen monotherapy. Therapy failure occurred in 73 patients (38%), of which 61 patients (84%) had progressive disease and 12 patients (16%) showed stable disease ≤6 months. One hundred twenty patients (62%) of these 193 patients had experienced a clinical benefit from first-line tamoxifen monotherapy, of which 11 patients (66%) had a complete response, 30 patients (25%) showed a partial response, and 79 patients (66%) showed stable disease > 6 months.

RNA isolation and qRT-PCR

Tissue processing, RNA isolation, cDNA synthesis, and qRT-PCR were performed as described previously by Sieuwerts *et al* [11]. qRT-PCR reactions were performed in 25 µl reaction volume on an ABI Prism 7700 Sequence Detection System (Applied Biosystems, Nieuwerkerk aan den IJssel, the Netherlands), in accordance with the recommended protocol. Commercially available Assay-on-
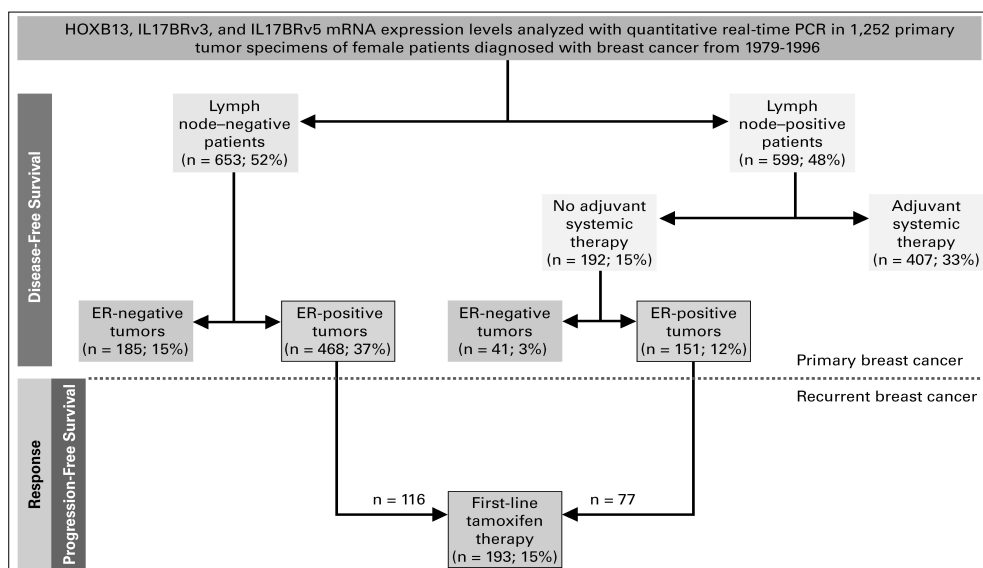

Figure 1. Study design and patient subsets (framed boxes) analyzed.
Relationships with tumor aggressiveness were evaluated in estrogen receptor-positive tumors from patients who did not receive adjuvant systemic therapy. Associations with response to first-line tamoxifen monotherapy were analyzed in 193 patients. PCR, polymerase chain reaction; ER, estrogen receptor.

Demand kits (Applied Biosystems) were used for *HOXB13* (Hs00197189_m1) and *IL17BR* (Hs00218889_m1; Hs00914532_m1). We used a primer set (Hs00914532_m1; defined as *IL17BRps3*), located in the 3' end region of *IL17BR* (from exons 9 to 10), which is comparable to the assay of Ma *et al* [2] and the primer set (Hs00218889_m1; defined as *IL17BRps5*) used by Reid *et al* [4], located in the 5' end region (from exons 1 to 2). Both primer sets amplify two published variants described in the Entrez Gene database [4,6] of the National Center for Biotechnology Information (Bethesda, MD). Primer sequences for the three reference genes (*ie*, *porphobilinogen deaminase*, *hypoxanthine-guanine phosphoribosyltransferase*, and *β-2-microglobulin*) and for the *ER* and *PGR* have all been previously described [11].

Forty rounds of amplification were performed according to the supplier's protocol, and at the end of the amplification fluorescent signals of the TaqMan probes (Applied Biosystems) were used to generate cycle threshold (Ct) values from which mRNA expression levels were calculated. Expression levels of *HOXB13* and *IL17BR* were normalized against average expression levels of three reference genes as follows [11]:

mRNA target$2^{(\text{mean Ct Ref} - \text{mean Ct target})}$. When amplification rounds exceeded the manufacturer's defined detection threshold of the ABI Prism 7700 Sequence Detection System (Ct values 35 to 40; Applied Biosystems, http://docs.appliedbiosystems.com/pebiodocs/04371095.pdf), quantities were considered to be undetectable and were set to 50% of the expression level measurable at the detection threshold.

Data analysis and statistics

The relationship between *HOXB13*, *IL17BR*, and a *HOXB13*-to-*IL17BR* ratio as continuous variables with patient and tumor characteristics were investigated with the use of nonparametric methods (*ie*, Spearman rank correlations for continuous variables and Wilcoxon rank sum test or Kruskal-Wallis exact test for ordered variables). Cox regression analysis was applied

to compute the hazard ratio (HR), which correlates expression levels of the variables with overall survival (OS), DFS, progression-free survival (PFS), and postrelapse survival (PRS), respectively. In multivariate analysis, Cox proportional hazards regression models were applied to compare the variables with traditional factors. The model for OS and DFS included age, menopausal status, tumor size, lymph node status, grade, and log *ER* and log *PGR* mRNA levels. The model for PRS and PFS included age, menopausal status, DFS, site of relapse, and log *ER* and log *PGR* mRNA levels [12]. The proportional hazards assumption was not violated for *HOXB13*, *IL17BRps3*, and *IL17BRps5* in any of the analyses. Logistic regression analysis was performed to calculate the odds ratio (OR) that defines the relation between expression ratio levels and response. Both HR and OR were calculated on log-transformed variables and were represented with their 95% CI.

Only when the test for trend for a continuous variable was statistically significant, a cutoff point was considered justified. To define cutoff points, isotonic regression was used to find the points where the monotonic relationship between the measured level and the hazard ratio showed a distinct change. The cutoff with the largest statistically significant change in hazard ratio corrected for multiple testing was used [12].

Ma *et al* [7] and Erlander *et al* [8] have described cutoff points for untreated patients (cutoff=1.00) and for adjuvant tamoxifen-treated patients (cutoff=0.06) that separated (tamoxifen-treated) nonrecurrence cases from recurrent cases. These predefined cutoff points were not directly applicable to our normalized data set because of differences in assays, reference genes, qRT-PCR machines, and sample specimens. As a result, our data were standardized for each gene via a z-transformation step. In concordance with Ma *et al* [7], a composite index was generated by taking the difference between the standardized *HOXB13* and *IL17BR* expression levels.

Based on the cutoff points, survival curves were generated using the Kaplan-Meier method, and

Table 2. Cox univariate and multivariate analysis for disease-free survival in ER-positive primary breast tumors from 468 lymph node-negative patients who did not receive adjuvant systemic therapy.

Factor of Base Model	No. of Patients	%	Univariate Analysis			Multivariate Analysis		
			HR	95% CI	P	HR	95% CI	P
Age, years								
≤ 40	53	11	1.00			1.00		
41-55	162	35	0.65	0.44 to 0.95	.026	0.67	0.45 to 1.00	.051
56-70	149	32	0.55	0.37 to 0.82	.004	0.52	0.27 to 1.00	.052
> 70	104	22	0.40	0.25 to 0.65	< .001	0.38	0.18 to 0.78	.008
Menopausal status								
Premenopausal	183	39	1.00			1.00		
Postmenopausal	285	61	0.71	0.54 to 0.93	.012	1.02	0.59 to 1.77	.94
Tumor size								
pT1, < 2 cm	215	46	1.00			1.00		
pT2, > 2-5 cm	230	49	1.11	0.85 to 1.46	.16	1.08	0.81 to 1.42	.61
pT3, > 5 cm + pT4	23	5	1.35	0.70 to 2.59	.37	1.58	0.82 to 3.07	.18
Grade*								
Poor	223	48	1.00			1.00		
Good/moderate	94	20	0.64	0.44 to 0.93	.021	0.68	0.46 to 1.00	.050
ER-α mRNA level								
Continuous	468	100	0.87	0.78 to 0.97	.014	1.02	0.88 to 1.17	.81
PgR mRNA level								
Continuous	468	100	0.91	0.86 to 0.97	.003	0.91	0.85 to 0.98	.014
Factors analyzed						Additions to the base model		
HOXB13 to IL17BRps3								
Ratio as continuous variable	468	100	1.05	1.02 to 1.09	.002	1.04	1.01 to 1.08	.015
Index and predefined cutoff point*								
Low, ≤ 1.00	418	88	1.00			1.00		
High, > 1.00	50	12	1.69	1.15 to 2.51	.008	1.74	1.17 to 2.59	.006
HOXB13 to IL17BRps5								
Ratio as continuous variable	468	100	1.06	1.03 to 1.09	< .001	1.05	1.02 to 1.08	.004
Index and predefined cutoff point†								
Low, ≤ 1.00	419	88	1.00			1.00		
High, > 1.00	49	12	1.59	1.07 to 2.37	.022	1.61	1.08 to 2.41	.019

Abbreviations: ER, estrogen receptor; HR, hazard ratio; PgR, progesterone receptor.

* In 151 samples (32%), grade was unknown. For this subset, the HR was 1.04 (95% CI, 0.77 to 1.39; P=0.82) and 1.18 (95% CI, 0.87 to 1.61; P=0.29) in univariate analysis and multivariate analysis, respectively.

† Predefined cutoff point for the HOXB13-to-IL17BR index was determined by Ma et al [7] in a training set at 1.00 for untreated patients.

a log-rank test was used to test for differences. Computations were performed with the STATA statistical package, release 9.1 (STATA Corp, College Station, TX). All *P* values were two-sided, and *P*<0.05 was considered statistically significant.

RESULTS

Associations of HOXB13 and IL17BR with clinicopathologic factors

The mRNA expression levels of *HOXB13*, *IL17BRps3*, and *IL17BRps5* were measured in 1,252 primary breast tumors by qRT-PCR and normalized against our reference genes. *HOXB13* expression levels showed a weak but significant inverse association with those of *IL17BR* (Spearman's rho=-0.16; *P*<0.0001), whereas expression levels of *IL17BRps3* and *IL17BRps5* correlated significantly (Spearman's rho=0.91; *P*<0.0001). In 448 tumors (36%), *HOXB13* expression levels were below detection level (see Patients and methods).

Table 1 shows median expression levels and the interquartile range of all three transcripts and their relation with patient and tumor characteristics. The differences in *IL17BR* expression levels measured with *ps3* and *ps5* only reflect assay performance. *HOXB13* levels associate significantly with grade and inversely with steroid hormone receptor status. The median expression level of *HOXB13* was 17 x higher in poorly differentiated tumors compared with good/moderately differentiated tumors. In contrast, the median *HOXB13* expression level was 25 x lower in ER-positive tumors compared with ER-negative tumors. Undetectable levels of *HOXB13* were significantly more prevalent in ER-positive tumors, with 379 (41%) out of 917, compared with ER-negative tumors, with

69 (21%) out of 335; *P<0.001*.

Except for tumor size, *IL17BR* levels were significantly associated with all clinicopathologic parameters studied (*ie*, positively with age and menopausal status, and negatively with grade and nodal status). ER-positive tumors showed a two-fold higher median *IL17BR* expression level than ER-negative tumors.

Next, expression levels of *HOXB13* were divided by *IL17BR* to generate a *HOXB13*-to-*IL17BR* expression ratio. In all 1,252 tumors, the *HOXB13*-to-*IL17BR* ratio measured as univariate log-transformed continuous variable was associated with a poor DFS (HR*ps3*=1.04 [95% CI, 1.02 to 1.06; *P<0.001*] and HR*ps5*=1.05 [95% CI, 1.03 to 1.06; *P<0.001*], respectively) and a poor OS (HR*ps3*=1.06 [95% CI, 1.04 to 1.08; *P<0.001*] and HR*ps5*=1.06 [95% CI, 1.04 to 1.08; *P<0.001*], respectively).

HOXB13-to-IL17BR ratio and tumor aggressiveness

To test for a relation between expression ratio and tumor aggressiveness, we included LNN patients with ER-positive tumors who did not receive adjuvant systemic therapy. Patients with ER-positive tumors were selected because only these patients are eligible for tamoxifen therapy. Thus 468 ER-positive primary breast tumors were analyzed (Figure 1). Of these patients, 217 (46%) had a relapse during the follow-up period. The *HOXB13*-to-*IL17BR* ratio as a univariate continuous variable was significantly associated with a poor DFS (Table 2) and a poor OS (HR*ps3*=1.06 [95% CI, 1.02 to 1.10; *P*=0.001] and HR*ps5*=1.07 [95% CI, 1.03 to 1.10; *P<0.001*], respectively). When added to the traditional factors of the base multivariate model, the *HOXB13*-to-*IL17BR* ratios contributed significantly to the model for DFS (Table 2) and OS (*P≤0.001*; data not shown).

The prognostic value of *HOXB13*-to-*IL17BR* ratios was also explored in ER-positive tumors from 151 LNP untreated patients, who were mainly enrolled in the early 1980s. In univariate analysis, the *HOXB13*-to-*IL17BR* ratio in these LNP patients associated with a poor DFS (HR*ps3*=1.05 [95% CI, 1.01 to 1.09; *P*=0.023], and HR*ps5*=1.05 [95% CI, 1.01 to 1.10;

P=0.016], respectively) and a poor OS (HR*ps3*=1.09 [95% CI, 1.04 to 1.14; *P<0.001*] and HR*ps5*=1.09 [95% CI, 1.04 to 1.14; *P<0.001*], respectively). In the multivariate model, the*HOXB13*-to-*IL17BR* ratio was significantly associated with OS (*P<0.001*), but not with DFS (*P*=0.065).

Based on a predefined cutoff point (1.00) for untreated patients [7,8] a *HOXB13*-to-*IL17BR* index was dichotomized. In the LNN-untreated 468 patients cohort, this dichotomized index had a significant relationship with a poor DFS in univariate analysis (HR*ps3*=1.69 and HR*ps5*=1.59) and multivariate analysis (HR*ps3*=1.74 and HR*ps5*=1.61; Table 2). However, the dichotomized index was not related with DFS in the LNP-untreated cohort of 151 patients (data not shown).

HOXB13-to-IL17BR expression ratio and response to first-line tamoxifen monotherapy

Expression levels were evaluated in 193 ER-positive primary breast tumors from patients whose relapse was treated with first-line tamoxifen monotherapy (Figure 1). These patients had not received any (neo)adjuvant systemic (*ie*, endocrine or chemotherapy) treatment.

The *HOXB13*-to-*IL17BR* ratio, as a univariate continuous variable, was significantly related with a poor response (OR*ps3*=0.93 [95% CI, 0.87 to 0.99]; *P*=0.027 and OR*ps5*=0.92 [95% CI, 0.86 to 0.98]; *P*=0.015, respectively), a short PFS (Table 3), and a poor PRS (HR*ps3* 1.07 [95% CI, 1.03 to 1.11; *P<0.001*], and HR*ps5* 1.07 [95%CI, 1.03 to 1.11; *P<0.001*], respectively). In multivariate analysis, however, the *HOXB13*-to-*IL17BR* ratio retained only its significant association for PFS (Table 3) and PRS (*P<0.001*; data not shown).

The significant findings in univariate analysis justified the search for a predictive cutoff point. Isotonic regression analysis defined optimal cutoff points for PFS at 2.99 and 16.44 for *HOXB13*-to-*IL17BRps3* and *IL17BRps5* ratio with 26 (13%) and 28 (15%) tumors classified as high, respectively. This resulted in an OR*ps3* for response of 0.18 and 0.16 ([95% CI, 0.06 to 0.45]; *P<0.001*) and an OR*ps5* of 0.12 and 0.12

Table 3. Cox univariate analysis and multivariate analysis for progression-free survival in ER-positive tumors from 193 patients whose recurrence was treated with received first-line tamoxifen monotherapy.

Factor of Base Model	No. of Patients	%	Univariate Analysis			Multivariate Analysis		
			HR	95% CI	P	HR	95% CI	P
Age, years								
≤ 40	17	9	1.00			1.00		
41-55	55	28	0.92	0.43 to 1.96	.83	0.61	0.27 to 1.39	.24
56-70	83	43	0.78	0.38 to 1.62	.51	0.38	0.14 to 1.02	.054
> 70	38	20	0.65	0.31 to 1.38	.26	0.32	0.12 to 0.86	.025
Menopausal status								
Premenopausal	56	29	1.00			1.00		
Postmenopausal	137	71	0.92	0.64 to 1.32	.659	2.24	1.17 to 4.30	.016
Disease-free survival								
≤ 1 year	30	16	1.00			1.00		
1-3 years	97	50	0.53	0.35 to 0.82	.004	0.54	0.33 to 0.88	.012
> 3 years	66	34	0.41	0.26 to 0.66	< .001	0.39	0.23 to 0.67	< .001
Dominant site of relapse								
Soft tissue	22	11	1.00			1.00		
Bone	92	48	1.26	0.76 to 2.10	.37	1.05	0.61 to 1.81	.86
Viscera	79	41	1.31	0.78 to 2.19	.31	1.20	0.70 to 2.07	.51
ER-α mRNA level								
Continuous	193	100	0.85	0.74 to 0.96	.012	0.87	0.75 to 1.01	.058
PgR mRNA level								
Continuous	193	100	0.93	0.87 to 1.00	.054	0.97	0.90 to 1.05	.41
Factors analyzed						Additions to the base model		
HOXB13 to IL17BRps3								
Ratio as continuous variable	193	100	1.08	1.05 to 1.12	< .001	1.07	1.04 to 1.11	< .001
Ratio cutoff point for PFS								
Low, ≤ 2.99	167	87	1.00			1.00		
High, > 2.99	26	13	3.43	2.18 to 5.40	< .001	2.97	1.82 to 4.86	< .001
Index and predefined cutoff point*								
Low, ≤ 0.06	128	66	1.00			1.00		
High, > 0.06	65	34	2.15	1.55 to 2.97	< .001	1.95	1.39 to 2.73	< .001
HOXB13 to IL17BRps5								
Ratio as continuous variable	193	100	1.09	1.05 to 1.13	< .001	1.08	1.04 to 1.12	< .001
Ratio cutoff point for PFS								
Low, ≤ 16.45	165	85	1.00			1.00		
High, > 16.45	28	15	3.85	2.47 to 6.00	< .001	3.31	2.05 to 5.34	< .001
Index and predefined cutoff point*								
Low, ≤ 0.06	120	62	1.00			1.00		
High, > 0.06	73	38	2.39	1.73 to 3.29	< .001	2.12	1.52 to 2.97	< .001

Abbreviations: ER, estrogen receptor; HR, hazard ratio; PgR, progesterone receptor; PFS, progression-free survival.

* Predefined cutoff point for the HOXB13-to-IL17BR index was determined by Ma et al [7] and set at 0.06 for adjuvant tamoxifen-treated patients.

([95% CI, 0.04 to 0.33]; P<0.001) in univariate and multivariate analyses, respectively. The univariate HR for PFS of the dichotomized HOXB13-to-IL17BRps3 and IL17BRps5 ratio were 3.43 and 3.85 (both P<0.001; Table 3). When added to the multivariate base model, high levels of HOXB13-to-IL17BR ratios were independently associated with a poor PFS (Table 3; both P<0.001).

We also evaluated a previously defined cutoff point of a HOXB13-to-IL17BR index for tamoxifen response in an adjuvant setting by Ma et al [7]. This cutoff point (0.06) classified 65 (34%) and 73 (38%) of the tumors as high for HOXB13-to-IL17BRps3 and IL17BRps5 indexes, respectively. In univariate analysis, the OR for response of the HOXB13-to-IL17BR index based on this predefined cutoff point was ORps3=0.59 (95% CI, 0.32 to 1.09; P=0.09) and ORps5=0.42 (95% CI, 0.23 to 0.76; P=0.004), and it resulted in a significant association with PFS (ie, HRps3=2.15 and HRps5=2.39; Table 3). In multivariate analysis, the two-gene index remained only significantly associated with a shorter PFS (Table 3).

The predictive value of HOXB13-to-IL17BRps3 is visualized with Kaplan-Meier curves in Figure 2. Similar results were obtained for the HOXB13-to-IL17BRps5 ratio.

DISCUSSION

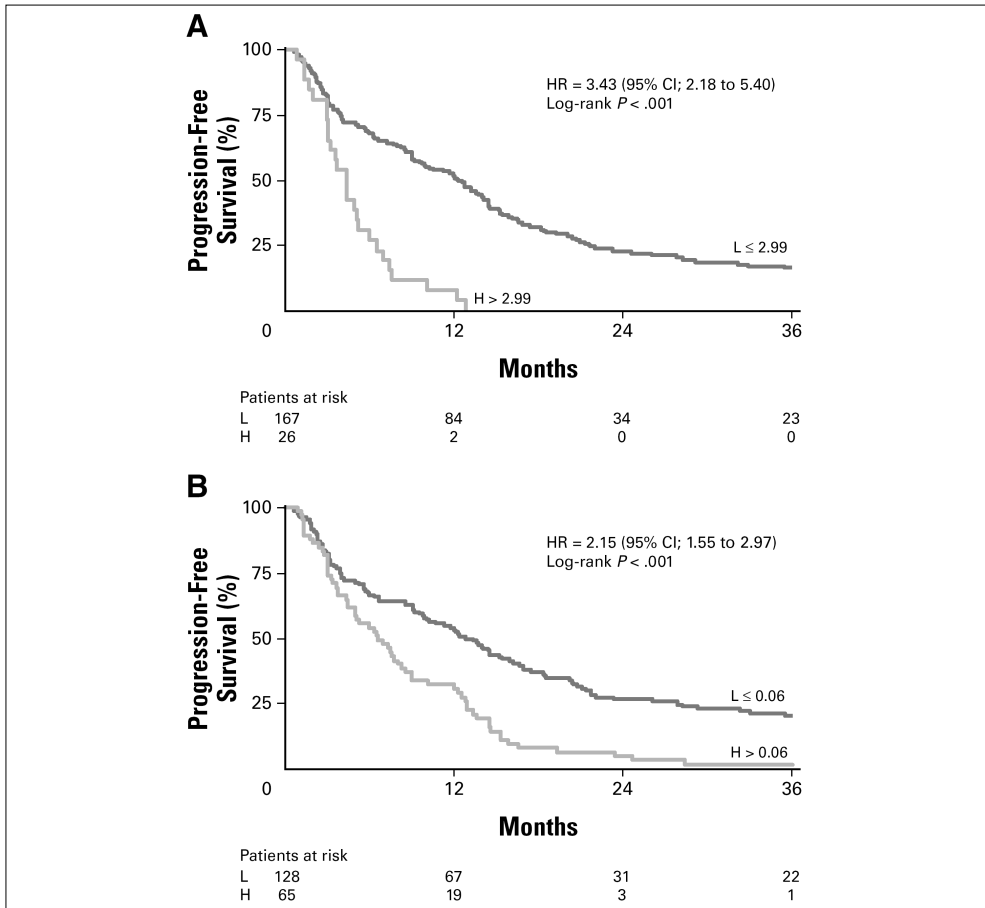Ma et al [2] used microarrays to analyze ER-positive tumors from patients treated with adju-

A

HR = 3.43 (95% CI; 2.18 to 5.40)
Log-rank *P* < .001

L ≤ 2.99

H > 2.99

Patients at risk

L	167	84	34	23
H	26	2	0	0

B

HR = 2.15 (95% CI; 1.55 to 2.97)
Log-rank *P* < .001

L ≤ 0.06

H > 0.06

Patients at risk

L	128	67	31	22
H	65	19	3	1

Figure 2. Relationship between dichotomized HOXB13-to-IL17BRv3 expression levels and progression-free survival curves ana-lyzed in 193 patients with recurrent disease treated with first-line tamoxifen monotherapy.
A cutoff point for advanced tamoxifen (A: 2.99) and a predefined cutoff point for adjuvant tamoxifen (B: 0.06) [7] were used to dichotomize the HOXB13-to-IL17BR ratio.

vant tamoxifen. They identified *HOXB13* and *IL17BR* as being differentially expressed between relapsed patients and disease-free patients. However, in the adjuvant setting, one cannot discriminate between tumor aggressive-ness and response to treatment [6]. The data were confirmed with qRT-PCR on FFPE-derived RNA in a small patient cohort that was not similar to the original training set. It is gen-erally accepted that RNA from FFPE samples is significantly degraded and, therefore, of lower quality compared to RNA from frozen samples. This article describes expression levels of

HOXB13 and *IL17BR* measured with qRT-PCR on frozen tissue–derived RNA in a large number of tumors. Based on this technical approach and the large sample size, a *HOXB13*-to-*IL17BR* expression ratio can be more accurately quanti-fied and related to outcome and clinicopatho-logic data. Up to now, this is the only study that allows for a relation of *HOXB13*-to-*IL17BR* expression levels with both tumor aggressive-ness and response to first-line tamoxifen monotherapy.

Our study supports the finding that a *HOXB13*-to-*IL17BR* ratio has prognostic value in LNN-

untreated patients [7,8]. In contrast to others [4,13], we found in a larger cohort of LNP-untreated patients a statistically significant association with disease outcome in univariate analysis. Interestingly, our findings demonstrated for the first time the relationship of a *HOXB13*-to-*IL17BR* ratio with response to first-line tamoxifen monotherapy. We showed in patients with recurrent disease that high *HOXB13*-to-*IL17BR* ratio levels were associated with a poor response to therapy and a short PFS, independent of traditional clinical and pathologic predictive factors.

For their analysis of *IL17BR* expression levels, Reid *et al* [4] used a primer set in the 5' end region of *IL17BR*, whereas Ma *et al* [2] applied a primer set in the 3' end region. Because of the difference in primer design, we have evaluated both primer sets. The 3' end primer set (*ps3*) of *IL17BR* revealed 6 x higher expression levels compared with levels determined with a 5' end primer set (*ps5*). Despite this six-fold difference, levels of both correlated significantly. As a consequence, corresponding *HOXB13*-to-*IL17BR* ratios showed equivalent performances. The *HOXB13* gene is localized at the edge of a *HOXB*-gene cluster at chromosome 17q21 and belongs to the canonical family of homeobox (*HOX*) genes [14]. *HOX* proteins often require other homeodomain proteins to form DNA-binding complexes [15,16]. Our data revealed that in 36% of breast tumors, *HOXB13* expression was below detection level. The observed absence of *HOXB13* expression in these tumors may be caused by a chromosomal deletion of the gene but also may be due to epigenetic silencing, such as promotor methylation. In renal cell carcinoma, complete methylation of 5' CpG islands of *HOXB13* and corresponding loss of mRNA and protein expression were reported to correlate with tumor progression [17]. In contrast, *HOXB13* was absent in normal breast and prostate tissue, whereas elevated levels were detected in breast and prostate tumor tissue [2,18,19]. In prostate cancer cell lines, it was shown that *HOXB13* functions as an androgen receptor (AR) repressor to modulate hormone-activated AR signaling and, in contrast with observations in tumor tissue, to suppress cell growth [15]. Likewise, we and others found that the absence of *HOXB13* expression was predominantly observed (85%) in ER-positive breast tumors. This relation between ER expression and transcriptional repression of *HOXB13* needs further investigation.

In conclusion, this retrospective qRT-PCR study provides evidence that high *HOXB13*-to-*IL17BR* expression levels are associated with both tumor aggressiveness and tamoxifen monotherapy failure.

ACKNOWLEDGEMENT

REFERENCES

1. Effects of chemotherapy and hormonal therapy for early breast cancer on recurrence and 15-year survival: an overview of the randomised trials. Lancet 2005;365: 1687-717.

2. Ma XJ, Wang Z, Ryan PD, Isakoff SJ, Barmettler A, Fuller A, Muir B, Mohapatra G, Salunga R, Tuggle JT, Tran Y, Tran D, Tassin A, Amon P, Wang W, Enright E, Stecker K, Estepa-Sabal E, Smith B, Younger J, Balis U, Michaelson J, Bhan A, Habin K, Baer TM, Brugge J, Haber DA, Erlander MG, Sgroi DC. A two-gene expression ratio predicts clinical outcome in breast cancer patients treated with tamoxifen. Cancer Cell 2004;5:607-16.

3. Jansen MP, Foekens JA, van Staveren IL, Dirkzwager-Kiel MM, Ritstier K, Look MP, Meijer-van Gelder ME, Sieuwerts AM, Portengen H, Dorssers LC, Klijn JG, Berns EM. Molecular classification of tamoxifen-resistant breast carcinomas by gene expression profiling. J Clin Oncol 2005;23:732-40.

4. Reid JF, Lusa L, De Cecco L, Coradini D, Veneroni S, Daidone MG, Gariboldi M, Pierotti MA. Limits of predictive models using microarray data for breast cancer clinical treatment outcome. J Natl Cancer Inst 2005;97:927-30.

5. Fan C, Oh DS, Wessels L, Weigelt B, Nuyten DS, Nobel AB, van't Veer LJ, Perou CM. Concordance among gene-expression-based predictors for breast cancer. N Engl J Med 2006;355:560-9.

6. Jansen MP, Foekens JA, Klijn JG, Berns EM. Re: Limits of predictive models using microarray data for breast cancer clinical treatment outcome. J Natl Cancer Inst 2005;97:1851-2; author reply 1852-3.

7. Ma X, Hilsenbeck S, Wang W, Ding L, Sgroi DC, Bender RA, Osborne CK, Allred DC, Erlander M. The HOXB13:IL17BR expression index is a prognostic factor in early stage breast cancer. J Clin Oncol 2006; 24:4611-9.

8. Erlander MG, Ma XJ, Hilsenbeck SG, Sgroi DC, Osborne CK, Allred DC. Validation of HOXB13, IL17BR and CHDH as predictors of clinical outcome of adjuvant tamoxifen monotherapy in breast cancer. Breast Cancer Res Treat 2005;94:33-4.

9. Hayward JL, Carbone PP, Heuson JC, Kumaoka S, Segaloff A, Rubens RD. Assessment of response to therapy in advanced breast cancer: a project of the Programme on Clinical Oncology of the International Union Against Cancer, Geneva, Switzerland. Cancer 1977;39:1289-94.

10. Foekens JA, Peters HA, Grebenchtchikov N, Look MP, Meijer-van Gelder ME, Geurts-Moespot A, van der Kwast TH, Sweep CG, Klijn JG. High tumor levels of vascular endothelial growth factor predict poor response to systemic therapy in advanced breast cancer. Cancer Res 2001;61:5407-14.

11. Sieuwerts AM, Meijer-van Gelder ME, Timmermans M, Trapman AM, Rodriguez Garcia R, Arnold M, Goedheer AJ, Portengen H, Klijn JG, Foekens JA. How ADAM-9 and ADAM-11 differentially from estrogen receptor predict response to tamoxifen treatment in patients with recurrent breast cancer: a retrospective study. Clin Cancer Res 2005;11:7311-21.

12. Meijer-van Gelder ME, Look MP, Peters HA, Schmitt M, Brunner N, Harbeck N, Klijn JG, Foekens JA. Urokinase-type plasminogen activator system in breast cancer: association with tamoxifen therapy in recurrent disease. Cancer Res 2004;64:4563-8.

13. Goetz MP, Suman VJ, Ingle JN, Nibbe AM, Visscher DW, Reynolds CA, Lingle WL, Erlander M, Ma XJ, Sgroi DC, Perez EA, Couch FJ. A two-gene expression ratio of homeobox 13 and interleukin-17B receptor for prediction of recurrence and survival in women receiving adjuvant tamoxifen. Clin Cancer Res 2006;12: 2080-2087.

14. Grier DG, Thompson A, Kwasniewska A, McGonigle GJ, Halliday HL, Lappin TR. The pathophysiology of HOX genes and their role in cancer. J Pathol 2005;205: 154-71.

15. Jung C, Kim RS, Zhang HJ, Lee SJ, Jeng MH. HOXB13 induces growth suppression of prostate cancer cells as a repressor of hormone-activated androgen receptor signaling. Cancer Res 2004;64:9185-92.

16. Jung C, Kim RS, Lee SJ, Wang C, Jeng MH. HOXB13 homeodomain protein suppresses the growth of prostate cancer cells by the negative regulation of T-cell factor 4. Cancer Res 2004;64:3046-51.

17. Okuda H, Toyota M, Ishida W, Furihata M, Tsuchiya M, Kamada M, Tokino T, Shuin T. Epigenetic inactivation of the candidate tumor suppressor gene HOXB13 in human renal cell carcinoma. Oncogene 2006;25:1733-42.

18. Cantile M, Pettinato G, Procino A, Feliciello I, Cindolo L, Cillo C. In vivo expression of the whole HOX gene network in human breast cancer. Eur J Cancer 2003;39: 257-64.

19. Edwards S, Campbell C, Flohr P, Shipley J, Giddings I, Te-Poele R, Dodson A, Foster C, Clark J, Jhavar S, Kovacs G, Cooper CS. Expression analysis onto microarrays of randomly selected cDNA clones highlights HOXB13 as a marker of human prostate cancer. Br J Cancer 2005;92:376-81.

CHAPTER SEVEN

Identification of alternatively spliced TIMP1 mRNA in cancer cell lines and colon cancer tissue

Pernille A. Usher[1], Anieta M. Sieuwerts[2], Annette Bartels[1], Ulrik Lademann[1],
Hans J. Nielsen[3], Lars Holten-Andersen[1], John A. Foekens[2],
Nils Brünner[1] and Hanne Offenberg[1]

[1]Department of Veterinary Pathobiology, Faculty of Life Sciences,
University of Copenhagen, Frederiksberg C, Denmark
[2]Department of Medical Oncology, Erasmus MC, Rotterdam, The Netherlands
[3]Department of Surgical Gastroenterology, University Hospital Hvidovre, Denmark

ABSTRACT

TIMP-1 is a promising new candidate as a prognostic marker in colorectal and breast cancer. We now describe the discovery of two alternatively spliced variants of *TIMP1* mRNA.

The two variants lacking exon 2 (*del-2*) and 5 (*del-5*), respectively, were identified in human cancer cell lines by RT-PCR. The *del-2* variant was furthermore detected in extracts from 12 colorectal cancer tissue samples. By western blotting additional bands of lower molecular mass than full-length TIMP-1 were identified in tumor tissue, but not in plasma samples obtained from cancer patients.

The two splice variants of TIMP-1 may hold important clinical information, and either alone or in combination with measurement of full-length TIMP-1 they may improve the prognostic and/or predictive value of TIMP-1 analyses.

INTRODUCTION

Despite an increasing knowledge on the molecular mechanisms underlying malignant transformation and dissemination of disease, the overall survival rates for the most common malignancies in the Western world have only improved slightly over the last decade. The obvious challenge in future management of cancer patients is therefore to improve existing therapy and/or to develop new therapy strategies. Another approach is to improve detection of early cancer disease, as patients diagnosed at the early stages of *e.g.* colorectal cancer often will be cured by primary surgery alone [1]. Furthermore, since stratification of cancer patients for therapy is based on prognostic evaluations, this calls for new and better prognostic markers. Tissue inhibitor of metalloproteinases-1 (TIMP-1) is a promising new marker for early detection and prognostic stratification of patients suffering from colorectal cancer [2, 3]. In addition, TIMP-1 also carries the potential as a predictive marker for response to chemotherapy [4, 5].

TIMP-1 is a naturally occurring inhibitor of matrix metalloproteinases (MMPs), a large family of proteases involved in many physiological and pathological processes like embryonic development, tissue morphogenesis, wound healing, inflammation and cancer invasion (for reviews see [6, 7]). Four TIMPs (TIMP-1 to -4) have been identified and they differ in tissue distribution and ability to inhibit different MMPs [8]. Mature TIMP-1 is a 28.5 kDa glycoprotein, consisting of 184 amino acid residues. The unprocessed precursor contains a signal peptide of 23 residues, which is cleaved in the maturation of the protein [9]. TIMP-1 contains two sites of N-glycan linkage and six disulfide bonds. The latter is folding the protein into a two-domain structure. These disulfide bonds renders TIMP-1 very robust to changes in pH, temperature and denaturing conditions [10]. The MMP-inhibitory activity has been located to the N-terminal domain of TIMP-1, which forms non-covalent complexes with MMPs or proforms of these, in particular proMMP-9 [11]. Although now named for its ability to inhibit MMPs, TIMP-1 was first identified for its growth stimulating activity of erythroid progenitors [12], and its mitogenic ability has since been demonstrated in many cell types [13, 14]. TIMP-1 has also been shown to inhibit apoptosis [15, 16] and to participate in regulation of angiogenesis [17]. It therefore seems that TIMP-1 is a multifunctional protein demonstrating a range of activities that in relation to cancer can be both tumor promoting and suppressing. Some functions of TIMP-1 can be ascribed to its MMP inhibitory ability, while others appear to be independent of binding to MMPs.

TIMP-1 may exist in multiple molecular forms in the cancer environment and subsequently in the circulation, *e.g.* in complex with other proteins like MMPs [18] or as different glycosylation variants [19]. The clinical value of TIMP-1 measurements may be improved by detection of specific forms of TIMP-1, as shown in breast cancer, where measurement of unbound TIMP-1 versus total TIMP-1 adds to the prognostic

evaluation of the patients [2, 20]. We now describe the expression of two newly discovered splice variants of *TIMP1* mRNA in cancer cell lines and in colon cancer tissue. They may hold important clinical information and could either alone or in combination with measurement of full-length TIMP-1 improve the already established clinical value of TIMP-1 as a biological tumor marker.

MATERIALS AND METHODS

Cell culture

The following human breast cancer cell lines were used: MDA-MB-231-BAG [21], MDA-MB-435-BAG [21], CAMA-1, EVSA-T, ZR75.1, T47-D, SKBR-3 and MCF7-S1 (kindly provided by Professor Marja Jäättela, Danish Cancer Society, Copenhagen, Denmark). Furthermore, three colon cancer cell lines DLD-1, LoVo and LS 174T (all from ATCC, Manassas, USA) as well as the prostate cancer cell line PC-3, the human acute promyelocytic leukemia cell line HL-60 (kindly provided by Professor Hau C. Kwaan, Northwestern University, Chicago, USA) and the endothelial cell line EAHY-926 were used. MCF7-S1 cells were propagated in RPMI medium supplemented with 10% heat inactivated fetal calf serum (FCS) and HL-60 cells were propagated in IMDM medium with 20% FCS. ZR75.1, T47-D, SKBR-3 and EAHY-926 were propagated in HAMF/DME medium with 10% FCS, 0.15% Na_2HCO_3 and 45 µg/ml Gentamycin. ZR75.1 cells were furthermore supplemented with 10 nM estradiol and to EAHY-926 cells 1x HAT medium was added. DLD-1 cells were propagated in modified RPMI-1640 medium (ATCC) supplemented with 10% FCS. LoVo cells were propagated in modified F-12K medium (ATCC) supplemented with 10% FCS. LS 174T cell were propagated in modified EMEM (ATCC) supplemented with 10% FCS. All other cell lines were propagated in DMEM medium. MDA-MB-231-BAG and MDA-MB-435-BAG cells were supplemented with 10% FCS and CAMA-1, EVSA-T and PC-3 cells with 5% FCS. All media (except for the colon cancer cell lines) were purchased from Invitrogen, Taastrup, Denmark and were supplemented with penicillin and streptomycin. The cells were grown at 37º C in a humidified air atmosphere with 5% CO_2.

Patient material

Tumor tissue and blood samples from 12 patients who underwent surgery for colorectal cancer (CRC) were obtained from Hvidovre Hospital, Denmark, in accordance with an approval by the Scientific Ethical Committee for Copenhagen and Frederiksberg, Denmark (Journal no. KF 01-078/93) and with informed consent from the patients. The tissue samples were taken from the peripheral area of the tumor, snap frozen in liquid nitrogen and stored at -80º C. At the time of surgical removal of the tumor, blood samples were collected and EDTA plasma samples prepared according to a previously described protocol [22]. A pool of control EDTA plasma and platelets were obtained from the blood bank at Rigshospitalet, Copenhagen, Denmark.

Each tissue sample was divided into three parts. One part was used for RNA extraction and RT-PCR and one part was used for protein extraction and ELISA. The middle part of each tissue was thawed and fixed in 4% neutral buffered paraformaldehyde overnight at 4° C and processed for paraffin embedding prior to histological analyses. The diagnosis of colon cancer was confirmed in H&E stained sections of the paraffin embedded material and the relative area of neoplastic cells was estimated (0 -100%).

For western blotting analysis we obtained an additional 6 CRC tissue samples from the same source as the 12 CRC samples described above.

RNA extraction and reverse transcription

RNA was extracted from tissue samples or cells using a spin column kit (SV Total RNA isolation system, Promega, Madison, USA) according to the manufacturer's instructions. This procedure includes an on-column DNase treatment, minimizing the risk of DNA contamination. Prior to extraction approximately 30 mg of

tissue sample was homogenized in 1 ml lysis buffer. The cells were grown to a confluency of approximately 60% in 900 ml flasks, washed twice in PBS and lysed in 0.5 ml lysis buffer. RNA was extracted from 175 µl lysate and the concentration of total RNA was measured spectrophotometrically.

One microgram of total RNA was transcribed into cDNA using the First Strand cDNA Synthesis Kit (Fermentas, Helsingborg, Sweden). The total volume of the reaction was 25 µl consisting of 1x reaction buffer, 0.8 mM dNTPs, 20 U RiboLock RNase inhibitor, 0.5 µg oligo(dT) primer, 0.2 µg random hexamer primer and 40 U M-MuLV Reverse Transcriptase. Samples were incubated at 25º C for 10 min, followed by 42º C for 1 h. The reaction was terminated by incubating at 95º C for 5 min followed by cooling on ice.

PCR

All primer sets used were intron-spanning to avoid false positive results from contaminating genomic DNA. Prior to PCR with *TIMP1* primers all cDNA samples were subjected to PCR with primers for *GAPDH* (Table 1) to ensure that RNA extraction and reverse transcription (RT) were carried out efficiently. PCR was performed in 25 µl reactions containing 1x HotStarTaq Mastermix (Qiagen Nordic, West Sussex, UK), 1 µM of each gene-specific primer and 1 µl cDNA. Reaction conditions were 95º C for 15 min followed by 40 cycles of 94º C for 1 min, 60º C for 30 s and 72º C for 1 min.

PCR products were separated on a 1.5 % agarose gel (Fermentas, Sweden) stained with ethidium bromide and visualized by UV light.

Quantitative real-time PCR (qPCR)

In order to estimate the expression level of the *del-2 TIMP1* variant compared with full-length *TIMP1*, a qPCR assay determining relative expression levels was developed. Relative quantification was chosen in contrast to absolute quantification, since tumor samples contain various amounts of cells expressing *TIMP1*. The absolute amount of transcript will therefore depend on the composition of each sample. Relative quantification using either total *TIMP1* or full-length *TIMP1* as reference gene will reflect only changes in transcription of the cells expressing *TIMP1*.

qPCR was carried out using SYBR Green I detection and the LightCycler System 2.0 (Roche Diagnostics, Hvidovre, Denmark) essentially as previously described [23]. PCR conditions for each primer set were optimized by determining the $MgCl_2$ concentration and annealing temperature at which only the specific product was seen. Reactions were carried out in 20 µl volumes consisting of 1x FastStart Master SYBR Green Mix, 5 mM $MgCl_2$ and 0.5 µM of the gene-specific primer. The amplification program was as follows: Preincubation for Fast Start Polymerase activation at 95º C for 10 min, followed by 45 amplification cycles (95º C for 5 s (20º C/s), 65º C for 10 s (20º C/s), and 72º C for 6-10 s (20º C/s). SYBR Green fluorescence was acquired at 72º C in each amplifica-

Table 1. Primers used for RT-PCR and qPCR analyses.

Gene	Specificity	Forward primer 5' → 3'	Reverse primer 5' → 3'	Product size (bp)
TIMP-1	All exon-skipping variants[a]	Forward exon 1 CCCTAGCGTGGACATTTATC	Reverse exon 6 AAGGTGACGGGACTGGAAG	648 (full-length)
TIMP-1	Full-length + del-2	Forward exon 1 CCCTAGCGTGGACATTTATC	Reverse exon 3 GGTATAAGGTGGTCTGGTTG	263 + 134
TIMP-1	Full-length + del-5	Forward exon 4 ACTTCCACAGGTCCCACAAC	Reverse exon 6 AAGGTGACGGGACTGGAAG	252 + 127
TIMP-1	Full-length[b]	Forward exon 2 CTTCTGGCATCCTGTTGTTG	Reverse exon 3 GGTATAAGGTGGTCTGGTTG	153
TIMP-1	Del-2[b]	Forward exon 1/3 CCCAGAGAGACACCAGAGTCA	Reverse exon 4 GTGGGACCTGTGGAAGTATC	196
GAPDH	Full-length	CAATGACCCCTTCATTGACC	TTCACACCCATGACGAACAT	309

[a] Except variants lacking exon 1 or 6.
[b] qPCR assay.

tion cycle. After the end of the last cycle the melting curve was generated by starting the fluorescence acquisition at 65º C and taking measurements every 0.1 s until 95º C was reached.

A standard curve for each primer set was generated using 10-fold dilutions of a pool of tumor cDNA. The standard curve was used to correct for differences in PCR efficiencies between primer sets. Dilutions of tumor cDNA samples were chosen for the generation of standard curves to ensure the same PCR efficiency in standards and samples. Relative quantification was done using the Relative Quantification software (LightCycler 2.0, Roche, Denmark).

Protein extraction for western blotting and ELISA

The frozen tissue samples used for ELISA were fragmented on dry ice using a pestle and mortar device (Arrow Fastener CO Inc., Saddle Brook, N.J., USA). The powdered tissue was weighed and dissolved in Camiolo buffer (75 mM CH_3COOK, 0.3 M NaCl, 0.1 M L-argenine, 10 mM EDTA, 0.25% Triton X-100, pH 4.2) in a 3:1 ratio of buffer to tissue. Samples were centrifuged for 1 h at 20,000 g, and the supernatant containing the proteins was used for further analysis. For western blotting, the tissue powder was dissolved in modified RIPA buffer (50 mM Tris-HCl (pH 7.4), 1% NP-40, 0.25% Na-deoxycholate, 150 mM NaCl, 1 mM EDTA) supplemented with protease inhibitors (Pefabloc, Aprotinin, Leupeptin, Pepstatin: 1 µg/ml of each).

The tumor cell lines were seeded in Petri dishes ($1x10^6$/ dish). After 24 h, the cells were harvested in ice-cold PBS by scraping followed by centrifugation for 5 min at 400 *g*. Platelets were centrifuged for 5 min at 300 *g*. The tumor cells and platelets were resuspended in lysis buffer (25 mM Hepes, 5 mM $MgCl_2$, 1 mM EDTA, 0.5% Triton; pH 7.5) supplemented with protease inhibitors (see above), incubated for 30 min on ice followed by centrifugation for 5 min at 20,000 *g*. Protein concentration in plasma, and tissue samples and in cell lysates was determined by the BCA Protein assay kit (Pierce, Rockford, IL, USA).

Western blotting

Protein samples were mixed with 0.25 x volume of 4 x Laemmli sample buffer, boiled for 5 min and equal amounts of protein (100 or 150 µg) were separated on a 12% polyacrylamide gel and blotted on nitrocellulose membrane. The blot was blocked in PBS containing 0.1% Tween 20 and 5% dry milk powder for 1 h, and then incubated overnight with monoclonal anti-human TIMP-1 (VT7; 1 µg/ml) [24]. Subsequently, the blot was washed 3 x 10 min in PBS containing 0.1% Tween 20, incubated with horseradish peroxidase (HRP)- conjugated goat anti-mouse antibody diluted 1:1000 (DAKO, Glostrup, Denmark) in PBS with 0.1% Tween 20 and 1% dry milk powder for 1 h followed by 3 x 10 min washing in PBS with 0.1% Tween 20. The blot was developed by the ECL+ detection system (Amersham, UK) according to the manufacturer's instructions. Recombinant human TIMP-1 (rhTIMP-1) and platelet lysate were used as positive controls, and as a control for the sensitivity of the assay we also included a pool of control EDTA plasma (see Patient material) with a known low level of TIMP-1 (Table 2).

ELISA

A well established sandwich ELISA was used to measure total levels of human TIMP-1 in tissue and plasma samples [22]. In brief, the immunoassay employs an affinity-purified polyclonal sheep anti-TIMP-1 antibody as cap-

Table 2. TIMP-1 levels in plasma and tumor extracts measured by ELISA.

Sample number	EDTA plasma TIMP-1 (ng/ml)	Tumor extracts TIMP-1 (ng/mg protein)	Tumor area (%)[a]
1	213	33.17	25
2	274.5	28.29	75
3	511.1	7	10
4	272.1	12.67	75
5	523.8	6.7	10
6	530	19.34	75
7	530	29.5	50
8	115.8	10.78	90
9	258.5	28.92	90
10	395.2	13.02	50
11	160.8	14.1	10
12	131.7	19.27	5
Control plasma	45.7		

[a] *Relative area of neoplastic cells in tissue section.*

ture antibody and a monoclonal anti-TIMP-1 antibody for detection. The complex was detected with alkaline phosphatase-conjugated rabbit anti-mouse antibodies (Dako, Denmark), that enables a kinetic rate assay. The plate was read at 405 nm, and the rate of the color development was collected automatically over a 1 h period in a Power Wave$_x$ Microplate Reader (Biotek Instruments Inc., VT, USA) and the results were evaluated using the KC4 software (Biotek Instruments Inc., USA). A four-parameter fitted standard curve was generated from which the TIMP-1 concentration of each sample was calculated. TIMP-1 concentrations in tissue samples were normalized for differences in protein concentrations.

Generation and sequencing of TIMP1 cDNA fragments

Full-length human *TIMP1* cDNA (Genbank accession no. NM_003254) was used as a template to generate two non-overlapping cDNA fragments of *TIMP1* by PCR named *TIMP1 01* (56-378 bp) and *TIMP1 02* (398-680 bp). The PCR reactions were carried out with upstream primers flanked by a *T3* RNA polymerase site and downstream primers flanked by a *T7* RNA polymerase site (polymerase sites in bold). The primers used for fragment *01* were: up 5'-**CAT TAA CCC TCA CTA AAG GGA GA**A CCC ACC ATG GCC CCC TTG-3' and down 5'-**TAA TAC GAC TCA CTA TAG GGA G**AC TCC TCG CTG CGG TTG TGG-3', and for fragment *02*: up 5'-**CAT TAA CCC TCA CTA AAG GGA GA**G CAG GAT GGA CTC TTG CAC A-3' and down 5'-**TAA TAC GAC TCA CTA TAG GGA G**TA TCT GGG ACC GCA GGG ACT-3'. The PCR was carried out in a 25 µl reaction containing 1xTaq buffer, 0.2 mM dNTP mix, 2 mM MgCl$_2$, 1 µM of each primer, 1 U Taq polymerase and 0.1-0.5 µg cDNA template using standard reagents from Fermentas (Sweden). The PCR products were analyzed by gel electrophoresis and purified using MinElute Gel Extraction kit from Qiagen Nordic (UK) according to the manufacturer's instructions.

For the two splice variants of *TIMP1* lacking

exon 2 (*del-2*) or exon 5 (*del-5*), RT-PCR products from cell lines and colon cancer tissue samples were gel purified as described above and used as a template for a PCR reaction with the following *T3* and *T7* flanked primers: up 5'-**CAT TAA CCC TCA CTA AAG GGA GA**A GTG GGT GGA TGA GTA ATG C-3' and down 5'-**TAA TAC GAC TCA CTA TAG GGA G**TC TGG TTG ACT TCT GGT GTC C-3'.

All *TIMP1* fragments generated with *T3* and *T7* flanked primers were sequenced (AGOWA, Berlin, Germany) with both *T3* and *T7* primers and the sequences were confirmed by BLAST search.

Preparation of digoxigenin-labeled RNA probes

Antisense and sense RNA probes were synthesized by *in vitro* transcription from *TIMP1* fragment *01*, *02* and *del-2* variant using *T3* and *T7* polymerases and Dig RNA labeling mix (Roche, Basel, Schwitzerland) according to the manufacturer's instructions. The labeled probes were purified using RNeasy MinElute Cleanup Kit (Qiagen, UK) and the yield of labeled probe was estimated by spot blot analysis. Antisense and corresponding sense probes were adjusted to the same concentration and diluted with deionized formamide to a final concentration of 50%.

In situ hybridization

Paraffin sections were cut at 3 µm, dried overnight, dewaxed and treated with 10-15 µg/ml of proteinase K for 5 min, dehydrated and air-dried before 25 µl of hybridization solution containing 5 µl probe (50 ng) was added to each section. Hybridization was carried out overnight at 42° C. After hybridization, the sections were washed with 2x SSC/0.1% SDS for 1 h and with 0.5x SSC/0.1% SDS for 30 min at 55° C. The sections were then treated with RNase A for 10 min at 37°C to remove non-hybridized probe followed by a final stringency wash with 0.1x SSC/0.1% SDS for 30 min at 37° C. Prior to immunological detection of hybridized probe, the sections were blocked with 5% BSA in 0.1 M Tris, 0.15 M NaCl pH 7.5 containing 0.1% Triton X-100 for 30 min. Alkaline phosphatase-

labeled anti-digoxigenin antibody diluted 1:500 was then applied to the sections for 2 h, and the reaction was visualized by incubating the sections with NBT/BCIP (Roche, Schwitzerland) overnight in the dark. The sections were counter-stained with Mayer's hematoxylin and mounted with Glycergel (Dako, Denmark). Sense probes were applied to each case as negative controls. For each *in situ* hybridization experiment, a positive control case (human colon carcinoma known to contain *TIMP1* mRNA) was included.

Immunohistochemistry

Paraffin sections (3 μm) were dewaxed in xylene and rehydrated through a graded series of ethanol. Antigen retrieval was carried out by boiling the sections for 10 minutes in a conventional microwave oven in 10 mM citrate buffer pH 6.00 followed by 30 min in the hot buffer at room temperature. To block endogenous peroxidase activity, the sections were treated with 0.5% hydrogen peroxide in 99% ethanol for 10 min. Sections were incubated at 4° C overnight with primary antibodies diluted to the following IgG concentrations: 0.25 μg/ml monoclonal anti-TIMP-1 antibody, clone VT7 [24] and 3.75 μg/ml monoclonal anti-α-smooth muscle actin (α-SMA; Dako, Denmark). Anti-TIMP-1 antibody was detected with HRP-labeled PowerVision Kit, (ImmunoVision Technologies, Brisbane, CA, USA) and anti-α-SMA antibody was detected with HRP-labeled rabbit Envision (Dako, Denmark). The reactions were in all cases visualized by incubating the sections with 0.1% diaminobenzidine containing 0.02% H_2O_2 for 5 min. The sections were counterstained with Mayer's hematoxylin. For each tissue sample a negative control was performed on a serial section, where the primary antibody was substituted by an irrelevant monoclonal antibody against trinitrophenyl hapten (TNP) (IgG_1 subtype) diluted to the same IgG concentration as the respective primary antibodies. For each immunohistochemical experiment, a positive control case (human colon carcinoma known to contain TIMP-1) was included.

RESULTS

RT-PCR

The *TIMP1* gene consists of 6 exons and the initial RT-PCR screening of the cultured cell lines was carried out using a forward primer in exon 1 and a reverse primer in exon 6 (Table 1 and Figure 1A). After detection of more than one PCR product, indicating various splice variants, RT-PCR was performed using combinations of primers located 2 exons apart to identify any exon-skipping variants. All cell lines except EVSA-T and CAMA-1 expressed more than one *TIMP1* transcript (Figure 1A). These were identified as a variant lacking exon 2 (*del-2*) (Figure 1B), and in MDA-MB-231-BAG, MDA-MB-435-BAG, PC-3 and EAHY-926
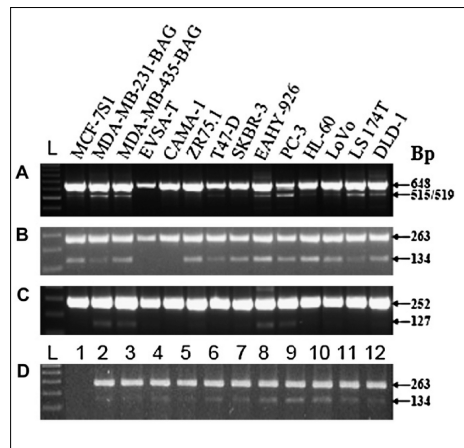

Figure 1. RT-PCR on cultured cell lines (A–C) and colon cancer tissue samples (D).
The following primer combinations were used. Panel A: forward exon 1 and reverse exon 6; panel B and D: forward exon 1 and reverse exon 3; panel C: forward exon 4 and reverse exon 6. Full-length TIMP1 mRNA was detected in all cell lines (A, upper band at 648 bp), and all cell lines except EVSA-T and CAMA express more than one transcript, most abundantly a second transcript of 515/519 bp (lower band in A). RT-PCR with primers located in exon 1 and 3 shows that all cell lines except EVSA-T and CAMA express del-2 variant (B, lower band at 134 bp), and RT-PCR with primers located in exon 4 and 6 shows that MDA-MB-231-BAG, MDA-MD-435-BAG, EAHY-926 and PC-3 cell lines express del-5 variant (C, lower band at 127 bp). Both full-length TIMP1 and del-2 variant mRNA were detected in 11 of the 12 colon cancer tissue samples (D). L: 100 bp DNA ladder.

cells also a variant lacking exon 5 (*del-5*) (Figure 1C). The identification of full-length, *del-2* and *del-5* transcripts was confirmed by sequencing. No variants lacking exon 3 or 4 could be detected. MDA-MB-231-BAG, MDA-MB-435-BAG and PC-3 cells also expressed additional variants, which could not be identified by the single exon-skipping analysis and were therefore not analysed further.

Screening of the 12 colon cancer tissue samples revealed both full-length and *del-2* variant in 11 samples (Figure 1D). In one of the samples no transcript could be detected when the primer located in exon 1 was used. However amplification with both *GAPDH* primers and *TIMP1* primers other than the one located in exon 1

revealed that there was *TIMP1* expression in this sample (data not shown). qPCR in which the primer partly located in exon 1 (see below) was used, showed that in this sample the *del-2* variant was also expressed. The results indicate that in this sample exon 1 is either partially missing or the sequence located at the 5' end is altered compared to the other samples. No *del-5* variant could be detected in any of the 12 tissue samples.

qPCR

To detect full-length *TIMP1* transcript, the forward primer located in exon 2 was combined with the reverse primer located in exon 3 (Table
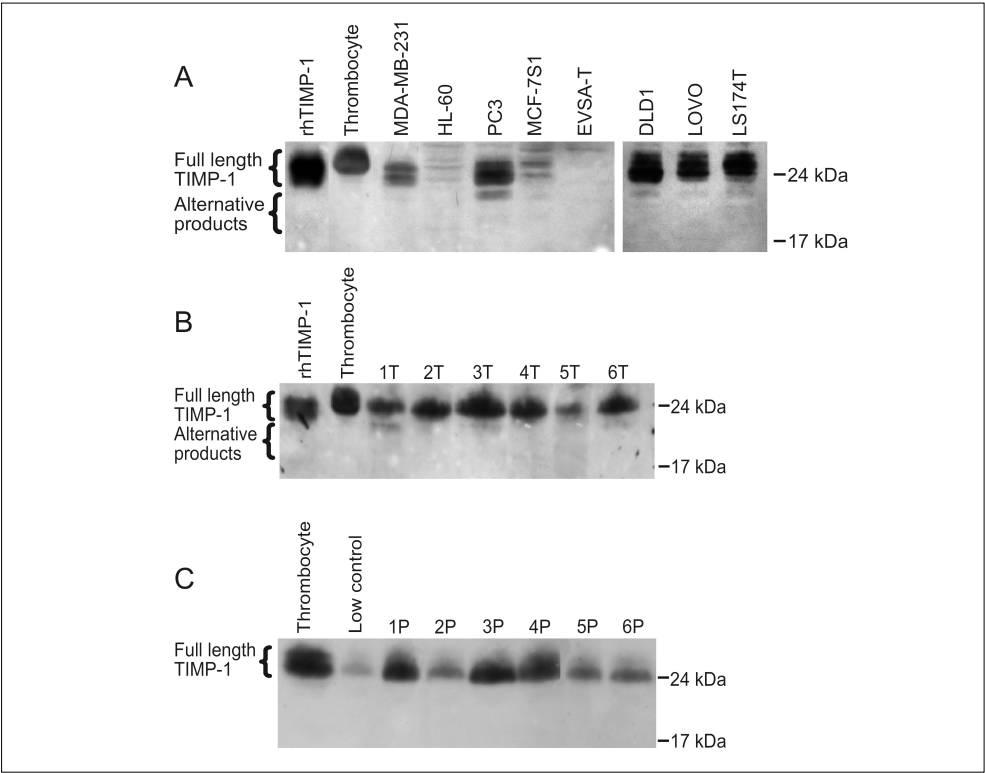

Figure 2. Detection of TIMP-1 and alternative TIMP-1 products in cancer cell lines (A), lysates of tumor samples from CRC patients (B) and in plasma from CRC patients (C).
Equal amounts of protein were separated by SDS-PAGE, and TIMP-1 was subsequently detected with a monoclonal anti-TIMP-1 antibody (VT7). Low control, platelet lysate (contains high TIMP-1 protein levels) and recombinant human (rh) TIMP-1 serve as controls. The plasma samples are representative of a total of 12 samples analysed. The experiment was repeated once with similar results.

1). To detect only the *del-2* transcript a forward primer designed to anneal to the last 18 bases of exon 1 and the first 3 bases of exon 3 (Table 1) was combined with a reverse primer in exon 4. In the 12 CRC samples, the mean relative expression level of the *del-2* variant compared to the full-length transcript was 0.00802 (± 0.00206 SD). This means that the variant is transcribed at a level approximately 1/1000 of the full-length transcript. The cancer cell lines generally displayed a higher level of *del-2* variant expression ranging from 0.0021 to 0.05.

Western blot analysis

Next, it was investigated if the splice variants detected by RT-PCR and qPCR also generated a protein product detectable by western blotting analysis. To analyse if the presence of different transcripts results in different protein expression we chose to analyse one cell line that only expresses full-length *TIMP1* mRNA (EVSA-T), 2 cell lines that express both full-length *TIMP1* mRNA and the *del-2* variant (MCF-7S1 and HL-60) and 2 cell lines that express both full-length *TIMP1* mRNA, the *del-2* variant and the *del-5* variant. We also included all three colon cancer cell lines to compare with the tumor tissue. As shown in Figure 2A, all the tumor cell lines, except for EVSA-T, expressed full-length TIMP-1 protein, although at different levels of expression. The anti-TIMP-1 antibody recognized two bands around 24 kDa in the positive controls and in the tumor cell lines, probably representing glycosylation variants of full-length TIMP-1. Below full-length TIMP-1 additional bands were detected, in particular in PC-3, DLD-1, LoVo and LS 174T cell lines. When tumor tissue extracts from CRC patients were analysed for presence of TIMP-1 protein, additional bands were detected below full length TIMP-1 in tissue sample 1, 3 and 6 (Figure 2B). Both cells and tumor extracts were lysed in a buffer containing a cocktail of protease inhibitors minimizing the risk of breakdown products, and therefore the alternative products may represent splice variants. When plasma samples from CRC patients were analyzed by western blotting no alternative TIMP-1 products were detected (Figure 2C).

ELISA

ELISA detecting the amount of total TIMP-1 protein was performed on both plasma samples and tumor tissue extracts. The results are displayed in Table 2. Compared with a control plasma pool, it is evident that all the plasma samples from CRC patients displayed an elevated level of TIMP-1 protein (mean 326.4 ± 163.4 ng/ml), supporting our previous reports [2, 25]. In the tumor tissue samples, the mean concentration of TIMP-1 was 18.6 ± 9.3 ng/mg of protein. In order to evaluate if the tumor extract levels were elevated we would need to compare with a matched sample of normal colon tissue, which unfortunately was not available for this study. There was no obvious correlation between TIMP-1 levels in plasma samples and tumor extracts. As TIMP-1 levels in the tumor tissue samples are likely to reflect the amount of tumor tissue/invasive front present in the sample, we evaluated histopathologically a section taken from the middle part of each biopsy. However, there was no apparent correlation between TIMP-1 levels in the tumor extracts and the relative area of neoplastic cells in the corresponding tissue sections (Table 2).

Localization of TIMP1 mRNA and TIMP-1 protein

TIMP1 full-length mRNA expression was detected in 9 of the 12 colon cancer samples by *in situ* hybridization. The positive signal was seen in single cells located adjacent to tumor cells. The cells were elongated and resembled in all cases fibroblasts (Figure 3A and C). No signal was observed in tumor cells in any of the samples. The specificity of the *in situ* hybridization signal was evaluated by using probes transcribed from two non-overlapping fragments of *TIMP1* cDNA. In all 9 positive samples, the two non-overlapping antisense probes gave identical hybridization patterns (Figure 3A and C), while no specific signal was seen with the two corresponding sense probes (Figure 3D). The intensity of the hybridization signal was generally weaker than the signal observed in the positive control tissue, possibly due to differences in fix-
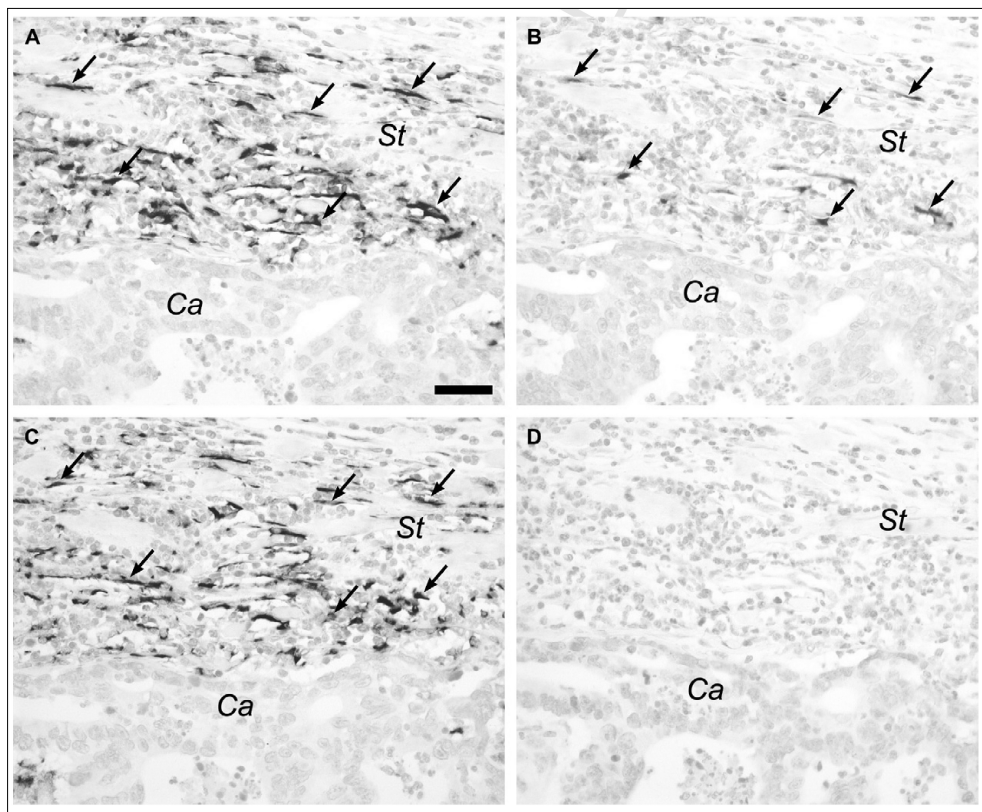
Figure 3. TIMP1 expressions in colon cancer.
Serial sections from a colon adenocarcinoma were hybridized with antisense or sense probes for full-length TIMP1(A, C, D) or exon 2 splice variant of TIMP1(B). Full-length TIMP1 mRNA is seen in fibroblast-like cells localized in the stroma (St) adjacent to the cancer cells (Ca) with similar hybridization patterns seen with two non-overlapping antisense probes (transcribed from pTIMP1 01 and 02) (arrows in A and C). The exon 2 variant of TIMP1 mRNA is detected in some of the same fibroblast-like cells seen in a parallel section (arrows in B). No signal is detected with a sense probe corresponding to the antisense probe shown in panel A (D). Scale bar: A–D=50 μm.

ation procedure. The 12 colon cancer samples were also hybridized with a specific antisense probe against the *TIMP1 del-2* splice variant, and a very weak signal was observed in 2 of the samples. However a stronger signal was seen in the control tissue, were the positive cells co-localized with a proportion of cells expressing full-length *TIMP1* mRNA (Figure 3B).

TIMP-1 protein was detected in all 12 colon cancer samples by immunohistochemistry using a monoclonal antibody against human TIMP-1. This antibody recognizes a linear epitope located in the C terminal end of TIMP-1 translated from part of exon 6 [24]. Intense positive immunostaining was seen in fibroblast-like cells in all samples (Figure 4B), and in addition tumor cells also showed weak staining in 9 of the 12 samples investigated. No staining was observed in any of the samples when the primary antibody was replaced by an irrelevant control antibody against TNP (Figure 4D).

There was a good correlation between TIMP-1 immunohistochemistry and *in situ* hybridization for full-length *TIMP1* mRNA performed on serial sections (Figure 4A and B). The positive cells were further characterized by immuno-staining with a monoclonal antibody against α-SMA. On serial sections, *TIMP1* mRNA and

TIMP-1 protein positive cells co-localized with a sub-population of α-SMA positive cells (Figure 4A-C), indicating that the TIMP-1 expressing cells are smooth muscle cells or myofibroblasts.

DISCUSSION

By screening tumor tissue from 12 patients suffering from colorectal cancer and a panel of human cancer cell lines, we have in addition to full-length *TIMP1* mRNA, identified two exon-skipping splice variants. In most cell lines and in all the cancerous tissue samples we detected a variant of *TIMP1* lacking exon 2 (*del-2*), and in a few of the cell lines a variant lacking exon 5 (*del-5*). The observed splice variants were all sequenced, confirming that they represented *TIMP1* transcripts.

In full-length *TIMP1* mRNA the translation is initiated from the first ATG site in exon 2. Sequence analysis of information on the *del-2* variant (Ensembl gene report OTTHUMG00000021447), revealed that the most likely initiation site containing part of the Kozak consensus sequence [26] is located at the end of exon 3 (Figure 5). This does not change the reading frame, but results in a shorter protein (143 amino acids) lacking the signal pep-
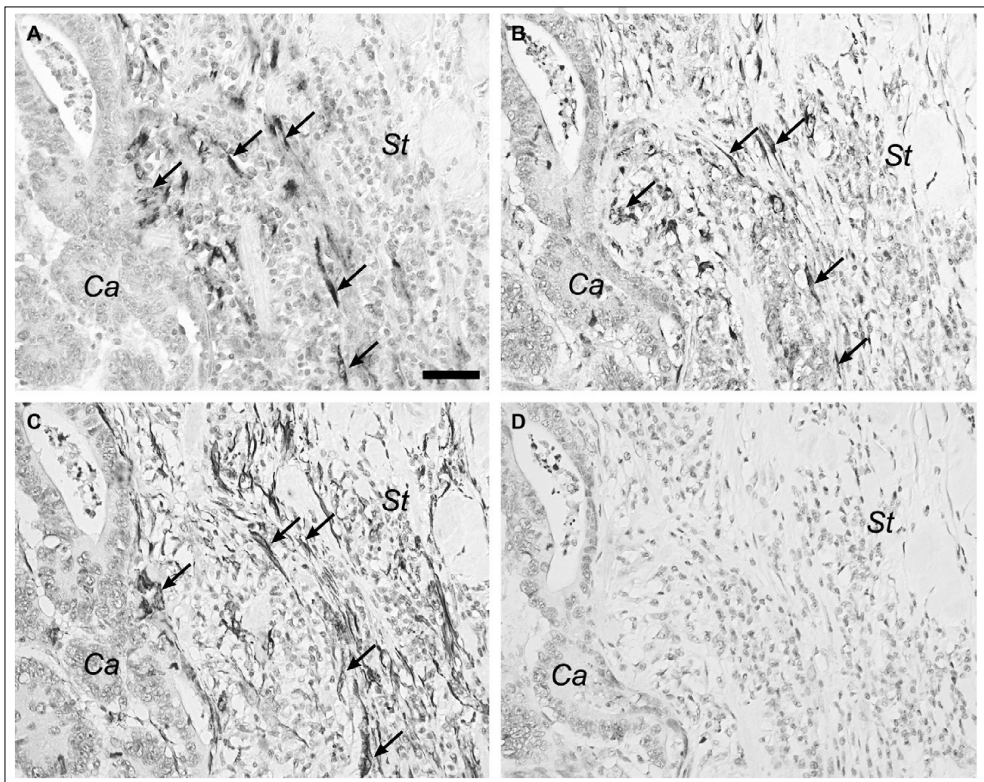

Figure 4. Identification of TIMP-1 positive cells in colon cancer.
Serial sections from a colon adenocarcinoma were processed for in situ hybridization with TIMP1 antisense probe 01 (A), or immunostained with monoclonal antibodies against TIMP-1 (B) or a-SMA (C). TIMP1 mRNA expressing cells (arrows in A) are seen in the stroma (St) with no signal observed in the cancer cells (Ca), and immunoreactivity for TIMP-1 is detected in the same cells (arrows in B). TIMP1 mRNA and protein co-localize with a sub-population of a-SMA positive cells, as seen on an adjacent section (arrows in C). No immunoreactivity is seen when the primary antibody is substituted with an irrelevant antibody against TNP (D). Scale bar: A–D=50 μm.
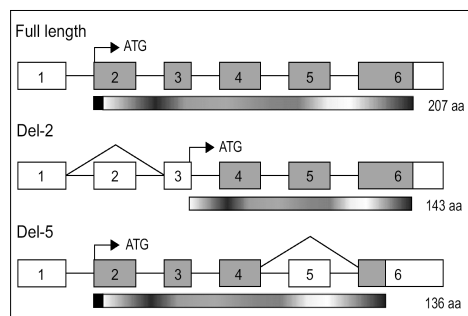
Figure 5. Schematic representation of full-length and alternatively spliced TIMP-1.
Exons are numbered from 1 to 6 and translated regions are shown in grey. White boxes indicate untranslated regions. Translation initiation sites are marked by black arrow and ATG. The corresponding translated proteins are shown underneath the mRNAs and the theoretical size is marked with number of amino acids (aa). The signal peptide sequences are shown as black boxes at the N-terminal end of full-length TIMP-1 and the del-5 variant. The translation initiation site in del-2 TIMP1 is shifted from exon 2 to exon 3, which results in a shorter protein lacking the signal peptide. A theoretical translation of the del-5 variant results in a protein consisting of 136 aa due to a shift in reading frame of the exon 6 sequence.

tide sequence, which directs full-length TIMP-1 to the secretory pathway. Thus, this variant, if translated, is probably a soluble, intracellular protein. In the *del-5* variant, any translation initiation is likely to start at the same ATG site in exon 2 as full-length *TIMP1*. However, a theoretical translation (ExPASy translation tool) gives a shift in the reading frame of the exon 6 sequence with an introduction of a new stop codon, which would result in a protein consisting of 136 amino acids (Figure 5). Full-length TIMP-1 is N-glycosylated at position 53 and 101 [27], and although the second site is retained in the shorter del-2 variant, it is unlikely to be exposed to the N-glycosylation machinery because of the lack of signal peptide, and thus may not be glycosylated *in vivo*. Although residues throughout the TIMP-1 molecule are involved in inhibition of MMPs, the main inhibitory activity has been assigned to the N-terminal end of the molecule [11], more specifically to a region surrounding the second disulfide knot [28]. Part of this region is missing in a putative del-2 variant of TIMP-1, which may therefore have compromised MMP

inhibitory activity. The del-5 variant of TIMP-1 is more likely to retain its inhibitory activity.

By performing western blotting analyses on the tumor tissue samples, we could in addition to full-length TIMP-1 demonstrate additional TIMP-1 bands of lower molecular mass. However, these extra products are absent in the plasma samples suggesting that they could represent the exon-2 variant, which if translated would not be secreted into the circulation because of the lacking signal peptide. Even though the *del-2* mRNA transcript was expressed in all the analysed cell lines (except EVSA-T) we were only able to detect additional TIMP-1 bands of lower molecular mass in the PC-3, DLD-1, LoVo and LS 174T cell lines. The western blot analyses show different levels of TIMP-1 in the cell lines and we could only detect the additional TIMP-1 band in cells with high expression of the full-length TIMP-1 protein. The additional TIMP-1 bands could therefore be present in the other cell lines as well, however, below detection level. This is further supported by the finding that the *del-2* variant mRNA is expressed at a much lower level than full-length *TIMP1* mRNA.

When we quantified the total level of TIMP-1 protein by using a thoroughly validated ELISA assay, there was no correlation between tumor extracts and plasma either. This however, could be explained by the fact that a tumor extract only represents a small part of the whole tumor, not necessarily from the invasive front, where we have previously demonstrated that the *TIMP1* expressing fibroblast-like cells are localized [29]. These fibroblast-like cells are in this study further characterized as myofibroblasts or smooth muscle cells, and are now shown to also express the *del-2* variant, although at a much lower level than full-length *TIMP1*, which is in agreement with our qPCR data.

The paradox of raised levels of inhibitors of tissue-degrading enzymes in advanced disease is well-described, but little is known about the biology of this phenomenon. High levels of TIMP-1 in the circulation and in tumor extracts may simply reflect the raised levels of MMPs, but there is increasing data describing tumor-

promoting activities of TIMP-1 independent of MMP inhibition, including inhibition of apoptosis. It is possible that different variant forms of TIMP-1 are responsible for the diverse and contrasting functions of the protein, similarly to what has been found for other cancer-related proteins [30]. A further investigation of this requires expression and characterization of the variant forms of the protein.

The prognostic value of TIMP-1 has been described at both mRNA and protein level. In breast cancer however, the mRNA data are somewhat conflicting. One semi-quantitative study has shown an inverse correlation between high level of *TIMP1* expression and lymph node metastasis [31], whereas other investigators have found high *TIMP1* mRNA levels to be correlated with poor prognosis [32, 33]. However, Span *et al*. found no association between levels of full-length *TIMP1* mRNA and disease progression, when measured by a quantitative RT-PCR assay [34]. At the protein level, high TIMP-1 has repeatedly proved to be a marker of poor prognosis in both colorectal and breast cancer [2, 3, 20, 35, 36], making measurements of TIMP-1 protein more attractive in the clinical setting. The development of quantitative assays specific for full-length and del-2 variant of TIMP-1 may improve the prognostic and predictive value and be useful in the management of cancer patients.

REFERENCES

1. Ouyang DL, Chen JJ, Getzenberg RH, Schoen RE. Noninvasive testing for colorectal cancer: a review. Am J Gastroenterol 2005;100:1393-403.

2. Holten-Andersen MN, Christensen IJ, Nielsen HJ, Stephens RW, Jensen V, Nielsen OH, Sorensen S, Overgaard J, Lilja H, Harris A, Murphy G, Brunner N. Total levels of tissue inhibitor of metalloproteinases 1 in plasma yield high diagnostic sensitivity and specificity in patients with colon cancer. Clin Cancer Res 2002;8: 156-64.

3. Waas ET, Hendriks T, Lomme RM, Wobbes T. Plasma levels of matrix metalloproteinase-2 and tissue inhibitor of metalloproteinase-1 correlate with disease stage and survival in colorectal cancer patients. Dis Colon Rectum 2005;48:700-10.

4. Davidsen ML, Wurtz SO, Romer MU, Sorensen NM, Johansen SK, Christensen IJ, Larsen JK, Offenberg H, Brunner N, Lademann U. TIMP-1 gene deficiency increases tumour cell sensitivity to chemotherapy-induced apoptosis. Br J Cancer 2006;95:1114-20.

5. Schrohl AS, Meijer-van Gelder ME, Holten-Andersen MN, Christensen IJ, Look MP, Mouridsen HT, Brunner N, Foekens JA. Primary tumor levels of tissue inhibitor of metalloproteinases-1 are predictive of resistance to chemotherapy in patients with metastatic breast cancer. Clin Cancer Res 2006;12:7054-8.

6. Egeblad M, Werb Z. New functions for the matrix metalloproteinases in cancer progression. Nat Rev Cancer 2002;2:161-74.

7. Lemaitre V, D'Armiento J. Matrix metalloproteinases in development and disease. Birth Defects Res C Embryo Today 2006;78:1-10.

8. Baker AH, Edwards DR, Murphy G. Metalloproteinase inhibitors: biological actions and therapeutic opportunities. J Cell Sci 2002;115:3719-27.

9. Brew K, Dinakarpandian D, Nagase H. Tissue inhibitors of metalloproteinases: evolution, structure and function. Biochim Biophys Acta 2000;1477:267-83.

10. Stricklin GP, Welgus HG. Human skin fibroblast collagenase inhibitor. Purification and biochemical characterization. J Biol Chem 1983;258:12252-8.

11. Murphy G, Houbrechts A, Cockett MI, Williamson RA, O'Shea M, Docherty AJ. The N-terminal domain of tissue inhibitor of metalloproteinases retains metalloproteinase inhibitory activity. Biochemistry 1991;30:8097-102.

12. Westbrook CA, Gasson JC, Gerber SE, Selsted ME, Golde DW. Purification and characterization of human T-lymphocyte-derived erythroid-potentiating activity. J Biol Chem 1984;259:9992-6.

13. Bertaux B, Hornebeck W, Eisen AZ, Dubertret L. Growth stimulation of human keratinocytes by tissue inhibitor of metalloproteinases. J Invest Dermatol 1991; 97:679-85.

14. Hayakawa T, Yamashita K, Tanzawa K, Uchijima E, Iwata K. Growth-promoting activity of tissue inhibitor of metalloproteinases-1 (TIMP-1) for a wide range of cells. A possible new growth factor in serum. FEBS Lett 1992;298:29-32.

15. Guedez L, Stetler-Stevenson WG, Wolff L, Wang J, Fukushima P, Mansoor A, Stetler-Stevenson M. In vitro suppression of programmed cell death of B cells by tissue inhibitor of metalloproteinases-1. J Clin Invest 1998;102:2002-10.

16. Liu XW, Taube ME, Jung KK, Dong Z, Lee YJ, Roshy S, Sloane BF, Fridman R, Kim HR. Tissue inhibitor of metalloproteinase-1 protects human breast epithelial cells from extrinsic cell death: a potential oncogenic activity of tissue inhibitor of metalloproteinase-1. Cancer Res 2005;65:898-906.

17. Akahane T, Akahane M, Shah A, Connor CM, Thorgeirsson UP. TIMP-1 inhibits microvascular endothelial cell migration by MMP-dependent and MMP-independent mechanisms. Exp Cell Res 2004; 301:158-67.

18. Holten-Andersen MN, Christensen IJ, Nielsen HJ, Lilja H, Murphy G, Jensen V, Brunner N, Piironen T. Measurement of the noncomplexed free fraction of tissue inhibitor of metalloproteinases 1 in plasma by immunoassay. Clin Chem 2002;48:1305-13.

19. Thaysen-Andersen M, Thogersen IB, Nielsen HJ, Lademann U, Brunner N, Enghild JJ, Hojrup P. Rapid and individual-specific glycoprofiling of the low abundance N-glycosylated protein tissue inhibitor of metalloproteinases-1. Mol Cell Proteomics 2007;6:638-47.

20. Wurtz SO, Christensen IJ, Schrohl AS, Mouridsen H, Lademann U, Jensen V, Brunner N. Measurement of the uncomplexed fraction of tissue inhibitor of metalloproteinases-1 in the prognostic evaluation of primary breast cancer patients. Mol Cell Proteomics 2005;4:483-91.

21. Brunner N, Thompson EW, Spang-Thomsen M, Rygaard J, Dano K, Zwiebel JA. lacZ transduced human breast cancer xenografts as an in vivo model for the study of invasion and metastasis. Eur J Cancer 1992; 28A:1989-95.

22. Holten-Andersen MN, Murphy G, Nielsen HJ, Pedersen AN, Christensen IJ, Hoyer-Hansen G, Brunner N, Stephens RW. Quantitation of TIMP-1 in plasma of healthy blood donors and patients with advanced cancer. Br J Cancer 1999;80:495-503.

23. Offenberg H, Thomsen PD. Functional challenge affects aquaporin mRNA abundance in mouse blastocysts. Mol Reprod Dev 2005;71:422-30.

24. Moller Sorensen N, Dowell BL, Stewart KD, Jensen V, Larsen L, Lademann U, Murphy G, Nielsen HJ, Brunner N, Davis GJ. Establishment and characterization of 7 new monoclonal antibodies to tissue inhibitor of metalloproteinases-1. Tumour Biol 2005;26:71-80.

25. Holten-Andersen MN, Stephens RW, Nielsen HJ, Murphy G, Christensen IJ, Stetler-Stevenson W, Brunner N. High preoperative plasma tissue inhibitor of metalloproteinase-1 levels are associated with short survival of patients with colorectal cancer. Clin Cancer Res 2000;6:4292-9.

26. Kozak M. At least six nucleotides preceding the AUG initiator codon enhance translation in mammalian cells. J Mol Biol 1987;196:947-50.

27. Gomez DE, Alonso DF, Yoshiji H, Thorgeirsson UP. Tissue inhibitors of metalloproteinases: structure, regulation and biological functions. Eur J Cell Biol 1997;74:111-22.

28. Bodden MK, Harber GJ, Birkedal-Hansen B, Windsor LJ, Caterina NC, Engler JA, Birkedal-Hansen H. Functional domains of human TIMP-1 (tissue inhibitor of metalloproteinases). J Biol Chem 1994;269:18943-52.

29. Holten-Andersen MN, Hansen U, Brunner N, Nielsen HJ, Illemann M, Nielsen BS. Localization of tissue inhibitor of metalloproteinases 1 (TIMP-1) in human colorectal adenoma and adenocarcinoma. Int J Cancer 2005;113:198-206.

30. Venables JP. Unbalanced alternative splicing and its significance in cancer. Bioessays 2006;28:378-86.

31. Inoue H, Mimori K, Shiraishi T, Kataoka A, Sadanaga N, Ueo H, Barnard GF, Mori M. Expression of tissue inhibitor of matrix metalloproteinase-1 in human breast carcinoma. Oncol Rep 2000;7:871-4.

32. Nakopoulou L, Giannopoulou I, Stefanaki K, Panayotopoulou E, Tsirmpa I, Alexandrou P, Mavrommatis J, Katsarou S, Davaris P. Enhanced mRNA expression of tissue inhibitor of metalloproteinase-1 (TIMP-1) in breast carcinomas is correlated with adverse prognosis. J Pathol 2002;197:307-13.

33. Ree AH, Florenes VA, Berg JP, Maelandsmo GM, Nesland JM, Fodstad O. High levels of messenger RNAs for tissue inhibitors of metalloproteinases (TIMP-1 and TIMP-2) in primary breast carcinomas are associated with development of distant metastases. Clin Cancer Res 1997;3:1623-8.

34. Span PN, Lindberg RL, Manders P, Tjan-Heijnen VC, Heuvel JJ, Beex LV, Sweep CG. Tissue inhibitors of metalloproteinase expression in human breast cancer: TIMP-3 is associated with adjuvant endocrine therapy success. J Pathol 2004;202:395-402.

35. Schrohl AS, Christensen IJ, Pedersen AN, Jensen V, Mouridsen H, Murphy G, Foekens JA, Brunner N, Holten-Andersen MN. Tumor tissue concentrations of the proteinase inhibitors tissue inhibitor of metalloproteinases-1 (TIMP-1) and plasminogen activator inhibitor type 1 (PAI-1) are complementary in determining prognosis in primary breast cancer. Mol Cell Proteomics 2003;2:164-72.

36. Schrohl AS, Holten-Andersen MN, Peters HA, Look MP, Meijer-van Gelder ME, Klijn JG, Brunner N, Foekens JA. Tumor tissue levels of tissue inhibitor of metalloproteinase-1 as a prognostic marker in primary breast cancer. Clin Cancer Res 2004;10:2289-98.

Concentrations of TIMP1 mRNA splice variants and TIMP-1 protein are differentially associated with prognosis in primary breast cancer

Anieta M. Sieuwerts[1], Pernille A. Usher[2], Marion E. Meijer-van Gelder[1], Mieke Timmermans[1], John W.M. Martens[1], Nils Brünner[2], Jan G.M. Klijn[1], Hanne Offenberg[2] and John A. Foekens[1]

[1]Department of Medical Oncology, Erasmus MC, Rotterdam, The Netherlands
[2]Department of Veterinary Pathobiology, Faculty of Life Sciences, University of Copenhagen, Frederiksberg C, Denmark

ABSTRACT

Background: TIMP-1 protein is a prognostic factor for recurrence-free and overall survival (OS) time in breast cancer. We evaluated the prognostic value of *TIMP1* mRNA and a novel *TIMP1* mRNA splice variant in 1,301 primary breast cancer patients.

Methods: We measured mRNA transcripts of full-length *TIMP1* (*TIMP1-v1*) and the novel splice variant lacking exon 2 (*TIMP1-v2*) by use of real-time RT-PCR in frozen primary tumor samples. Transcript concentrations are correlated with histomorphological and biological factors, TIMP-1 protein, and distant metastasis-free survival (MFS) and OS time.

Results: *TIMP1-v1* and *TIMP1-v2* alone were not informative with respect to predicting prognosis. However, the PCR assay designed to measure the combination of *v1+v2* showed that high concentrations of this combination were associated with good prognosis. In Cox multivariate regression analysis, which also included the traditional prognostic factors, increasing concentrations were independently associated with prolonged MFS (P=0.004) and OS (P=0.048). Including TIMP-1 protein and *TIMP1-v1+v2* mRNA together in the multivariate model revealed that protein and mRNA were both independently associated with prognosis, with hazard ratios pointing in opposite directions.

Conclusion: High concentrations of *TIMP1-v1+v2* mRNA are associated with good prognosis in patients with primary breast cancer. Since high concentrations of TIMP-1 protein are associated with poor prognosis, the presence of possible posttranscriptional mechanisms requires further investigation.

INTRODUCTION

Tissue inhibitor of metalloproteinases-1 (TIMP-1) is one of the naturally occurring inhibitors of matrix metalloproteinases (MMPs). A number of studies have demonstrated an association between high tumor-tissue concentrations of *TIMP1* mRNA and TIMP-1 protein and a poor prognosis for breast cancer patients [1–7]. However, TIMP-1 overexpression in malignant cells has also been associated with decreased proliferation [8] and with favorable clinical outcome, particularly in lymph node–negative (LNN) patients [8, 9], or was not associated with breast cancer prognosis at all [10]. One of the reasons for these contradictory reports might be the multifunctional roles ascribed to this protein. TIMP-1 not only inhibits MMPs [11, 12] but also affects cellular proliferation [13, 14], apoptosis [15–17], and angiogenesis [18], both dependent on and independent of its MMP-inhibiting function. Furthermore, TIMP-1 may exist in multiple molecular forms in the cancer environment and in circulation, *e.g.*, in complex with other proteins or as differentially glycosylated variants. Cox regression analysis of recurrence-free survival in breast cancer patients suggested that a score based on both uncomplexed and total TIMP-1, reflecting the tumor level of TIMP-1/MMP complexes, would be a more precise estimate of prognosis than total TIMP-1 alone [19].

In analogy with free and complexed TIMP-1 protein, the prognostic value of TIMP-1 may be improved by detection of specific splice variants of *TIMP1* mRNA. Furthermore, biological understanding of TIMP-1 protein and its gene might help in understanding the controversial findings about TIMP-1 with respect to tumor development and prognosis. To address this, we analyzed mRNA concentrations of the common full-length variant of *TIMP1* (*v1*) and a newly discovered splice variant (*v2*) lacking exon 2 (see also chapter 7 of this thesis) in a large cohort of 1,301 primary breast tumors. We related *TIMP1-v1* and *v2* expression with histomorphological and clinical factors, mRNA expression of the proliferation marker *Ki-67*, and total TIMP-1 protein concentrations. Finally, we investigated whether mRNA expression of the *TIMP1* splice variants adds to the prognostic value of total TIMP-1 protein.

PATIENTS AND METHODS

Patients

A protocol for studying biological markers associated with disease outcome was approved by the medical ethics committee of the Erasmus Medical Center Rotterdam, The Netherlands (MEC 02.953). The present study, in which coded tumor tissues were used, was performed in accordance with the Code of Conduct of the Federation of Medical Scientific Societies in the Netherlands (http://www.fmwv.nl/). Tumor samples were originally submitted to our reference laboratory from 25 regional hospitals for measurements of steroid hormone receptors. Guidelines for primary treatment were similar for all hospitals. To avoid bias, tumors were selected from our tumor bank at the Erasmus Medical Center (Rotterdam, The Netherlands) by processing all available frozen tumor samples from female patients with breast cancer who entered the clinic during 1979–2001 from whom detailed clinical follow-up was available. Further inclusion criteria were as follows: >100 mg frozen tissue available, invasive breast cancer, no previous other cancer (except basal cell skin cancer or early-stage cervical cancer stage Ia/Ib), no second primary breast tumor at first relapse, no adjuvant systemic treatment for the LNN patients, and >30% epithelial tumor cell nuclei. Of the remaining samples, 8% were excluded because of poor RNA quality.

The remaining 1,301 patients were treated either with breast-conserving surgery (44%) or with modified mastectomy (56%); 931 patients (72%) received adjuvant radiotherapy. During this period, 195 of the 620 lymph node–positive (LNP) patients did not receive adjuvant systemic therapy; 425 of the LNP patients were treated with adjuvant systemic therapy, of these patients 197 received hormonal therapy, 210 chemotherapy, and 18 received combination therapy. Routine postsurgical follow-up and definition of time to metastasis were as described [20]. Median follow-up was 92 months (range 3–248 months). Six hundred sixty-nine (51%) patients developed a distant metastasis and count as events in the analysis

for metastasis-free survival (MFS). Seventy-two patients (6%) died without evidence of disease and were censored at last follow-up in the analysis of MFS. Five hundred twenty-six patients (40%) died after a previous relapse. Thus, 598 patients (46%) were counted as events in the analysis of overall survival (OS). Tumor staging was according to the Union Internationale Contre le Cancer tumor node metastasis classification. Other relevant patient and tumor characteristics are listed in Table 1 (see also Table 1 in the Data Supplement that accompanies the online version of this article at http://www.clinchem.org/content/vol53/issue7).

Tissue processing and estimation of the amount of epithelial tumor cells

We processed tissue and estimated amount of invasive tumor cells as described [21, 22]. Only specimens with at least 30% of the nuclei of epithelial tumor cell origin and distributed uniformly over at least 70% of the hematoxylin-eosin–stained tissue section area were included. Furthermore, we dichotomized our tumor cohort at the median of 70% tumor cell nuclei in stroma-rich tumors (primary tumors containing ≥30% stromal components) and stroma-poor tumors (primary tumors containing at least 70% tumor cells).

RNA isolation, cDNA synthesis, and quantification of specific mRNA species

RNA isolation, cDNA synthesis, quantification of specific mRNA species, and quality control checks were done as described in detail [21]. We performed real-time RT-PCR in an ABI Prism 7700 Sequence Detection System (Applied Biosystems) and a Mx3000P™ Real-Time PCR System (Stratagene) using both Assay-on-Demand from Applied Biosystems and the intron-spanning forward and reverse primer combinations at the conditions shown in Table 2A. RT-PCR products generated with these primers by cell lines and cancer tissue samples were gel-purified and sequenced (AGOWA, Berlin, Germany), and sequences were confirmed by BLAST search as described [23]. Primer sequences for *ESR1*, *PGR*, and the

Table 1. Associations of TIMP1 mRNA variant concentrations with histomorphological and clinical factors.

| Characteristic | No. patients | **Median mRNA concentrations** (relative to reference housekeeping gene set) | | |
		TIMP1-v1 ($x10^1$)	*TIMP1-v2* ($x10^{-4}$)	*TIMP1-v1+2* ($x10^{-1}$)
All patients	1301	1.26	2.46	2.61
Age, years				
≤40	161	1.08	2.86	1.82
41–55	495	1.18	2.85	2.19
56–70	431	1.36	2.19	2.76
>70	214	1.48	1.68	4.76
		$P < 0.001^d$	$P < 0.001^d$	$P < 0.001^d$
Menopausal status				
Premenopausal	548	1.17	2.93	2.18
Postmenopausal	753	1.35	2.18	2.94
		$P < 0.001^e$	$P < 0.001^e$	$P < 0.001^e$
ER mRNA status[a]				
Negative	317	1.03	2.42	0.98
Positive	984	1.33	2.46	3.59
		$P < 0.001^e$	$P = 0.54^e$	$P < 0.001^e$
PGR mRNA status[a]				
Negative	512	1.17	2.37	1.20
Positive	789	1.33	2.55	3.93
		$P < 0.001^e$	$P = 0.44^e$	$P < 0.001^e$
Grade				
Poor	722	1.17	2.49	2.10
Unknown	397	1.35	2.34	3.01
Moderate and good	182	1.43	2.47	4.47
		$P < 0.001^f$	$P = 0.48^f$	$P < 0.001^f$
Pathologic tumor size				
≤2 cm	408	1.35	2.74	3.02
>2 cm	893	1.21	2.37	2.40
		$P = 0.03^e$	$P = 0.33^e$	$P = 0.005^e$
Lymph nodes involved				
No (LNN)	681	1.29	2.23	2.68
Yes (LNP)	620	1.20	2.74	2.54
		$P = 0.20^e$	$P = 0.002^e$	$P = 0.25^e$
Stromal content[b]				
Stroma-rich	960	1.27	2.81	2.52
Stroma-poor	341	1.20	1.78	2.88
		$P = 0.43^e$	$P < 0.001^e$	$P = 0.12^e$
Histologic type[c]				
IDC	713	1.21	2.48	2.36
DCIS + IDC	163	1.30	2.69	2.76
ILC	100	1.50	3.30	3.15
		$P = 0.03^f$	$P = 0.01^f$	$P = 0.006^f$

See Supplemental Data Table 1 in the online Data Supplement (http://www.clinchem.org/content/vol53/issue7) for the 25% to 75% interquartile mRNA range. IDC, infiltrating ductal carcinoma; DCIS, ductal carcinoma in situ; ILC, infiltrating lobular carcinoma.

[a]*Cutpoint used for ER mRNA positive ≥ 0.2, for PGR mRNA positive ≥ 0.1.*

[b]*Dichotomized at the median level of 70% tumor cells with tumors with over 70% epithelial tumor cells grouped in the stroma-poor subgroup.*

[c]*Because only the major histological types are shown, numbers do not add up to 1301.*

[d]*Spearman rank correlation test.*

[e]*Mann-Whitney U test.*

[f]*Kruskal-Wallis test, including a Wilcoxon-type test for trend when appropriate.*

housekeeping genes have all been described, as have the PCR reactions and validations performed to ensure PCR specificity [21]. To measure concentrations of the proliferation marker *Ki-67*, we used the Hs00606991_m1 Assay-on-Demand from Applied Biosystems. Concentrations of the target genes, expressed relative to our housekeeping set [low-abundance housekeeping gene hydroxymethylbilane synthase (*HMBS*, formerly porphobilinogen deaminase, *PBGD*), medium-abundance hypoxanthine-guanine phosphoribosyltransferase (*HPRT*), and high-abundance β–2-microglobulin (*B2M*)], were quantified as follows, as described [21]:

mRNA target $= 2^{(\text{mean Ct housekeeping - mean Ct target})}$.

ESR1 and PGR mRNA receptor status

We established mRNA cutpoints to define tumors as steroid hormone positive at 0.2 for estrogen receptor (*ER*) and 0.1 for progesterone receptor (*PGR*). We compared these mRNA cutoffs with the established protein cutpoints of 10 fmol/mg protein in the 1,203 samples with known protein concentrations as established by ELISA. For *ER*, sensitivity and specificity were 93% and 72%, respectively, and positive and negative predictive accuracy were 90% and 81%. For *PGR*, sensitivity and specificity were 84% and 83%, respectively, and positive and negative predictive accuracy rates were 90% and 75%.

Table 2A. Intron-skipping TIMP1 variant-specific primers and probes used for sequencing and real-time RT-PCR.

Gene	specificity	Forward primer Sequence 5'→3'	Reverse primer Sequence 5'→3'	Size (bp)
TIMP1-v1 [a]	variant 1 (common)	*exon 2* CTTCTGGCATCCTGTTGTTG	*exon 3* GGTATAAGGTGGTCTGGTTG	153
TIMP1-v1+2 [b]	variant 1+ variant 2	*exon 1* CCCTAGCGTGGACATTTATC	*exon 3* GGTATAAGGTGGTCTGGTTG	263 + 134
TIMP1-v2 [c]	variant 2 (*del-2*)	*exon 1* CCCTAGCGTGGACATTTATC *del-2 specific probe (exon 1 → 3)*	*exon 3* GGTATAAGGTGGTCTGGTTG AGAGACACCAGAGTCATCAGGGC	134

[a] Assay performed in SYBR-green PCR-master-mixture (Applied Biosystems).
[b] Assay performed in Platinum SYBR Green qPCR SuperMix-UDG (Invitrogen).
[c] Assay performed with Taqman probes in Universal PCR-master-mixture (Applied Biosystems).

Table 2B. mRNA concentrations of TIMP1 variants.

	Fold difference (in reference to housekeeping set)		
	TIMP1-v1 (x 10^1)	*TIMP1-v1+2* (x 10^{-1})	*TIMP1-v2* (x 10^{-4})
Primary breast tumors	1.50	2.64	2.86
Primary breast fibroblast strain 19T [24]	55.64	3.05	11.78
EAHY-926 endothelial cells	1.80	0.18	13.71
MDA-MB-231	0.20	0.22	88.51
MDA-MB-435	0.30	0.14	24.89
MCF7	0.35	0.25	3.88
ZR75.1	0.34	0.44	0.0007
SKBR-3	0.06	0.02	0.0000
T47-D	0.0016	0.0019	0.0000
EVSA-T	0.0002	0.0003	0.0000
CAMA-1	0.0026	0.0030	0.0000

In our initial screening, we measured TIMP1 mRNA transcript concentrations of the two variants (see Table 2A for assay specifics) in a representative selection of 180 primary breast cancer tumors and various cultured cell lines.

Table 3. Spearman rank correlations between mRNA concentrations measured by real-time RT-PCR.

Gene assay	No. samples	Spearman rank correlation	TIMP1-v1	TIMP1-v2	TIMP1-v1+2
TIMP1-v1	1301	r_s		0.07	0.51
		P		0.01	<0.001
TIMP1-v2	1301	r_s			0.04
		P			0.16
Ki-67	1293	r_s	–0.09	0.01	–0.31
		P	0.002	0.76	<0.001

ELISA

To compare *TIMP1* mRNA concentrations with TIMP-1 protein, we used protein concentrations that were previously measured in cytosol preparations of the same tumors [6].

Statistics

Computations were done with the use of the STATA statistical package, release 9 (STATA). We assessed differences in concentrations with the Mann–Whitney *U*-test or Kruskal–Wallis test. In these tests, patient and tumor characteristics were used as grouping variables. We tested the strengths of the associations between continuous variables with the Spearman rank correlation (r_s). Variables were either log-transformed or Box-Cox–transformed to reduce the skewness. We investigated the prognostic values of the clinical and biological variables, with MFS and OS as the endpoints in the univariate, multivariate, and interaction analyses, with the use of the Cox proportional hazards model. The hazard ratio (HR) and its 95% CI were derived from these results. The proportionality assumption was investigated with a test based on the Schoenfeld residuals. We used Kaplan-Meier survival plots and log-rank tests for trend to assess the differences in time of the predicted high-risk, intermediate-risk, and low-risk groups of patients. All tests were 2-sided, and $P<0.05$ was considered statistically significant.

RESULTS

Correlations between real-time TIMP1 PCR assays

In our initial screening using combinations of primers located 2 exons apart to cover the 6 exons of *TIMP1*, we measured mRNA transcripts of 2 variants of *TIMP1* in a set of cultured cell lines and primary breast tumors: full-length *TIMP1* (*v1*) and a novel variant lacking exon 2 (*v2*). The identification of these mRNA variants was confirmed by gel electrophoresis and sequence analysis and was further evaluated by real-time RT-PCR with the assays shown in Table 2A in a representative selection of 180 primary breast tumors and various cell lines (Table 2B). In these analyses, only EVSA-T and CAMA-1 cells lacked expression of *TIMP1-v2* (Table 2B). Although with our TaqMan probe–based *TIMP1-v2* assay we were unable to detect *v2* transcripts above baseline in ZR75.1 and T47-D cells within 45 amplification rounds, gel analysis showed that a faint 134 bp product representative for *TIMP1-v2* was produced by these cells when amplified in 45 cycles with our SYBR-based *TIMP1-v1+2* assay. The highest expression of *TIMP1* mRNA was measured in a primary breast tumor–derived fibroblast strain [24] (Table 2B, 19T).

All tumors readily expressed *TIMP1-v1* mRNA; for only 16 of 1,301 tumors were we unable to detect *v2* transcripts within 45 amplification rounds. Because TIMP-1 protein overexpression has been inversely associated with cell proliferation [8], we matched our *TIMP1* PCR data with those of the proliferation marker *Ki-67* measured in the same preparations. The strength

Table 4. Cox univariate and multivariate analysis for 5-year MFS as a function of TIMP1 variants in primary breast tumors from 1,301 breast cancer patients.

Factor	No. patients	Univariate analysis			Multivariate analysis		
		HR	95% CI	P	HR	95% CI	P
					Base model		
Age at start of therapy, years							
≤40	161	1			1		
41–50	495	0.84	0.65–1.08		0.81	0.62–1.05	
51–70	431	0.88	0.68–1.14		0.72	0.49–1.06	
>70	214	0.67	0.49–0.92	0.09	0.55	0.36–0.85	0.046
Menopausal status at start of therapy							
Premenopausal	548	1			1		
Postmenopausal	753	1.02	0.86–1.20	0.84	1.25	0.93–1.68	0.14
Tumor size							
pT1, ≤2 cm	408	1			1		
pT2, >2- ≤5 cm	747	1.83	1.49-2.24		1.50	1.22-1.85	
pT3, >5 cm, + pT4	146	3.07	2.34-4.02	<0.001	2.05	1.53-2.75	<0.001
Lymph nodes involved							
0	681	1			1		
1–3	276	1.47	1.18–1.82		1.41	1.12–1.76	
>3	344	2.62	2.17–3.15	<0.001	2.34	1.91–2.87	<0.001
Grade							
Poor	722	1			1		
Unknown	397	0.88	0.73–1.05		0.97	0.80–1.16	
Moderate	182	0.48	0.36–0.65	<0.001	0.61	0.45–0.83	0.003
ER status, mRNA level							
Negative, <0.2	317	1			1		
Positive, ≥0.2	984	0.64	0.53–0.77	<0.001	0.73	0.58–0.93	0.009
PGR status, mRNA level							
Negative, <0.1	512	1			1		
Positive, ≥0.1	789	0.61	0.52–0.72	<0.001	0.75	0.60–0.92	0.008
					Additions to the base model[a]		
TIMP1-v1 mRNA level							
Log-transformed continuous	1301	0.89	0.78–1.02	0.11	0.98	0.86–1.13	0.83
TIMP1-v1+2 mRNA level							
Log-transformed continuous	1301	0.80	0.75–0.86	<0.001	0.89	0.82–0.96	0.004
TIMP1-v2 mRNA level							
Box-Cox–transformed continuous	1301	0.94	0.64–1.39	0.78	0.72	0.48–1.08	0.12
TIMP1-v1+2 mRNA level[b]							
Low	433	1			1		
Intermediate	434	0.72	0.59–0.87		0.85	0.69–1.04	
High	434	0.52	0.42–0.64	<0.001	0.71	0.56–0.90	0.017

[a] TIMP1 variants were separately introduced to the base multivariate model that included the following factors: age, menopausal status, nodal status, pathologic tumor size, grade, and ER and PGR status.
[b] Categorized by 3 equal parts in high, intermediate, and low concentrations.

of the associations between *TIMP1-v1*, *TIMP1-v2*, *TIMP1-v1+2*, and *Ki-67* mRNA are summarized in Table 3. Whereas *TIMP1-v1+2* showed a statistically significant association with *TIMP1-v1*, no correlation was observed with *TIMP1-v2* (Spearman r_s=0.51 and 0.04, respec-

tively). *TIMP1-v1+2*, compared with *TIMP1-v1* and *TIMP1-v2* separately, showed the strongest (inverse) correlation with *Ki-67* (r_s=-0.31, -0.09, and 0.01, respectively).
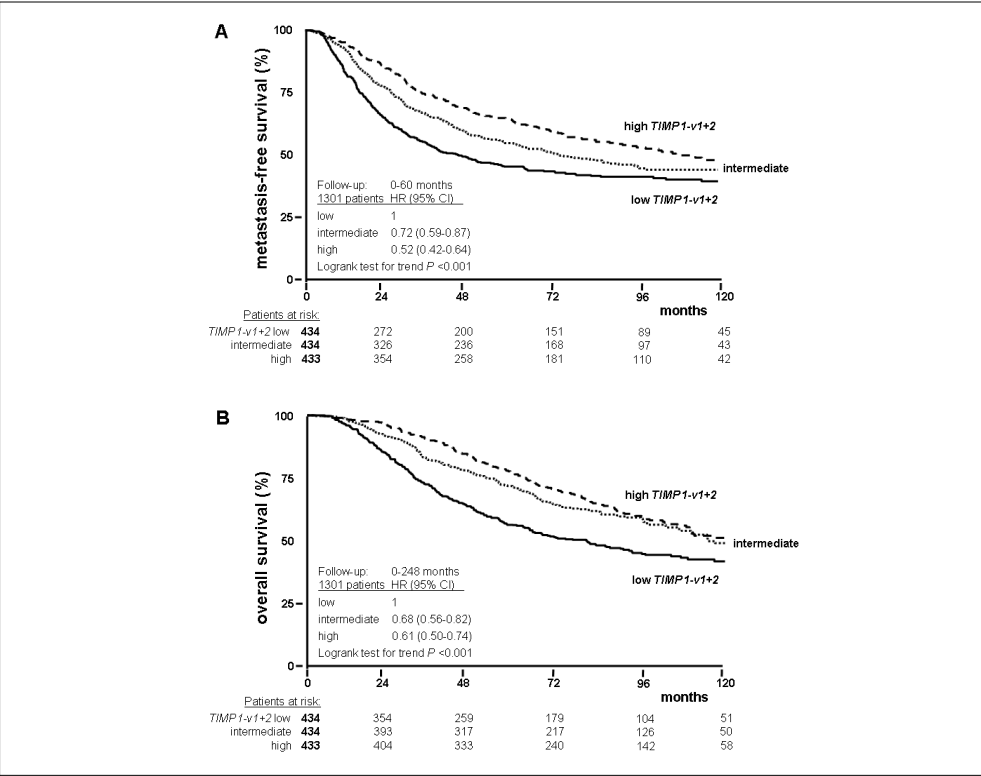
Figure 1. Relationship between TIMP1-v1+2, divided in 3 equal parts in high, intermediate, and low concentrations, and MFS (A) and OS (B) in 1,301 primary breast cancer patients.
Patients at risk are indicated.

Associations with histomorphological and clinical factors

Associations of mRNA expression of *TIMP1-v1*, *TIMP1-v2*, and *TIMP1-v1+2* with patient and tumor characteristics are shown in Table 1. Most notable are the opposing results of the *TIMP1-v2* assay with the *TIMP1-v1* and *TIMP1-v1+2* assays. Whereas concentrations assessed with the *TIMP1-v2* assay were negatively associated with age, and were lower in postmenopausal patients, results were the opposite for the other 2 *TIMP1* assays. Furthermore, only for the *TIMP1-v2* assay were concentrations significantly lower in the group of LNN patients compared with the group of LNP patients, and higher in the stroma-rich tumors compared with the group of stroma-poor

tumors. On the other hand, concentrations measured with the *TIMP1-v1* and *TIMP1-v1+2* assays were significantly higher in ER-positive tumors compared with ER-negative tumors. No such difference was observed for concentrations measured with the *TIMP1-v2* assay. Also with respect to grade and tumor size, only the *TIMP1-v1* and *TIMP1-v1+2* assays showed a relation *i.e.* higher concentrations in the prognostically more favorable tumors. Finally, for all *TIMP1* variants, concentrations were higher in infiltrating lobular carcinoma compared with infiltrating ductal carcinoma.

Table 5. Cox univariate analysis for distant metastasis-free and overall survival before and after categorizing tumors according to histomorphological and clinical criteria.

TIMP1 assay	Histomorphological and clinical subgroup		MFS[a]			OS		
Log-transformed continuous variable	Factor	No. patients	HR	95% CI	P	HR	95% CI	P
	Nodal status							
TIMP1-v2	LNP	620	0.51	0.31–0.85	0.010	0.64	0.39–1.04	0.08
TIMP1-v1+2	LNN	681	0.81	0.73–0.90	<0.001	0.89	0.80–0.99	0.027
TIMP1-v1+2	LNP	620	0.80	0.73–0.87	<0.001	0.82	0.75–0.89	<0.001
	ER status[b]							
TIMP1-v2	Negative	317	0.44	0.20–0.99	0.047	0.43	0.20–0.93	0.033
TIMP1-v1+2	Positive	984	0.78	0.72–0.86	<0.001	0.85	0.78–0.92	<0.001

[a] Restricted to the first 5 years of follow-up.
[b] ER cutpoint of mRNA ≥ 0.2.

Univariate and multivariate analysis for MFS and OS

To assess a possible relationship of *TIMP1* mRNA with prognosis, we first performed Cox univariate analyses for MFS and OS as a function of continuous *TIMP1* mRNA concentrations. Because the proportional hazards assumption was violated for the total follow-up time, we restricted our exploration of the relationships of *TIMP1* with MFS to the first 5 years of follow-up, with 571 failures in the 1,301 patients. In these analyses, only concentrations measured with the *TIMP1-v1+2* assay were significantly associated with MFS (HR 0.80, *P*<0.001) and OS (HR 0.85, *P*<0.001). Next, the *TIMP1* variants were separately introduced to the base multivariate model that included the factors of age, menopausal status, nodal status, tumor size, grade, *ER*, and *PGR* (Table 4). Of the three *TIMP1* assays, only the assay measuring both variant 1 and variant 2 (*TIMP1-v1+2*) contributed significantly to the multivariate model for MFS (HR 0.89, *P*=0.004) (Table 4) and OS (HR 0.92, *P*=0.048) (data not shown in a table). Adding *Ki-67* and adjuvant systemic therapy or radiotherapy to the multivariate model that included *TIMP1-v1+2* did not alter the coefficients of *TIMP1-v1+2*. To visualize the prognostic value of *TIMP1-v1+2* in Kaplan-Meier curves, we divided mRNA concentration curves into 3 equal parts (low, intermediate, and high). These curves are shown in Figure 1A for MFS and Figure 1B for OS.

Nodal and ER status

We next performed exploratory Cox univariate analyses for MFS and OS as a function of mRNA expression in the clinically relevant subgroups of LNN, LNP, ER-positive and ER-negative patients. Only those analyses that gave significant results after concentrations were entered as transformed continuous variables are shown in Table 5. *TIMP1-v1* mRNA concentrations alone were not significantly associated with nodal status and steroid hormone receptor status. But the following two divergent observations between the various assays are notable. First, whereas concentrations measured with the *TIMP1-v2* assay were associated with good prognosis only in the subgroup of LNP patients, the association of increasing concentrations measured with the *TIMP1-v1+2* assay and good prognosis were independent of nodal status. Second, whereas increasing concentrations of *TIMP1-v1+2* were associated with good prognosis exclusively in the group of ER-positive tumors, concentrations measured with the *TIMP1-v2* assay were associated with good prognosis only in the group of ER-negative tumors.

Correlations between TIMP1 mRNA and protein

To compare *TIMP1* mRNA with total TIMP-1 protein, we made use of protein concentrations that were previously measured with ELISA in

cytosol preparations of the same tumors [6]. In the 839 tumors with both measures, the highest correlation between total protein and mRNA was observed for the real-time RT-PCR assay able to measure *TIMP1-v1* (r_s=0.34, P<0.001). The strength of the association was lower for the PCR assay able to measure both variant 1 and 2 (*TIMP1-v1+2*) (r_s=0.28, P<0.001) and inverse for the *TIMP1-v2* assay (r_s=0.11, P=0.01).

To ensure that our cohort of 1,301 patients did not differ from the cohort of 2,984 patients with protein data, we repeated all analyses for the overlapping cohort of 839 patients. We divided the protein concentrations in 3 equal parts to classify the tumors at the protein level as TIMP-1 low, intermediate, or high. High and intermediate *vs* low concentrations of TIMP-1 protein were significantly associated with shorter MFS in univariate analysis (HR intermediate *vs* low 1.56, HR high *vs* low 1.37, P=0.002) and multivariate analysis (HR intermediate *vs* low 1.42, HR high *vs* low 1.42, P=0.010), which is in agreement with the original study, in which high tumor tissue concentrations of TIMP-1 protein were identified as an independent marker of poor prognosis in 2,984 primary breast cancers [6].

Next, we similarly compared the prognostic value of mRNA concentrations measured with our *TIMP1-v1*, *v1+2*, and *v2* PCR assays in these 839 patients. Only increasing concentrations of *TIMP1-v1+2* mRNA were significantly associated with a prolonged MFS in univariate analysis (HR intermediate *vs* low 0.81, HR high *vs* low 0.59, P<0.001) and multivariate analysis (HR intermediate *vs* low 0.89, HR high *vs* low 0.66, P=0.020).

Finally, we explored a potential interaction between TIMP-1 protein and *TIMP1* mRNA with respect to MFS. No such interaction was observed (P=0.56). Including log-transformed continuous concentrations of both TIMP-1 protein and *TIMP1-v1+2* mRNA to the base multivariate model for MFS revealed that TIMP-1 protein and *TIMP1-v1+2* mRNA were both independently associated with prognosis, with HRs pointing in opposite directions (HR 1.36, 95% CI 1.16 −1.61, P=0.001, n=839 for protein and HR 0.78, 95% CI 0.69–0.87, P=0.001, n=839 for mRNA).

DISCUSSION

Many research groups have investigated the link between prognosis in breast cancer and TIMP-1 protein or mRNA measured in primary tumors and TIMP-1 protein in serum/plasma, with conflicting results [1–10]. In agreement with earlier studies on *TIMP1* mRNA [9, 10], but in contrast to other studies [1, 3, 4], we were unable to confirm that high concentrations of *TIMP1* mRNA were associated with poor prognosis similar to results for TIMP-1 protein. However, mRNA transcript concentrations cannot always be compared with protein concentrations. This was confirmed in this study, in which we found a rather poor correlation between full-length *TIMP1* mRNA and TIMP-1 protein. In our view, the apparently contrasting findings between the prognostic value of *TIMP1* mRNA expression and TIMP-1 protein suggests that key regulators of TIMP-1 protein involved in an adverse outcome act posttranscriptionally. Such regulatory mechanisms affecting protein concentrations, activity, and stability can act at the level of mRNA translation, protein folding, glycosylation, and (proteosomal) protein degradation. This possibility needs further investigation.

Our main purpose was to investigate the potential prognostic value of *TIMP1* mRNA and a newly discovered splice variant to gain more knowledge on the biology of TIMP-1 in breast cancer. To address this, our retrospective study that included RNA preparations from tumor tissue obtained from 1,301 patients suffering from primary breast cancer is, to the best of our knowledge, the largest study performed on the mRNA concentrations of *TIMP1* to date. Because of different assay conditions, absolute values of real-time RT-PCR assays can be compared only within an assay, and values from different assays, such as our 2 assays measuring individual transcripts of *TIMP-v1* and *TIMP-v2*, cannot simply be added. With our multiplex *TIMP1-v1+2* assay that measures both transcripts in the same reaction with the same

primer pairs, we corrected as much as possible for such differences in assay conditions. However, by measuring both transcripts in the same reaction, we cannot exclude that the shorter (*v2*) variant was favored relative to the larger (*v1*) variant.

All tumors expressed full-length *TIMP1-v1* mRNA; we were unable to detect *v2* transcripts for only 16 of 1301 tumors. Sequence analysis of *TIMP1-v2* has already revealed that this variant lacking exon 2, if translated, is probably a soluble, intracellular protein lacking part of the region that directs the main inhibitory MMP activity (see also chapter 7 of this thesis). It is therefore unlikely that a putative protein of *TIMP1-v2* forms complexes with MMPs, and thus it probably exhibits a biological function different from full-length TIMP-1—indeed, our data suggest that. We found that *TIMP1-v1* mRNA concentrations increase with age, are higher in *ER/PGR*-positive tumors, and are higher in smaller-sized and moderately to well differentiated tumors. In contrast to some reports [3, 4, 9], but in agreement with another report [10], *TIMP1-v1* mRNA concentrations were not different in our cohort of 620 LNP patients compared with the group of 681 LNN patients. These discrepancies might be due to the relatively small sample sizes in the earlier studies (n=30 LNN and 24 LNP [3]; n=49 LNN and 66 LNP [4]).

Separate evaluation of *TIMP1-v2* in our patient cohort revealed a strong inverse correlation with age and no correlation with *ER*, *PGR*, grade, and tumor size. In addition, only for *TIMP1-v2*, concentrations were higher in stroma-rich compared with stroma-poor primary breast tumors. The lack of a correlation between *ER* and *TIMP1-v2* concentrations suggests that *TIMP1-v2*, unlike *TIMP1-v1*, is regulated by an ER-independent mechanism. Moreover, the lower *TIMP1-v2* and higher *TIMP1-v1* mRNA concentrations in the older age group support our hypothesis that *v2* is regulated by a different mechanism. Another observation we made is the relatively strong negative correlation between the proliferation marker *Ki-67* and *TIMP1-v1+2*. No such correlation was observed for the *TIMP1* assays able to measure the variants separately. This finding suggests that only the combined action of full-length TIMP-1 and its del-2 variant are effectively able to downregulate proliferation or to monitor reduced proliferation.

We recently raised the hypothesis that high concentrations of total TIMP-1 protein are not necessarily associated with poor prognosis but that the association depends on the ratio of uncomplexed/total TIMP-1 [19]. In analogy with this, our present study shows that *TIMP1-v1* mRNA and *TIMP1-v2* mRNA alone were not associated with prognosis. However, our real-time RT-PCR assay developed to measure both transcripts at the same time revealed that high mRNA concentrations of the combination of both variants were associated with low tumor aggressiveness. Whether changing the balance between full-length TIMP-1 and its variant lacking exon 2 has potential as a possible therapeutic approach to reduce tumor aggressiveness remains to be investigated. To establish this, and since it is only the actual protein that is biologically active, variant-specific immunohistochemistry and a quantitative assay (ELISA) able to measure the putative del-2 protein in relation to full-length TIMP-1 protein are required.

In conclusion, this retrospective study on a large cohort of primary breast cancers provides evidence that the combined expression of full-length *TIMP1-v1* mRNA and its *v2* variant lacking exon 2 are associated with low tumor aggressiveness. This splice variant-dependent association might help our understanding of the role of TIMP-1 with respect to breast cancer.

ACKNOWLEDGEMENTS

REFERENCES

1. Ree AH, Florenes VA, Berg JP, Maelandsmo GM, Nesland JM, Fodstad O. High levels of messenger RNAs for tissue inhibitors of metalloproteinases (TIMP-1 and TIMP-2) in primary breast carcinomas are associated with development of distant metastases. Clin Cancer Res 1997;3:1623-8.

2. McCarthy K, Maguire T, McGreal G, McDermott E, O'Higgins N, Duffy MJ. High levels of tissue inhibitor of metalloproteinase-1 predict poor outcome in patients with breast cancer. Int J Cancer 1999;84:44-8.

3. Castello R, Estelles A, Vazquez C, Falco C, Espana F, Almenar SM, Fuster C, Aznar J. Quantitative real-time reverse transcription-PCR assay for urokinase plasminogen activator, plasminogen activator inhibitor type 1, and tissue metalloproteinase inhibitor type 1 gene expressions in primary breast cancer. Clin Chem 2002; 48:1288-95.

4. Nakopoulou L, Giannopoulou I, Stefanaki K, Panayotopoulou E, Tsirmpa I, Alexandrou P, Mavrommatis J, Katsarou S, Davaris P. Enhanced mRNA expression of tissue inhibitor of metalloproteinase-1 (TIMP-1) in breast carcinomas is correlated with adverse prognosis. J Pathol 2002;197: 307-13.

5. Schrohl AS, Christensen IJ, Pedersen AN, Jensen V, Mouridsen H, Murphy G, Foekens JA, Brunner N, Holten-Andersen MN. Tumor tissue concentrations of the proteinase inhibitors tissue inhibitor of metalloproteinases-1 (TIMP-1) and plasminogen activator inhibitor type 1 (PAI-1) are complementary in determining prognosis in primary breast cancer. Mol Cell Proteomics 2003;2:164-72.

6. Schrohl AS, Holten-Andersen MN, Peters HA, Look MP, Meijer-van Gelder ME, Klijn JG, Brunner N, Foekens JA. Tumor tissue levels of tissue inhibitor of metalloproteinase-1 as a prognostic marker in primary breast cancer. Clin Cancer Res 2004;10:2289-98.

7. Kuvaja P, Talvensaari-Mattila A, Paakko P, Turpeenniemi-Hujanen T. The absence of immunoreactivity for tissue inhibitor of metalloproteinase-1 (TIMP-1), but not for TIMP-2, protein is associated with a favorable prognosis in aggressive breast carcinoma. Oncology 2005;68:196-203.

8. Nakopoulou L, Giannopoulou I, Lazaris A, Alexandrou P, Tsirmpa I, Markaki S, Panayotopoulou E, Keramopoulos A. The favorable prognostic impact of tissue inhibitor of matrix metalloproteinases-1 protein overexpression in breast cancer cells. Apmis 2003;111: 1027-36.

9. Inoue H, Mimori K, Shiraishi T, Kataoka A, Sadanaga N, Ueo H, Barnard GF, Mori M. Expression of tissue inhibitor of matrix metalloproteinase-1 in human breast carcinoma. Oncol Rep 2000;7:871-4.

10. Span PN, Lindberg RL, Manders P, Tjan-Heijnen VC, Heuvel JJ, Beex LV, Sweep CG. Tissue inhibitors of metalloproteinase expression in human breast cancer: TIMP-3 is associated with adjuvant endocrine therapy success. J Pathol 2004;202:395-402.

11. Jiang Y, Goldberg ID, Shi YE. Complex roles of tissue inhibitors of metalloproteinases in cancer. Oncogene 2002;21:2245-52.

12. Wurtz SO, Schrohl AS, Sorensen NM, Lademann U, Christensen IJ, Mouridsen H, Brunner N. Tissue inhibitor of metalloproteinases-1 in breast cancer. Endocr Relat Cancer 2005;12:215-27.

13. Luparello C, Avanzato G, Carella C, Pucci-Minafra I. Tissue inhibitor of metalloprotease (TIMP)-1 and proliferative behaviour of clonal breast cancer cells. Breast Cancer Res Treat 1999;54:235-44.

14. Porter JF, Shen S, Denhardt DT. Tissue inhibitor of metalloproteinase-1 stimulates proliferation of human cancer cells by inhibiting a metalloproteinase. Br J Cancer 2004;90:463-70.

15. Li G, Fridman R, Kim HR. Tissue inhibitor of metalloproteinase-1 inhibits apoptosis of human breast epithelial cells. Cancer Res 1999;59:6267-75.

16. Lee SJ, Yoo HJ, Bae YS, Kim HJ, Lee ST. TIMP-1 inhibits apoptosis in breast carcinoma cells via a pathway involving pertussis toxin-sensitive G protein and c-Src. Biochem Biophys Res Commun 2003;312: 1196-201.

17. Liu XW, Taube ME, Jung KK, Dong Z, Lee YJ, Roshy S, Sloane BF, Fridman R, Kim HR. Tissue inhibitor of metalloproteinase-1 protects human breast epithelial cells from extrinsic cell death: a potential oncogenic activity of tissue inhibitor of metalloproteinase-1. Cancer Res 2005;65:898-906.

18. Tomlinson J, Barsky SH, Nelson S, Singer S, Pezeshki B, Lee MC, Eilber F, Nguyen M. Different patterns of angiogenesis in sarcomas and carcinomas. Clin Cancer Res 1999;5:3516-22.

19. Wurtz SO, Christensen IJ, Schrohl AS, Mouridsen H, Lademann U, Jensen V, Brunner N. Measurement of the uncomplexed fraction of tissue inhibitor of metalloproteinases-1 in the prognostic evaluation of primary breast cancer patients. Mol Cell Proteomics 2005;4:483-91.

20. Wang Y, Klijn JG, Zhang Y, Sieuwerts AM, Look MP, Yang F, Talantov D, Timmermans M, Meijer-van Gelder ME, Yu J, Jatkoe T, Berns EM, Atkins D, Foekens JA. Gene-expression profiles to predict distant metastasis of lymph-node-negative primary breast cancer. Lancet 2005;365:671-9.

21. Sieuwerts AM, Meijer-van Gelder ME, Timmermans M, Trapman AM, Rodriguez Garcia R, Arnold M, Goedheer AJ, Portengen H, Klijn JG, Foekens JA. How ADAM-9 and ADAM-11 differentially from estrogen receptor predict response to tamoxifen treatment in patients with recurrent breast cancer: a retrospective study. Clin Cancer Res 2005;11:7311-21.

22. Sieuwerts AM, Look MP, Meijer-van Gelder ME, Timmermans M, Trapman AM, Rodriguez Garcia R, Arnold M, Goedheer AJ, de Weerd V, Portengen H, Klijn JG, Foekens JA. Which cyclin E prevails as prognostic marker for breast cancer? Results from a retrospective study involving 635 lymph node-negative breast cancer patients. Clin Cancer Res 2006;12:3319-28.

23. Holten-Andersen MN, Hansen U, Brunner N, Nielsen HJ, Illemann M, Nielsen BS. Localization of tissue inhibitor of metalloproteinases 1 (TIMP-1) in human colorectal adenoma and adenocarcinoma. Int J Cancer 2005;113:198-206.

24. Martens JW, Sieuwerts AM, Bolt-deVries J, Bosma PT, Swiggers SJ, Klijn JG, Foekens JA. Aging of stromal-derived human breast fibroblasts might contribute to breast cancer progression. Thromb Haemost 2003;89:393-404.

Pathway analysis of gene signatures predicting metastasis of node-negative primary breast cancer

Jack X. Yu[1], Anieta M. Sieuwerts[2], Yi Zhang[1], John W.M. Martens[2], Marcel Smid[2], Jan G.M. Klijn[2], Yixin Wang[1,3] and John A. Foekens[2]

[1]Veridex LLC, a Johnson & Johnson Company, 3210 Merryfield Row, San Diego, CA 92121, USA
[2]Department of Medical Oncology, Erasmus MC, Rotterdam, The Netherlands
[3]Veridex LCC, a Johnson & Johnson Company, 33 Technology Drive, Warren, NJ 07059, USA

ABSTRACT

Background: Published prognostic gene signatures in breast cancer have few genes in common. Here we provide a rationale for this observation by studying the prognostic power and the underlying biological pathways of different gene signatures.

Methods: Gene signatures to predict the development of metastases in estrogen receptor-positive and estrogen receptor-negative tumors were identified using 500 re-sampled training sets and mapping to Gene Ontology Biological Process to identify over-represented pathways. The Global Test program confirmed that gene expression profilings in the common pathways were associated with the metastasis of the patients.

Results: The apoptotic pathway and cell division, or cell growth regulation and G-protein coupled receptor signal transduction, were most significantly associated with the metastatic capability of estrogen receptor-positive or estrogen-negative tumors, respectively. A gene signature derived of the common pathways predicted metastasis in an independent cohort. Mapping of the pathways represented by different published prognostic signatures showed that they share 53% of the identified pathways.

Conclusions: We show that divergent gene sets classifying patients for the same clinical endpoint represent similar biological processes and that pathway-derived signatures can be used to predict prognosis. Furthermore, our study reveals that the underlying biology related to aggressiveness of estrogen receptor subgroups of breast cancer is quite different.

INTRODUCTION

Microarray technology has become a popular tool to classify breast cancer patients into histological subtypes, subgroups with a different prognosis, different site of relapse, and different types of response to treatment [1-9]. A major challenge for application of gene expression profiling is stability of the gene list as a signature [10]. Considering that many genes have correlated expression on a gene expression array, especially for genes involved in the same biological process, it is quite possible that different genes may be present in different signatures when different training sets of patients and different statistical tools are used. Furthermore, genes are usually included in a classifier applying stringent statistical criteria. At these strict significance levels, there is only a small chance for any specific gene to be included. Reproducibility in gene signatures identified in different datasets is thus unlikely [11]. To our knowledge, so far prognostic gene signatures were identified based on the performance of individual genes, regardless of their biological functions. We and others have previously suggested that it might be more appropriate to interrogate the gene lists for biological themes, rather than individual genes [8, 12-19]. Moreover, identification of the distinct biological processes between subtypes of cancer patients is more relevant to understand the mechanism of the disease development and for targeted drug development.

In this study we associated biological processes with the tumor's metastatic capability. We re-sampled our data set numerous times to get multiple gene lists whose expression correlated with patients' survival. Based on these gene lists, over-represented pathways defined in Gene Ontology Biological Process (GOBP) were identified for estrogen receptor (ER)-positive or ER-negative breast cancer patients, separately. One step further, we compared the pathways represented by different published prognostic gene signatures with the over-represented pathways associated with metastatic capability. This study also demonstrated it is feasible to construct a gene signature from the key pathways to predict clinical outcomes.

MATERIALS AND METHODS

Patient population

The study was approved by the Medical Ethics Committee of the Erasmus MC Rotterdam, The Netherlands (MEC 02.953), and was performed in accordance to the Code of Conduct of the Federation of Medical Scientific Societies in the Netherlands [20]. A cohort of 344 breast tumor samples from our tumor bank at the Erasmus Medical Center (Rotterdam, Netherlands) was used in this study. All these samples were from patients with lymph node-negative breast cancer who had not received any adjuvant systemic therapy, and had more than 70% tumor content. Among them, 286 samples had been used to derive a 76-gene signature to predict distant metastasis [8]. Fifty-eight additional ER-negative cases were included to increase the numbers in this subgroup. According to our previous study [21], array-measured *ESR1* status and clinical ER status have the best correlation when the cutoff is set at 1000, after scaling the average intensity of probe sets on an Affymetrix HG-U133A chip to 600. Using array-based *ESR1* status allows us to avoid the variations of the measures of ER by either immunohisto-chemistry or biochemical assays, as well as including tumors whose ER status is undetermined. Therefore, ER status for a patient was determined based on the expression level of the *ESR1* gene on the chip in this study. A sample is considered ER-positive if its *ESR1* expression level is higher than 1000. Otherwise, the sample is ER-negative [21]. As a result, there are 221 ER-positive and 123 ER-negative patients in the 344-patient population. The mean age of the patients was 53 years (median 52, range 26-83 years), 197 (57%) were premenopausal and 147 (43%) postmenopausal. T1 tumors (≤ 2 cm) were present in 168 patients (49%), T2 tumors (>2-5 cm) in 163 patients (47%), T3/4 tumors (>5 cm) in 12 patients (3%), and 1 patient had unknown tumor stage. Pathological examination was carried out by regional pathologists as described previously [22] and the histological grade was coded as poor in 184 patients (54%), moderate in 45 patients (13%), good in 7 patients (2%), and unknown for 108 patients (31%). During follow-up 103 patients showed a relapse within 5 years and were counted as failures in the analysis for DMFS. Eighty-two patients died after a previous relapse. The median follow-up time of patients still alive was 101 months (range 61-171 months).

RNA isolation and hybridization

Total RNA was extracted from 20-40 cryostat sections of 30 μm thickness with RNAzol B (Campro Scientific, Veenendaal, Netherlands). After being biotinylated, targets were hybridized to Affymetrix HG-U133A chips as described [8]. Gene expression signals were calculated using Affymetrix GeneChip analysis software MAS 5.0. Chips with an average intensity less than 40 or a background higher than 100 were removed. Global scaling was performed to bring the average signal intensity of a chip to a target of 600 before data analysis. For the validation dataset [23], quantile normalization was performed and ANOVA was used to eliminate batch effects from different sample preparation methods, RNA extraction methods, different hybridization protocols and scanners.

Multiple gene signatures

For ER-positive and ER-negative patients, 80 samples were randomly selected as a training set and univariate Cox proportional-hazards regression was performed to identify genes whose expression patterns were most correlated to patients' DMFS time. Our previous analysis suggested that 80 patients represent a minimum size of the training set for producing a prognostic gene signature with stable performance [8]. Because the majority of the published gene expression signatures had less than 100 genes, the top 100 genes from the Cox regression were used as a signature to predict tumor recurrence for the remaining patients. A relapse score for a patient was used to calculate a patient's risk of distant metastasis and was defined as the linear combination of logarithmically transformed gene expression

levels weighted by the standardized Cox regression coefficient as described [8]. ROC analysis with distant metastasis within 5 years as a defining point was conducted. Patients who did not have 5-year follow-up were excluded from ROC analysis. The AUC of the ROC plots was used as a measure of the performance of a signature in the test set. The above procedure was repeated 500 times (Figure 1). Thus, 500 signatures of 100 genes each were obtained for both the ER-positive and ER-negative subgroups. The frequency of the selected genes in the 500 signatures was calculated and the genes were ranked based on the frequency.

As a control, the patient survival data for the ER-positive patients or ER-negative patients was permuted randomly and re-assigned to the chip data. As described above, 80 chips were then randomly selected as a training set and the top 100 genes were selected using the Cox modeling based on the permuted clinical information. The clinical information was permuted 10 times. For each permutation of the survival data, 50 training sets of 80 patients were created. For each training set, the top 100 genes were obtained as a control gene list based on the Cox modeling. Thus, a total of 500 control signatures were obtained. The predictive performance of the 100 genes was examined in the remaining patients. A ROC analysis was conducted and AUC was calculated in the test set.

Mapping signatures to GOBP and identification of over-represented pathways

To identify over-representation of biological pathways in the signatures, genes on the Affymetrix HG-U133A chip were mapped to the categories of GOBP based on the annotation table downloaded from [24]. Categories that contained at least 10 probe sets from the HG-U133A chip were retained for subsequent pathway analysis. As a result, 304 categories were used for following pathway analysis. The 100 genes of each signature were mapped to GOBP. Hypergeometric distribution probabilities for all included GOBP categories were calculated for each signature to evaluate its statistical significance. A pathway that had a hypergeometric distribution probability < 0.05 and was hit by two or more genes from the 100 genes was considered an over-represented pathway in a signature. The total number of times a pathway occurred in the 500 signatures was considered as the frequency of over-representation. To evaluate the relationship between a pathway as a whole and the clinical outcome, each of the top 20 over-represented pathways that have the highest frequencies in the 500 signatures were subjected to Global Test program [12, 14]. The Global Test examines the association of a group of genes as a whole to a specific clinical parameter such as DMFS. The contribution of individual genes in the top over-represented pathways to the association was also evaluated.

Building pathway-based signatures

To explore the possibility of using the genes from over-represented pathways as a signature to predict distant metastasis, the top two pathways for ER-positive and ER-negative tumors that were in the top 20 list based on frequency of over-representation and had the smallest *P* values with the Global Test program were chosen to build a gene signature. First, genes in the pathway were selected if their z-score was greater than 1.96 from the Global Test program. A z-score greater than 1.96 indicates that the association of the gene expression with DMFS time is significant ($P<0.05$) [12, 14]. To determine the optimal number of genes in a given pathway used for building the signature, combinations of gene markers were tested by adding one gene at a time according to their z-scores. The number of significant genes that gave the highest AUC value of the ROC analysis with distant metastasis within 5 years as the defining point was considered optimal and used to build a pathway-based signature.

The relapse score for a given patient was calculated as the difference between the linear combination of the logarithmically transformed expression signals weighted by their z-scores for negatively correlated genes and that for positively correlated genes. The predicting performance of the gene signature was evaluated by ROC and Kaplan-Meier survival analysis in an independent patient group [23] for ER-positive patients and ER-negative patients both separately and combined.

Comparing multiple gene signatures

To compare the genes from various prognostic signatures for breast cancer, five gene signatures were selected [3, 8, 23, 25, 26]. Identity of the genes between the signatures was determined by BLAST program. To examine the representation of the top 20 pathways in the signatures, genes in each of the signatures were mapped to GOBP.

Data availability

The microarray data analyzed in this paper have been submitted to the NCBI/Genbank GEO database (series entry GSE2034 for the first 286 patients, and GSE5327 for the additional 58 patients). The microarray and clinical data used for the independent validation testing set analysis were obtained from the GEO database with accession number GSE2990.
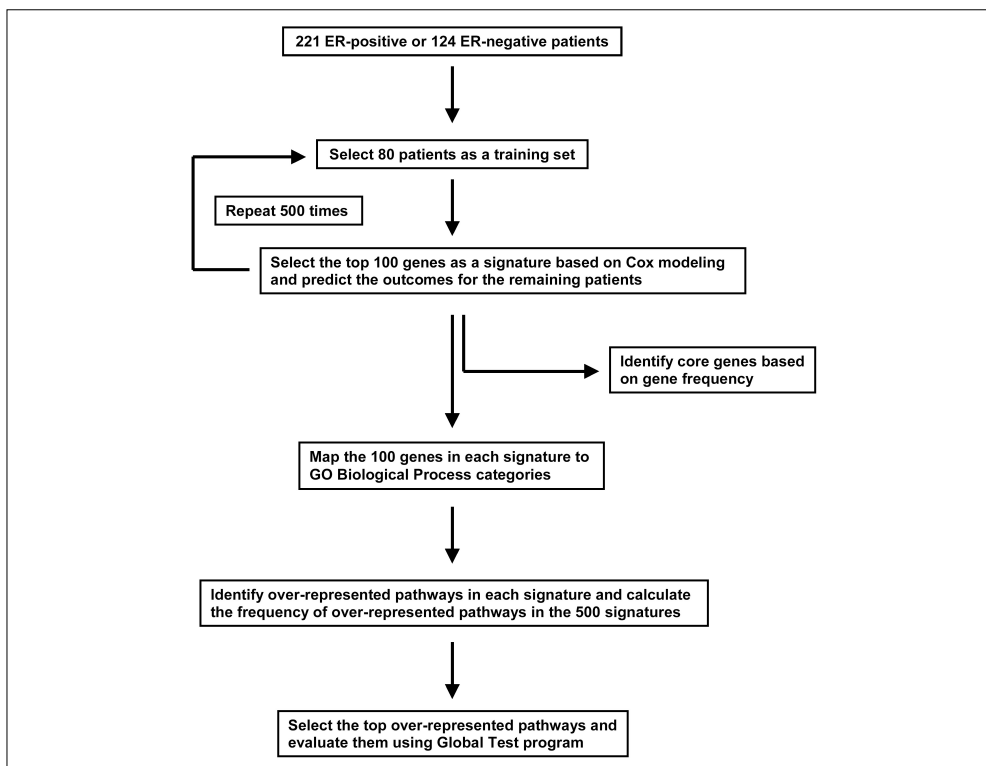

Figure 1. Work flow of data analysis for deriving core genes and over-represented pathways.
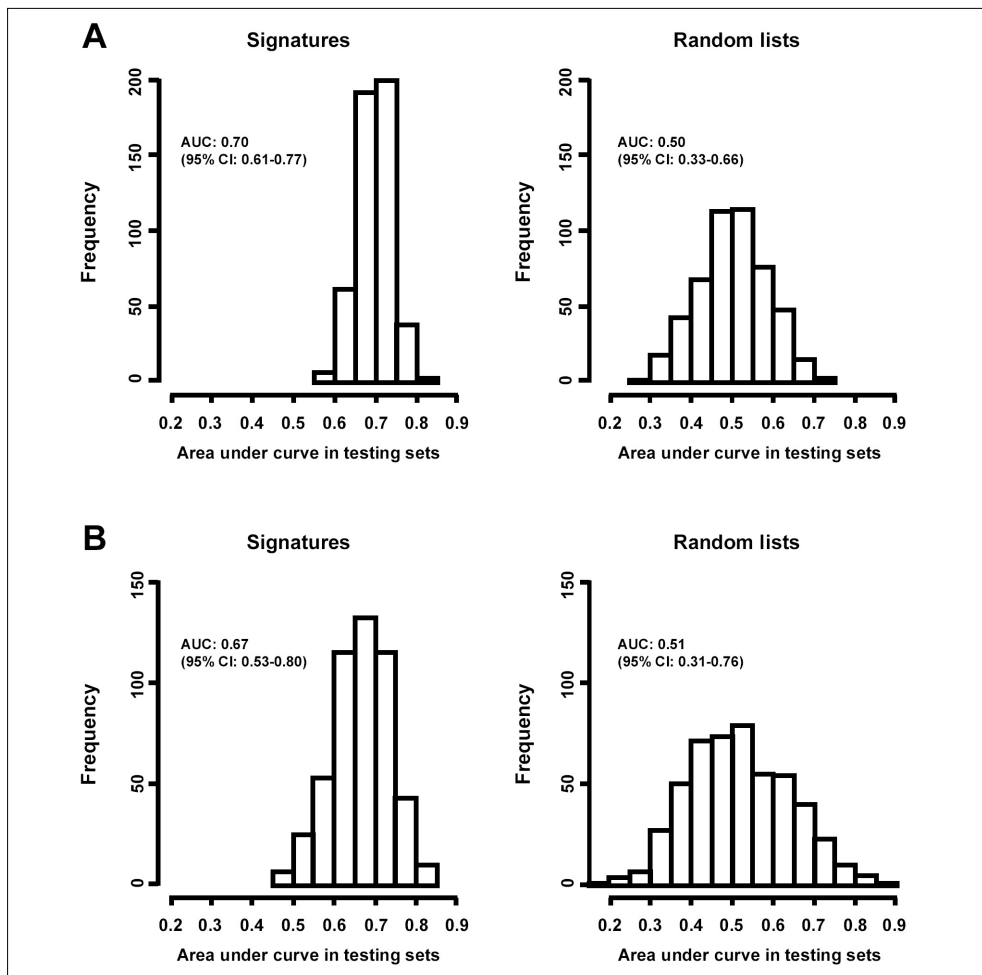
Figure 2. Evaluation of the 500 gene signatures.
Each of the 100-gene signatures for 80 randomly selected tumors in the training set was used to predict relapsed patients in the corresponding test set. Its performance was measured by the AUC of the ROC analysis. (A) Performance of the gene signatures for ER-positive patients in test sets. (B) Performance of the gene signatures for ER-negative patients in test sets. (Left) Frequency of AUC in 500 prognostic signatures panels as derived following the flow chart presented in Figure 1. (Right) Frequency of AUC in 500 random gene lists. To generate a gene list as a control, the survival data for the ER-positive patients or ER-negative patients was permutated randomly and reassigned to the chip data.

RESULTS

Multiple gene signatures

Using re-sampling, we constructed a total of 1,000 prognostic gene signatures derived from different patient groups aiming to improve understanding of the underlying biological processes of breast cancer metastasis. Since gene expression patterns of ER-subgroups of breast tumors are quite different [1-4, 8, 27] data analysis to derive gene signatures and subsequent pathway analysis were

Table 1. Genes with highest frequencies in 500 signatures.

Gene title	Gene symbol	Frequency
Top 20 core genes from ER-positive tumors		
KIAA0241 protein	*KIAA0241*	321
CD44 antigen (homing function and Indian blood group system)	*CD44*	286
ATP-binding cassette, sub-family C (CFTR/MRP), member 5	*ABCC5*	251
serine/threonine kinase 6	*STK6*	245
cytochrome c, somatic	*CYCS*	235
KIAA0406 gene product	*KIA0406*	212
uridine-cytidine kinase 1-like 1	*UCKL1*	201
zinc finger, CCHC domain containing 8	*ZCCHC8*	188
Rac GTPase activating protein 1	*RACGAP1*	186
staufen, RNA binding protein (Drosophila)	*STAU*	176
lactamase, beta 2	*LACTB2*	175
eukaryotic translation elongation factor 1 alpha 2	*EEF1A2*	172
RAE1 RNA export 1 homolog (S. pombe)	*RAE1*	153
tuftelin 1	*TUFT1*	150
zinc finger protein 36, C3H type-like 2	*ZFP36L2*	150
origin recognition complex, subunit 6 homolog-like (yeast)	*ORC6L*	143
zinc finger protein 623	*ZNF623*	140
extra spindle poles like 1	*ESPL1*	139
transcription elongation factor B (SIII), polypeptide 1	*TCEB1*	138
ribosomal protein S6 kinase, 70kDa, polypeptide 1	*RPS6KB1*	127
Top 20 core genes from ER-negative tumors		
zinc finger protein, multitype 2	*ZFPM2*	445
ribosomal protein L26-like 1	*RPL26L1*	372
hypothetical protein FLJ14346	*FLJ14346*	372
mitogen-activated protein kinase-activated protein kinase 2	*MAPKAPK2*	347
collagen, type II, alpha 1	*COL2A1*	340
muscleblind-like 2 (Drosophila)	*MBNL2*	320
G protein-coupled receptor 124	*GPR124*	314
splicing factor, arginine/serine-rich 11	*SFRS11*	300
heterogeneous nuclear ribonucleoprotein A1	*HNRPA1*	297
CDC42 binding protein kinase alpha (DMPK-like)	*CDC42BPA*	296
regulator of G-protein signalling 4	*RGS4*	276
transient receptor potential cation channel, subfamily C, member 1	*TRPC1*	265
transcription factor 8 (represses interleukin 2 expression)	*TCF8*	263
chromosome 6 open reading frame 210	*C6orf210*	262
dynamin 3	*DNM3*	260
centrosome protein Cep63	*Cep63*	251
tumor necrosis factor (ligand) superfamily, member 13	*TNFSF13*	251
dapper, antagonist of beta-catenin, homolog 1 (Xenopus laevis)	*DACT1*	248
heterogeneous nuclear ribonucleoprotein A1	*HNRPA1*	245
reversion-inducing-cysteine-rich protein with kazal motifs	*RECK*	243

The top 20 genes are ranked by their frequency in the 500 signatures of 100 genes for ER-positive and ER-negative tumors (for details see Figure 1).

conducted separately [8]. For both ER-positive and ER-negative patients, 80 samples were randomly selected as a training set and the 100 genes most significantly associated with distant metastasis-free survival (DMFS) were used as a signature to predict tumor recurrence for the remaining ER-positive and ER-negative patients, respectively (Figure 1). The area under the curve (AUC) of receiver operating characteristic (ROC) analysis with distant metastasis within 5 years as a defining point was used as a measure of the performance of a signature in a corresponding test set. The above procedure was repeated 500 times. The average of AUCs for the 500 signatures in the ER-positive test sets was 0.70 (95% confidence interval (CI): 0.61-0.77) whereas the average of AUCs for 500 random gene lists

Table 2. Top 20 pathways in the 500 signatures of ER-positive and ER-negative tumors evaluated by Global Test.

Pathways	GO_ID	P	Frequency
ER-positive tumors			
Apoptosis	6915	3.06E-7	250
Regulation of cell cycle	74	2.46E-5	203
Protein amino acid phosphorylation	6468	2.48E-5	114
Cytokinesis	910	6.13E-5	165
Cell motility	6928	0.00015	93
Cell cycle	7049	0.00028	138
Cell surface receptor-linked signal transd.	7166	0.00033	172
Mitosis	7067	0.00036	256
Intracellular protein transport	6886	0.00054	141
Mitotic chromosome segregation	70	0.00057	98
Ubiquitin-dependent protein catabolism	6511	0.00074	158
DNA repair	6281	0.00079	156
Induction of apoptosis	6917	0.00083	115
Immune response	6955	0.00094	167
Protein biosynthesis	6412	0.0010	145
DNA replication	6260	0.0015	92
Oncogenesis	7048	0.0020	228
Metabolism	8152	0.0021	83
Cellular defense response	6968	0.0025	131
Chemotaxis	6935	0.0027	89
ER-negative tumors			
Regulation of cell growth	1558	0.00012	136
Regul. of G-coupled receptor signaling	8277	0.00013	153
Skeletal development	1501	0.00024	160
Protein amino acid phosphorylation	6468	0.0051	151
Cell adhesion	7155	0.0065	110
Carbohydrate metabolism	5975	0.0066	86
Nuclear mRNA splicing, via spliceosome	398	0.0067	203
Signal transduction	7165	0.0078	160
Cation transport	6812	0.0098	160
Calciumion transport	6816	0.010	93
Protein modification	6464	0.011	132
Intracellular signaling cascade	7242	0.012	135
mRNA processing	6397	0.012	81
RNA splicing	8380	0.014	192
Endocytosis	6897	0.026	166
Regul. of transcription from PolII promoter	6357	0.031	109
Regulation of cell cycle	74	0.043	88
Protein complex assembly	6461	0.048	183
Protein biosynthesis	6412	0.063	99
Cell cycle	7049	0.084	72

Each of the top 20 over-represented pathways that have the highest frequencies in the 500 signatures of ER-positive and ER-negative tumors were subjected to Global Test program [12, 14]. The Global Test examines the association of a group of genes as a whole to a specific clinical parameter, in this case DMFS, and generates an asymptotic theory P value for the pathway. The pathways are ranked by their P value in the respective ER-subgroup of tumors.

was 0.50 (95% CI: 0.33-0.66), indicating a non-random prediction for the true test sets (Figure 2A). For ER-negative datasets, these values of average AUCs were 0.67 (95% CI: 0.53-0.80) and 0.51 (95% CI: 0.31-0.76), respectively (Figure 2B). The results demonstrate that depending on the training set different gene signatures can be identified with comparable performance. This could explain the results obtained by earlier studies, which reported different gene signatures with similar power to predict risk

groups. The 20 most frequently found genes in the 500 signatures for ER-positive and ER-negative tumors are listed in Table 1. The most frequent genes were KIAA0241 protein (*KIAA0241*) for ER-positive tumors, and zinc finger protein multitype 2 (*ZFPM2*) for ER-negative tumors. There was no overlap between genes of the ER-positive and -negative core gene lists suggesting that different molecular mechanisms are associated with the subtypes of breast cancer disease.

Over-represented pathways in gene signatures and Global Test

The 100 genes in each of the 500 signatures for ER-positive and ER-negative tumors were mapped to the categories of GOBP. For a given gene signature, a pathway (or category) that had a hypergeometric distribution probability smaller than 0.05 and included two or more genes was considered an over-represented pathway. The "inclusion of 2 or more genes" as a selection criterion in addition to the statistical significance was to avoid selecting statistically significant pathways containing only one gene in the signature. The frequency of over-representation of GOBP in the 500 signatures for ER-positive and ER-negative dataset was calculated. Like the observation of most frequently found genes, the biological pathways over-represented in the gene signatures are distinct for ER-positive and ER-negative tumors (Table 2).

For ER-positive tumors, cell division-related processes and immune-response-related pathways are frequently found in the top 20 over-represented pathways. All of the 20 pathways had a significant association with DMFS as analyzed by the Global Test program [12, 14], with the 2 most significant being "apoptosis" (mainly containing genes of the extrinsic apoptotic pathway) and "regulation of cell cycle" (Table 2). For ER-negative tumors, many of the top 20 pathways are related with RNA processing, transportation and signal transduction. Eighteen of the top 20 pathways demonstrated a significant association with DMFS in the Global Test, the 2 most significant being "regulation of cell growth" and "regulation of G-protein coupled receptor signaling" (Table 2).

The contribution and significance of individual genes in the top over-represented pathways to the association with DMFS were determined for ER-positive (see Additional Data Files 1 and 2 available on line) and ER-negative tumors (see Additional Data Files 3 and 4 available on line). Genes can either show a positive association with DMFS, indicating a higher expression in tumors without metastatic capability, or a negative association, indicative of a higher expression in metastatic tumors. In ER-positive tumors, pathways with a mixed association include the 2 most significant pathways "apoptosis" and "regulation of cell cycle" (Figure 3A). There were also a number of pathways that had a predominant positive or negative correlation with DMFS. For example, the pathway "immune response" is associated with 379 probe sets, of which the majority showed positive correlation to DMFS (Figure 3A). Similarly in the biological processes "cellular defense response" and "chemotaxis", most genes displayed a strong positive correlation with DMFS (see Additional Data File 1). On the other hand, genes in "mitosis" (Figure 3A), "mitotic chromosome segregation" and "cell cycle" showed a predominant negative correlation with DMFS (see Additional Data File 1).

In ER-negative tumors (Figure 3B), examples of pathways with genes that had both positive and negative correlation to DMFS include "regulation of cell growth", the most significant pathway, and "cell adhesion". Of the top 20 pathways in ER-negative tumors, none showed a dominant positive association with DMFS. Although for some pathways most genes correlated negatively with DMFS (see Additional Data File 3), including "regulation of G-protein coupled receptor signaling" and "skeletal development" (Figure 3B), ranked among the top 3 pathways in significance (Table 2). Of the top 20 core pathways 4 overlapped between ER-positive and -negative tumors, *i.e.*, "regulation of cell cycle", "protein amino acid phosphorylation", "protein biosynthesis", and "cell cycle" (Table 2).
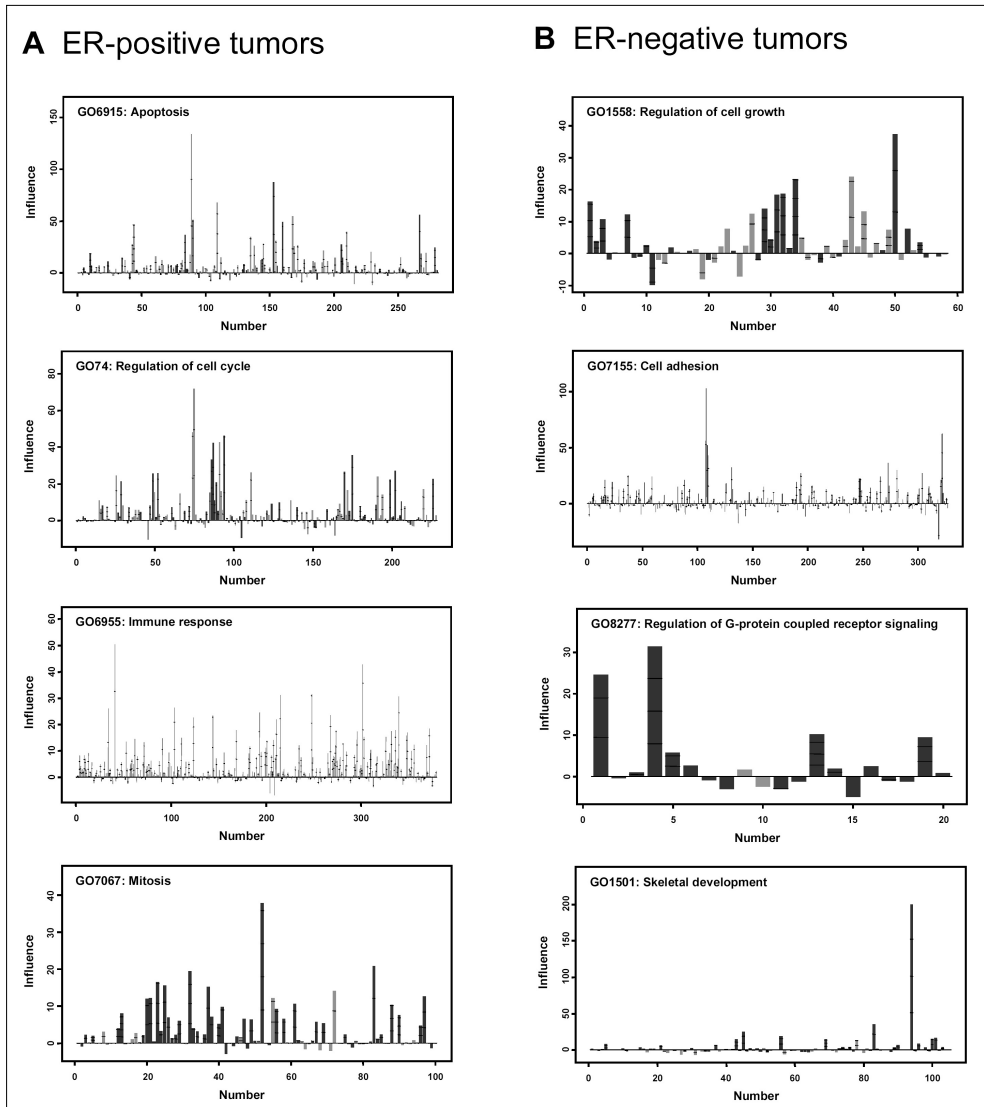
A ER-positive tumors   **B** ER-negative tumors

Figure 3. Association of the expression of individual genes with DMFS time for selected over-represented pathways.
The Geneplot function in the Global Test program [12, 14] was applied and the contribution of the individual genes in each selected pathway is plotted. The numbers at the X-axis represent the number of genes in the respective pathway in ER-positive (Left) or ER-negative tumors (Right). The values at the Y-axis, represent the contribution (influence) of each individual gene in the selected pathway with DMFS. Negative values indicate there is no association between the gene expression and DMFS. Horizontal markers in a bar indicates one standard deviation away from the reference point, two or more horizontal markers in a bar indicate that the association of the corresponding gene with DMFS is statistically significant. The grey bars reflect genes that are positively associated with DMFS, indicating a higher expression in tumors without metastatic capability. The black bars reflect genes that are negatively associated with DMFS, indicative of higher expression in tumors with metastatic capability. (A) ER-positive tumors: from top to bottom: "apoptosis" pathway consisting of 282 genes, "regulation of cell cycle" pathway consisting of 228 genes, "immune response" pathway consisting of 379 genes, and "mitosis" pathway consisting of 100 genes. (B) ER-negative tumors: from top to bottom: "regulation of cell growth" pathway consisting of 58 genes, "cell adhesion" pathway consisting of 327 genes, "regulation of G-coupled receptor signaling" pathway consisting of 20 genes, and "skeletal development" pathway consisting of 105 genes.
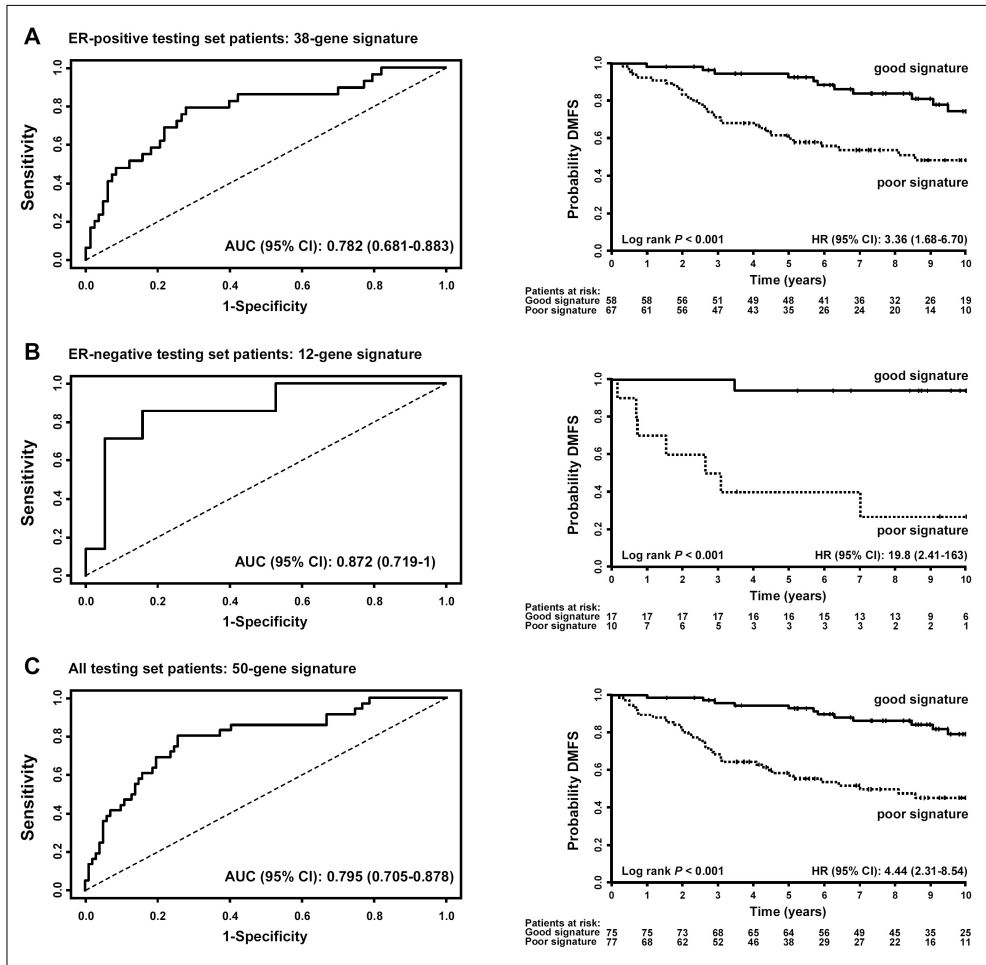
Figure 4. Validation of pathway-based breast cancer classifiers constructed from the optimal significant genes.
The 152-patient test set [23] consisted of 125 ER-positive tumors and 27 ER-negative tumors based on the expression level of ER gene on the chip. (A) ROC (Left) and Kaplan-Meier (Right) analysis of the 38-gene probe set signature (see also Table 3A and 3B) for ER-positive tumors. Thirteen patients with less than 5-year follow-up were excluded from ROC analysis. (B) ROC (Left) and Kaplan-Meier (Right) analysis of the 12-gene probe set signature (see also Table 3C and 3D) for ER-negative tumors. One patient with less than 5-year follow-up was excluded from ROC analysis. (C) ROC (Left) and Kaplan-Meier (Right) analysis of a combined 50-gene probe set signature for ER-positive and ER-negative tumors. Fourteen patients with less than 5-year follow-up were excluded from ROC analysis.

Pathway-derived gene expression profiles as a predictor

In an attempt to use gene expression profiles in the most significant biological processes to predict distant metastases we used the genes of the top 2 significant pathways in both ER-positive and -negative tumors (Table 3) to construct a gene signature for the prediction of distant recurrence. A 50-gene signature was constructed by combining the 38 genes(represented by 38 unique probe sets) from the top 2 ER-positive pathways ("apoptosis", "regulation of cell cycle") and 12 genes for the top 2 ER-negative pathways ("regulation of cell growth", "regulation of G-coupled receptor signaling").

Table 3. Genes used for prediction in top pathways.

A: Significant genes in the "apoptosis" pathways in ER-positive tumors

Probe Set	z-score	DMFS	Gene Symbol	Gene Title
208905_at	4.29	-	CYCS	cytochrome c, somatic
204817_at	3.73	-	ESPL1	extra spindle poles like 1
38158_at	3.41	-	ESPL1	extra spindle poles like 1
204947_at	3.04	-	E2F1	E2F transcription factor 1
201111_at	3.04	-	CSE1L	CSE1 chromosome segregation 1-like
201636_at	2.97	-	FXR1	fragile X mental retardation, autosomal homolog 1
220048_at	2.82	-	EDAR	ectodysplasin A receptor
210766_s_at	2.75	-	CSE1L	CSE1 chromosome segregation 1-like
221567_at	2.66	-	NOL3	nucleolar protein 3 (apoptosis repressor with CARD domain)
213829_x_at	2.65	-	TNFRSF6B	tumor necrosis factor receptor superfamily, member 6b, decoy
201112_s_at	2.57	-	CSE1L	CSE1 chromosome segregation 1-like
212353_at	2.51	-	SULF1	sulfatase 1
208822_s_at	2.47	-	DAP3	death associated protein 3
209462_at	2.37	-	APLP1	amyloid beta (A4) precursor-like protein 1
203005_at	2.29	-	LTBR	lymphotoxin beta receptor (TNFR superfamily, member 3)
202731_at	4.01	+	PDCD4	programmed cell death 4
206150_at	3.57	+	TNFRSF7	tumor necrosis factor receptor superfamily, member 7
202730_s_at	3.18	+	PDCD4	programmed cell death 4
209539_at	3.14	+	ARHGEF6	Rac/Cdc42 guanine nucleotide exchange factor (GEF) 6
212593_s_at	3.07	+	PDCD4	programmed cell death 4
204933_s_at	2.96	+	TNFRSF11B	tumor necrosis factor receptor superfamily, member 11b
209831_x_at	2.43	+	DNASE2	deoxyribonuclease II, lysosomal
203187_at	2.38	+	DOCK1	dedicator of cytokinesis 1
210164_at	2.34	+	GZMB	granzyme B

B: Significant genes in the "regulation of cell cycle" pathway in ER-positive tumors

Probe Set	z-score	DMFS	Gene Symbol	Gene Title
204817_at	3.73	-	ESPL1	extra spindle poles like 1 (S. cerevisiae)
38158_at	3.41	-	ESPL1	extra spindle poles like 1 (S. cerevisiae)
214710_s_at	3.10	-	CCNB1	cyclin B1
212426_s_at	3.08	-	YWHAQ	tyrosine 3-/tryptophan 5-monooxygenase activation protein
204009_s_at	3.08	-	KRAS	v-Ki-ras2 Kirsten rat sarcoma viral oncogene homolog
204947_at	3.04	-	E2F1	E2F transcription factor 1
201947_s_at	3.04	-	CCT2	chaperonin containing TCP1, subunit 2 (beta)
204822_at	2.91	-	TTK	TTK protein kinase
209096_at	2.57	-	UBE2V2	ubiquitin-conjugating enzyme E2 variant 2
204826_at	2.53	-	CCNF	cyclin F
212022_s_at	2.46	-	MKI67	antigen identified by monoclonal antibody Ki-67
202647_s_at	2.42	-	NRAS	neuroblastoma RAS viral (v-ras) oncogene homolog
201076_at	3.09	+	NHP2L1	NHP2 non-histone chromosome protein 2-like 1 (S. cerevisiae)
201601_x_at	3.00	+	IFITM1	interferon induced transmembrane protein 1 (9-27)
204015_s_at	2.90	+	DUSP4	dual specificity phosphatase 4
220407_s_at	2.68	+	TGFB2	transforming growth factor, beta 2
206404_at	2.38	+	FGF9	fibroblast growth factor 9 (glia-activating factor)

Table 3. continued. Genes used for prediction in top pathways.

C: Significant genes in the "regulation of cell growth" pathway in ER-negative tumors

Probe Set	z-score	DMFS	Gene Symbol	Gene Title
209648_x_at	4.01	-	SOCS5	suppressor of cytokine signaling 5
208127_s_at	3.75	-	SOCS5	suppressor of cytokine signaling 5
209550_at	3.18	-	NDN	necdin homolog (mouse)
201162_at	3.14	-	IGFBP7	insulin-like growth factor binding protein 7
213910_at	2.87	-	IGFBP7	insulin-like growth factor binding protein 7
212279_at	2.91	+	MAC30	hypothetical protein MAC30
213337_s_at	2.88	+	SOCS1	suppressor of cytokine signaling 1

D: Significant genes in the "regulation of G-protein coupled receptor signaling" pathway in ER-negative tumors

Probe Set	z-score	DMFS	Gene Symbol	Gene Title
204337_at	3.99	-	RGS4	regulator of G-protein signalling 4
209324_s_at	3.73	-	RGS16	regulator of G-protein signalling 16
220300_at	2.61	-	RGS3	regulator of G-protein signalling 3
202388_at	2.61	-	RGS2	regulator of G-protein signalling 2, 24kDa
204396_s_at	2.34	-	GRK5	G protein-coupled receptor kinase 5

Genes in the top 2 significant prognostic pathways in both ER-positive and ER-negative tumors were sorted based on their "z-score" (significance), reflecting their association with distant metastasis-free survival time (DMFS) time. To find the optimal number of genes as a signature, ROC analyses, with 5-year DMFS as defining point, with an increasing number of genes were conducted in the training set of ER-positive tumors or ER-negative tumors. For ER-positive tumors, in the "apoptosis" pathway, 24 probe sets (reaching an AUC of 0.784) were considered optimal. For the "regulation of cell cycle" pathway in ER-positive tumors, 17 probe sets (AUC of 0.777) were considered optimal. For ER-negative tumors, the optimal number of probe sets was 7 (AUC of 0.790) for the "regulation for cell growth" pathway, and 5 (AUC of 0.788) for the "regulation of G-protein coupled receptor signaling" pathway, respectively. The selected unique probe sets for the top 2 pathways for ER-positive and ER-negative tumors were subsequently used to construct prognostic gene signatures separately for the 2 ER-subgroups of tumors (see Figure 4).

This signature was further validated using an independent 152-patient cohort [5], which consisted of 125 ER-positive tumors and 27 ER-negative tumors (after removing 36 lymph node-positive patients and a patient who died 15 days after surgery). When the 38-gene probe set was applied to the 125 ER-positive patients, a ROC analysis gave an AUC of 0.782 (95% CI: 0.681-0.883) (Figure 4A, left), and Kaplan-Meier analysis for DMFS showed a clear separation in risk groups ($P<0.001$, HR: 3.36 and 95% CI: 1.68-6.70) (Figure 4A, right). For the 12-gene probe set for the 27 ER-negative patients, an AUC of 0.872 (95% CI: 0.719-1) (Figure 4B, left) and separation between risk groups with a $P<0.001$ and a HR of 19.8 (95% CI: 2.41-163) (Figure 4B, right) was obtained. The combined 50-gene probe set signature for ER-positive and ER-negative patients gave an AUC of 0.795 (95% CI: 0.705-0.878) (Figure 4C, left) and a $P<0.001$ and a HR of 4.44 (95% CI: 2.31-8.54) for separation between risk groups (Figure 4C, right).

Pathway analysis of published prognostic gene signatures

To compare genes from various prognostic signatures for breast cancer, five published gene signatures were selected [3, 8, 23, 25, 26]. We first compared the gene sequence identity between each pair of the gene signatures and found, consistent with previous reports, very few overlapping genes (Table 4). The grade index gene expression signature comprising 97 genes, of which most are associated with cell cycle regulation and proliferation [23], showed the highest number of overlapping genes between the various signatures ranging from 5 of the 16 genes of Genomic Health [25] to 10 with Yu's 62 genes [26]. The other 4 gene signatures showed only 1 gene overlap in a pair-wise comparison, and there was no common gene for all signatures. In spite of the low number of overlapping genes across signatures, we hypothesized that the representation of common pathways in the various signatures may underlie their

Table 4. Number of common genes between different gene signatures for breast cancer prognosis.

	Wang's 76 genes	**van 't Veer's 70 genes**	**Paik's 16 genes**	**Yu's 62 genes**
Wang's 76 genes[a]		*CCNE2*	No genes	No genes
van 't Veer's 70 genes[b]	*CNNE2*		*SCUBE2*	*AA962149*
Paik's 16 genes[c]	No genes	*SCUBE2*		*BIRC5*
Yu's 62 genes[a]	No genes	*AA962149*	*BIRC5*	
Sotiriou's 97 genes[a]	*PLK1, FEN1, CCNE2, GTSE1, KPNA2, MLF1IP, POLQ*	*MELK, CENPA, CCNE2, GMPS, DC13, PRC1, NUSAP1, KNTC2*	*MYBL2, BIRC5, STK6, MKI67, CCNB1*	*URCC6, FOXM1, DLG7, DKFZp686L20222, DC13, FLJ32241, HSP1CDC21, CDC2, KIF11, EXO1*

[a]*Affymetrix HG-U133A Genechip*
[b]*Agilent Hu25K microarray*
[c]*No genome-wide assessment; RT-PCR.*
To compare genes from various prognostic signatures for breast cancer, five gene signatures were selected, the 76-gene signature [8], the 70-gene signature [3], the 16-gene signature [25], the 62-gene signature [26], and the 97-gene signature [23]. Identity of genes was determined by BLAST program when gene signatures were derived from different platforms. Except for the 97-gene expression grade index [23], which showed an overlap with 5 to 10 genes with the other gene signatures, a maximum overlap of only 1 identical gene was found between the other gene signatures. The initially reported 3-gene overlap between the 76-gene and the 70-gene prognostic signatures [8] included genes with high similarity in sequences. In this study, only genes with an identical sequence in two signatures are considered overlapped based on results from BLAST program. Therefore, CCNE2 gene is the only common gene between the two signatures.

individual prognostic value [8]. Therefore, we examined the representation of the core prognostic pathways (Table 2) in the 5 signatures. The Genomic Health 16-gene signature mapped to 10 of the 36 distinct core pathways (20 for both ER-positive and -negative tumors but 10 counting the 4 overlapping pathways once) whereas it mapped to a total of 25 out of 304 GOBPs. The statistical significance for the enrichment of GOBP, as computed by hypergeometric distribution probability was 2×10^{-5}. Each of the other 4 signatures have 62 or more genes and were mapped to 19 (53%) distinct prognostic pathways and their statistical significance of enrichment was 1×10^{-7} for Wang and van 't Veer, 1×10^{-6} for Sotiriou and 6×10^{-11} for Yu's signature (Table 5). Of these 19 pathways, 9 were identical for all 4 signatures, *i.e.*, "mitosis", "apoptosis", "regulation of cell cycle", "DNA repair", "cell cycle", "protein amino acid phosphorylation", "DNA replication", "intracellular signaling cascade", and "cell adhesion".

Table 5. Mapping various gene signatures to core pathways.

Pathways	GO_ID	Published gene signatures[a]				
		Wang	Van 't Veer	Paik	Yu	Sotiriou
ER-positive tumors						
Apoptosis	6915	X	X	X	X	X
Regulation of cell cycle	74	X	X	X	X	X
Protein amino acid phosphorylation	6468	X	X	X	X	X
Cytokinesis	910	X	X	X		X
Cell motility	6928				X	X
Cell cycle	7049	X	X	X	X	X
Cell surface receptor-linked signal transd.	7166			X		
Mitosis	7067	X	X	X	X	X
Intracellular protein transport	6886	X	X			X
Mitotic chromosome segregation	70	X	X			X
Ubiquitin-dependent protein catabolism	6511		X		X	X
DNA repair	6281	X	X		X	X
Induction of apoptosis	6917	X				
Immune response	6955	X			X	X
Protein biosynthesis	6412			X	X	X
DNA replication	6260	X	X		X	X
Oncogenesis	7048			X	X	X
Metabolism	8152	X	X			
Cellular defense response	6968	X			X	X
Chemotaxis	6935				X	X
ER-negative tumors						
Regulation of cell growth	1558		X			
Regul. of G-coupled receptor signaling	8277					
Skeletal development	1501	X	X			
Protein amino acid phosphorylation	6468	X	X	X	X	X
Cell adhesion	7155	X	X		X	X
Carbohydrate metabolism	5975	X	X			
Nuclear mRNA splicing, via spliceosome	398					
Signal transduction	7165	X	X	X	X	
Cation transport	6812					
Calciumion transport	6816					
Protein modification	6464					
Intracellular signaling cascade	7242	X	X		X	X
mRNA processing	6397					
RNA splicing	8380					
Endocytosis	6897					
Regul. of transcription from PolII promoter	6357				X	
Regulation of cell cycle	74	X	X	X		
Protein complex assembly	6461		X		X	
Protein biosynthesis	6412			X		X
Cell cycle	7049	X	X	X	X	X

[a]Published gene signatures that were studied include the 76-gene signature [8], the 70-gene signature [3], the 16-gene signature [25], the 62-gene signature [26], and the 97-gene signature [23]. Individual genes in each signature were mapped to the top 20 core pathways for ER-positive and ER-negative tumors, a cross indicates a match.

DISCUSSION

Gene-expression profiling for separating patients into different subtypes and risk groups have been focused on the identification of differential expression of individual genes rather than obtaining biological insight. In the present study we have used an alternative approach to identify in ER-positive and ER-negative populations of breast cancer patients the underlying biological processes associated with metastasis. Using a stringent re-sampling and permutation methodology we were able to show that indeed multiple signatures can be identified showing similar prognostic power while the genes from these different samplings have similar functions. Similar observations were made when we mapped the core prognostic pathways to 5 published prognostic signatures [3, 8, 23, 25, 26]. Thus, we showed that in spite of the low number of overlapping genes between the various published gene signatures, the signatures had many pathways in common, implying that different prognostic gene signatures represent common biology. In a recent study, comparing the prognostic performance of different gene-signatures, agreement in outcome predictions were found as well [28]. However, in contrast to our present approach, the underlying pathways were not investigated. Instead, the performance of various gene signatures on a single patient cohort, heterogeneous with respect to nodal status and adjuvant systemic therapy [29], was compared [28]. It is important to note, however, that although similar pathways are represented in various signatures, it does not necessarily mean the individual genes in a pathway are equally significant or are all similarly associated with tumor aggressiveness (see Additional Data Files 1 and 3).

The fact that none of the 20 genes most frequently present in the 500 signatures for the ER-positive tumors were among the top 20 core gene list of the ER-negative tumors, was not surprising and is in line with the fact that ER-subgroups of tumors are biologically very different entities [1-4, 8, 27]. Furthermore, although among the top 20 over-represented pathways, 4 were common for ER-positive tumors and ER-negative tumors, there were in total only 2 shared genes pointing into the same direction with respect to metastatic capability of the tumors. Both genes, *KIAA0256* in the "protein biosynthesis" pathway and *CCNT2* in the "cell cycle pathway", were associated with an aggressive tumor behavior. These results imply that the underlying biological processes between ER-subgroups of tumors with respect to their metastatic behavior have little if any in common. Of the top 20 core prognostic pathways for the ER-positive tumors many biological processes are related to cell division activities, immunity, signal transduction, and extrinsic apoptosis-related biological processes. The cell division-related pathways have predominantly negative correlation with survival time, while immune-related pathways have predominantly positive correlation. This indicates that ER-positive tumors with metastatic capability tend to have higher cell division rates, are more resistant to external apoptotic stimuli, and induce a poor immune reaction in the host body. In ER-positive tumors, one or more of these pathways, or genes in these pathways, have also been described to be associated with the efficacy of tamoxifen therapy in recurrent breast cancer [7], in the various prognostic signatures described in the present paper [8, 23, 25, 26], as well as in other published signatures not specifically designed for ER-positive tumors, such as the 70-gene prognostic signature [3], the stromal signatures [30], and the hypoxia signature [31]. The differences in metastatic behavior between ER-subgroups of tumors is further substantiated by the finding that in ER-negative tumors other pathways showed the strongest involvement, including those related with cell growth regulation, possibly through JAK/STAT signaling, and modulation of G-protein receptor signal transduction, RNA splicing or processing, and ion transport. No comparison can be made with the literature since no other studies so far have described prognostic of predictive pathways specifically in ER-negative breast cancer.

We were able to construct a 50-gene signature by combining the genes from the 2 most significant ER-positive and ER-negative pathways. This signature was validated and performed well on an independent published patient cohort [23], herewith showing the feasibility to derive a gene signature from biological pathways. Although further methodology and analysis would be required to optimize

the selection of such a pathway-based prognostic signature, our example provides not only a new way to derive gene signatures for cancer prognosis, but also gives insight into the distinct biological processes between subgroups of tumors.

CONCLUSIONS

Our study for the first time applied a method that systematically evaluated the biological pathways related to patient outcomes of breast cancer and showed that various published prognostic gene signatures providing similar outcome predictions are based on the representation of largely overlapping biological processes. Identification of the key biological processes, rather than the assessment of signatures based on individual genes, allows not only to build a biological meaningful gene signature from functionally related genes, but also provides insight into the mechanism of the disease development and, as spin off, potential targets for future drug development. In this respect, as pharmacologic inhibitors for specific pathways become available for the clinic, the signatures that define tumors according to their vital pathways may provide crucial guidance for designing appropriate drug combinations [32].

ADDITIONAL DATA FILES

The following Additional Data Files are available with the online version of this paper:
-    Additional Data File 1: Top 20 prognostic pathways in ER-positive tumors
-    Additional Data File 2: Significant genes in the top 20 prognostic pathways for ER-positive tumors
-    Additional Data File 3: Top 20 prognostic pathways in ER-negative tumors
-    Additional Data File 4: Significant genes in the top 20 prognostic pathways for ER-negative tumors

ACKNOWLEDGEMENTS

REFERENCES

1. Perou CM, Sorlie T, Eisen MB, van de Rijn M, Jeffrey SS, Rees CA, Pollack JR, Ross DT, Johnsen H, Akslen LA, Fluge O, Pergamenschikov A, Williams C, Zhu SX, Lonning PE, Borresen-Dale AL, Brown PO, Botstein D. Molecular portraits of human breast tumours. Nature 2000;406:747-52.

2. Sorlie T, Perou CM, Tibshirani R, Aas T, Geisler S, Johnsen H, Hastie T, Eisen MB, van de Rijn M, Jeffrey SS, Thorsen T, Quist H, Matese JC, Brown PO, Botstein D, Eystein Lonning P, Borresen-Dale AL. Gene expression patterns of breast carcinomas distinguish tumor subclasses with clinical implications. Proc Natl Acad Sci U S A 2001;98:10869-74.

3. van 't Veer LJ, Dai H, van de Vijver MJ, He YD, Hart AA, Mao M, Peterse HL, van der Kooy K, Marton MJ, Witteveen AT, Schreiber GJ, Kerkhoven RM, Roberts C, Linsley PS, Bernards R, Friend SH. Gene expression profiling predicts clinical outcome of breast cancer. Nature 2002;415:530-6.

4. Sorlie T, Tibshirani R, Parker J, Hastie T, Marron JS, Nobel A, Deng S, Johnsen H, Pesich R, Geisler S, Demeter J, Perou CM, Lonning PE, Brown PO, Borresen-Dale AL, Botstein D. Repeated observation of breast tumor subtypes in independent gene expression data sets. Proc Natl Acad Sci U S A 2003;100:8418-23.

5. Sotiriou C, Neo SY, McShane LM, Korn EL, Long PM, Jazaeri A, Martiat P, Fox SB, Harris AL, Liu ET. Breast cancer classification and prognosis based on gene expression profiles from a population-based study. Proc Natl Acad Sci U S A 2003;100:10393-8.

6. Brenton JD, Carey LA, Ahmed AA, Caldas C. Molecular classification and molecular forecasting of breast cancer: ready for clinical application? J Clin Oncol 2005;23:7350-60.

7. Jansen MP, Foekens JA, van Staveren IL, Dirkzwager-Kiel MM, Ritstier K, Look MP, Meijer-van Gelder ME, Sieuwerts AM, Portengen H, Dorssers LC, Klijn JG, Berns EM. Molecular classification of tamoxifen-resistant breast carcinomas by gene expression profiling. J Clin Oncol 2005;23:732-40.

8. Wang Y, Klijn JG, Zhang Y, Sieuwerts AM, Look MP, Yang F, Talantov D, Timmermans M, Meijer-van Gelder ME, Yu J, Jatkoe T, Berns EM, Atkins D, Foekens JA: Gene-expression profiles to predict distant metastasis of lymph-node-negative primary breast cancer. Lancet 2005;365:671-679.

9. Smid M, Wang Y, Klijn JG, Sieuwerts AM, Zhang Y, Atkins D, Martens JW, Foekens JA. Genes associated with breast cancer metastatic to bone. J Clin Oncol 2006; 24:2261-7.

10. Michiels S, Koscielny S, Hill C. Prediction of cancer outcome with microarrays: a multiple random validation strategy. Lancet 2005;365:488-92.

11. Simon R. Development and evaluation of therapeutically relevant predictive classifiers using gene expression profiling. J Natl Cancer Inst 2006;98:1169-71.

12. Goeman JJ, van de Geer SA, de Kort F, van Houwelingen HC. A global test for groups of genes: testing association with a clinical outcome. Bioinformatics 2004;20:93-9.

13. Vogelstein B, Kinzler KW. Cancer genes and the pathways they control. Nat Med 2004;10:789-99.

14. Goeman JJ, Oosting J, Cleton-Jansen AM, Anninga JK, van Houwelingen HC. Testing association of a pathway with survival using gene expression data. Bioinformatics 2005;21:1950-7.

15. Segal E, Friedman N, Kaminski N, Regev A, Koller D. From signatures to models: understanding cancer using microarrays. Nat Genet 2005;37 Suppl:S38-45.

16. Subramanian A, Tamayo P, Mootha VK, Mukherjee S, Ebert BL, Gillette MA, Paulovich A, Pomeroy SL, Golub TR, Lander ES, Mesirov JP. Gene set enrichment analysis: a knowledge-based approach for interpreting genome-wide expression profiles. Proc Natl Acad Sci U S A 2005;102:15545-50.

17. Tian L, Greenberg SA, Kong SW, Altschuler J, Kohane IS, Park PJ. Discovering statistically significant pathways in expression profiling studies. Proc Natl Acad Sci U S A 2005;102:13544-9.

18. Adler AS, Lin M, Horlings H, Nuyten DS, van de Vijver MJ, Chang HY. Genetic regulators of large-scale transcriptional signatures in cancer. Nat Genet 2006;38:421-30.

19. Tinker AV, Boussioutas A, Bowtell DD. The challenges of gene expression microarrays for the study of human cancer. Cancer Cell 200;9:333-9.

20. www.fmwv.nl.

21. Foekens JA, Atkins D, Zhang Y, Sweep FC, Harbeck N, Paradiso A, Cufer T, Sieuwerts AM, Talantov D, Span PN, Tjan-Heijnen VC, Zito AF, Specht K, Hoefler H, Golouh R, Schittulli F, Schmitt M, Beex LV, Klijn JG, Wang Y. Multicenter validation of a gene expression-based prognostic signature in lymph node-negative primary breast cancer. J Clin Oncol 2006; 24:1665-71.

22. Foekens JA, Portengen H, van Putten WL, Trapman AM, Reubi JC, Alexieva-Figusch J, Klijn JG. Prognostic value of receptors for insulin-like growth factor 1, somatostatin, and epidermal growth factor in human breast cancer. Cancer Res 1989;49:7002-9.

23. Sotiriou C, Wirapati P, Loi S, Harris A, Fox S, Smeds J, Nordgren H, Farmer P, Praz V,Haibe-Kains B, Desmedt C, Larsimont D, Cardoso F, Peterse H, Nuyten D, Buyse M, van de Vijver MJ, Bergh J, Piccart M, Delorenzi M. Gene expression profiling in breast cancer: understanding the molecular basis of histologic grade to improve prognosis. J Natl Cancer Inst 2006;98:262-72.

24. www.affymetrix.com.

25. Paik S, Shak S, Tang G, Kim C, Baker J, Cronin M, Baehner FL, Walker MG, Watson D, Park T, Hiller W, Fisher ER, Wickerham DL, Brynat J, Wolmark N. A multigene assay to predict recurrence of tamoxifen-treated, node-negative breast cancer. N Engl J Med 2004;351:2817-26.

26. Yu K, Lee CH, Tan PH, Hong GS, Wee SB, Wong CY, Tan P. A molecular signature of the Nottingham prognostic index in breast cancer. Cancer Res 2004;64: 2962-8.

27. Gruvberger S, Ringner M, Chen Y, Panavally S, Saal LH, Borg A, Ferno M, Peterson C, Meltzer PS. Estrogen receptor status in breast cancer is associated with remarkably distinct gene expression patterns. Cancer Res 2001;61:5979-84.

28. Fan C, Oh DS, Wessels L, Weigelt B, Nuyten DS, Nobel AB, van't Veer LJ, Perou CM. Concordance among gene-expression-based predictors for breast cancer. N Engl J Med 2006;355:560-9.

29. van de Vijver MJ, He YD, van't Veer LJ, Dai H, Hart AA, Voskuil DW, Schreiber GJ, Peterse JL, Roberts C, Marton MJ, Parrish M, Atsma D, Witteveen A, Glas A, Delahaye L, van der Velde T, Bartelink H, Rodenhuis S, Rutgers ET, Friend SH, Bernards, R. A gene-expression signature as a predictor of survival in breast cancer. N Engl J Med 2002;347: 1999-2009.

30. West RB, Nuyten DS, Subramanian S, Nielsen TO, Corless CL, Rubin BP, Montgomery K, Zhu S, Patel R, Hernandez-Boussard T, Goldblum JR, Brown PO, van de Vijver M, van de Rijn M. Determination of stromal signatures in breast carcinoma. PLoS Biol 2005; 3:e187.

31. Winter SC, Buffa FM, Silva P, Miller C, Valentine HR, Turley H, Shah KA, Cox GJ, Corbridge RJ, Homer JJ, Musgrove R, Slevin N, Sloan P, Price P, West CM, Harris AL. Relation of a hypoxia metagene derived from head and neck cancer to prognosis of multiple cancers. Cancer Res 2007;67:3441-9.

32. Massague J. Sorting out breast-cancer gene signatures. N Engl J Med 2007;356:294-7.

General discussion and future perspectives

10. GENERAL DISCUSSION AND FUTURE PERSPECTIVES

The aims of this thesis were firstly to gain insight into the interaction between breast tumor cells and the surrounding stromal fibroblasts. Secondly, to integrate the concept of a multi-cellular program in which the epithelial tumor cells, the tumor-associated fibroblasts, and diverse other cells in the tumor micro-environment are active participants, in our search for novel prognostic and predictive biomarkers. Finally, to place the concept of biomarkers in a larger context by looking at pathways rather than individual biomarkers.

In this general discussion I would like to take the opportunity to discuss in more depth three concepts that emerged from the studies described in this thesis in relation to future perspectives:
1)   if and how assessment of stromal content may aid to put a putative tumor marker in a biological context;
2)   if and how genes localized on the long arm of chromosome 17q may play a dominant role in tamoxifen responsiveness;
3)   if and how there is a future for testing biomarkers with real-time RT-PCR.

10.1 Stromal content in breast cancer subtypes

Three studies presented in this thesis (described in chapter 4, 5 and 8) show that additional prognostic and/or predictive information can be obtained if tumors are subdivided at the median level of 70% epithelial tumor cell nuclei in stroma-rich (tumors with 30% or more nuclei from stromal origin) and stroma-poor (tumors with over 70% tumor cell nuclei from epithelial origin), with the relatively large group of tumors with 70% epithelial tumor cell nuclei grouped with the stroma-rich tumors [1]. The rationale for this was that certain genes, like specific matrix metalloproteases and their inhibitors, are known to be mainly expressed in the stroma, while others, such as *ESR1* (*ER-alpha*), are predominantly expressed by the epithelial cancer cells.

Such cell-type specific localizations were confirmed in this thesis using real-time RT-PCR, *in situ* hybridization, western blotting and immunostaining. In chapter 2 and 3 for example we compared mRNA levels of various genes in breast fibroblasts derived from breast tumor tissue and adjacent 'normal' breast tissue and showed that gene and protein expression levels of tumor-derived fibroblasts in response to either external stimuli [2] or during aging [3] can differ significantly from those of fibroblasts derived from a location adjacent to normal breast tissue. For the tissue inhibitor of metalloproteinases-1 (TIMP-1), highest expression was measured in fibroblasts located adjacent to tumor cells [4, 5]. Further investigation revealed that concentrations of full-length *TIMP1* mRNA did not differ between stroma-rich and stroma-poor tumors. However, mRNA levels of the novel by us identified *TIMP1* splice variant lacking exon 2 (*TIMP1-v2*), were higher in stroma-rich compared with stroma-poor primary breast tumors [5]. These and other observations supported our hypothesis that *TIMP1-v2*, with clinical features distinct from full-length *TIMP1*, is regulated by a different, ER-independent, mechanism. In chapter 4 we showed that ER-alpha staining was mainly localized to the nuclei of epithelial tumor cells. Immunohistochemical staining of ADAM-9 and ADAM-11 protein in human breast carcinomas yielded heterogeneous results with both proteins found in epithelial tumor cells, adipocytes, smooth muscle cells of vessel walls, and the myoepithelial and luminal layers of non-neoplastic epithelium of the mammary gland [1].

In chapter 4 we were able to demonstrate that especially for primary tumors containing a large proportion of stromal cells, the assessment of mRNA expression levels of the disintegrin and metalloproteinase *ADAM9* and *ADAM11* can be useful to identify patients with recurrent breast cancer who are likely to benefit or fail from tamoxifen therapy [1]. In addition, we showed in chapter 5 that patients with high levels of *CCNE1* had an increased risk ($P=0.03$) to develop a metastasis within 5

years if their primary tumor was stroma-rich compared with patients with a high level of *CCNE1* combined with a stroma-poor primary tumor [6]. Thus, it has been established in this thesis that the prognostic and predictive value of biological factors, among which CCNE-1, ER-alpha, ADAM-9, ADAM-11 and TIMP-1, may be further refined by dividing tumor samples at the median level of 70% epithelial tumor cell nuclei in a cohort of stroma-poor tumors and a cohort of stroma-rich tumors.

Although we have shown that this pragmatic subdivision in stroma-poor and stroma-rich enabled us to discriminate between breast cancer subtypes with specific clinical implications, thus far no rationale other than that some biomarkers are known to be expressed more frequently in either the epithelial tumor cells or the stromal cells was given. However, another obvious explanation for the differences in gene expression levels we measured in the stroma-poor and stroma-rich cohorts might be the influence of the housekeeper set used in our studies to normalize the real-time RT-PCR gene expression data. To accurately quantify gene expression, the measured amount of mRNA from the gene of interest was divided by the amount of mRNA from a reference housekeeping gene set measured in the same sample to normalize for possible variation in the amount and quality of mRNA between different samples. Such a normalization is only valid provided that the expression of the reference gene is very similar across all the samples. Choosing a reference gene fulfilling this criterion is therefore of high importance, and often challenging, because only very few genes show equal levels of expression across a range of different conditions or tissues [7-10]. To smoothen the possible differential influence of one specific housekeeping gene for a specific condition, *i.e.* stromal content, we choose to use a set of 3 different housekeeping genes: the low abundance hydroxymethylbilane synthase (*HMBS*, formerly porpholilinogen deaminase, *PBGD*), the medium abundance hypoxanthine-guanine phosphoribosyl-transferase 1 (*HPRT1*), and the high abundance beta-2-microgobulin (*B2M*). Comparing the levels of our housekeeping set after splitting tumor samples at the median level of 70% tumor cell nuclei, with the group of 70% tumor cell nuclei grouped with the stroma-rich, in stroma-poor (n=390) and stroma-rich (n=1290), showed no significant differences between the two groups (Mann-Whitney U test P=0.999). Hence, the differences in gene expression levels we measured in the stroma-poor and stroma-rich cohorts are not the result of our normalization method.

But before considering applying this relatively simple method for high throughput screening, an understanding of what this subdivision in stroma-rich and stroma-poor implies in terms of histology is essential. Please refer to table 10.1.1 for a summary of the significant differences we observed and that are discussed in more detail below.
For the purpose of this general discussion we investigated if the various histological types described in table 1.1.1 of this thesis display a preference for stroma-rich or for stroma-poor tumors. In the 1137 primary breast tumors with known histology we noticed that stroma-poor tumors were significantly associated with infiltrating lobular carcinoma (ILC; chi-squared=3.88, P=0.049, n=110) and mucinous tumors (chi-squared=5.19, P<0.0001, n=36). Infiltrating ductal carcinoma (IDC) on the other hand were mainly of the stroma-rich phenotype (chi-squared=5.19, P=0.023, n=921). No such differences in stromal distribution were seen for the remaining tumor types (LCIS, DCIS, medullary, papillary, and tubular). These data imply that the stroma-poor phenotype is in general associated with the less common ILC subtype and the clinically more favorable mucinous type. The stroma-rich phenotype is more likely to resemble an IDC, the most common histologic breast cancer type.
But these observations, with IDC comprising about 80% of the invasive breast cancers, still do not sufficiently explain our findings described in chapter 4, 5 and 8 that stroma-rich and stroma-poor primary breast tumors might behave quite different with respect to prognosis. Another way to approach the clinical implications of our pragmatic division in stroma-rich and stroma-poor is to look at possible differences in grading in these 2 phenotypes. For the 978 primary tumors with known grade and tumor cell content no significant differences were observed in this respect: stroma-rich and stroma-poor

tumors were equally distributed over the n=198 low to moderate grade tumors with an overall favorable prognosis and the n=780 more aggressive high-grade tumors.

Fortunately, in this genomics era sophisticated microarray based methods are available to supplement the histological grading data provided by the pathologist. So how do microarray based grading signatures compare with our empirical distribution in stroma-rich and stroma-poor? To further explore this, we used our distribution in stroma-poor (n=102) and stroma-rich (n=203) after splitting samples at the median level of 70% tumor cell nuclei to classify 305 lymph-node negative primary breast tumors with known tumor cell content essentially like described by Smid *et al*., [11]. Modulated genes were identified in the two groups using Significance Analysis of Microarrays (SAM) with a 10% false discovery rate (FDR) cut-off. These analyses showed that of the almost 450,000 probe sets representing more than 39,000 transcripts, 1,268 probe sets were significantly higher expressed in the stroma-rich subgroup and only one probe set (220942_x_at; representing the E2-induced *E2IG5* gene) was higher expressed in the stroma-poor group. When including only the 191 ER-positive breast tumors present in this cohort, the distribution did not change much with 197 probe sets representing 153 known genes and 11 yet unidentified transcripts higher expressed in the stroma-rich group of 122 tumors and only 2 genes (*ESR1* and *FAM134B*, a gene coding for the hypothetical protein FLJ20152 or LOC54463), higher expressed in the stroma-poor group of 69 tumors. In the 114 ER-negative breast tumors 58 probe sets, representing 48 known genes and 4 yet unidentified transcripts, were higher expressed in the stroma-rich group of 81 tumors and not one single gene was higher expressed in the stroma-poor group of 33 tumors. Of note, for the highly expressed genes in these stroma-rich ER-positive (153 known genes) and ER-negative (48 known genes) cohorts only 8 genes overlapped (*CCL19*, *CCND2*, *DCN*, *FBLN1*, *HLA-DOB*, *ITM2C*, *KLRB1*, and *PTGDS*).

Next, we similarly tried matching our stroma-rich and stroma-poor phenotypes with three microarray based signatures aimed at classifying breast carcinomas based on gene expression patterns: two grading signatures that specifically focus on the stromal micro-environment of the epithelial tumor cells [13, 15], and the intrinsic breast cancer subtypes described by Perou and Sorlie [16-19].
In the stromal-related wound healing signature that, based on gene expression profiles of fibroblasts from ten anatomic sites, reflects the multifaceted role of fibroblasts in wound healing [12-14], stroma-rich and stroma-poor tumors were evenly distributed over the tumors exhibiting this wound healing signature and those that did not. Differences between the two phenotypes were however observed based on the stromal signature introduced by West *et al* [15]. This signature is based on differences between two types of fibroblastic tumors: the locally aggressive desmoid-type fibromatosis (DTF) and the generally benign solitary fibrous tumors (SFT). DTF expresses numerous collagens that are present in a fibrotic response. Numerous myofibroblastic genes are also expressed by DTF. In contrast, SFT express collagens and other extracellular matrix proteins that are typically found in the basement membrane. DTF tumors express several genes of the *ADAM* and *MMP* families involved in extracellular matrix remodeling, which might be relevant to the more infiltrative behavior of these tumors [15]. SFT express few of these genes and the ADAMs that are expressed in SFT (*ADAM22* and *ADAM23*) are probably more involved in cell adhesion than in extracellular matrix remodeling. In addition, DTF tumors express growth factors involved in the profibrotic response, such as transforming growth factor beta and connective tissue growth factor [15]. Clustering our tumors according to these signatures revealed that the SFT subtype could be subdivided in 3 different groups (SFT-a, SFT-b and SFT-c). Stroma-rich tumors were most abundant in the 125 tumors defined by the expression of DTF genes and stroma-poor tumors were most abundant in the 83 tumors defined by expression of genes of for the SFT-c subtype (chi-squared=11.6, *P*=0.0006). Thus, according to these observations, our stroma-rich primary breast tumors are representative for the more aggressive DTF genotype.
Finally, the intrinsic breast cancer subtypes (n=67 luminal A, n=74 luminal B, n=64 ERBB2, n=17

normal-like and n=83 basal tumors) were identified in our cohort like described [11]. These intrinsic subtypes showed a significant ($P<0.0001$) relationship with the stromal subgroups. Stroma-rich tumors were most abundant in the ERBB2+ subtype ($P=0.002$) but were found less than would be expected in the luminal A subtype ($P<0.0001$). Survival analyses in a prospective study on a subcohort of uniformly treated patients with locally advanced breast cancer showed significantly different outcomes for the patients belonging to the various intrinsic breast cancer subtypes. These correlations with clinical outcome included a significant difference in outcome for the two estrogen receptor-positive (luminal A versus B+C) groups, with the best prognosis associated with the luminal A subtype. Furthermore, the basal-like and ERBB2+ subtypes were associated with the shortest relapse-free survival [17]. According these data, stroma-rich tumors are characterized by a higher proportion of the more aggressive ERBB2+ subtype and stroma-poor tumors by a higher proportion of the aggressive luminal A subtype.

To summarize the above, when compared to stroma-poor tumors, stroma-rich tumors are more likely to express higher gene levels, especially genes associated with DTF tumors, are more likely to be an IDC,

Table 10.1.1. Associations of stromal content with histological and genotypic features.

Grouping variables / Sub cohort	Stroma-poor* over 70% tumor nuclei	Stroma-rich* 30 – 70% tumor nuclei
Histology		
ILC	↑	
IDC		↑
mucinous	↑	
Histologic grade	→	→
Housekeeping gene set [1, 5, 6]	→	→
No of highly expressed probes ** [11]		
ER+ and ER-	1	1268
ER+	2	197
ER-	0	58
Wound healing signature [12-14]	→	→
Stromal signature [15]		
DTF		↑
SFT-c	↑	
Intrinsic breast cancer subtypes [16-19]		
Luminal A	↑	
ERBB2+		↑

*   Dichotomized at the median level of 70% epithelial tumor cells with tumors with at least 70% epithelial tumor cells grouped in the stroma-poor, i.e. predominantly epithelial, subgroup.
**   Significantly higher expressed genes were identified in the two groups using SAM with a 10% FDR cut-off.
↑   Histological or genotypic feature more frequently expressed by the specified stromal phenotype.

and are more likely to be of the ERBB2+ breast cancer subtype. All features associated with poor prognosis. Stroma-poor tumors on the other hand are more likely to express genes associated with the generally benign SFT tumors, are more likely to be mucinous or an ILC, and are more likely to be of the luminal A subtype. All features associated with a better prognosis.

Thus, solely based on tumor cellularity we have been able to roughly discriminate between histological phenotypes and microarray based genotypes with different prognostic features. However, we do definitely not advocate that such a rough assessment of tumor cellularity can replace these methods. But when the more laborious and expensive molecular profiling approach is not feasible, our relatively easy to perform pragmatic approach should be taken into consideration to add information to the traditional prognostic and predictive parameters. In addition, the observations described underline the notion that cancer should be seen as a multi-type cellular program in which the epithelial tumor cells themselves, the tumor-associated fibroblasts, and diverse other cell types in the tumor micro-environment are active participants [13, 20-22].

10.2 Overrepresentation of genes associated with tamoxifen responsiveness on chromosome 17q12-25?

Using microsatellite length polymorphisms, comparative genomic hybridization (CGH) and molecular cytogenetics (FISH), frequent allelic losses and gains on chromosome 17q have been detected in cell lines and sporadic breast carcinoma [23-30]. These and other studies suggest that chromosome 17q accomodates potential tumor suppressor genes as well as oncogenes.

In a recent study we discovered a set of markers predictive for the type of response to endocrine therapy with the antiestrogen tamoxifen using gene expression profiling [31]. In total, 81 genes were differentially expressed in the responsive and non-responsive groups. When assigning these genes to chromosomes, we observed that a relatively high number of 8 genes (nearly 10% in stead of the 3.2% expected on this chromosomal arm that contains 997 out of 31,210 Ensembl genes) was localized to chromosome 17q12-q25: *EZH1*, *FMNL*, *KIAA0563*, *APPBP2* and *CDC42EP4*, for which high levels were associated with favorable response to tamoxifen, and *LOC117584*, *COL1A1* and *NAT9* for which high levels were associated with adverse response to tamoxifen. Interestingly, two additional studies included in this thesis describe markers located on 17q that correlate with tamoxifen response: *HOXB13* [32] and *ADAM11* [1]. In addition, unpublished data of our group indicate that high levels of the eukaryotic translation initiation factor *EIF1* (*SUI1*) on 17q21.2 are associated with favorable response to tamoxifen while high levels of *TIMP2* on 17q25 are associated with adverse response to tamoxifen.

Besides the above mentioned genes located on 17q and linked by work of our group to tamoxifen responsiveness, 17q harbors two additional interesting genes that have drawn much attention in the past years: the familial susceptibility tumor suppressor gene *BRCA1* [33] and the in breast cancer often amplified *ERBB2* oncogene. These two genes might, in addition to the widely demonstrated association with prognosis, be related to tamoxifen response. Although it is not yet clear whether tamoxifen can reduce breast cancer incidence in women with *BRCA* mutations in general, use of tamoxifen does reduce the risk of contralateral breast cancer [34]. Patients with *ERBB2* amplification have lower ER levels and have been shown to be, albeit modestly, less responsive to tamoxifen [35-38]. This was confirmed in our own studies where we found amplified levels of *ERBB2* and the co-amplified *GRB7* as measured by real-time RT-PCR significantly associated with reduced tamoxifen responsiveness (unpublished data).

As demonstrated for the ERBB2-blocking antibody trastuzumab (Herceptin) [39-41], especially agents blocking expression of genes or gene products for which high levels are associated with unfavorable response to tamoxifen are therapeutically interesting. Therefore genes with increased expression levels in tamoxifen unresponsive cases, such as the genes depicted with a downward arrow in figure 10.2.1, are expected to be the most promising candidates for targeted therapy. Another interesting approach might however be to induce genes, such as *ADAM11* and others depicted with an upward arrow in figure 10.2.1, for which high expression has been associated with treatment benefit.

In view of another publication included in this thesis, where we showed that aging accompanied by telomere loss could contribute to breast cancer progression [3], it is noteworthy that telomeric length on 17q shortens more than global telomere length in the development of breast cancer [42, 43]. This increased level of telomere shortening on 17q may be involved in the chromosomal instability of 17q and the progression of DCIS to IDC [43]. By using telomerase RNA (TERC) and dyskerin, the reverse transcriptase enzyme telomerase (TERT) is able to maintain telomere length [44]. With respect to tamoxifen sensitivity, an increase of telomerase activity has been implicated in the transition from a tamoxifen sensitive to tamoxifen resistant phenotype [45-47]. It will therefore be interesting to see if artificially decreasing telomere length, for example by blocking TERT activity with antibodies or through mRNA silencing, is able to reverse tamoxifen resistance and how this correlates with

Gene symbol	tamoxifen response*	Gene description and alisases	Cytogenetic location
VTN	→	• Vitronectin, serum spreading factor; complement S-protein; somatomedin B • Hs.592130	17q11
NR1D1	→	• nuclear receptor subfamily 1, group D; member 1; hRev; THRA1;THRAL; ear-1 • Hs.592130	17q11.2
LOC 117584	↓	• transcribed locus 117584 • Hs.594059	17q12
ERBB2	↓	• v-erb-b2 erythroblastic leukemia viral oncogene homolog 2; neuro/glioblastoma derived oncogene homolog (avian); NGL; NEU; HER-2; HER2 • Hs.446352	17q11.2-17q21.1
GRB7	↓	• growth factor receptor-bound protein 7 • Hs.86859	17q11.2-17q21
EZH1	↑	• enhancer of zeste (Drosophila) homolog 1; KIAA0388 • Hs.194669	17q21.1-17q21.3
BRCA1	?	• breast cancer 1, early onset, • PSCP, BRCC1, IRIS, RNF53 • Hs.194143	17q21
FMNL1	↑	• formin-like; chromosome 17 open reading frame 1; C17orf1; C17orf1B; HREP • Hs.100217	17q21
EIF1	↑	• eukaryotic translation initiation factor 1; EIF-1; ISO1; A121; SUI1; EIF1A • Hs.150580	17q21.2
ADAM11	↑	• a disintegrin and metalloproteinase domain 11; MDC • Hs.6088	17q21.3
KIAA 0563	↑	• KIAA0563 protein; LRRC37A leucine rich repeat containing 37A; DKFZp686N1231 • Hs.656994	17q21.31
APPBP2	↑	• amyloid beta precursor protein (cytoplasmic tail) binding protein 2; PAT1 • Hs.84084	17q21-17q23
HOXB13	↓	• homeo box B13; human homeodomain protein HOXB13 • Hs.66731	17q21.31
COL1A1	↓	• collagen, type I, alpha 1 • Hs.172928	17q21.33
TIMP2	↓	• tissue inhibitor metallopeptidase inhibitor 2 • Hs.633514	17q25
NAT9	↓	• N-acetyltransferase 9; DKFZP564C103; EBSP • Hs.144058	17q25.2
CDC42EP4	↑	• CDC42 effector protein (Rho GTPase binding) 4; CEP4; KAIA1777; BORG4 • Hs.176479	17q24-17q25

Chromosome ideogram labels: 17p13, 17p12, 17p11.2, 17p11.1, 17q11.1, 17q11.2, 17q12, 17q21, 17q22, 17q23, 17q24, 17q25

Figure 10.2.1. Genes associated with tamoxifen responsiveness on chromosome 17q12-25.

*   →   *Gene expression levels are not associated with response to tamoxifen treatment for metastatic disease.*
         ↑   *Gene expression levels are higher in tamoxifen responsive cases and/or lower in unresponsive cases.*
         ↓   *Gene expression levels are lower in tamoxifen responsive cases and/or higher in unresponsive cases.*

expression of genes located on 17q.

In figure 10.2.1 our findings with respect to genes located at 17q in relation to tamoxifen responsiveness are summarized. Here it is also shown that we observed no correlation between tamoxifen response and vitronectin (*VTN*) located on 17q11 and *NR1D1* on 17q11.2. This indicates that a possible association of genes located on 17q and tamoxifen responsiveness could be confined to genes located upstream 17q11. Taken together, our data suggest that a condensation of genes localized on the long arm of chromosome 17q12-25 are, in addition to their association with breast cancer biology in general, associated with tamoxifen responsiveness.

10.3 Is there a future for the discovery or validation of biomarkers by real-time PCR?

Surprisingly in this high-throughput era, the only established breast biomarkers are currently the serum-based cancer antigens CA 15-3, CA 125, CA 27-29 and CEA, the tissue-based ER and PgR, markers measuring DNA-ploidy/content and/or cellular proliferation, the oncogene ERBB2, the tumor suppressor gene p53, and the protease uPA and its inhibitor PAI-1 [40, 41, 48].

In aid of the urgently needed establishment of new biomarkers, our department decided to process the Rotterdam fresh frozen human breast tumor tissue bank, containing over 5,000 tissues with clinical follow-up available, into a RNA, DNA and protein bank. These three banks now enable us to characterize the breast tumors by means of genomics and proteomics. In chapter 6 of this thesis a detailed overview of the RNA collection stored in this bank with sufficient clinical follow-up for reliable statistical analyses is presented [32]. These RNA samples were the very important source of clinical samples discussed in this thesis [1, 5, 6, 32, 49]. In addition to the data presented in these published studies, we have so far tested an impressive set of over 300 other genes by real-time RT-PCR. In most cases over 600 lymph node-negative patients who did not receive any adjuvant systemic therapy were analyzed to evaluate the prognostic value of genes, very similarly as described in chapter 5 of this thesis [6]. To evaluate the predictive value, in most cases at least 190 hormone naïve patients with ER-positive primary breast tumors treated with tamoxifen for recurrent breast cancer, were evaluated as described in chapter 4 [1] and 6 [32]. Perhaps disappointing, relatively few of these markers fulfil the criteria of a clinically attractive biomarker in this stage. Furthermore, with a rapidly expanding field of tumor associated biomarkers and a concomitant increase in published reports, it has become increasingly apparent that a strong need exists to establish consensus guidelines for the development and use of established as well as novel tumor associated markers [40, 50, 51]. For this purpose, the tumor marker utility grading system (TMUGS) has been introduced as a framework tool to define the quality of data that exist and to place the available data into one or several levels of evidence (LOE-5 to LOE-1) (table 1.4.1) [52].

Despite the large number of samples we have analyzed in the different studies included in this thesis, the putative biomarkers that emerged (*ADAM-9*, *ADAM-11*, *CCNE1*, *CCNE2*, *HOXB13*-to-*IL17BR* ratio, and *TIMP1-v1+v2*) do not exceed evidence-based level 3 (LOE-3; evidence from large but retrospective studies from which variable numbers of samples are available or selected). To reach LOE-2 (evidence from a study in which marker data are determined in relationship to a prospective therapeutic trial that is performed to test a therapeutic hypothesis but not specifically designed to test the marker utility), we need access to new tumor material from such a prospective trial and preferably also optimize our qRT-PCR assays for formalin-fixed paraffin-embedded (FFPE) tissues. Literature and data base searches might tell whether other groups have taken up on the putative new biomarker, in which case those data might help to reach LOE-2. Only then can the markers that are discussed in this thesis even be considered for entering LOE-1 (evidence from a single, high-powered, prospective, controlled study that is specifically designed to test marker or evidence from meta-analysis and/or overview of level II or III studies.). Taking this into consideration, there is still a long way to go for the biomarkers discussed in this thesis. Does this mean that in our search for new biomarkers the future for

real-time PCR looks bleak? No, I do not think so. Firstly, we have already shown that contributions of our group can result in biomarkers entering LOE-1 [53]. Secondly, even when no antibodies are available, real-time RT-PCR at least allows assessment of mRNA levels of candidate markers, nowadays also in FFPE tissue. Although gene expression profiling methods are definitely more comprehensive, especially low expressed tags might be adversely biased and validation at the single gene level by real-time RT-PCR will remain essential. In addition, the amount of valuable patient material, elaborate equipment and costs required to perform these genome-wide screenings must be taken into consideration. Thirdly, for example a 21 multigene real-time RT-PCR based assay (Oncotype DX™) to predict recurrence of tamoxifen-treated, node-negative breast cancer [54], and a FDA approved 2-gene (mammaglobin (*MGB1*) and cytokeratin 19 (*KRT19*)) RT-PCR assay (GeneSearch™) to detect the spread of breast cancer into the lymph nodes have already entered the clinic.

Taken together, real-time PCR is a sensitive, fast, quantitative, and cost-effective method suitable for high-throughput screening. In this thesis it has been shown that real-time RT-PCR is indeed a powerful method to quantify mRNA levels of genes that are differentially expressed in primary tumors of breast cancer patients with different prognostic and predictive features. Therefore, the single gene or multiplex real-time PCR approach will remain an important quantification method for fast screening of diagnostic markers and therapeutic targets that are already established or that emerge from the literature and microarray based techniques.

REFERENCES

1. Sieuwerts AM, Meijer-van Gelder ME, Timmermans M, Trapman AM, Rodriguez Garcia R, Arnold M, Goedheer AJ, Portengen H, Klijn JG, Foekens JA. How ADAM-9 and ADAM-11 differentially from estrogen receptor predict response to tamoxifen treatment in patients with recurrent breast cancer: a retrospective study. Clin Cancer Res 2005;11:7311-21.

2. Sieuwerts AM, Martens JW, Dorssers LC, Klijn JG, Foekens JA. Differential effects of fibroblast growth factors on expression of genes of the plasminogen activator and insulin-like growth factor systems by human breast fibroblasts. Thromb Haemost 2002;87: 674-83.

3. Martens JW, Sieuwerts AM, Bolt-deVries J, Bosma PT, Swiggers SJ, Klijn JG, Foekens JA. Aging of stromal-derived human breast fibroblasts might contribute to breast cancer progression. Thromb Haemost 2003;89:393-404.

4. Usher PA, Sieuwerts AM, Bartels A, Lademann U, Nielsen HJ, Holten-Andersen L, Foekens JA, Brunner N, Offenberg H. Identification of alternatively spliced TIMP-1 mRNA in cancer cell lines and colon cancer tissue. Mol Oncol 2007;1:205-215.

5. Sieuwerts AM, Usher PA, Meijer-van Gelder ME, Timmermans M, Martens JW, Brunner N, Klijn JG, Offenberg H, Foekens JA. Concentrations of TIMP1 mRNA splice variants and TIMP-1 protein are differentially associated with prognosis in primary breast cancer. Clin Chem 2007;53:1280-8.

6. Sieuwerts AM, Look MP, Meijer-van Gelder ME, Timmermans M, Trapman AM, Rodriguez Garcia R, Arnold M, Goedheer AJ, de Weerd V, Portengen H, Klijn JG, Foekens JA. Which cyclin E prevails as prognostic marker for breast cancer? Results from a retrospective study involving 635 lymph node-negative breast cancer patients. Clin Cancer Res 2006;12:3319-28.

7. Szabo A, Perou CM, Karaca M, Perreard L, Quackenbush JF, Bernard PS. Statistical modeling for selecting housekeeper genes. Genome Biol 2004;5:R59.

8. Janssens N, Janicot M, Perera T, Bakker A. Housekeeping genes as internal standards in cancer research. Mol Diagn 2004;8:107-13.

9. Nailis H, Coenye T, Van Nieuwerburgh F, Deforce D, Nelis HJ. Development and evaluation of different normalization strategies for gene expression studies in Candida albicans biofilms by real-time PCR. BMC Mol Biol 2006;7:25.

10. Nolan T, Hands RE, Bustin SA. Quantification of mRNA using real-time RT-PCR. Nat Protoc 2006;1: 1559-82.

11. Smid M, Wang Y, Zhang Y, Sieuwerts A, Yu J, Klijn J, Foekens J, Martens J. Subtypes of breast cancer show preferential site of relapse. (submitted) 2007.

12. Chang HY, Chi JT, Dudoit S, Bondre C, van de Rijn M, Botstein D, Brown PO. Diversity, topographic differentiation, and positional memory in human fibroblasts. Proc Natl Acad Sci USA 2002;99:12877-82.

13. Chang HY, Sneddon JB, Alizadeh AA, Sood R, West RB, Montgomery K, Chi JT, van de Rijn M, Botstein D, Brown PO. Gene expression signature of fibroblast serum response predicts human cancer progression: similarities between tumors and wounds. PLoS Biol 2004;2:206-214.

14. Chang HY, Nuyten DS, Sneddon JB, Hastie T, Tibshirani R, Sorlie T, Dai H, He YD, van't Veer LJ, Bartelink H, van de Rijn M, Brown PO, van de Vijver MJ. Robustness, scalability, and integration of a wound-response gene expression signature in predicting breast cancer survival. Proc Natl Acad Sci U S A 2005; 102:3738-43.

15. West RB, Nuyten DS, Subramanian S, Nielsen TO, Corless CL, Rubin BP, Montgomery K, Zhu S, Patel R, Hernandez-Boussard T, Goldblum JR, Brown PO, van de Vijver M, van de Rijn M. Determination of stromal signatures in breast carcinoma. PLoS Biol 2005; 3:1101-1110.

16. Perou CM, Sorlie T, Eisen MB, van de Rijn M, Jeffrey SS, Rees CA, Pollack JR, Ross DT, Johnsen H, Akslen LA, Fluge O, Pergamenschikov A, Williams C, Zhu SX, Lonning PE, Borresen-Dale AL, Brown PO, Botstein D. Molecular portraits of human breast tumours. Nature 2000;406:747-52.

17. Sorlie T, Perou CM, Tibshirani R, Aas T, Geisler S, Johnsen H, Hastie T, Eisen MB, van de Rijn M, Jeffrey SS, Thorsen T, Quist H, Matese JC, Brown PO, Botstein D, Eystein Lonning P, Borresen-Dale AL. Gene expression patterns of breast carcinomas distinguish tumor subclasses with clinical implications. Proc Natl Acad Sci U S A 2001;98:10869-74.

18. Sorlie T, Tibshirani R, Parker J, Hastie T, Marron JS, Nobel A, Deng S, Johnsen H, Pesich R, Geisler S, Demeter J, Perou CM, Lonning PE, Brown PO, Borresen-Dale AL, Botstein D. Repeated observation of breast tumor subtypes in independent gene expression data sets. Proc Natl Acad Sci U S A 2003;100:8418-23.

19. Sorlie T, Perou CM, Fan C, Geisler S, Aas T, Nobel A, Anker G, Akslen LA, Botstein D, Borresen-Dale AL, Lonning PE. Gene expression profiles do not consistently predict the clinical treatment response in locally advanced breast cancer. Mol Cancer Ther 2006; 5:2914-8.

20. Shekhar MP, Pauley R, Heppner G. Host microenvironment in breast cancer development: extracellular matrix-stromal cell contribution to neoplastic phenotype of epithelial cells in the breast. Breast Cancer Res 2003;5:130-5.

21. Radisky DC, Bissell MJ. Cancer. Respect thy neighbor! Science 2004;303:775-7.

22. Orimo A, Weinberg RA. Stromal fibroblasts in cancer: a novel tumor-promoting cell type. Cell Cycle 2006;5: 1597-601.

23. Futreal PA, Soderkvist P, Marks JR, Iglehart JD, Cochran C, Barrett JC, Wiseman RW. Detection of frequent allelic loss on proximal chromosome 17q in sporadic breast carcinoma using microsatellite length polymorphisms. Cancer Res 1992;52:2624-7.

24. Cropp CS, Champeme MH, Lidereau R, Callahan R. Identification of three regions on chromosome 17q in primary human breast carcinomas which are frequently deleted. Cancer Res 1993;53:5617-9.

25. Orsetti B, Courjal F, Cuny M, Rodriguez C, Theillet C. 17q21-q25 aberrations in breast cancer: combined allelotyping and CGH analysis reveals 5 regions of allelic imbalance among which two correspond to DNA amplification. Oncogene 1999;18:6262-70.

26. Osborne RJ, Hamshere MG. A genome-wide map showing common regions of loss of heterozygosity/ allelic imbalance in breast cancer. Cancer Res 2000;60: 3706-12.

27. Hyman E, Kauraniemi P, Hautaniemi S, Wolf M, Mousses S, Rozenblum E, Ringner M, Sauter G, Monni O, Elkahloun A, Kallioniemi OP, Kallioniemi A. Impact of DNA amplification on gene expression patterns in breast cancer. Cancer Res 2002;62:6240-5.

28. Harkes IC, Elstrodt F, Dinjens WN, Molier M, Klijn JG, Berns EM, Schutte M. Allelotype of 28 human breast cancer cell lines and xenografts. Br J Cancer 2003;89: 2289-92.

29. Orsetti B, Nugoli M, Cervera N, Lasorsa L, Chuchana P, Ursule L, Nguyen C, Redon R, du Manoir S, Rodriguez C, Theillet C. Genomic and expression profiling of chromosome 17 in breast cancer reveals complex patterns of alterations and novel candidate genes. Cancer Res 2004;64:6453-60.

30. De Marchis L, Cropp C, Sheng ZM, Bargo S, Callahan R. Candidate target genes for loss of heterozygosity on human chromosome 17q21. Br J Cancer 2004;90:2384-9.

31. Jansen MP, Foekens JA, van Staveren IL, Dirkzwager-Kiel MM, Ritstier K, Look MP, Meijer-van Gelder ME, Sieuwerts AM, Portengen H, Dorssers LC, Klijn JG, Berns EM. Molecular classification of tamoxifen-resistant breast carcinomas by gene expression profiling. J Clin Oncol 2005;23:732-40.

32. Jansen MP, Sieuwerts AM, Look MP, Ritstier K, Meijer-van Gelder ME, van Staveren IL, Klijn JG, Foekens JA, Berns EM. HOXB13-to-IL17BR expression ratio is related with tumor aggressiveness and response to tamoxifen of recurrent breast cancer: a retrospective study. J Clin Oncol 2007;25:662-8.

33. Hall JM, Lee MK, Newman B, Morrow JE, Anderson LA, Huey B, King MC. Linkage of early-onset familial breast cancer to chromosome 17q21. Science 1990;250: 1684-9.

34. Narod SA, Brunet JS, Ghadirian P, Robson M, Heimdal K, Neuhausen SL, Stoppa-Lyonnet D, Lerman C, Pasini B, de los Rios P, Weber B, Lynch H. Tamoxifen and risk of contralateral breast cancer in BRCA1 and BRCA2 mutation carriers: a case-control study. Hereditary Breast Cancer Clinical Study Group. Lancet 2000;356: 1876-81.

35. Berns EM, Foekens JA, van Staveren IL, van Putten WL, de Koning HY, Portengen H, Klijn JG. Oncogene amplification and prognosis in breast cancer: relationship with systemic treatment. Gene 1995;159: 11-8.

36. Klijn JGM, Berns EMJJ, Foekens JA. Prognostic and predictive factors and targets for therapy in breast cancer. In: Breast cancer: prognosis, treatment and prevention. (J.R. Pasqualini, ed), Marcel Dekker Inc., New York 2002:79-90.

37. Arpino G, Green SJ, Allred DC, Lew D, Martino S, Osborne CK, Elledge RM. HER-2 amplification, HER-1 expression, and tamoxifen response in estrogen receptor-positive metastatic breast cancer: a southwest oncology group study. Clin Cancer Res 2004;10:5670-6.

38. Ponzone R, Montemurro F, Maggiorotto F, Robba C, Gregori D, Jacomuzzi ME, Kubatzki F, Marenco D, Dominguez A, Biglia N, Sismondi P. Clinical outcome of adjuvant endocrine treatment according to PR and HER-2 status in early breast cancer. Ann Oncol 2006; 17:1631-6.

39. Duffy MJ. Predictive markers in breast and other cancers: a review. Clin Chem 2005;51:494-503.

40. Goldhirsch A, Glick JH, Gelber RD, Coates AS, Thurlimann B, Senn HJ. Meeting highlights: international expert consensus on the primary therapy of early breast cancer 2005. Ann Oncol 2005;16:1569-83.

41. Molina R, Barak V, van Dalen A, Duffy MJ, Einarsson R, Gion M, Goike H, Lamerz R, Nap M, Soletormos G, Stieber P. Tumor markers in breast cancer- European Group on Tumor Markers recommendations. Tumour Biol 2005;26:281-93.

42. Zou Y, Sfeir A, Gryaznov SM, Shay JW, Wright WE. Does a sentinel or a subset of short telomeres determine replicative senescence? Mol Biol Cell 2004;15:3709-18.

43. Rashid-Kolvear F, Pintilie M, Done SJ. Telomere length on chromosome 17q shortens more than global telomere length in the development of breast cancer. Neoplasia 2007;9:265-70.

44. Cohen SB, Graham ME, Lovrecz GO, Bache N, Robinson PJ, Reddel RR. Protein composition of catalytically active human telomerase from immortal cells. Science 2007;315:1850-3.

45. Wang Z, Kyo S, Maida Y, Takakura M, Tanaka M, Yatabe N, Kanaya T, Nakamura M, Koike K, Hisamoto K, Ohmichi M, Inoue M. Tamoxifen regulates human telomerase reverse transcriptase (hTERT) gene expression differently in breast and endometrial cancer cells. Oncogene 2002;21:3517-24.

46. Gao J, Chen D, Tian Y, Zhang J, Cai K. Effect of estrogen on telomerase activity in human breast cancer cells. J Huazhong Univ Sci Technolog Med Sci 2003; 23:286-7,293.

47. Park WC, Liu H, Macgregor Schafer J, Jordan VC. Deregulation of estrogen induced telomerase activity in tamoxifen-resistant breast cancer cells. Int J Oncol 2005; 27:1459-66.

48. Bast RC, Jr., Ravdin P, Hayes DF, Bates S, Fritsche H, Jr., Jessup JM, Kemeny N, Locker GY, Mennel RG, Somerfield MR. 2000 update of recommendations for the use of tumor markers in breast and colorectal cancer: clinical practice guidelines of the American Society of Clinical Oncology. J Clin Oncol 2001;19:1865-78.

49. Yu J, Sieuwerts AM, Zhang Y, Martens JW, Smid M, Klijn JG, Wang Y, Foekens JA. Pathway analysis of gene signatures predicting metastasis of node-negative primary breast cancer. BMC Cancer 2007;7:182.

50. Schmitt M, Harbeck N, Daidone MG, Brynner N, Duffy MJ, Foekens JA, Sweep FC. Identification, validation, and clinical implementation of tumor-associated biomarkers to improve therapy concepts, survival, and quality of life of cancer patients: tasks of the Receptor and Biomarker Group of the European Organization for Research and Treatment of Cancer. Int J Oncol 2004;25: 1397-406.

51. Williams C, Brunskill S, Altman D, Briggs A, Campbell H, Clarke M, Glanville J, Gray A, Harris A, Johnston K, Lodge M. Cost-effectiveness of using prognostic information to select women with breast cancer for adjuvant systemic therapy. Health Technol Assess 2006; 10:iii-iv,ix-xi,1-204.

52. Hayes DF, Bast RC, Desch CE, Fritsche H, Jr., Kemeny NE, Jessup JM, Locker GY, Macdonald JS, Mennel RG, Norton L, Ravdin P, Taube S, Winn RJ. Tumor marker utility grading system: a framework to evaluate clinical utility of tumor markers. J Natl Cancer Inst 1996;88: 1456-66.

53. Look MP, van Putten WL, Duffy MJ, Harbeck N, Christensen IJ, Thomssen C, Kates R, Spyratos F, Ferno M, Eppenberger-Castori S, Sweep CG, Ulm K, Peyrat JP, Martin PM, Magdelenat H, Brunner N, Duggan C, Lisboa BW, Bendahl PO, Quillien V, Daver A, Ricolleau G, Meijer-van Gelder ME, Manders P, Fiets WE, Blankenstein MA, Broet P, Romain S, Daxenbichler G, Windbichler G, Cufer T, Borstnar S, Kueng W, Beex LV, Klijn JG, O'Higgins N, Eppenberger U, Janicke F, Schmitt M, Foekens JA. Pooled analysis of prognostic impact of urokinase-type plasminogen activator and its inhibitor PAI-1 in 8377 breast cancer patients. J Natl Cancer Inst 2002;94:116-28.

54. Paik S, Shak S, Tang G, Kim C, Baker J, Cronin M, Baehner FL, Walker MG, Watson D, Park T, Hiller W, Fisher ER, Wickerham DL, Bryant J, Wolmark N. A multigene assay to predict recurrence of tamoxifen-treated, node-negative breast cancer. N Engl J Med 2004;351:2817-26.

CHAPTER ELEVEN

Summary

Samenvatting

11.1 SUMMARY

The aims of this thesis and outlined in more detail below were firstly to gain insight into the interaction between breast tumor cells and the surrounding stromal fibroblasts. Secondly, to integrate this concept of a multi-type cellular program in which the epithelial tumor cells, the tumor-associated fibroblasts, and diverse other cells in the tumor micro-environment are active participants, in our search for novel prognostic and predictive biomarkers. Finally, to place the concept of biomarkers in a larger context by looking at pathways rather then individual biomarkers. The more specific subjects discussed in this thesis were: 1) studies on the interaction between different biological systems, 2) studies on prognosis, and 3) studies on prediction to tamoxifen therapy response.

General introduction

To familiarize the reader with basic aspects of breast cancer and histological and molecular techniques used to study breast cancer relevant for this thesis, a general introduction was provided in **chapter 1**. To summarize this chapter, breast cancer is the most common type of cancer and accounts for about 30% of all cancers in women. In the well developed countries for women between 35-55 years of age it is overall even the main cause of death. Early detection and new treatment modalities, in part based on new insights, have improved clinical outcome and survival rates. The difficulty with breast cancer is that it is a heterogeneous disease which encompasses several entities with distinct prognosis. Furthermore, now there is an increasing insight that signals provided by the tissue supporting the epithelial cancer cells, *i.e.*, the stroma, can be responsible for genetic alterations that underlie tumor formation, can stimulate tumor growth and progression, and can dictate both therapeutic response and ultimate clinical outcome. So, cancer should be seen as a multicellular process in which the epithelial tumor cells themselves, the tumor-associated fibroblasts, and diverse other cells in the tumor micro-environment are active participants. To aid the clinician in the management of this heterogeneous and multi-type cellular disease, breast cancer is characterized by histology, stage, grade, and expression of biomarkers. Biomarkers are biological substances normally present in small amounts in tumor tissues or body fluids and encompass a wide variety of molecules, including transcription factors, cell surface receptors, and secreted proteins. These biomarkers are measured in the management of breast cancer patients for the following purposes: 1) early detection, 2) monitoring of advanced breast cancer patients, 3) prediction of prognosis, 4) prediction of site of relapse, and 5) prediction of therapeutic response. For this thesis it is important to understand the difference between a prognostic and a predictive biomarker: a prognostic marker predicts disease recurrence or tumor progression, independently of future treatment effects. A predictive biomarker predicts response or resistance to a specific therapy. Any change in disease status must be reflected by a change in the biomarker status. Surprisingly in this high-throughput era, the only established breast biomarkers are currently the serum-based cancer antigens CA 15-3, CA 125, CA 27-29 and CEA, the tissue-based estrogen and progesterone receptors, markers measuring DNA-content and/or cellular proliferation, the oncogene ERBB2, the tumor suppressor gene p53, the protease uPA and its inhibitor PAI-1, and two markers for hereditary breast cancer susceptibility (BRCA1 and BRCA2). In brief there is still an urgent need for new biomarkers.

Methods

The techniques to search for new biomarkers, to validate their usefulness, and assign biological functions has made great progress in this computerized era of proteomics to study proteins and genomics to study genes. Quantitative real-time reverse transcriptase polymerase chain reaction (real-time RT-PCR or qRT-PCR) is one of the methods that enables quantification of gene products as they accumulate in "real-time" during the PCR amplification process. With scientists pinning their hopes for new diagnostics and cures on molecular biomarkers, they need access to human tissue samples from large numbers of patients. For this, biobanks with stored tissues, body fluids and related products such as DNA, RNA and protein lysates are essential. One such well characterized fresh frozen breast tumor tissue bank has been established by the department of Medical Oncology, Erasmus Medical Center, Rotterdam, The Netherlands. This fresh frozen breast tumor tissue bank currently contains over 14,000 samples that are collected since 1978 and stored in liquid nitrogen immediately after surgery. Of 5,500 patients a computerized database with updated clinical follow-up is available. In addition, information on high quality extracts of DNA from 3,000 tissues, RNA from 2,000 tissues, and protein from over 10,000 tissues are stored in computerized databases. These RNA samples have been the very important source of clinical samples for the marker discovery studies discussed in this thesis.

Results and conclusions

To achieve the aims set for this thesis, the role of peri-tumoral fibroblasts in relation to the expression of components of the plasminogen activator (PA) system and the insulin-like growth factor (IGF) system in normal- and tumor-tissue-derived human breast fibroblasts exposed to various fibroblast growth factors (FGFs) was investigated in **chapter 2**. The *in vitro* data presented proposed that of the FGFs studied (FGF-1, -2, -4, -5, and -7), FGF-2 is the most attractive target for therapeutical strategies aimed at diminishing the contribution of stromal fibroblasts in the PA-directed proteolysis.

With our aging population, especially the age-related increase in breast cancer incidence is worrying. In **chapter 3** the role of peri-tumoral fibroblasts was investigated in relation to this important aspect. For this, we have investigated whether breast fibroblasts aged *in vitro* through passage in culture displayed altered levels of components of the PA system and growth factors that are known to modulate that system. Our results showed that aging accompanied by telomere loss induces *PAI-1* and *FGF-1* mRNA expression in all breast fibroblast strains, increases *uPA* and decreases *IGF-1* mRNA expression in a subset, and increases matrix metalloproteinases-2 (MMP-2) protein expression only in tumor-derived breast fibroblasts. Thus, the aging-dependent levels of these biomarkers in stromal breast fibroblasts could contribute to breast cancer progression.

In **chapter 4** the importance of the multi-cellular notion was experienced in the clinical setting. Here we evaluated the predictive value of the disintegrin and metalloproteinases, ADAM-9, ADAM-10, ADAM-11, and ADAM-12, and of the matrix metalloproteinases, MMP-2 and MMP-9, in patients with recurrent breast cancer treated with tamoxifen. The data showed that especially for primary tumors containing a high proportion of stromal elements, the assessment of mRNA expression levels of *ADAM-9* and *ADAM-11* could be useful to identify patients with recurrent breast cancer who are likely to benefit or fail from tamoxifen therapy.

One of the applications of qRT-PCR is validation of putative biomarkers that emerge from microarray experiments in a larger patient cohort. One such biomarker is cyclin E2 (*CCNE2*), a gene that overlapped between two independently established prognostic gene signatures. In **chapter 5** we described the prognostic evaluation of cyclin E with this quantitative method in a large cohort of 635 lymph node-negative (LNN) breast cancer patients that did not receive systemic adjuvant therapy. The study showed that both *CCNE1* and *CCNE2* qualified as independent prognostic markers for LNN breast cancer patients, and that *CCNE1* may provide additional information for specific subgroups of patients with stroma-enriched primary tumors.

Another validation study, discussed in **chapter 6**, concerned the *HOXB13*-to-*IL17BR* expression ratio that was previously identified to predict clinical outcome of breast cancer patients treated with adjuvant tamoxifen. Here we demonstrated that, in addition to tamoxifen therapy failure for advanced disease, high *HOXB13*-to-*IL17BR* ratio expression levels are also associated with intrinsic tumor aggressiveness.

Having discovered and identified two alternatively spliced variants of tissue inhibitor of metalloproteinases-1 (*TIMP1*) mRNA in cancer cell lines and colon cancer tissue (**chapter 7**), the prognostic value of these variants were tested in 1301 primary breast cancer specimens (**chapter 8**). While high concentrations of TIMP-1 protein are associated with poor prognosis, high concentrations of *TIMP1-v1+2* mRNA measured in the primary tumors of breast cancer patients were associated with good prognosis. Such a differential association, implicating the presence of possible posttranscriptional mechanisms, might help our understanding of the role of TIMP-1 with respect to breast cancer progression.

As discussed in chapter 5, published prognostic gene signatures in breast cancer have few genes in common. In **chapter 9** we demonstrated that these divergent gene sets classifying patients for the same clinical endpoint represented similar biological processes and that pathway-derived signatures can be used to predict prognosis. Such signatures that define tumors according to their vital pathways may provide crucial guidance for designing appropriate drug combinations

General discussion and future perspectives

Finally, in **chapter 10**, three concepts that have emerged from the studies described in this thesis in relation to future perspectives were discussed in more depth, leading to the following conclusions and recommendations:

Firstly, solely based on tumor cellularity (ratio of epithelial tumor cells over stromal cells) we were able to roughly distinguish between histological phenotypes and microarray based genotypes with different prognostic features. In addition, the observations underlined the notion that cancer should be seen as a multicellular program in which the epithelial tumor cells themselves, the tumor-associated fibroblasts, and diverse other cells in the tumor micro-environment are active participants.

Secondly, work of our group showed that a condensation of genes localized on the long arm of chromosome 17q12-25 is, in addition to an association of genes in this region with breast cancer risk in general, associated with sensitivity to tamoxifen. Especially the genes located in this chromosomal area with increased expression levels in tamoxifen unresponsive cases were proposed as promising candidates for targeted therapy.

Lastly, it has been shown in this thesis that qRT-PCR is a sensitive, fast, quantitative, and cost-effective method, extremely suitable to quantify mRNA levels of genes that are differentially expressed in the primary tumors of breast cancer patients with different prognostic and predictive features. Even when no antibodies are available to detect protein, qRT-PCR at least enables quantitative assessment of mRNA levels of candidate markers, nowadays also in formalin-fixed paraffin-embedded (FFPE) tissue. Therefore, there is no doubt that the single gene or multiplex qRT-PCR approach will remain an important quantitative method for fast screening of diagnostic markers and therapeutic targets.

11.2 SAMENVATTING

Het eerste doel van het in dit proefschrift beschreven onderzoek was inzicht te krijgen in de wisselwerking tussen borsttumorcellen en de cellen in het omringende stroma. Een tweede doel was om dit idee van een multitype cellulaire tumor, waarin naast epitheliale tumorcellen ook tumor-geassocieerde fibroblasten en diverse andere typen cellen een actieve rol spelen, te integreren in onze zoektocht naar nieuwe prognostische en predicatieve markers. Ten slotte was er het doel om het concept van biomarkers in een groter geheel te plaatsen door naar de biologische paden te kijken waar ze onderdeel van zijn, in plaats van naar de individuele biomarkers. Meer specifiek: de onderwerpen die in dit proefschrift beschreven werden zijn: 1) studies naar de wisselwerking tussen verschillende biologische systemen, 2) studies met betrekking tot prognose, en 3) studies met betrekking tot het voorspellen of een patiënt wel of niet zal reageren op tamoxifen therapie.

Algemene inleiding

Om de lezer meer bekend te maken met het basisprincipe van borstkanker en de histologische en moleculaire technieken die worden gebruikt om borstkanker te bestuderen, is er een algemene inleiding opgenomen in **hoofdstuk 1**. Samengevat is in dit hoofdstuk uitgelegd dat borstkanker de bij vrouwen meest voorkomende soort kanker is, verantwoordelijk voor 30% van alle vrouwelijke kankerpatiënten. In de westerse wereld is het zelfs de belangrijkste doodsoorzaak voor vrouwen in de leeftijd van 35 tot 55 jaar. Vroege opsporing en nieuwe behandelingsmethodes, deels gebaseerd op nieuwe inzichten, hebben tot een verbetering in de behandeling en een daling van sterfte ten gevolge van borstkanker geleid. Maar het probleem met borstkanker is dat het een heterogene ziekte is die meerdere vormen omvat, ieder met een eigen specifiek ziekteverloop. Bovendien is er nu groeiend inzicht dat het weefsel dat de tumorcellen omgeeft (het stroma), signalen kan afgeven die mogelijk verantwoordelijk zijn voor de genetische veranderingen die voorafgaan aan het ontstaan van een tumor, tumorgroei en uitzaaiingen bevorderen, sturing geven aan de manier waarop een tumor op therapie reageert en het uiteindelijke ziekteverloop bepalen. Daarom moet kanker worden gezien als een multitype cellulair proces waarin de epitheliale tumorcellen zelf, de tumorgeassocieerde fibroblasten en diverse andere cellen die zich in een tumor in de directe omgeving van de epitheliale tumorcellen bevinden, allen een actieve rol spelen. Om de dokter te helpen met de behandeling van deze heterogene en multitype cellulaire ziekte, wordt kanker gekarakteriseerd door histologie, stagering, gradering en expressie van biomarkers. Biomarkers zijn biologische stoffen die gewoonlijk in kleine hoeveelheid in tumorweefsel of lichaamsvocht aanwezig zijn en omvatten een grote verscheidenheid aan moleculen zoals transcriptie factoren, celreceptoren en uitgescheiden eiwitten. Deze biomarkers worden tijdens de begeleiding van de borstkankerpatiënt om de volgende redenen gemeten: 1) voor vroege opsporing, 2) ter begeleiding van patiënten met uitgezaaide ziekte, 3) om het ziekteverloop te voorspellen, 4) om te voorspellen waar de uitzaaiing van de tumor zal plaatsvinden, en 5) om te voorspellen of de patiënt zal reageren op een therapie. Het is voor dit proefschrift belangrijk het verschil tussen een prognostische en een predicatieve biomarker te begrijpen: een prognostische biomarker voorspelt de kans op terugkeer van de ziekte of op tumorgroei, onafhankelijk van toekomstige behandelingseffecten. Een predicatieve biomarker voorspelt of de patient zal reageren op een specifieke behandeling. Elke verandering in het verloop van de ziekte moet worden weerspiegeld door een verandering in de waarden van de biomarker. Verrassend genoeg in deze 'high-throughput' eeuw, zijn de enige algemeen erkende biomarkers voor borstkanker momenteel de in bloedserum aanwezige antistoffen CA 15-3, CA 125, CA 27-29 en CEA, en de in tumorweefsel gemeten receptoren voor oestrogeen en progesteron, markers die de hoeveelheid DNA en/of celdelingsnelheid meten, het oncogen ERBB2, het tumorsuppressor gen p53, de eiwitafbrekende protease uPA en zijn remmer PAI-1, en twee markers om de gevoeligheid voor erfelijke borstkanker te meten (BRCA1 en BRCA2). Kortom, er is een dringende vraag naar nieuwe biomarkers.

Methodes

De technieken om naar nieuwe biomarkers te zoeken, hun bruikbaarheid te testen en om ze een biologische functie te geven, hebben een grote vooruitgang gemaakt in deze gecomputeriseerde eeuw van 'proteomics' om eiwitten te bestuderen en 'genomics' om genen te bestuderen. Kwantitatieve real-time reverse transcriptase polymerase chain reaction (real-time RT-PCR of qRT-PCR) is een van de methodes die het mogelijk maakt genproducten te kwantificeren als zij zich ophopen in de tijd ("real-time") tijdens het PCR amplificatieproces. Wetenschappelijke onderzoekers, die voor nieuwe diagnostiek- en therapiemethodes hun hoop hebben gevestigd op moleculaire markers, moeten kunnen beschikken over materialen van een grote verscheidenheid aan patiënten. Hiertoe zijn biobanken met opgeslagen weefsels, lichaamsvochten en gerelateerde producten zoals DNA, RNA en eiwitextracten uiterst belangrijk. Een voorbeeld van zo'n goed gekarakteriseerde bank met vers ingevroren borstkankerweefsel is opgezet door de afdeling Medische Oncologie aan het Erasmus Medisch Centrum te Rotterdam in Nederland. Deze bank bevat momenteel meer dan 14,000 monsters van borstkankerweefsel die sinds 1978 zijn verzameld, en direct na de operatie opgeslagen zijn in vloeibare stikstof. Van 5,500 patiënten is er een geautomatiseerd bestand met bijgewerkte klinische gegevens beschikbaar. Bovendien is er informatie betreffende de hoge kwaliteitsextracten van DNA uit 3,000 weefsels, van RNA uit 2,000 weefsels, en van eiwit uit 10,000 weefsels opgeslagen in geautomatiseerde gegevensbestanden. De klinische RNA monsters zijn een zeer belangrijke bron geweest voor de studies om nieuwe markers te ontdekken zoals deze in dit proefschrift worden beschreven.

Resultaten en conclusies

Om de doelstellingen te bereiken die voor dit proefschrift waren opgesteld, is in **hoofdstuk 2** de rol van normale en met tumorweefsel geassocieerde fibroblasten onderzocht in relatie tot expressie van componenten van het plasminogeenactivator (PA) systeem en het 'insuline-like-groeifactor' (IGF) systeem, voor en nadat deze fibroblasten aan verschillende groeifactoren voor fibroblasten (FGFs) waren blootgesteld. De *in vitro* data die in dit hoofdstuk gegeven worden, suggereerden dat van de bestudeerde FGFs (FGF-1, -2, -4, 5, en -7), FGF-2 het meest interessante doelwit is voor therapeutische strategieën die gericht zijn op het verminderen van de bijdrage van de stromale fibroblasten in het proces van de -door het PA-systeem aangestuurde- eiwitafbraak.

Door de toenemende vergrijzing van de bevolking is met name de leeftijdsgebonden toename in de borstkankerincidentie zorgwerkend. In **hoofdstuk 3** is de functie van normale en met tumorweefsel geassocieerde fibroblasten in relatie tot dit belangrijke onderwerp onderzocht. Hiertoe hebben we bekeken of fibroblasten, die we in het laboratorium in kweek hebben laten verouderen, veranderingen gaven in de concentraties van bestanddelen van het PA systeem en van groeifactoren waarvan bekend is dat ze het PA-systeem beinvloeden. Onze resultaten lieten zien dat veroudering gecombineerd met verlies van telomeerlengte in alle fibroblastkweken gepaard ging met een toename in de productie van *PAI-1* en *FGF-1* mRNA, in een subset van de fibroblastkweken met een toename van *uPA* en een afname van *IGF-1* mRNA, en alleen in fibroblasten afkomstig uit tumorweefsel met een toename in de eiwitproductie van matrixmetalloproteinases-2 (MMP-2). Derhalve kunnen de leeftijdsafhankelijke veranderingen van biomarkers in stromale borstfibroblasten bijdragen aan borstkankerprogressie.

In **hoofdstuk 4** is het belang van het multitype cellulaire concept in een klinische setting ondervonden. Hier hebben we in patiënten, die met tamoxifen waren behandeld voor uitgezaaide borstkanker, gekeken naar de predicatieve waarde van de disintegrine en metalloproteinases ADAM-9, ADAM-10, ADAM-11, en ADAM-12, en de matrixmetalloproteinases MMP-2 en MMP-9. De analyses lieten zien dat met name voor primaire tumoren die voor een groot deel uit stromale bestanddelen bestaan, het bepalen van *ADAM-9* en *ADAM-10* mRNA concentraties bruikbaar zou kunnen zijn om patiënten te

identificeren die een grotere kans hebben wel of niet te reageren op een behandeling met tamoxifen voor teruggekeerde borstkanker.

Een van de toepassingen van qRT-PCR is het in een groter patiëntenbestand valideren van in microarray-experimenten gevonden vermoedelijke biomarkers. Een voorbeeld van zo'n biomarker is cycline E2 (*CCNE2*), een gen dat voorkwam in twee onafhankelijk tot stand gekomen prognostische genprofielen. In **hoofdstuk 5** hebben we beschreven hoe we met deze kwantitatieve methode de prognostische waarde van cycline E hebben geëvalueerd in een groot bestand van 635 borstkanker patiënten met negatieve lymfklieren (LNN) die geen systemische aanvullende behandeling hadden gehad. De studie liet zien dat zowel *CCNE1* als *CCNE2* kwalificeerden als onafhankelijke prognostische markers voor LNN borstkankerpatiënten, en dat *CCNE1* extra informatie kan geven voor specifieke subgroepen patiënten met stroma-rijke primaire tumoren.

Een andere controlestudie, beschreven in **hoofdstuk 6**, betrof de *HOXB13-IL17BR* ratio, een ratio die al eerder was geïdentificeerd als een maat op grond waarvan het ziekteverloop kon worden voorspeld van borstkankerpatiënten die adjuvant behandeld waren met tamoxifen. Hier hebben wij aangetoond dat een hoge *HOXB13-IL17BR* ratio, bovenop de associatie met het falen van tamoxifen therapie voor uitgezaaide ziekte, ook geassocieerd is met de intrinsieke agressiviteit van een tumor.

Nadat wij twee alternatief gesplitste varianten van 'tissue-inhibitor of metalloproteinases-1' (*TIMP1*) mRNA hadden ontdekt en deze verder hadden geïdentificeerd in kankercellijnen en darmkankerweefsel (**hoofdstuk 7**), hebben wij de prognostische waarde van deze varianten verder onderzocht in 1301 primaire borstkankermonsters (**hoofdstuk 8**). Terwijl hoge concentraties TIMP-1 eiwit worden geassocieerd met een slechte prognose, vonden wij dat in de primaire borstkanker gemeten hoge concentraties *TIMP1-v1+2* mRNA zijn geassocieerd met een goede prognose. Een dergelijke differentiële associatie, mogelijk een aanwijzing voor de aanwezigheid van posttranscriptionele mechanismes, zou ons kunnen helpen de rol van TIMP-1 ten aanzien van borstkankerprogressie beter te begrijpen.

Zoals besproken in hoofdstuk 5, hebben gepubliceerde prognostische genprofielen maar een paar gemeenschappelijke genen. In **hoofdstuk 9** hebben we aangetoond dat deze uiteenlopende genensets, die patiënten voor eenzelfde klinisch eindpunt classificeren, deel uitmaken van overeenkomstige biologische processen, en dat het daarom beter is om een voorspelling te geven op grond van profielen die zulke biologische paden beschrijven. Zulke profielen, die tumoren karakteriseren op grond van biologisch actieve paden, zouden cruciale informatie kunnen verschaffen die nodig is om geschikte medicijncombinaties te ontwikkelen.

Algemene discussie en toekomstvooruitzichten

In **hoofdstuk 10** tenslotte, zijn drie onderdelen verder uitgewerkt die gemeenschappelijk uit de beschreven studies naar voren kwamen. Dit resulteerde in de volgende conclusies en aanbevelingen:

Ten eerste, enkel en alleen gebaseerd op de samenstelling van de tumor (de verhouding tussen epitheliale tumorcellen en stromale cellen), zijn we in staat geweest een grof onderscheid te maken tussen histologische fenotypen en op microarray gebaseerde genotypen met verschillende prognostische eigenschappen. Bovendien onderstreepten deze waarnemingen het belang van de opvatting dat kanker gezien moet worden als een proces waarin meerdere celtypen, zoals de epitheliale tumorcellen zelf, de tumorgeassocieerde fibroblasten en diverse andere cellen die zich in een tumoromgeving bevinden, actieve deelnemers zijn.

Ten tweede bleek uit werk van onze groep dat een concentratie van genen op de lange arm van chromosoom 17q12-25, aanvullend op de associatie van genen in dit gebied met het risico op borstkanker in het algemeen, geassocieerd is met gevoeligheid voor tamoxifen. Met name de genen in dit chromosomale gebied die een verhoogde expressie laten zien in tamoxifen ongevoelige tumoren, werden als veelbelovende kandidaten voor doelgerichte therapie aanbevolen.

Ten slotte is in dit proefschrift aangetoond dat qRT-PCR een gevoelige, snelle, kwantitatieve, kostenbesparende methode is, die uitermate geschikt is om mRNA concentraties te meten van genen die verschillend tot expressie komen in de primaire tumoren van borstkankerpatiënten met verschillende prognostische en predicatieve kenmerken. Zelfs wanneer er geen antilichamen beschikbaar zijn om eiwit aan te tonen, is men met qRT-PCR in ieder geval in staat de mRNA concentraties kwantitatief te meten, vandaag de dag ook in formaline-gefixeerd weefsel dat in paraffine is ingebed. Er bestaat daarom geen twijfel dat het meten van een enkel gen, of meerdere genen in een multiplex reactie, met behulp van qRT-PCR een belangrijke kwantitatieve methode zal blijven om snel te screenen op diagnostische en therapeutische markers.

LIST OF PUBLICATIONS

PUBLICATIONS ANIETA M. SIEUWERTS

Recent puplications with first authorship included in the thesis

1. **Sieuwerts AM**, Usher PA, Meijer-van Gelder ME, Timmermans M, Martens JWM, Brünner N, Klijn JGM, Offenberg H and Foekens JA. Concentrations of TIMP1 mRNA splice variants and TIMP-1 protein are differentially associated with prognosis in primary breast cancer. Clin Chem 2007;53 (7):1280-1288.

2. **Sieuwerts AM***, Jansen MP*, Look MP, Ritstier K, Meijer-van Gelder ME, van Staveren IL, Klijn JGM, Foekens JA and Berns EM. HOXB13-to-IL17BR expression ratio is related with tumor aggressiveness and response to tamoxifen of recurrent breast cancer: a retrospective study. J Clin Oncol 2007;25:662-668.
   *both authors contributed equally to the publication

3. **Sieuwerts AM**, Look MP, Meijer-van Gelder ME, Timmermans M, Trapman AM, Rodriguez Garcia R, Arnold M, Goedheer AJ, de Weerd V, Portengen H, Klijn JGM and Foekens JA. Which cyclin E prevails as prognostic marker for breast cancer? Results from a retrospective study involving 635 lymph node-negative breast cancer patients. Clin Cancer Res 2006;12:3319-3328.

4. **Sieuwerts AM**, Meijer-van Gelder ME, Timmermans M, Trapman AM, Rodriguez Garcia R, Arnold M, Goedheer AJ, Portengen H, Klijn JGM and Foekens JA. How ADAM-9 and ADAM-11 differentially from estrogen receptor predict response to tamoxifen treatment in patients with recurrent breast cancer: a retrospective study. Clin Cancer Res 2005;11:7311-7321.

5. **Sieuwerts AM**, Martens JWM, Dorssers LCJ, Klijn JGM and Foekens JA. Differential effects of fibroblast growth factors on the plasminogen-activator and insulin-like-growth-factor systems in human breast fibroblasts. Thromb Haemost 2002;87:674-683.

Recent publications with second authorship included in the thesis

6. Yu JA, **Sieuwerts AM**, Zhang Y, Martens JMW, Smid M, Klijn JGM, Wang Y and Foekens JA. Pathway analysis of gene signatures predicting metastasis of node-negative primary breast cancer. BMC Cancer 2007;7:182.

7. Usher PA, **Sieuwerts AM**, Bartels A, Lademann U, Nielsen HJ, Holten-Andersen L, Foekens JA, Brünner N and Offenberg H. Identification of alternatively spliced TIMP-1 mRNA in cancer cell lines and colon cancer tissue. Mol Oncol 2007;1:205-215.

8. Martens JWM, **Sieuwerts AM**, Bolt-de Vries J, Bosma PT, Swiggers SJJ, Klijn JGM and Foekens JA. Ageing of stromal-derived human breast fibroblasts might contribute to breast cancer progression. Thromb Haemost 2003;89:393-404.

Previous publications with first authorship

9. **Sieuwerts AM**, Klijn JGM and Foekens JA. Insulin-like-growth-factor-1 (IGF-1) and urokinase-type-plasminogen-activator (uPA) are inversely related in human breast fibroblasts. Mol Cell Endocrinol 1999;154:179-185.

10. **Sieuwerts AM**, Klijn JGM, Henzen-Logmans SC and Foekens JA. Cytokine-regulated urokinase-type plasminogen activator (uPA) production by human breast fibroblasts in vitro. Breast Cancer Res Treatm 1999;55:9-20.

11. **Sieuwerts AM**, Klijn JGM, Henzen-Logmans SC, Bouwman I, van Roozendaal CEP, Peters HA, Setyono-Han B and Foekens JA. Urokinase-type plasminogen activator (uPA) production by primary human breast (myo)-fibroblasts in vitro: influence of transforming growth factor-β1 (TGFβ1) compared to factor(s) released by human epithelial carcinoma cells. Int J Cancer 1998;76:829-835.

12. **Sieuwerts AM**, Klijn JGM and Foekens JA. Assessment of the invasive potential of human gynaecological tumor cell lines with the in vitro Boyden chamber assay: influences of filteradhesion. Clin Exp Metas 1997;15:53-62.

13. **Sieuwerts AM**, Klijn JGM, Peters HA and Foekens JA. The MTT assay scrutinized: how to use this assay reliably to measure metabolic activity of cell cultures in vitro for the assessment of growth characteristics, IC50-values and cell survival. Eur J Clin Chem Clin Biochem 1995;33:813-823.

Other publications with second authorship

14. Kotzsch M, **Sieuwerts AM**, Grosser M, Meye A, Fuessel S, Meijer-van Gelder ME, Smid M, Schmitt M, Baretton G, Luther T, Magdolen V, Foekens JA. Urokinase receptor splice variant uPAR-del4/5-associated gene expression in breast cancer: Identification of rab31 as an independent prognostic factor. Submitted.

15. Meijer D, **Sieuwerts AM**, Look MP, van Agthoven T, Foekens JA, Dorssers LCJ. FGFR4 predicts failure on tamoxifen therapy in patients with recurrent breast cancer. Submitted.

16. Zheng PP, **Sieuwerts AM**, Luider TM, van der Weiden M, Sillevis-Smitt PA, Kros JM. Differential expression of splicing variants of the human caldesmon gene (CALD1) in glioma neovascularization versus normal brain microvasculature. Am J Pathol 2004;164:2217-2228.

17. Bontenbal M, **Sieuwerts AM**, Peters HA, van Putten WLJ, Foekens JA and Klijn JGM. Uptake and distribution of doxorubicin in hormone-manipulated human breast cancer cells in vitro. Breast Cancer Res Treat 1998;51:139-148.

18. Foekens JA, **Sieuwerts AM**, Stuurman-Smeets EMJ, Peters HA and Klijn JGM. Effects of suramin on cell cycle kinetics of MCF-7 human breast cancer cells in vitro. Br J Cancer 1993;67:232-236.

19. Foekens JA, **Sieuwerts AM**, Stuurman-Smeets EMJ, Dorssers LCJ, Berns EMJJ and Klijn JGM. Pleiotropic actions of suramin on the proliferation of human breast cancer cells in vitro. Int J Cancer 1992;51:439-444.

20. Bontenbal M, **Sieuwerts AM**, Peters HA, Sonneveld P, Foekens JA and Klijn JGM. Manipulation of cell cycle kinetics; influence on the cytotoxicity of doxorubicin in human breast cancer cells. J Steroid Biochem Molec Biol 1990;37:1097-1102.

21. Bontenbal M, **Sieuwerts AM**, Klijn JGM, Peters HA, Krijnen HL, Sonneveld P and Foekens JA. Effect of hormonal manipulation on cell cycle kinetics and doxorubicin cytotoxicity of human breast cancer cells: analysis by dual-parameter flow cytometry. Br J Cancer 1989;60:688-692.

Additional publications with co-authorship

22. Smid M, Wang Y, Zhang Y, **Sieuwerts AM**, Yu J, Klijn JGM, Foekens JA, Martens JWM. Subtypes of breast cancer show preferential site of relapse. Submitted.

23. Smid M, Wang Y, Klijn JG, **Sieuwerts AM**, Zhang Y, Atkins D, Martens JW, Foekens JA. Genes associated with breast cancer metastatic to bone. J Clin Oncol 2006;24:2261-2267.

24. Foekens JA, Atkins D, Zhang Y, Sweep FC, Harbeck N, Paradiso A, Cufer T, **Sieuwerts AM**, Talantov D, Span PN, Tjan-Heijnen VC, Zito AF, Specht K, Hoefler H, Golouh R, Schittulli F, Schmitt M, Beex LV, Klijn JG, Wang Y. Multicenter validation of a gene expression-based prognostic signature in lymph node-negative primary breast cancer. J Clin Oncol 2006;24:1665-1671.

25. Yang F, Foekens JA, Yu J, **Sieuwerts AM**, Timmermans M, Klijn JG, Atkins D, Wang Y, Jiang Y. Laser microdissection and microarray analysis of breast tumors reveal ER-alpha related genes and pathways. Oncogene 2006;25:1413-1419.

26. Setyono-Han B, Sturzebecher J, Schmalix WA, Muehlenweg B, **Sieuwerts AM**, Timmermans M, Magdolen V, Schmitt M, Klijn JG, Foekens JA. Suppression of rat breast cancer metastasis and reduction of primary tumour growth by the small synthetic urokinase inhibitor WX-UK1. Thromb Haemost 2005;93:779-786.

27. Jansen MP, Foekens JA, van Staveren IL, Dirkszwager-Kiel MM, Ritsier K, Look MP, Meijer-van Gelder ME, **Sieuwerts AM**, Portengen H, Dorssers LCJ, Klijn JGM and Berns EMJJ. Molecular classification of tamoxifen resistant breast carcinomas by gene expression profiling. J Clin Oncol 2005;23:732-740.

28. Wang Y, Klijn JGM, Zhang Y, **Sieuwerts AM**, Look MP, Yang F, Talantov D, Timmermans M, Meijer-van Gelder ME, Yu J, Jatkoe T, Berns EMJJ, Atkins D and Foekens JA. Gene expression profiles to predict distant metastasis of lymph-node-negative primary breast cancer. Lancet 2005; 365:671-679.

29. Martens JWM, Nimmrich I, Koenig T, Look MP, Harbeck N, Model F, Bolt-de Vries J, **Sieuwerts AM**, Portengen H, Meijer-van Gelder ME, Piepenbrock C, Olek A, Höfler H, Klijn JGM, Schmitt M, Maier S and Foekens JA. Association of DNA methylation of phosphoserine aminotransferase with response to endocrine therapy in patients with recurrent breast cancer. Cancer Res 2005;15:4101-4117.

30. Van Roozendaal CEP, Klijn JGM, **Sieuwerts AM**, Henzen-Logmans SC and Foekens JA. Role of urokinase plasminogen activator in human breast cancer: active involvement of stromal fibroblasts. Fibrinolysis 1996;10(Suppl.2):79-83.

31. Klijn JGM, Setyono-Han B, Bakker GH, van der Burg MEL, Bontenbal M, Peters HA, **Sieuwerts AM**, Berns PMJJ and Foekens JA. Growth factor-receptor pathway interfering treatment by somatostatin analogs and suramin: (pre)clinical studies. J Steroid Biochem Molec Biol 1990;37: 1089-1096.

CURRICULUM VITAE

CURRICULUM VITAE ANIETA M. SIEUWERTS

Anieta M. Sieuwerts was born on November 27th, 1957 in 's Hertogenbosch, The Netherlands. After passing her high school exam at the Casimir College in Vlaardingen in 1976 she followed several studies and had several jobs before she, aged 25, finally found her niche at the Life Science school (HLO-biochemistry) in Rotterdam to become a technician. She started her scientific career in 1987 in the department of Medical Oncology at the Dr. Daniel den Hoed Clinic in Rotterdam as a research technician helping others with their research. A few years later she was given the opportunity to perform and publish her own research ranging from evaluation of *in vitro* MTT- and invasion assays to scientific research articles related to urokinase-type plasminogen activator production by human breast fibroblasts. During this time she was promoted to senior research technician. Due to the rapid development in the field of genomics and proteomics, her department decided to process their frozen human breast tumor tissue bank into a RNA, DNA and protein bank. In 2003 she initiated this process with respect to methodology and quality controls and supervised a team of technicians processing these samples. In this period she also started to work as a PhD student at the department of Medical Oncology, Erasmus Medical Center Rotterdam, the Netherlands, under the supervision of Prof.dr. J.G.M Klijn and Dr. J.A. Foekens. Since 2004 she is employed as a scientific research assistant and manages this RNA, DNA and protein bank. In this capacity she is engaged in studies that involve SNP arrays, methylation assays, gene expression arrays, real-time PCR, western blotting, ELISA, and immunohistochemistry. Because of the uniqueness of this bank, this resource is, together with her expertise, also extensively used in collaborative studies with other European and American research groups. Several of the publications released in between 2005 to 2007 are the first examples of these fruitful cooperations. In 2005 she received the '*AACR-GlaxoSmithKline Outstanding Clinical Scholar Award* ' for her retrospective study on how ADAM-9 and ADAM-11 differentially from estrogen receptor predict response to tamoxifen treatment in patients with recurrent breast cancer. After obtaining her doctor's degree she intends to continue her work at the Department of Medical Oncology at the Erasmus Medical Center in Rotterdam.

DANKWOORD

DANKWOORD

En dan nu het dankwoord. Sommige mensen vinden dit het leukste om te schrijven, ik vind het iets minder leuk, bang als ik ben iemand ten onrechte te vergeten. Mocht dat ondanks mijn beste bedoelingen toch het geval zijn, bij deze mijn oprechte verontschuldigingen!

In de eerste plaats wil ik mijn ouders bedanken die mij alle ruimte hebben gegeven om een goede opleiding te volgen. Mede dankzij jullie onvoorwaardelijke ondersteuning heb ik het zover geschopt.

Zonder het vertrouwen en de hulp tot in de late uurtjes van mijn promotor professor Jan Klijn en mijn copromotor dr. John Foekens had ik het natuurlijk nooit tot dit hoofdstuk kunnen brengen. John, ik heb niet veel ervaring met leidinggevenden, maar voor mij ben je het beste wat mij had kunnen overkomen. Ik hoop dat onze toekomst net zo prettig en harmonieus gaat verlopen als ons verleden. Hier wil ik ook graag de leden van de leescommissie, professor Fred Sweep, professor Lex van Eggermont en dr. Els Berns, bedanken die, weliswaar voordat ze wisten hoe dik het boekwerk ging worden, zonder aarzeling hebben toegezegd zich aan deze taak te willen wijden en dat vervolgens ook met verve hebben gedaan. Mede dankzij de snelle actie van de leescommissie heb ik voldoende tijd gehad om dit boekje een mooie afwerking te geven, nogmaals dank hiervoor.

Maar zonder Siert Bolt, Joan Bolt en Mieke Timmermans had dit boekje er nooit zo mooi en volledig uitgezien als nu. Siert, die met een ongekend enthousiasme de taak van DTP-er op zich heeft genomen, de onderhandelingen met de drukkers heeft gevoerd, mij attent maakte op onregelmatigheden, en tot het einde toe geduldig bleef als ik toch weer iets anders wilde. Joan en Siert, waar ik 's avonds altijd welkom was om onder het genot van koffie, sigaretten en een wijntje de stand van zaken door te nemen waarna ik dan weer enthousiast en vol goede moed met een dik pak papier huiswaarts ging. En mijn collega's door dik en dun, Joan en Mieke, wat gaan wij al lang mee zo samen. Mieke, ik zie het echt als een kroon op mijn werk dat jij de kaft van 'ons' boekje zo'n mooie en toepasselijke vorm hebt kunnen geven. En alsof dat niet genoeg was, wilde je je ook nog wel als paranimf inzetten voor de promotie. Zelfs voordat je wist dat je in het zeer goede gezelschap van John Martens zou toeven. John M, het 'jonkie' onder ons die ik echter in de paar jaren dat wij nu samen werken heb leren kennen als een eerlijke, betrouwbare, rechtdoorzee collega waar je op kan bouwen. Nooit te beroerd voor een praatje en altijd in voor een goede en open discussie. Een wereldgozer.

Het mag duidelijk zijn, voordat het tot een thesis kan komen, is er een hecht team nodig om resultaten te krijgen die de moeite van het opschrijven waard zijn. "Als je niet kunt delen, dan kun je ook niet vermenigvuldigen". Hiertoe wil ik hier eerst alle coauteurs van de publicaties die in deze thesis zijn opgenomen bedanken: Anita Trapman, Anneke Goedheer, Annette Bartels, Els Berns, Hanne Offenberg, Hans Jørgen Nielsen, Henk Portengen, Iris van Staveren, Jack Yu, Jan Klijn, Joan Bolt-de Vries, John Foekens, John Martens, Kirsten Ritstier, Lambert Dorssers, Lars Holten-Andersen, Marcel Smid, Marion Meijer-van Gelder, Maurice Jansen, Maxime Look, Mieke Timmermans, Miranda Arnold, Nils Brunner, Pernille Usher, Peter Bosma, Roberto Rodriguez Garcia, Susan Swiggers, Ulrik Lademann, Vanja de Weerd, Yi Zhang, en Yixin Wang.
Een voorbeeld van zo'n superteam dat hier zeker extra vermelding verdient, is het RDE team dat zich de afgelopen jaren zo nauwgezet en eensgezind heeft gewijd aan het opwerken van de RNA, DNA en Eiwit samples. Henk, kamergenoot, stadsgenoot, de laatste der Mohikanen. Dat waren toch leuke tijden zo 's morgens vroeg samen met jou in de auto op weg naar de Daniel en terug met Tiny die altijd wel iets leuks had te vertellen. Toen ik uiteindelijk dan toch zelf in het bezit van rijbewijs en eigen auto kwam, was dat afgelopen, maar nog wel veel contact via de e-mail waar jij altijd zo snel reageerde op mijn zoveelste verzoek voor database bestanden ten behoeve van de RDE-bank. Ik zal altijd met plezier

en ondertussen bijna met weemoed terugdenken aan wat ik van jou en Harry heb geleerd: ondanks jullie gemopper over dat jonge grut dat niet meer kan pipetteren, wat mij betreft niets dan goeds over de oude garde. Mieke Timmermans, met jouw uitgebreide kennis van alles wat met immunologie en histologie heeft te maken; zonder jouw expertise had een van de overkoepelende onderwerpen van deze thesis, de rol van stroma in borstkanker, nooit zo goed uit de verf kunnen komen. Anita Trapman, altijd in om een nieuwe techniek te leren en daardoor nu degene die als het nodig is overal inzetbaar is, geweldig toch? Anneke Goedheer, onze vliegende keep die als geen ander orde in de chaos wist te brengen; mens wat mis ik jouw droge humor en wervende activiteit op ons lab. Miranda Arnolds, nauwgezet en als geen ander in staat een nieuwe techniek uit te werken, complimenten hoor. Roberto Rodriguez Garcia, onze onverstoorbare steun en toeverlaat, nooit te beroerd iets aan te pakken. Anneke, Miranda en Roberto, ik wil jullie hier nogmaals bedanken voor alles wat jullie voor de RDE bank en mij hebben gedaan en kan alleen maar blij zijn dat jullie uiteindelijke ergens anders een goed plek hebben gevonden. Mensen komen, mensen gaan. Alhoewel het altijd moeilijk is als mensen weggaan, heb ik daarvoor in de plaats weer andere collega's gekregen waar ik minstens zoveel goede herinneringen aan heb. Wendy, jij kwam binnen als een verlegen stagiaire, maar kijk toch eens hoe je gegroeid bent. En Vanja, ik heb je door de drukte rond dit proefschrift misschien wat in de steek gelaten de afgelopen maanden. Maar als ik kijk hoe zelfstandig jij nu werkt, denk ik dat dit uiteindelijk alleen maar positief voor ons is geweest. Ik kijk er naar uit weer samen met jou nieuwe wetenschappelijke uitdagingen aan te gaan.

Drie andere collega's die hier zeker genoemd moeten worden, ons klinisch statistisch team, de drie M's, Maxime Look, Marion Meijer-van Gelder, en Marcel Smid. Ik realiseer mij ten volle dat ik enorm verwend ben met jullie drie die te allen tijden zo snel reageerden op mijn mailtjes met weer een nieuwe vraag. Maxime, die zelfs vanuit Australië de een na de andere statistische analyse voor mij deed zodat ik 's morgens vroeg bij het openen van mijn PC weer de nodige stof tot nadenken kon binnenhalen. Marion, altijd in voor een gezellig kletspraatje 's morgens vroeg, wat overigens meestal uitliep in discussies hoe we de klinische aspecten van het onderzoek gedegen konden aanpakken. Waarna jij, altijd met een positieve instelling, weer met lijsten met vragen van mij aan de slag ging. En Marcel met zijn kennis van de microarray data, die aan een half woord genoeg had om te begrijpen wat ik nu toch weer graag zou willen bekijken. Zonder jullie drie was dit proefschrift er echt nooit gekomen.

Laat ik hier nu vooral niet vergeten de mensen te bedanken die nog niet genoemd zijn maar met wie ik de afgelopen jaren zo prettig en collegiaal op het lab heb gewerkt: Antoinette, Arzu, Berthe, Buddy, Fons, Iris, Jord, Jozien, Kirsten, Maaike, Marijke, Maurice, en Mieke S.

Tenslotte, zeker meer dan een dankwoord voor mijn vriend en levenspartner, die er altijd was als het even tegenzat, maar waar ik gelukkig ook altijd samen de goede momenten mee heb kunnen delen en hoop te blijven delen. Albert, dank je wel voor het begrip dat je toonde als ik toch weer net iets langer bleef doorwerken als was afgesproken en voor de energie die je erin gestoken hebt om mij op gezette tijden bij die computer weg te halen. Jij maakt mij compleet.

Direct of indirect hebben jullie er allemaal voor gezorgd dat dit boekje er uiteindelijk is gekomen. Kortom, dit proefschrift ons proefschrift!